creative commons
COMMONS DEED

저작자표시-비영리-변경금지 2.0 대한민국

이용자는 아래의 조건을 따르는 경우에 한하여 자유롭게

- 이 저작물을 복제, 배포, 전송, 전시, 공연 및 방송할 수 있습니다.

다음과 같은 조건을 따라야 합니다:

저작자표시. 귀하는 원저작자를 표시하여야 합니다.

비영리. 귀하는 이 저작물을 영리 목적으로 이용할 수 없습니다.

변경금지. 귀하는 이 저작물을 개작, 변형 또는 가공할 수 없습니다.

- 귀하는, 이 저작물의 재이용이나 배포의 경우, 이 저작물에 적용된 이용허락조건을 명확하게 나타내어야 합니다.
- 저작권자로부터 별도의 허가를 받으면 이러한 조건들은 적용되지 않습니다.

저작권법에 따른 이용자의 권리는 위의 내용에 의하여 영향을 받지 않습니다.

이것은 이용허락규약(Legal Code)을 이해하기 쉽게 요약한 것입니다.

Disclaimer

dCollection

조선대학교
CHOSUN UNIVERSITY

[UCI]I804:24011-200000266485

February 2018

Ph.D. Dissertation

Biodiesel production from microalgae:

Optimization of microalgal growth and lipid accumulation using various cultivation techniques

Graduate School of Chosun University

Department of Environmental Engineering

Geun Ho Gim

조선대학교
CHOSUN UNIVERSITY

Biodiesel production from microalgae:

Optimization of microalgal growth and lipid accumulation using various cultivation techniques

미세조류를 이용한 바이오디젤 생산:

다양한 배양기술을 이용한

미세조류 생장 및 지질 축적의 최적화

February 23 2018

Graduate School of Chosun University

Department of Environmental Engineering

Geun Ho Gim

Collection @ chosun

조선대학교
CHOSUN UNIVERSITY

Biodiesel production from microalgae:

Optimization of microalgal growth and lipid accumulation using various cultivation techniques

Supervisor : Prof. Si Wouk Kim

A dissertation submitted to the Department of Environmental Engineering and the Graduate School of Chosun University in fulfillment of the requirement for the degree of Doctor of Philosophy

February 23 2018

Graduate School of Chosun University
Department of Environmental Engineering
Geun Ho Gim

Collection @ chosun

조선대학교
CHOSUN UNIVERSITY

This certifies that the degree of Doctor of Philosophy of Geun Ho Gim is approved by

Jin Cheol Yoo
Chair of committee

In Seop Chang
Committee member

Hyun Hwa Lee
Committee member

Baek Rock Oh
Committee member

Si Wouk Kim
Committee member

December 2017

Graduate School of Chosun University

Collection @ chosun

조선대학교
CHOSUN UNIVERSITY

Contents

Collection @ chosun

조선대학교
CHOSUN UNIVERSITY

Collection @ chosun

조선대학교
CHOSUN UNIVERSITY

Collection @ chosun

조선대학교
CHOSUN UNIVERSITY

Collection @ chosun

조선대학교
CHOSUN UNIVERSITY

Collection @ chosun

조선대학교
CHOSUN UNIVERSITY

List of Tables

Collection @ chosun

조선대학교
CHOSUN UNIVERSITY

Collection @ chosun

조선대학교
CHOSUN UNIVERSITY

List of Figures

Collection @ chosun

조선대학교
CHOSUN UNIVERSITY

Collection @ chosun

조선대학교
CHOSUN UNIVERSITY

Collection @ chosun

조선대학교
CHOSUN UNIVERSITY

Collection @ chosun

조선대학교
CHOSUN UNIVERSITY

ABSTRACT

The growth and lipid content of freshwater (*Chlorella* sp., *C. vulgaris* CCAP211/11B, *B. braunii* FC124, and *S. obliquus* R8) and marine microalgae (*I. galbana* LB987, *N. oculata* CCAP849/1, and *D. salina*) were investigated under different culture modes. Enhanced growth was occurred when they were cultivated under heterotrophic or mixotrophic conditions compared with photoautotrophic mode. Meanwhile, high lipid accumulation in the cells occurred when they were cultivated under photoautotrophic or mixotrophic conditions. During mixotrophic cultivation mode, light intensity had an impact on freshwater microalgal growth and lipid accumulation. Marine microalgal biomass production was not affected significantly by light intensity. However, both chlorophyll concentration and lipid content increased dramatically with increasing light intensity under mixotrophic culture mode. Additionally, in marine microalagae under photoautotrophic culture mode, low nitrogen concentration stimulated lipid production, but a decreasing lipid content and an increasing biomass were observed with increasing nitrogen concentration.

The effects of growth stimulators in oceanic sediment on biomass and lipid production of *B. braunii* LB572 and *P. tricornutum* B2089 in mixotrophic culture was also investigated. With the optimal mixing ratio of culture medium and oceanic sediment extract of 6:4 (v/v), specific growth rates of *B. braunii* LB572 and *P. tricornutum* B2089 increased 13.0 and 11.3-fold, respectively. Then, maximum biomass and lipid production of *B. braunii* LB572 was 5.54 and 3.09 g/L, and that of *P. tricornutum* B2089 was 6.41 and 3.61 g/L, respectively. Fe^{3+} and Ca^{2+} in sediment remarkably promoted biomass and lipid production, but Mg^{2+} did not. Humic acid extracted from sediment increased bioavailability of metal ions. Thus, low-cost oceanic sediment can supply sufficient growth stimulators for mass production of biomass and lipid in both microalgae.

Collection @ chosun

조선대학교
CHOSUN UNIVERSITY

Moreover, this study investigated the effect of light regimes on the cell growth, lipid accumulation and fatty acid composition of oleaginous microalgae under mixotrophic culture mode in a tubular photobioreactor. Biomass production gradually increased with increasing light intensity up to 200 μmol photon/m^2/s for *B. braunii* LB572 and 150 μmol photon/m^2/s for *P. tricornutum* B2089, respectively, but the lipid content of both microalgae tended to increase continuously up to 300 μmol photon/m^2/s. The effect of photoperiod was also similar to that of light intensity. Thus, the optimal photoperiod of the two microalgae was 18:6 h/L:D cycle, and the optimal light intensity was 200 μmol photon/m^2/s for *B. braunii* LB572 and 150 μmol photon/m^2/s for *P. tricornutum* B2089. Fatty acid composition in both microalgal cells was changed by the light intensity and photoperiods. The amounts of saturated and monounsaturated fatty acids in C16-C18 fatty acids, which were essential component for biodiesel, increased with increasing light intensity and duration time, but that of polyunsaturated fatty acids gradually decreased. Additionally, for optimization of microalgal cell disruption method, the six disruption methods (autoclave, sonication, bead-beater, microwave, french-press, and osmotic shock) for efficient lipid extraction of *B. braunii* LB572 and *P. tricornutum* B2089 were optimized. As a result, microwave disruption method was the most effective disruption for lipid extraction in both microalgae. The optimum conditions of microwave methods were as follows: microwave oven at 150 ℃ for 20 min with frequency of 1250 W and 2450 MHz.

In addition, biomass and lipid productivity of *B. braunii* LB572 and *P. tricornutum* B2089 were investigated in the continuous or repeated-batch culture under optimum light regimes. After cells of the two microalgae were cultured in the 12 L tubular-type photobioreactor (working volume 10 L) for 13 days, they were further cultured by different cultivation types. Each specific growth rate of *B. braunii* LB572 and *P. tricornutum* B2089 was 0.33 and 0.37 d^{-1}, respectively, when cultured in the batch cultivation. In the continuous cultivation, fresh medium was supplied to the reactor at a speed of 2.4 mL/min and the same volume of cell suspension was drained from the

Collection @ chosun

조선대학교
CHOSUN UNIVERSITY

reactor. The highest biomass and lipid productivity was found when the dilution rate was 0.35 d^{-1}, then those of *B. braunii* LB572 and *P. tricornutum* B2089 were 2.47 and 1.41 g/L/d and 4.24 and 2.45 g/L/d, respectively, which resulted in about 4 times higher than those obtained from the cells cultivated by batch culture mode. In addition, they were repeated-batch cultured for 30 days. 4 L of cell suspension was drained from the reactor at every 6 days and the same volume of fresh medium was supplied. After five times repeated-batch cultivation, the biomass and lipid productivity *B. braunii* LB572 was 2.71 and 4.84 g/L/d and those of *P. tricornutum* B2089 was 3.72 and 6.24 g/L/d, respectively. These results indicates that repeated-batch culture is better than continuous culture for biomass and lipid production.

Also, direct-transesterification condition was optimized for biodiesel production from the microalgal biomass, and the FAME yields of the two microalgae were investigated under the optimal conditions, which were as follows: 10 g biomass was treated with 6.0 mL sulfuric acid and 8.0 mL chloroform and boiled at 200 ℃ for 60 min. Under this condition, 70 mL methanol for *B. braunii* LB572 and 35 mL methanol for *P. tricornutum* B2089 were added, respectively. The inner pressure in the reactor was found to be about 75 bar at the optimum temperature of 200 ℃. In addition, FAME yield (from non-disrupted wet biomass) of *B. braunii* LB572 and *P. tricornutum* B2089 through this reaction were found to be 95.6 and 96.2% (of lipid), respectively.

Collection @ chosun

조선대학교
CHOSUN UNIVERSITY

Chapter I

General Introduction

Collection @ chosun

조선대학교
CHOSUN UNIVERSITY

1. Introduction

1-1. Bioenergy and biomass

Sustainable alternative and renewable energy development is highly needed because of the various global problems of existing fossil fuels, such as lack of fuel resources, energy saving, and increasing energy cost, and this importance of sustainable alternative energy research and development is gradually attention [Dragone et al., 2010; Jung et al., 2012]. Wind, solar, geothermal, hydro, and biomass represent a major alternative sources to fossil fuels currently in use. According to published by REN21 (Renewables Energy Policy Network for the 21st Century, renewables 2016 Global Status Report), renewable energy is firmly established as a competitive mainstream energy source in many countries around the world [Zervos, 2016].

2015s was a record years for the development and application of renewable energy, and the capacity of energy generation is steadily increasing. In addition, the use of renewable energy is also increasing in transportation fuels [Savin, 2012]. According to the International Energy Agency (IEA) [Fatih, 2015], oil accounted for 31.1% of the world's major energy consumption, followed by coal (28.9%), natural gas (21.4%), renewable energy (13.8%). Compared with the 1970s, the share of oil has declined, but the share of natural gas, coal, nuclear energy and renewable energy has increased. Demand for heating has dropped sharply since the oil crisis, but demand for transportation has increased steadily. Recently, coal has faced a new situation due to improved air pollution and greenhouse gas reduction policies (such as paris agreement), and renewable energy has grown at its fastest pace since the 2000s, in view of strengthening energy security and reducing greenhouse gas emissions (Fig. 1-1).

Collection @ chosun

조선대학교
CHOSUN UNIVERSITY

Bioenergy accounts for a larger share of the primary energy supply than any other renewable energy sources. Primary energy means that does not convert human engineered into natural resources (such as hydro, wind, geothermal, and solar power, etc.) and fossil resources (such as coal, oil, and natural gas). In 2015, the production of bioenergy has increased in response to rising energy demand and environmental considerations in some countries. However, the bioenergy sector is faces difficulties in terms of uncertainty in some markets, such as low oil prices and the commercialization of shale gas [Savin, 2012]. The recent commercialization of shale gas and the low cost policies of oil producing countries have reduced the need for research and development of bioenergy production. However, the reserves of fossil fuels and shale gas are limited, and research and development of bioenergy for greenhouse gas reduction should continue. On the other hand, Biomass-derived biofuels production is expected to provide a variety of opportunities in the upcoming era. It is expected to promote new employment in bio-energy production areas, replace fossil fuels in the long term, stabilize atmospheric greenhouse gas concentrations, promote desulfurization of transport fuels, and enhance the safety of energy supplies [Mata et al., 2010].

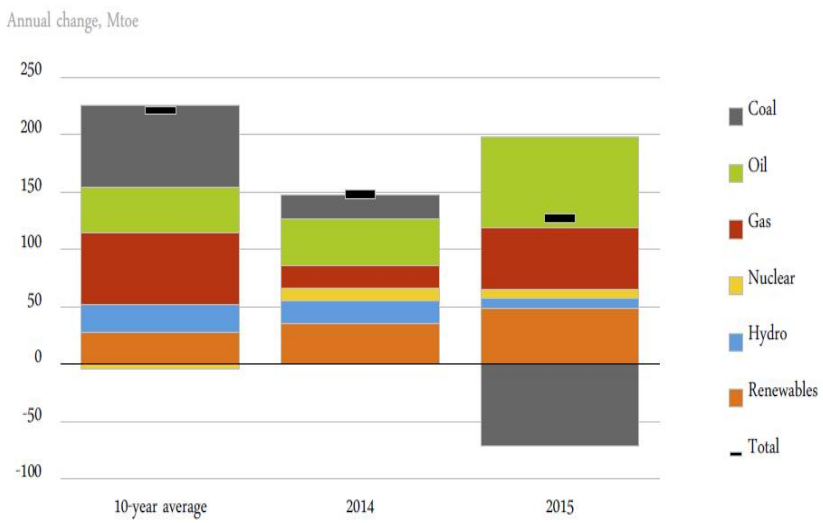

Fig. 1-1. Changes in global energy types since 2000s [BP, 2016].

Collection @ chosun

조선대학교
CHOSUN UNIVERSITY

1-1-1. Bioenergy production from Biomass

Bioenergy is the energy which is stored in biological matter or biomass, and bioenergy is a renewable energy source that is environmentally and sustainable and has high potential for global energy demand [Rosillo-Calle, 2016]. Biomass is a plant resource in which light energy is accumulated as chemical energy by photosynthesis. Because it is a resource that can be continuously produced through photosynthesis using solar energy, water, and carbon dioxide, which can be easily obtained from nature, mass production of biofuels can be continuously produced (Fig. 1-2).

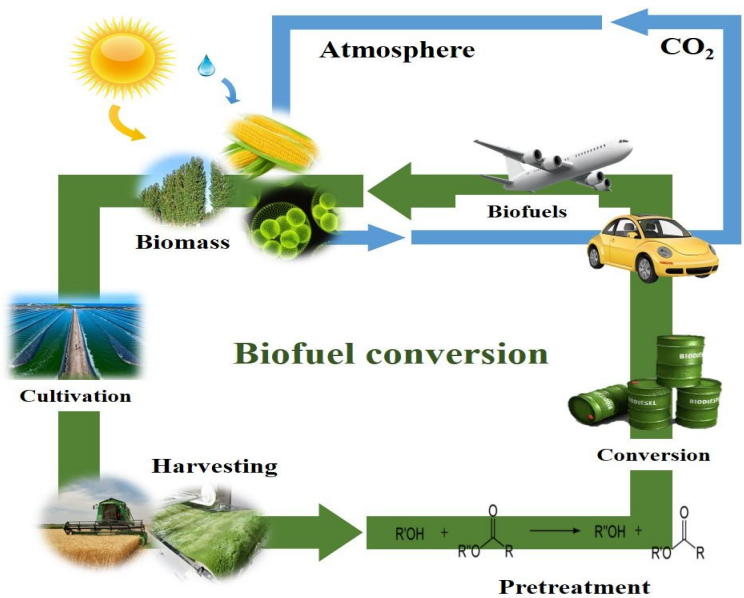

Fig. 1-2. Biological conversion of solar energy to chemical energy.

Collection @ chosun

조선대학교
CHOSUN UNIVERSITY

a. 1st generation biofuels

The most common type of biofuels today is so-called "1st generation biofuels (or 1st generation biomass)" that include ethanol, methanol. butanol. and pure vegetable oil (PPO). Sugarcane, corn, soybeans, potatoes, wheat, and sugarbeets are major sources of 1st-generation bioenergy in the bioenergy sector. However, price competition with food resources is inevitable for 1st generation biofuels [Bringezu et al., 2007].

b. 2nd generation biofuels

Therefore, recent studies have focused on the production of "2nd generation biofuel (such as 2nd generation biomass)" or advanced biofuels cause the potential non-sustainability of first generation fuels. The 2nd biomass is made from lignocellulosic biomass and agricultural waste. However, these feeders have no direct competition with human food resources (1st generation biofuel). On the other hand, in the case of arable land, a biofuel production could ultimately be a rival to food crops, also second generation biomass is very difficult to pre-treatment due to lignocellulose when producing biofuel [Eisentraut, 2010].

c. 3rd generation biofuels

Algal biofuel, the bioenenrgy of the next generation of bioenergy, are considered “3rd generation biofuel (of 3rd generation biomass)” [Dragone et al., 2010]. Algal crops can not be directly competitive with land-based foods and crops because they can be grown in water [Roesijadi et al., 2010]. Algae are organisms that ate like plants and vegetables. There are called “Macroalgae” and “Microalgae”. Macroalgae are commonly known as “seaweed”, that macro means big plant. and “Microalgae” are often “phytoplankton”, the word micro means small plant. Microalga uses light and carbon dioxide to reproduce itself with photosynthesis. Microalgae convert solar energy to chemical energy of carbohydrates, proteins and lipids through photosynthesis (Fig. 1-3), and their

Collection @ chosun

조선대학교
CHOSUN UNIVERSITY

growth is completed in only a few days [Sheehan et al., 1998]. The growth rate of microalgae can be accelerated by adding certain nutrients and sufficient aeration (containing carbon dioxide), but growth is possible where sunlight and some simple nutrients are needed [Aslan and kapdan, 2006; Pratoomyot et al., 2005; Renaud et al., 1999]. Microalgae has great potential to produce many types of biofuels as follows; production of methane by anaerobic digestion [Spolaore et al., 2006], biodiesel production from microalgal oil [Chen et al., 2011; Cheng et al, 2009; Converti et al., 2009; Doan et al., 2011; Dunahay et al., 1996; Jung et al., 2012; Mandal and Mallick, 2009; Miao and Wu, 2006; Sawayama et al., 1995; Scott et al., 2010; Xu et al., 2006; Yang et al., 2011], and photobiological produced biohydrogen [Akkerman et al., 2002; Fedorov et al., 2005; Ghirardi et al., 2000; Kapdan and Kargi, 2006; Melis, 2002].

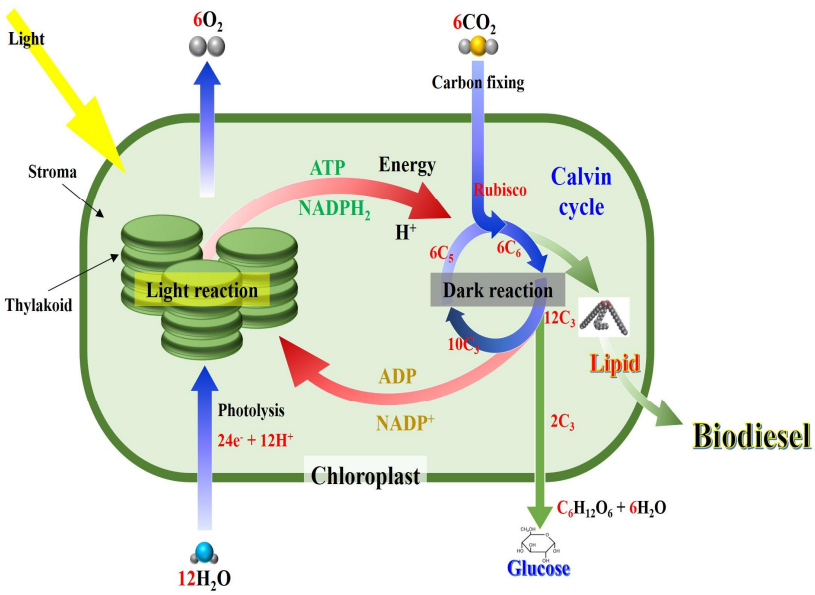

Fig. 1-3. Biodiesel production from microalgae by photosynthesis.

Collection @ chosun

조선대학교
CHOSUN UNIVERSITY

Benefits of biofuels (such as biodiesel) production using microalgal species are as follows. ① Microalgal strain can produce high biodiesel productivity because it growth more rapidly in crops and woody biomass and can be produced every year round [Schenk et al., 2008]. ② Water in necessary for microalgae and crops to grow, but water use is less than land-crops, which can reduce th load on freshwater [Dismukes et al., 2008]. ③ Also, microalgae can be cultivated in the presence of salt and adapt to various environmental culture conditions, so that they do not significantly affect microalgal biomass productivity [Searchinger et al., 2008]. ④ Most microalgae have fast growth rate (doubling time was about 3.5 h) and high total lipid contents (about 20-50%, w/w). It has a very high potential as an energy source for effective biodiesel production [Chisti, 2007; Metting, 1996; Spolaore et al., 2006]. ⑤ During the microalgal biomass production, it is possible to maintain and improve air quality through carbon dioxide fixation (1 kg of dry microalgal bioimass utllise about 1.83 kg of CO_2) [Chisti, 2007]. ⑥ Nutrients (Nitrogen, phosphorus, and carbon) for nicroalgal cultivation can be obtained from a variety wastewater and organic wastes, enabling an environmentally friendly microalgal culture process [Cantrell et al., 2008]. ⑦ After oil extraction from microalgal cells, it is possible to produce various high-value by-products such as proteins and residual biomass [Spolaore et al., 2006]. ⑧ Depending on the microalgal growth culture conditions changes can be controlled for each of the biochemical composition, and also total lipid accumulation in cells can be significantly improved [Qin, 2005].

1-2. Biodiesel production from microalgae

Biodiesel is an alternative fuel similar to conventional of fossil diesel. Biodiesel production and commercialization technology lasted for more than 50 years [Barnwal and Sharma, 2005; Demirbas, 2005; Felizardo et al., 2006; Fukuda et al., 2001; Knothe et al.,

Collection @ chosun

조선대학교
CHOSUN UNIVERSITY

1997; Kulkarni and Dalai, 2006; Meher et al., 2006; Van Gerpen, 2005]. As shown table 1-1, microalgae seem to be a powerful biodiesel source that can completely replace fossil fuels and unlike other biomass (corn and soybean), it is very effective in oil yield and land area [Chisti, 2007].

Table 1-1. Comparison of various biomass of biodiesel [Chisti, 2007]

Biomass	Oil Yield (L/ha)	Land area required (M ha)[a]	Percent of US cropping area[a]
Corn	172	1,540	846
Soybean	446	594	326
Canola	1,190	223	122
Jatropha	1,832	140	77
Coconut	2,689	99	54
Oil palm	5,950	45	24
Microalgae[b]	136,900	2	1.1
Microalgae[c]	58,700	4.5	2.5

[a] For meet 50% of the demand for the total transport fuels in the US.

[b] 70% oil (wet weight) in microalgal biomass

[c] 30% oil (wet weight) in microalgal biomass

In order to produce biodiesel from microalgae, selection of microalgae species, optimization of culture conditions, mass cultivation systems, and each of harvest-disruption-extraction-conversion process should be accompanied. Depending on the species of algae can be produced various bio-molecules such as lipid, hydrocarbons, proteins, pigment, and other components [Banerjee et al., 2002; Metzger and Largeau, 2005]. Although not all microalgal oils are satisfactory for biodiesel production, most microalgae species can produce oils suitable for biodiesel production. Significant funds are invested in research on high growth rates, cell density, and lipid content in biodiesel production from microalgae. However, there are many obstacles to overcome in order to improve microalgae culture and oil extraction methods as an economically feasible platform

Collection @ chosun

조선대학교
CHOSUN UNIVERSITY

to offset diesel conversion and by-product treatment methods and consquently reduce carbon dioxide emissions. The microalgal biofuels production diagram is shown Fig. 1-4, and key challenges include microalgal strain selection and development, cultivation technology, production, harvesting, by-product development, oil extraction, oil refining and residual utilization [Hannon et al., 2014].

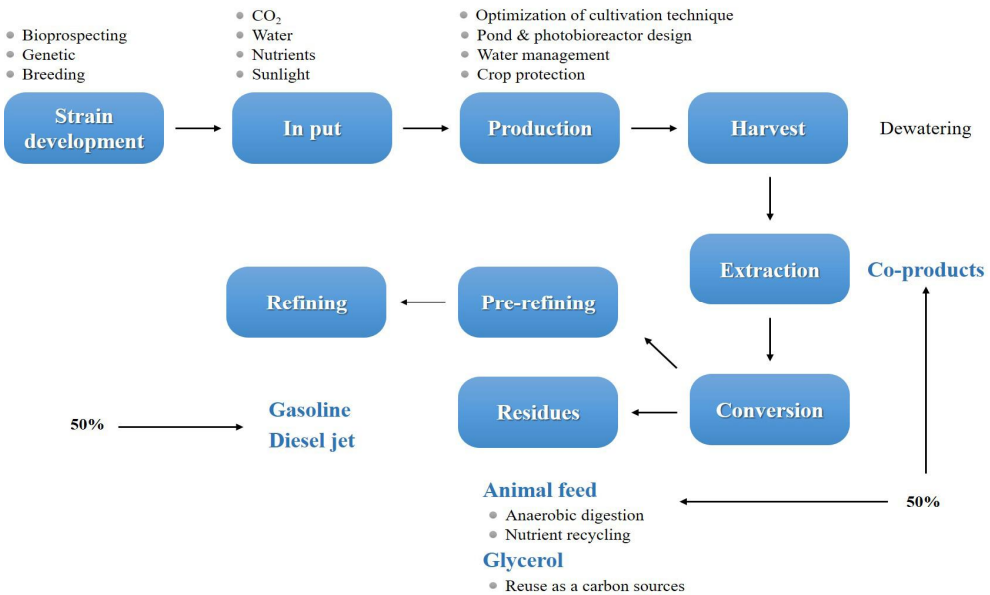

Fig. 1-4. Microalgal biofuels production diagram [Hannon et al., 2014].

1-2-1. Microalgal species

Microalgae is estimated to be inhabited in aquatic and terrestrial environments. There are currently more than 50,000 species and about 30,000 species have been studied and analyzed [Richmond, 2004]. Because microalgae vary in species diversity, the production of lipids, hydrocarbons, and other complex oils depends on the microalgal species specific [Banerjee et al., 2002; Metzger and Largeau, 2005]. Therefore, effective

Collection @ chosun

조선대학교
CHOSUN UNIVERSITY

microalgal strain selection and optimization is required from natural in order to increase the productivity of microalgal biodiesel [Lee et al., 2015]. There are 5 major factors considerations when electing microalgae as follows. ① It should be possible to convert effective light energy into biomass in various light conditions. The light conversion efficiency of microalgae is usually less than 5%, and microalgal growth is limited by photoinhibition effect under high light intensity. ② If oxygen is not released in the microalgal culture systems, high density culture of microalgae difficult due to the oxygen inhibition effect. Therefore, it is necessary to select a strain capable of culturing even at a high oxygen partial pressure. ③ For cultivate high cell density and open type culture systems of microalgae, it is essential to select and improve strains for resistant contamination from external organisms. ④ It is possible to improve biodiesel productivity through the improvement and selection of strains with high cell growth and lipid content. In recently, studies on the improvement of lipid accumulations through cultivation under depleted conditions of light, temperature, and nitrogen, and the like are active [Converti et al., 2009; Gim et al., 2016; Giridhar Babu et al., 2017; Gordillo et al., 1998; Khotimchenko and Yakovleva, 2005; Li et al., 2008; Merzlyak et al., 2007; Mock and Kroon, 2002; Pal et al., 2011; Qin, 2005; Sugimoto et al., 2008; Xin et al., 2010; Yeesang and Ceirsilp, 2011]. ⑤ After microalgae cultivation, selection and development of microalgae suitable for harvesting and extraction are needed. Especially, microalgae such as *Botryococcus* is able to reduce the harvest cost by forming floc at high concentration and thin-walled microalgae show an advance to promote lipid extraction.

a. Freshwater microalgae

○ ***Chlorella*** is able to growth in both aquatic and terrestrial habitats because of its simple life period and has a plant-like photosynthesis mechanism. This microalgal species are the most notable microorganisms for biodiesel production or other

Collection @ chosun

조선대학교
CHOSUN UNIVERSITY

application sectors. Recently, researches on biodiesel production for *C. vulgaris* [Church et al., 2017; Mohd-Sahib et al., 2017; Wong et al., 2017] and *Chlorella sorokiniana* [Giridhar Babu et al., 2017; Mandal et al., 2017] were very active. *Chlorella* strains, unicellular green algae, are spherical or ellipsoidal with a diameter of 2-10 μm and doubling time is 9-20 hr [Richmond and Hu, 2013; Rosenberg et al., 2014]. Chlorella contains about 60% protein, 10-15% carbohydrates, and 15-20% lipids and major compositions of fatty acids in lipid are the C16 and C18 groups. In particular, the lipid content of *Chlorella* can be increased up to 60% under nitrogen depletion and excess illumination conditions [Hu er al., 2008].

○ ***Scenedesmus*** is one of the common freshwater microalgal strain, like *Chlorella*. This species have many shapes and it is difficult to identify these microorganism visually with the eye. *Scenedesmus* can exist as unicells, but these strains may be present in the form of 4 or 8 cells like coenobia [Lürling, 1998] and the doubling time of this strain is 10 to 21 h [Gardner et al., 2012]. *Scenedesmus* is a microalgal strain capable of producing various bioenergy (bio-ethanol, hydrogen, and diesel) and is one of the major microalgae in biodiesel production research until recently [Abd El Baky et al., 2012; Mandal and Mallick, 2009]. *Scenedesmus* is highly biomass-producing in green algae and it is possible to produce better productivity by adding various organic carbon sources (heterotrphic cultivation) [Gim et al., 2014]. In addition, recent active research has shown that the total lipid content of *Scenedesmus* has been increased to about 60%, and it has attracted attention as a suitable strain for biodiesel production in the future [Banerjee, 2002; Mandal and Mallick, 2009].

○ ***Botryococcus braunii*** is colonial green alga, pyriform shaped planktonic microalga [Tasić et al., 2016], this strain is widely distributed is freshwater environments. Cell size (length × width) is in the range of 8-9 × 5 μm to 13 × 7-9 μm. *Botryococcus* is most promising for biofuel production, because that strain is produces a high

Collection @ chosun

조선대학교
CHOSUN UNIVERSITY

content of hydrocarbon and lipid in the cells, and the hydrocarbon and lipid content are up to 75 and 65% of dry weight [Banerjee et al., 2002; Chisti, 2007; Metzger and Largeau, 2005]. Moreover, its strain enriched in saturated and unsaturated fatty acids known as TAGs, which is well suited for biodiesel production [Kalacheva et al., 2002a and b]. However, *Botryococcus* has a slow growth rate compared to other microalgae species and is a major obstacle to commercial application use. The relatively slow doubling time of this strain is about 40 hours at optimal growth conditions [Wolf et al., 1985].

b. Marine microalgae

○ ***Dunaliella*** is a unicellular microalgae, motile, bi-flagellate, that is widespread in freshwater and seawater, and is a green algae (Chlorophyta, Chlorophyceae) [Borowitzka and Borowitzka, 1988]. In addition, the cell length is 5-29 μm (average 10.9-16.9 μm) and th doubling time is 6 hr in the optimum culture condition [Ben-Amotz, et al., 1991; Richmond and Hu, 2013; Tang et al., 2011; Zou et al., 2009]. This strain is a source of biological β-carotene and has since been commercially used as a natural source of valuable carotenoids in the pharmaceutical and functional food industries since the 1980s [Richmond and Hu, 2013]. In addition, *Dunaliella* species, *D. salina* and *Dunaliella tertiolecta* have been studied for the biodiesel production until recently. However, these species have low biomass production (about 1.0 g/L, dry weight) compared to high lipid content (up to 30-40%, w/w) and require much research on optimized culture condition [Abd El Baky et al., 2014; Gim et al., 2016].

○ ***Isochrysis*** is a genus of haptophytes, and includes the species such as *I. galbana*, *Isochrysis litoralis,* and *Isochrysis maritima*. Especially, this marine microalgal strain *I. galbana* is a golden-brown alga that accumulation of lipid and carbohydrate. Because of its high lipid contents, fast growth (doubling time is 38 h) [Kalplan et

Collection @ chosun

조선대학교
CHOSUN UNIVERSITY

al., 1986], and non-toxicity, *I. galbana* is a promising biomass for the production of a variety of livestock (and shellfish) food and biodiesel. Moreover, unlike most microalgae, there is no cell wall of *I. galbana*, so lipid extraction is relatively easy and extraction efficiency is easy to improved [Liu and Wang, 2014].

○ ***Nannochloropsis*** was first named by Hibberd [1981], and is a genus of microalgae within the heterokont family of eukaryotes that are being studied for microalgal biodiesel production. *Nannochloropsis* species have been shown to be suitable for biofuel production because of their ease of growth (doubling time is 23 h) and high lipid content (28.7-37.3% of dry weight) and mostly unsaturated fatty acids and palmitic acid. It also contains sufficient unsaturated fatty acids linolenic acid and polyunsaturated acids for high-quality biodiesel [Converti et al., 2009; Gim et al., 2016; Gouveia and Oliveira, 2009; Pal et al., 2011; Sukenik et al., 1989].

○ ***Phaeodactylum tricornutum*** is a diatom, and this is the only species in the genus *Phaeodactylum*. Unlike other diatoms, *P. tricornutum* grow in various forms (fusiform, triradiate, and oval) as the growth environment changes [de Martino et al., 2007]. *Phaeodactylum*, in this the cell size (length × width) is in the range of 10-20 × 3-4 μm and th doubling time is 18-21 hr in the optimum culture condition [Thomas and Dodson, 1968]. Moreover, in this unicellular microalgal strains can be accumulate lipids in the range 20-60% (dry weight) under suitable culture conditions [Valenzuela et al., 2013], and it can store carbon and energy in the from of neutral lipids, especially TAGs. Therefore, *P. tricornutum* has potential as a source for biodiesel production [Valenzuela et al., 2012].

Collection @ chosun

조선대학교
CHOSUN UNIVERSITY

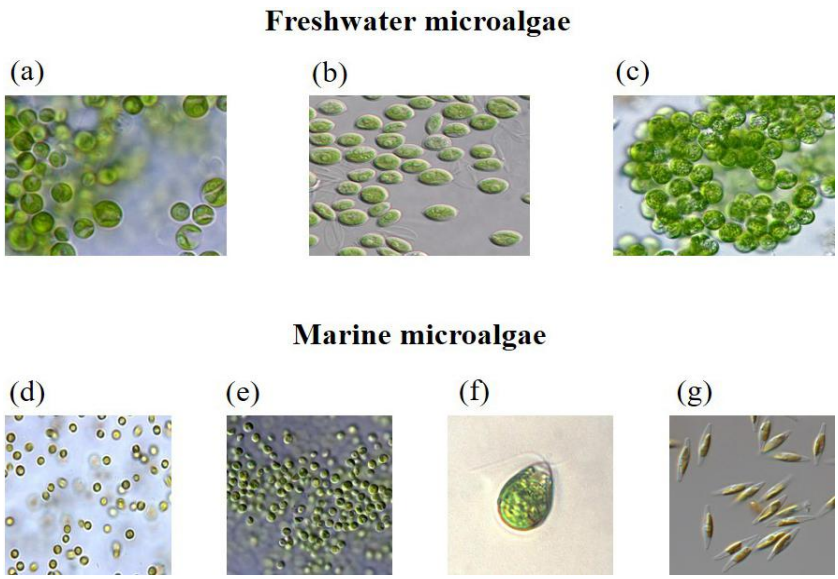

Fig. 1-5. Photographs of freshwater and marine microalgal species: (a) *C. vulgaris*; (b) *S. obliquus*; (c) *B. braunii*; (d) *I. galbana*; (e) *N. oculata*; (f) *D. salina*; (g) *P. tricornutum*.

1-2-2. Cultivation

For stable microalgae cultivation, modification and optimization study of microalgal culture medium, nutritions (Macronutrient, trace elements, and other organic carbon sources), environmental growth factors (light intensity, photo periods, temperature, and pH), various culture modes (photoautotrophic, heterotrophic, and mixotrophic culture mode), and reactor (open and closed system) should be performed indispensable.

a. Cultivation medium & nutrients

○ Growth medium for microalgal strain cultivation should be provided by various inorganic nutrients for algal cell formation and growth. Essential elements are nitrogen (N), phosphorus (P), iron, calcium, and sometimes silicon. The minimum nutrients requirement of stable microalgae cultivation can be estimated using the

Collection @ chosun

조선대학교
CHOSUN UNIVERSITY

approximate molecular formula of microalgal biomass as follows: $CO_{0.48}H_{1.83}N_{0.11}P_{0.01}$ [Grobbelaar, 2004]. Proper microalgal seeds management and maintenance of microalgae strains depend on the choice of growth medium and culture parameters. When selecting the culture medium, the microalgae species habitat environment should be identified. For example, in consideration of eutrophicate environment and nutritional deficiency environment, the microalgal culture medium suitable for the species should be selected [Barsanti and Gualtieri, 2006]. In addition, selection of nutrients (Nitrogen and Phosphorous), trace elements (iron, calcium, magnesium, and silicon), buffer solution, various vitamins, chelating agents, and various extract (such as soil) and proper concentration adjustments are required for the preparation of a suitable medium for microalgae.

b. Environmental growth factors

○ Microalgae culture temperature is one of the environmental factors which are very sensitive to microalgae growth and metabolism activity, and easy to control in microalgae cultivation. For reference, the total lipid content was increased 2 times by increasing the incubation temperature of *N. oculata* from 20 ℃ to 25 ℃ [Converti et al., 2009].

○ Light supply is a major environmental factor influencing phytoplankton physiology and is the most important factor affecting photosynthesis kinetics of microalgae [Khoeyi, et al., 2012]. According to previous studies, optimal growth of microalgae is possible under the optimum light condition, but when the light intensity is low or high, light inhibition phenomenon which inhibits microalgal growth is caused [Bouterfas et al., 2002].

Collection @ chosun

조선대학교
CHOSUN UNIVERSITY

c. Culture mode

○ Most algae groups refer to photoautotrophs, which produce carbohydrates and ATP through photosynthesis using sunlight as an energy source and carbon dioxide as a carbon source [Barsanti and Gualtieri, 2006], however, the production efficiency of microalgal growth and lipid accumulation are deteriorated due to the limit of light supply of microalgae in the culture medium under photoautotrophic culture mode. However, depending on the microalgal species, it is possible to cultivate in heterotrophic and mixrotrophic culture mode rather than photoautotrophic culture mode, and it is possible to high growth rate and lipid accumulation [Gim et al., 2014 and 2016]. Under light-free culture conditions in heterotrphic cultivation mode, microalgae growth using only organic carbon. Mixotrophic culture mode are grown by metabolic precesses combined with independent nutrients and heterotroph mode that use both organic and inorganic carbon. They use energy produced from organic compounds fro cell synthesis and store chemical energy converted from light energy [Chojnacka and Marquez-Rocha, 2004; Gim et al., 2014 and 2016]. Several microalgal strains which have been observed under photoauto-, hetero-, and mixotrophic conditions are *C. vulgaris* [Gim et al., 2014; Mitra et al., 2012], *Chlorella sorokiniana* [Wang et al., 2012], *Chlorella zofingiensis* [Liu et al., 2012], *Haematococcus pluvialis* [Kobayashi et al., 1992], *S. obliquus* [Gim et al., 2014], *B. braunii* [Gim et al., 2014; Zhang et al., 2011], *N. oculata* [Gim et al., 2016], I. *galbana* [Gim et al., 2016], and *D. salina* [Gim et al., 2016].

d. Mass cultivation & culture systems

○ The industrial use of microalgal strains for feed, food, functional and biofuels production is currently limited by various factors, including those related to massive scale cultivation. Mass production of microalgal biomass typically uses various culture systems in the indoor (such as photobioreactor) or outdoor (such as open

Collection @ chosun

조선대학교
CHOSUN UNIVERSITY

pond and raceway) processes. Universally, large-scale microalgal production systems are raceway pond [Terry and Raymond, 1985] and several photobioreactors [Tredici and Zittelli, 1998].

○ Since 1950s, mass cultivation of microalgae have been cultivated using raceway, it is difficult to control the temperature of the reactor depending on the external temperature and seasonal changes. However, carbon dioxide is readily available in the atmosphere and is more effective than photobioreactors. This open type reactor is susceptible to external other microorganisms contamination and uses natural light, making it difficult to provide effective illumination [Terry and Raymond, 1985].

○ On the other hand, photobioreactors (PBRs) are highly specialized mass cultivation systems that can be optimized for the biological and physical characteristics of microalgae cultured in closed system. In PBRs, microalgal cultured can be protected from a variety of external inflammatory factors, and the control of various influencing factors is flexible. Compared to opentype reactors, it is possible to develop modular processes with space-efficient design and carious functions. Currently, reactors for the microalgal mass production are vertical tubular [Kumar et al., 2011], bubble column [Doran, 1995], air-lift [Loubiere et al., 2009], flat-pannel [Barbosa et al., 2005; Zhang et al., 2001], horizontal [Tredici and Zittelli, 1998], helical type [Morita et al., 2001], stirred tank [Kumar et al., 2011], and hybrid type [Fernandez et al., 2001], etc. Each PBRs type has advantages and disadvantages. Depending on the species characteristics and application industries of microalgae, the choice of reactor is flexible.

Collection @ chosun

조선대학교
CHOSUN UNIVERSITY

1-2-3. Cell disruption

Optimization research of cell disruption processes are very important for effective lipid extraction from microalgal cells (Fig. 1-6) [Agerkvist and Enfors, 1990; Chen et al., 2009; Middelberg, 1995; Mutanda et al., 2011]. There are four main categories of microbial disruption, including microalgae. The selection of microalgal cell disruption methods has several influencing factors, especially, consideration should be given to microalgae such as cell wall toughness, economics, ease of scale-up, and deformation of lipid products. Mechanical or physical disruption methods are the least preferred method because they are not dependent on microalgae species and can cause less contamination and deformation of microalgal lipids. However, these methods generally require higher energy requirements than chemical or enzymatic methods and have less mechanical damage due to heat generation. Therefore, in order to produce biodiesel using microalgae, the most suirable cell disruption process for each strain should be studied [Harrison, 1991].

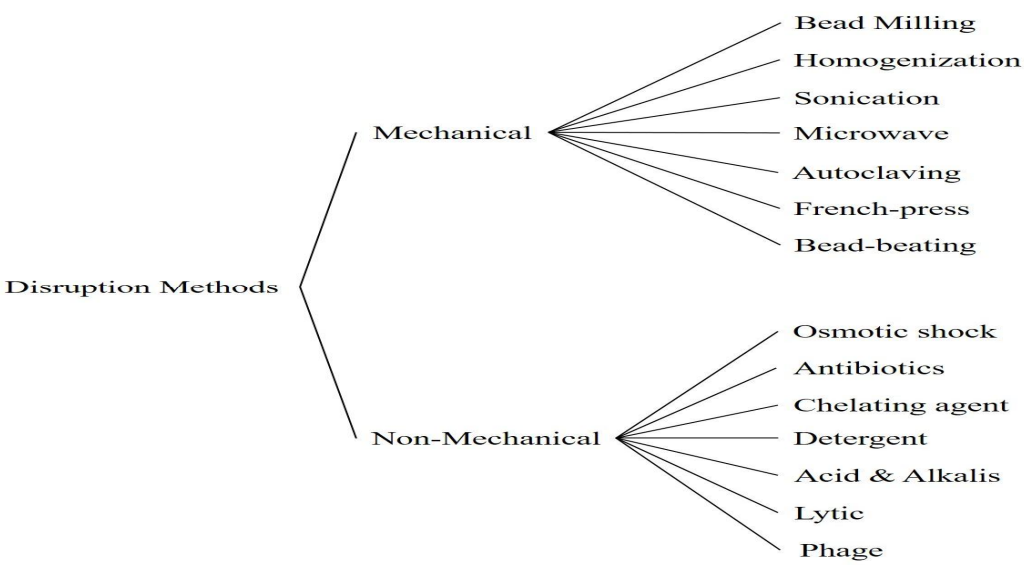

Fig. 1-6. Classification of various cell disruption methods [Günerken et al., 2015].

Collection @ chosun

조선대학교
CHOSUN UNIVERSITY

1-2-4. Biodiesel conversion

The parents oil (from microalgal lipid) used in biodiesel production is composed of triacylglycerides (TAGs), and TAGs is esterified with three fatty acid molecules and one glycerol molecules. In this reaction, 1 mole of triglyceride reacts with 3 moles of alcohol such as methanol to produce 1 mole of glycerol and 3 moles of methylester, and a catalyst is used for this reaction (Fig. 1-7). Catalyst are promoted in the transesterification, and the catalyst used in this reaction are mainly acids, alkalis, and enzymes [Fukuda et al., 2001; Meher et al., 2006]. The transesterification reaction using an alkali catalyst such as sodium hydroxide (or potassium) is much higher (approximately 4000 times) than the acid catalysis. However, when the free-fatty acid content of microalgae is high, the conversion efficiency of biodiesel due to the saponification reaction decrease [Fukuda et al., 2001]. Therefore, catalyst selection is very important for the optimization of transesterification process for biodiesel production from microalgae.

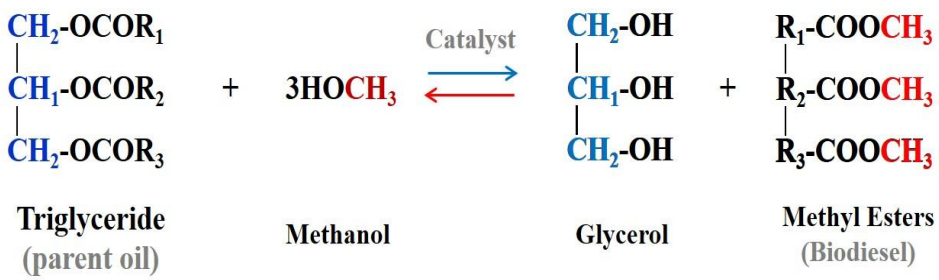

Fig. 1-7. Conversion of biodiesel to microalgae [Mata et al., 2010].

Collection @ chosun

조선대학교
CHOSUN UNIVERSITY

1-3. Overall research objective

After industrial revolution, energy depletion and global warming are one of the world's problems, seeking solutions around the world and international conventions (the Paris Climate Change Accord) are underway. Moreover, Korea is also confident that it will become a bioenergy powerhouse by researching bioenergy production such as biodiesel production using microalgae in order to solve the energy depletion and global warming problem to come.

Production of biodiesel using microalgae is carried out according to each step of cultivation-harvest-extraction-transesterification, and various studies are carried out for each step. Especially, since the cultivation process is the most expensive in the entire process, various researchers have been actively conducted for years to secure economical efficiency of the cultivation process. In order to ensure the economical efficiency of the culture process, development of microalgal strains (with high growth and lipid accumulation), new medium (contained organic carbon sources and various nutrients), and high efficiency photobioreactor are very important. In order to commercialize high-quality biodiesel, it is necessary to study changes fatty acid contents and composition of microalgal in the cells depending on various factors such as nutrients, trace metal ions, and photo regimes. Therefore, in this study, the research necessary for the production of biodiesel using microalgae was carried out as follows.

This study was carried out as follows to optimize culture conditions, culture mode (photoautotrophic, heterotrophic, and mixotrophic culture condition), and cell disruption methods in flask-scale for freshwater and marine microalgae, and to develop new media for high productivity of biomass and lipid of selected microalgae. First, for the present study, microalgae with a rapid growth rate and lipid content of less than 20% (w/w) were searched and selected. Secondly, biomass production and lipid content of freshwater and marine microalgae were investigated in various cultivation modes. And then,

Collection @ chosun

조선대학교
CHOSUN UNIVERSITY

the effect of light intensity on microalgal growth and lipid accumulation under mixotrophic culture mode was investigated (chapter II and III). In addition, effect on the growth and lipid accumulation of marine microalgae were carried out under depleted- and rich-nitrogen condition. In the next chapter, we have developed a new medium capable of promoting microalgal growth and lipid accumulation in oil-rich microalgae, and examined the effect of the oceanic sediments extract (such as, DOC and metal ions) on microalgal growth and lipid accumulation (chapter IV).

And, based on the results of the study on the flask-scale, a study was conducted for the mass cultivation and direct-transesterification of oil-rich microalgae using photobioreactor. In chapter V, effect of various light regimes on microalgal growth, lipid accumulation, and fatty acid composition were investigated for the high quality biodiesel production from microalgae under mixotrophic culture mode. Moreover, we investigated the optimal disruption method for efficient lipid extraction from microalgal cells.

In addition, biomass and lipid productivity of each microalgae were investigated through various cultivation systems (such as, batch-, repeated-batch, and continuous culture systems). Also, the transesterification was optimized to investigate the FAME yield and productivity from microalgal biomass cultured in a photobioreactor (Chapter VI).

Collection @ chosun

조선대학교
CHOSUN UNIVERSITY

Chapter II

Comparison of biomass production and total lipid content of freshwater green microalgae cultivated under various culture conditions

This chapter is published in Bioprocess & Biosystems Engineering 37 (2) 99-106 (2014)

Collection @ chosun

조선대학교
CHOSUN UNIVERSITY

1. Introduction

Microalgae are a potential renewable fuel source because of their high lipid content, abundance and fast growth rate as compared to other plants. Cost-effective biodiesel production from microalgae primarily depends on high biomass productivity, high lipid yields and efficient harvesting. Thus, there has been extensive research and development focused on photoautotrophic, heterotrophic and mixotrophic culture conditions to increase microalgae biomass production and total lipid content [Cho et al., 2007; Li et al., 2007; Liang et al., 2009; Mata et al., 2010; Mandal and Mallick, 2009; Miao and Wu, 2006; Xu et al., 2006; Yoo et al., 2010]. During photoautotrophic growth, microalgae harvest energy from sunlight and assimilate atmospheric CO_2. However, photoautotrophic growth is slow, costly, and results in low biomass production. The major limitations associated with photoautotrophic cultivation can be overcome by heterotrophic cultivation of microalgae using organic carbon sources. Heterotrophic growth uses sugars and organic acids to replace traditional light energy [Huang et al., 2010]. Glucose [Liang et al., 2009; Hongjin and Guangce, 2009; Leesing and Nantaso, 2010; Wan et al., 2011], sodium acetate [Hongjin and Guangce, 2009; Ratledge et al., 2001] and sodium bicarbonate [Yeh et al., 2010] are common carbon sources used for heterotrophic cultivation of microalgae. This mode of growth offers several advantages, including the elimination of light, good control of cultivation, high biomass production and high lipid content in cells [Mio and wu, 2006; Lee and Lee, 2002]. Conversely, mixotrophic cultivation uses light as the main energy source, although both organic carbon and inorganic carbon (CO_2) are simultaneously assimilated. Thus, mixotrophic cultivation is a good strategy to obtain a large biomass with high lipid content [Lee and Lee, 2002]. Mixotrophic cultivation offers the additional benefit that CO_2 released by the microalgae via metabolic processes can be trapped and reused for phototrophic cultivation [Mata et al., 2010].

Collection @ chosun

조선대학교
CHOSUN UNIVERSITY

A number of environmental factors such as salinity, nitrogen, iron and light intensity are also known to strongly influence microalgal growth and lipid content. Most research on microalgae has focused on the selection of cultivation conditions that lead to the highest lipid yield in the shortest time [Doan et al., 2011; Yeesang and Cheirsilp, 2011]. However, few studies have systematically compared biomass production and total lipid content in microalgae cultivated under various conditions.

In the present study, we compared the microalgal growth and total lipid content of four green microalgal species (*Chlorella* sp., *C. vulgaris* CCAP211/11B, *B. braunii* FC124 and *S. obliquus* R8) under autotrophic, heterotrophic and mixotrophic conditions. The influence of six carbon sources, different glucose concentrations and light irradiation on cell growth and total lipid content was also investigated.

Collection @ chosun

조선대학교
CHOSUN UNIVERSITY

2. Materials and methods

2-1. Microalgae and growth medium

Four green microalgal species were studied: *Chlorella* sp. (obtained from Prof. Eon Seon Jin of Hanyang University, Seoul, Korea), *C. vulgaris* CCAP211/11B (obtained from the Culture Collection of Algae and Protozoa, Argyll, UK), *S. obliquus* R8 (obtained from Dr. Yang Hetong of the Biotechnology Center, Shandong Academy of Science, PR China), and *B. braunii* FC124 (obtained from the Korea Marine Microalgae Culture Center, Busan, Korea).

The media used in this study were TAP (Tris-Acetate-Phosphate) medium [Harris, 1989] for *Chlorella* sp., BG11 (Blue-Green) medium [Stanier et al., 1971] for *C. vulgaris* CCAP211/11B, Bold's Basal medium [Bold, 1949] for *S. obliquus* R8, and Chu 13 medium [Chu, 1942] for *B. braunii* FC124. TAP medium contained the following (per liter, pH 7.0): 0.8 g NH_4Cl, 0.1 g $CaCl_2 \cdot 2H_2O$, 0.2 g $MgSO_4 \cdot 7H_2O$, 0.3 g K_2HPO_4, 0.05 g EDTA$\cdot 2H_2O$, 5 mg $FeSO_4 \cdot 7H_2O$, 22 mg $ZnSO_4 \cdot 7H_2O$, 5.2 mg H_3BO_3, 5.1 mg $MnCl_2 \cdot 4H_2O$, 1.1 mg $CuCl_2 \cdot 2H_2O$, 2.6 mg $Na_2MoO \cdot 2H_2O$, 1.6 mg $CoCl_2 \cdot 6H_2O$. BG11 medium contained the following (per liter, pH 7.1): 1.5 g $NaNO_3$, 0.04 g K_2HPO_4, 7.5 mg $MgSO_4 \cdot 7H_2O$, 36 mg $CaCl_2 \cdot 2H_2O$, 6 mg citric acid, 6 mg ammonium ferric citrate green, 1 mg Na_2EDTA, 0.02 g Na_2CO_3, 2.9 mg H_3BO_3, 1.8 mg $MnCl_2 \cdot 4H_2O$, 0.22 mg $ZnSO_4 \cdot 7H_2O$, 0.39 mg $Na_2MoO \cdot 2H_2O$, 0.08 mg $CuSO_4 \cdot 5H_2O$, 0.05 mg $Co(NO_3)_2 \cdot 2H_2O$. Bold's Basal medium contained the following (per liter, pH 6.8): 0.175 g KH_2PO_4, 0.025 g $CaCl_2 \cdot 2H_2O$, 7.5 mg $MgSO_4 \cdot 7H_2O$, 0.255 g $NaNO_3$, 0.075 g K_2HPO_4, 0.025 g NaCl, 0.01 g Na_2EDTA, 6.2 mg KOH, 5.0 mg $FeSO_4 \cdot 7H_2O$, 10 μL H_2SO_4, 10.9 mg H_3BO_3, 1.8 mg $MnCl_2 \cdot 4H_2O$, 0.2 mg $ZnSO_4 \cdot 7H_2O$, 0.4 mg $Na_2MoO \cdot 2H_2O$, 0.079 mg $CuSO_4 \cdot 5H_2O$, 0.05 mg $Co(NO_3)_2 \cdot 6H_2O$. Chu13 medium contained the following (per liter, pH 7.5): 0.4 g

Collection @ chosun

조선대학교
CHOSUN UNIVERSITY

KNO_3, 0.08 g K_2HPO_4, 0.107 g $CaCl_2 \cdot 2H_2O$, 0.2 g $MgSO_4 \cdot 7H_2O$, 0.02 g ferric citrate, 0.1 g citric acid, 0.02 mg $CoCl_2$, 5.7 mg H_3BO_3, 3.6 mg $MnCl_2 \cdot 4H_2O$, 0.4 mg $ZnSO_4 \cdot 7H_2O$, 0.16 g $CuSO_4 \cdot 5H_2O$, 0.084 mg Na_2MoO, 1 drop of 0.072 N-H_2SO_4.

2-2. Pre-cultivation condition

Each microalga was pre-cultured in a 500 mL Erlenmeyer flask containing modified medium with the pH adjusted to 6.8-7.5 at 25-27 ℃. The light intensity and illumination period (light:dark) provided for each microalga were the following: 100 μmol photon/m^2/s and 12:12 h (Light:dark cycle) for *Chlorella* sp.; 80 μmol photon/m^2/s and 12:12 h (Light: dark cycle) for *C. vulgaris* CCAP211/11B and *S. obliquus* R8; and 100 μmol photon/m^2/s and 16:8 h (Light:Dark cycle) for *B. braunii* FC124. The cultivation periods for each microalgal species were 12, 15, 20, and 30 days for *Chlorella* sp., *C. vulgaris* CCAP211/11B, *S. obliquus* R8, and *B. braunii* FC124, respectively.

2-3. Culture conditions

Photoautotrophic cultivation of the above four microalgae was performed under the same pre-cultivation conditions in 2 L Erlenmeyer flasks. The effects of various organic carbon sources such as glucose, xylose, rhamnose, fructose, sucrose, and galactose on heterotrophic cultivation (without light irradiation) of the four microalgae were studied. The initial concentration of each carbon source was 0.01 M. In addition, the influence of glucose concentration (0.2-2.0%, w/v) on microalgal growth under heterotrophic cultivation was determined. In the mixotrophic culture conditions, the start-up cultivation was the same as the photoautotrophic culture condition, with the exception of the initial glucose concentration (1%, w/v) for *Chlorella* sp., *C. vulgaris* CCAP211/11B, and *B. braunii*

Collection @ chosun

조선대학교
CHOSUN UNIVERSITY

FC124 and 2% (w/v) for *S. obliquus* R8). To study the effect of light intensity on microalgal growth and total lipid content, light intensities of 0, 15, 35, 80, 100, and 150 μmol photon/m^2/s were provided by a fluorescence lamp. Under mixotrophic conditions, *Chlorella* sp., *C. vulgaris* CCAP211/11B, *S. obliquus* R8, and *B. braunii* FC124 were cultivated for 11, 15, 12, and 20 days, respectively.

Collection @ chosun

조선대학교
CHOSUN UNIVERSITY

2-4. Estimation of biomass production

To estimate the dry weight of the microalgae, 100 mL of stationary microalgal cultures were centrifuged at 5000 x *g* for 30 min. The resulting pellets were washed three times with 0.9% (w/v) NaCl. After washing, the pellet fraction was filtered through a 0.8 μm glass membrane (Pall, USA), dried at 105 ℃ for 8 h in an electric oven (Advantec FUW243PA, Japan) and then weighed using an electronic balance.

2-5. Estimation of total lipid content

The cultured microalgal cells were harvested by centrifugation at 5000 x *g* for 30 min. The resulting cell pellet was frozen overnight at -30 ℃ and freeze-dried at -50 ℃ under vacuum. One gram of the dry cell biomass was blended with 200 mL of distilled water and the biomass mixture was disrupted by autoclaving at 121 ℃ with 0.2 MPa for 60 min. Analysis of the total lipid content from the microalgal biomass was performed according to the modified procedure described by Folch et al. [1957]. Briefly, the total lipid content was extracted with a mixture of chloroform-methanol (2:1, v/v) for 1 h and then separated into chloroform and aqueous methanol layers overnight. The chloroform layer was washed with distilled water and evaporated using a rotary vacuum evaporator (Rotavapor R-205; Buchi, Switzerland). All experiments were performed in triplicate and reported as average values with standard deviations.

Collection @ chosun

조선대학교
CHOSUN UNIVERSITY

3. Results and discussion

3-1. Effect of organic carbon sources on biomass production

The effect of different carbon sources on biomass production for the four microalgae grown under heterotrophic culture conditions is shown in Fig. 2-1. Six carbon sources (glucose, xylose, rhamnose, fructose, sucrose, and galactose) were used in these experiments. When the initial concentration of each carbon source was 0.01 M, significant biomass growth variations were observed for all four microalgal species. Among the various carbon sources, glucose was the most effective carbon source for microalgal growth, especially for *B. braunii* FC124 and *S. obliquus* R8, whereas the other carbon sources did not significantly stimulate biomass production.

This occurred because glucose is a simple hexose monosaccharide, which is first catabolised into glucose-6-phosphate (an important intermediate product for various metabolic precursors) and subsequently converted to pyruvate through anaerobic glycolysis, before entering into the mitochondrial TCA cycle where it is oxidatively phosphorylated for ATP production [Neilson and Lewin, 1974]. Other carbon sources require more complicated inter-conversion metabolic processes to provide energy for algal growth and lipid production. Although glucose and fructose have the same number of carbon atoms, fructose cannot be directly converted into glucose-6-phosphate in microalgae. The lowest biomass production was observed with sucrose supplementation because sucrose is a non-reducing disaccharide molecule consisting of equimolar amounts of glucose and fructose that must be hydrolyzed prior to glycolysis. Overall, it was clear that differences in biomass production resulted from differences in the metabolic pathways used for carbon among the four microalgal species.

Collection @ chosun

조선대학교
CHOSUN UNIVERSITY

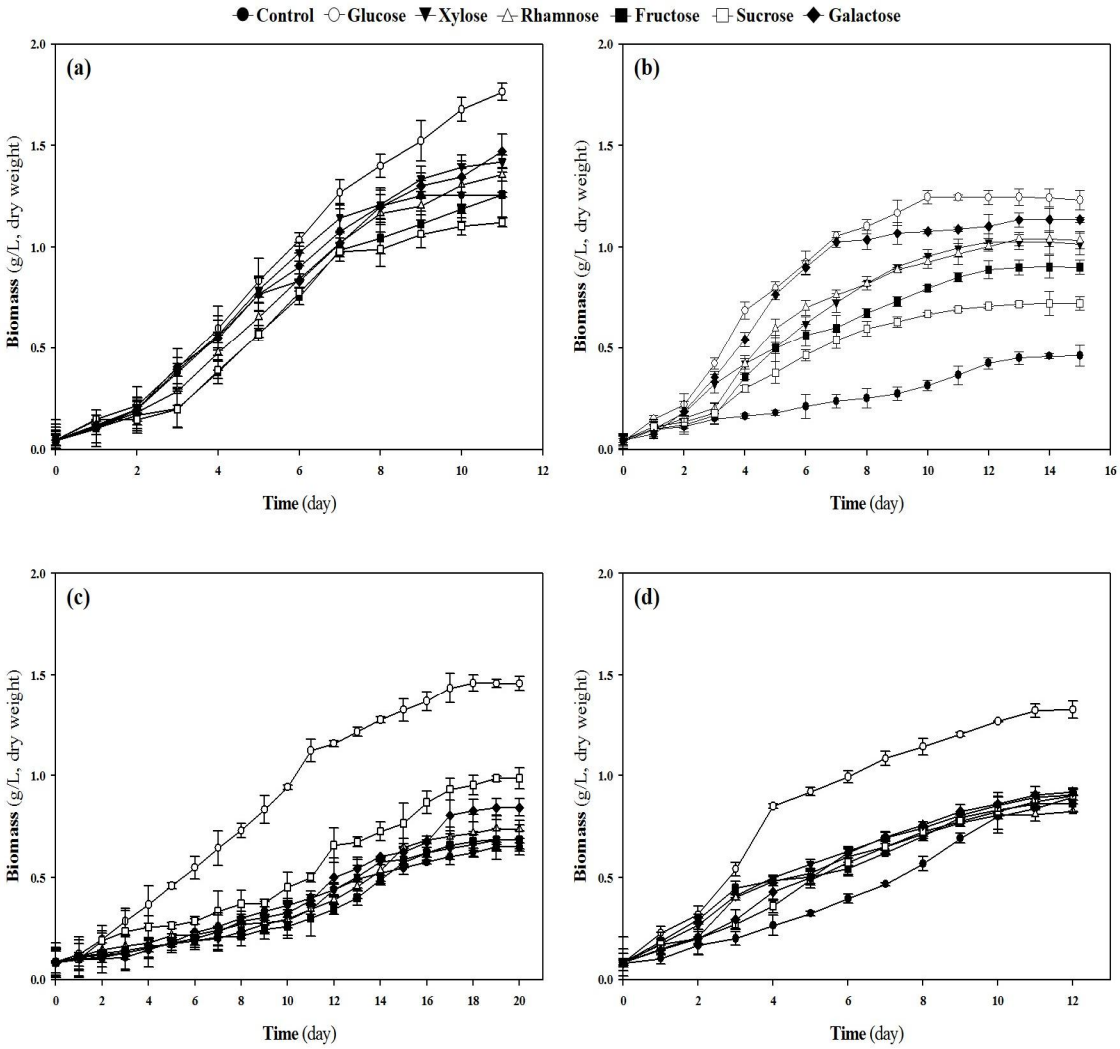

Fig. 2-1. Effect of various carbon sources (0.01 M) on biomass production on (a) *Chlorella* sp., (b) *C. vulgaris* CCAP211/11B, *B. braunii* FC124, and (d) *S. obliquus* R8, under heterotrophic cultivation.

Collection @ chosun

조선대학교
CHOSUN UNIVERSITY

3-2. Effect of glucose concentration on microalgal biomass

The effect of glucose concentration (0.2-2.0%, w/v) on microalgal biomass was monitored for the four microalgal species under heterotrophic cultivation conditions (Fig. 2-2). Generally, the biomasses of the four green microalgal species increased in proportion to glucose concentration. Among the cultures supplemented with glucose, the highest biomass production was achieved at a concentration of 1.0% (w/v) glucose, with higher concentrations severely inhibiting growth. Supplementation with 2.0% (w/v) glucose resulted in a 30-40% decrease in biomass production for most microalgae, because of substrate inhibition of growth; however, *S. obliquus* R8 exhibited a strong tolerance for high glucose concentrations (2.0%, w/v).

The results obtained in these studies are in accordance with previous reports. The concentration of glucose had a marked effect on the biomass yield. For example, *Chlorella protothecoides* and *Chlorella saccharophila* have been reported to grow heterotrophically by using organic compounds as carbon sources and produce higher biomass yields [Shi et al., 1999; Hosoglu et al., 2012]. Furthermore, Tan and Johns [1991] and Hongjin and Guangce [2009] reported that microalgal growth is strongly inhibited at high carbon concentrations.

Collection @ chosun

조선대학교
CHOSUN UNIVERSITY

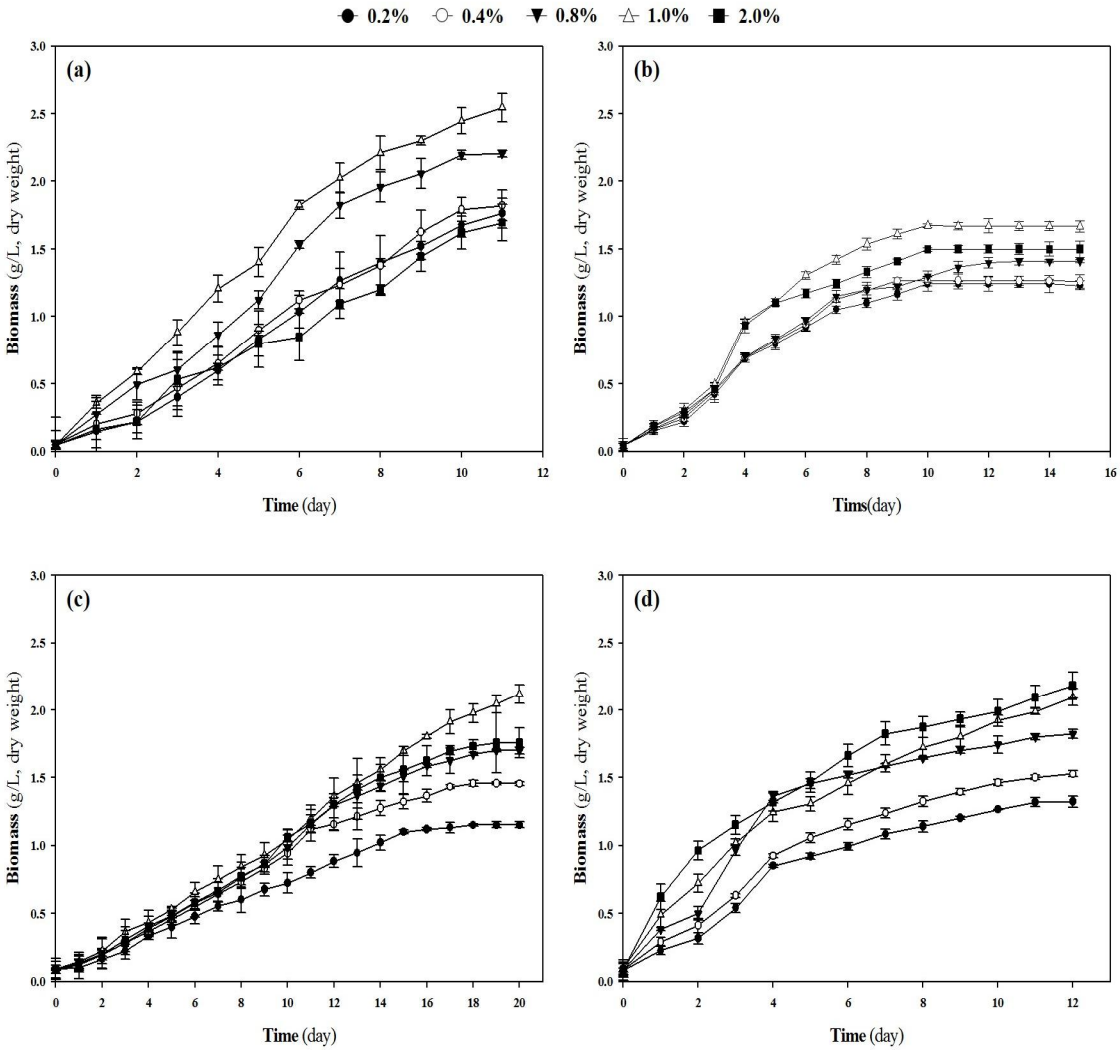

Fig. 2-2. Influence of glucose concentration on biomass production under heterotrophic cultivation of (a) *Chlorella* sp., (b) *C. vulgaris* CCAP211/11B, *B. braunii* FC124, and (d) *S. obliquus* R8, under heterotrophic cultivation.

Collection @ chosun

조선대학교
CHOSUN UNIVERSITY

3-3. Comparison of biomass and total lipid content under different culture conditions

Microalgal growth and total lipid content for all four microalgae under photoautotrophic, heterotrophic and mixotrophic cultivation were compared (Fig. 2-3). In this study, 1.0% (w/v) glucose was used in both the heterotrophic and mixotrophic (with light) conditions. The maximum biomass production under photoautotrophic, heterotrophic and mixotrophic culture conditions were as follows: 1.3, 2.5, and 2.7 g/L for *Chlorella* sp.; 0.5, 1.7, and 1.8 g/L for *C. vulgaris* CCAP211/11B; 1.1, 2.2, and 2.3 g/L for *S. obliquus* R8; and 0.6, 2.1, and 2.4 g/L for *B. braunii* FC124 (Fig. 2-3a). Biomass production under autotrophic culture conditions was significantly lower than heterotrophic and mixotrophic culture conditions. There are two primary reasons why these variations occurred: first, the microalgal cells transferred low amounts of light energy into ATP production [Yang et al., 2000]; and second, some of ATP produced during photochemical reactions was not utilized for anabolic processes [Yokota et al., 1989]. Due to the absence of light under heterotrophic culture conditions, the organic carbon source (glucose) was directly used for cell metabolism. Moreover, the growth of all four microalgal species was better under the mixotrophic conditions listed as follows: 100 μmol photon/m^2/s, 1% (w/v) glucose and 11 days incubation for *Chlorella* sp.; 100 μmol photon/m^2/s, 2% (w/v) glucose and 12 days incubation for *S. obliquus* R8; 80 μmol photon/m^2/s, 1% (w/v) glucose and 15 days incubation for *C. vulgaris* CCAP211/11B; and 80 μmol photon/m^2/s, 1% (w/v) glucose and 20 days incubation for *B. braunii* FC124. These results are in accordance with Liang et al. [2009] and Arroyo et al. [2011] who stated that mixotrophic cultivation produces higher biomass than heterotrophic and photoautotrophic cultivation. This phenomenon occurs because glucose and light energy can be metabolized to produce ATP and NAD(P)H production, thereby accelerating cell growth [Yang et al., 2000].

Collection @ chosun

조선대학교
CHOSUN UNIVERSITY

Total lipid contents of the four microalgal species under different growth modes were compared and are presented in Fig. 2-3b. Total lipid content was highest for mixotrophic cultivation and lowest for heterotrophic cultivation. Lipid production under heterotrophic condition decreased when compared with autotrophic and mixotrophic culture conditions: 21 and 49% (w/w) in *Chlorella* sp.; 23 and 40% (w/w) in *C. vulgaris* CCAP211/11B; 38 and 51% (w/w) for *S. obliquus* R8; and 41 and 55% (w/w) for *B. braunii* FC124. Based on the above experimental results, it was revealed that mixotrophic cultivation of the four microalgal species stimulated both biomass and total lipid production better than heterotrophic cultivation. As shown in Fig. 2-3a, lower lipid content was obtained in heterotrophic systems because most of the organic carbon was completely utilized for algal growth. In mixotrophic culture conditions, however, simultaneous assimilation of glucose (carbon source) and CO_2 took place in the algal cells. In the presence of light energy and glucose, most of the metabolizing enzyme spresent in the algal cells were more active. In particular, the activity of fatty acid synthesizing enzymes such as acetyl-CoA carboxylase, desaturatase, acyl-carrier protein synthase, and ATP: citrate lyase increased, resulting in an increase in the accumulation of lipids in the algal cells [Arroyo et al., 2011].

Collection @ chosun

조선대학교
CHOSUN UNIVERSITY

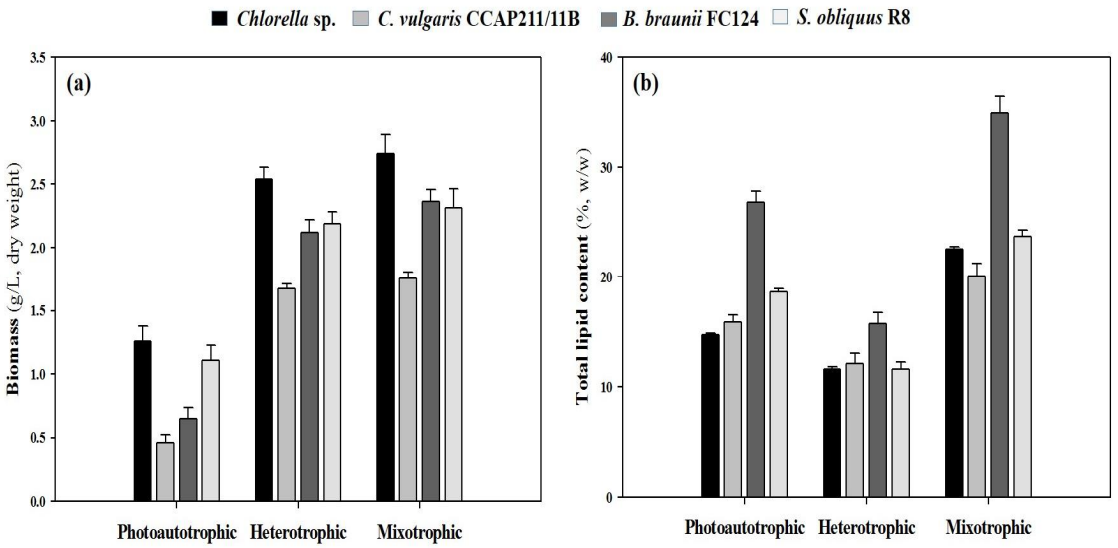

Fig. 2-3. Comparison of (a) biomass production and (b) total lipid content of four green microalgae under photoautotrophic, heterotrophic, and mixotrophic culture conditions.

3-4. Effect of light intensity on biomass and lipid production

Microalgal acclimatization can occur due to variations in environmental factors such as light intensity. When microalgae are cultured with carbon dioxide as a sole carbon source, cell growth, biochemical composition (structural and storage molecules) and lipid accumulation depend on the availability of light [Khotimchenko and Yakovleva, 2005]. Fig. 2-4 shows the effect of light intensity on biomass growth and total lipid content of the four microalgal species, which were cultured under mixotropic culture conditions. In our study, as light intensity increased from 0 to 150 μmol photon/m^2/s, no significant difference in biomass growth was found in *Chlorella* sp. and *C. vulgaris* CCAP211/11B. However, *B. braunii* FC124 showed higher biomass content (2.6 g/L) at 80 μmol photon/m^2/s of light irradiation, with higher light intensities inhibiting cell growth. Conversely, *S. obliquus* R8 growth increased with increasing light intensity.

Total lipid content in these four species increased in proportional to light intensity. *B. braunii* FC124 was found to be the highest lipid producing microalga (39.4%,

Collection @ chosun

조선대학교
CHOSUN UNIVERSITY

w/w) compared with the other species. These results are in good agreement with that of Tansakul et al. [2005]. According to the literature, light intensity has a profound impact on lipid accumulation; more specifically, higher light irradiance is favoured for lipid production rather than biomass growth. When microalgae are exposed to large quantities of light energy, metabolic flux generated from photosynthesis is directed to lipid accumulation [Tansakul el al. 2005] as free fatty acid synthesis is up regulated in chloroplasts [Sauer and Heise, 1984].

Furthermore, low light intensities may cause higher chlorophyll *a* (Chl *a*) content in cells [Guihéneuf et al., 2009]. Under low light conditions, the microalgal cells increase their photosynthetic pigments, such as Chl *a*, and antenna pigments to maximize their ability to harvest light for their normal growth requirements [Mock and Kroon, 2002]. In addition, the algal cells have a relatively large volume of chloroplasts, a high surface density of thylakoid membrane and a small volume of lipid storage bodies [Sukenik et al., 1989]. In contrast, at higher light intensities, the dimensions of microalgal light harvesting antenna pigments and Chl *a* content decreases and thylakoid membranes work more efficiently for lipid accumulation [Rammus, 1990].

Collection @ chosun

조선대학교
CHOSUN UNIVERSITY

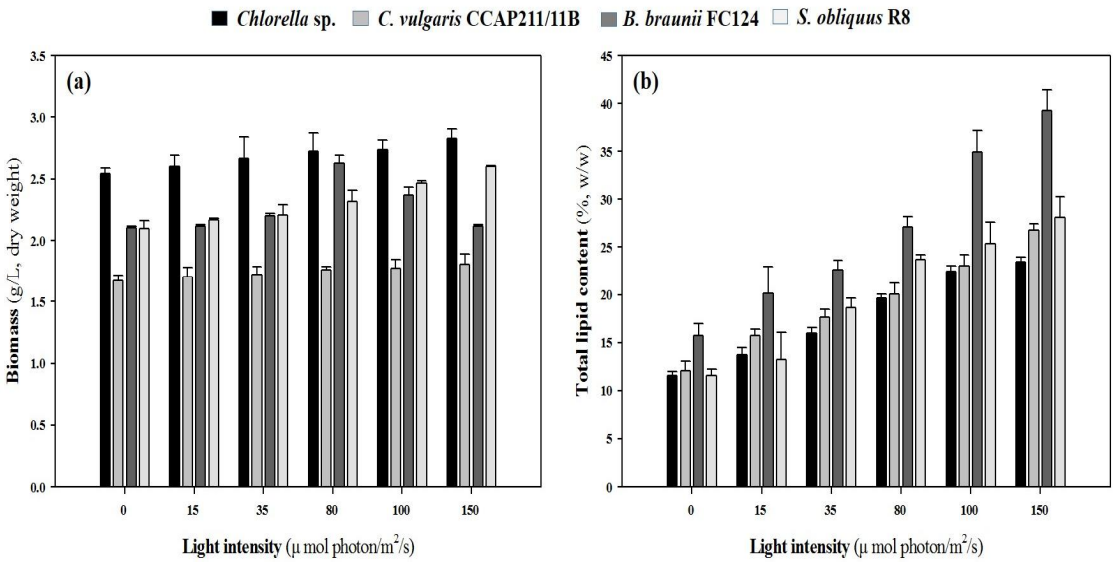

Fig. 2-4. Effect of light intensity on (a) biomass production and (b) total lipid content of four microalgae grown under mixotrophic condition.

Table 2-1 shows the biomass production and total lipid content for various microalgal species cultivated under different culture conditions. From this comparative analysis, it is evident that all four green microalgal species show relatively high total lipid content. Among them, *B. braunii* FC124 was found to be the best lipid producing microalgae under mixotrophic culture conditions (80 μmol photon/m^2/s, 1% glucose, and 20 days). Our study firmly proves that higher lipid production is obtained at lower light intensities (80 or 100 μmol photon/m^2/s). It is known that light intensity also influences the fatty acid composition of cells including triglyceric acid, glycolipids, phospholipids, and poly-unsaturated fatty acids. In the near future, the effect of light intensity on microalgal fatty acid composition profile during mixotrophic cultivation should be investigated.

Collection @ chosun

조선대학교 CHOSUN UNIVERSITY

Table 2-1. Comparison of biomass production and total lipid content of four green microalgae with related microalgae

Microalgae	Culture condition	Carbon sources	Light intensity (μmol photon/m^2/s)	Biomass production (g/L)	Total lipid contents (%, w/w)	Ref.
S. obliquus AS-6-1	Photobioreactor	CO_2	140	1.6	11.7	Ho et al., 2012
S. obliquus CNW-1	Photobioreactor	CO_2	140	1.4	9.2	Ho et al., 2012
S. obliquus ESP-5	Photobioreactor	CO_2	140	1.9	8.3	Ho et al., 2012
S. obliquus	Photobioreactor	12% CO_2	43.2	2.1	-	Morais et al., 2007
S. obliquus R8	Mixotrophic/Batch	2% glucose	100	2.3	23.7	in this study
Nannochloropsis sp.	Batch	CO_2	700	0.6	21.0	Pal et al., 2011
Dunaliella viridis	Batch	1% CO_2	1500	~0.6	31.8	Gordillo et al., 1998
D. salina DCCBC2	Photobioreactor	3% CO_2	100	3.2	-	Kim et al., 2012
C. protothecoides	Heterotrophic/Batch	Glucose	-	15.3	7.7	Chen and Walker, 2011
C. protothecoides	Heterotrophic/Batch	Pure glucose	-	19.2	9.8	Chen and Walker, 2011
C. protothecoides	Heterotrophic/Batch	Crude glucose	-	23.5	14.6	Chen and Walker, 2011
C. vulgaris LEB-104	Batch	5% CO_2	47.3	1.9	10.0	Sydney et al., 2010
C. vulgaris CCAP211/11B	Mixotrophic/Batch	1% glucose	80	1.8	20.1	in this study
Chlorella sp.	Mixotrophic/Batch	1% glucose	100	2.7	22.5	in this study
B. braunii SAG-3081	Batch	5% CO_2	47.3	3.1	33.0	Sydney et al., 2010
B. braunii FC124	Mixotrophic/Batch	1% glucose	80	2.4	34.9	in this study

Collection @ chosun

조선대학교
CHOSUN UNIVERSITY

Chapter III

Effect of carbon source and light intensity on the growth and total lipid production of three microalgae under different culture conditions

This chapter is published in Journal of Industrial Microbiology & Biotechnology 37 (2) 99-106 (2014)

Collection @ chosun

조선대학교
CHOSUN UNIVERSITY

1. Introduction

In recent years, many researchers have increased efforts to find a better alternative renewable fuel because of depletion of fossil fuels. Microalgae promise to be a suitable energy resource through the photoautotrophic mechanism that can convert atmospheric carbon dioxide into biomass, fatty acid, and lipids. The total lipid content of microalgae varies from 1 to 70% of the dry cell weight [Li et al., 2008; Spolaore et al., 2006; Xin et al., 2010]. The lipids present in microalgae are mainly in the form of esters of glycerol and fatty acids, which are suitable for producing biodiesel. Microalgae such as *Scenedesmus pectinatus* var XJ-1 [Xia et al., 2013], *Chlorella* sp. [Cheirsilp and Torpee, 2012], *Nannochloropsis* sp. [Cheirsilp and Torpee, 2012], and *Chlorella vulgaris* [Liang et al., 2009] generally are cultured photoautotrophically.

Unfortunately, the photoautotrophic cultivation of microalgae has many limitations, such as low biomass and lipid productivity, and this is mainly because of photolimitation (high cell density inhibits light penetration). Heterotrophic growth of microalgae can be performed in a culture medium supplemented with external organic/inorganic carbon sources. For heterotrophic microalgal cultivation, several carbon sources, such as glucose [Cerón-García et al., 2013, Gim et al., 2014; Ren et al., 2013], fructose [Gim et al., 2014; Ren et al., 2013], sucrose [Gim et al., 2014; Ren et al., 2013], glycerol [Cerón-García et al., 2013], and acetate [Vazhappilly and Chen, 1998], have been used. Heterotrophic cultivation offers many advantages, including good control of cultivation, higher biomass and lipid, and elimination of the requirement for light. However, mixotrophic growth that combines phototrophic and heterotrophic cultivation (i.e., with light and organic sources) is particularly useful for overcoming the problems imposed by phototrophic or heterotrophic growth [Gim et al., 2014]. One of the most notable advantages is that the CO_2 released from microalgae during carbon metabolism is trapped

Collection @ chosun

조선대학교
CHOSUN UNIVERSITY

and reused. Recently, many studies have focused on the enhanced biomass and lipid productivity achieved by mixotrophic cultures of microalgae such as *C. vulgaris* [Kong et al., 2013], *Scenedesmus* sp. ZTY3, and *Chlorella* sp. ZTY4 [Tian-Yuan et al., 2014].

Furthermore, it is known that many environmental factors influence the growth, lipid content, and fatty-acid composition of microalgae. Microalgal cultivation requires rigorous control of various factors, such as carbon sources, salinity, nitrogen, iron, pH, temperature, CO_2 concentration, and light intensity. It is most note worthy that carbon source, light-intensity and -wavelength have been reported to change the lipid metabolism in microalgae by enhancing the biomass production and lipid content, as shown for *Nannochloropsis* sp. [Das et al., 2011], *Haematococcus pluvialis* [Imamoglu et al., 2007], *Scenedesmus* sp. [Liu et al., 2012], and *C. vulgaris* ESP-31 [Yeh et al., 2010]. In addition, a number of nutritional factors, including phosphate [Gouveia and Olivira, 2009], sulfur [Sugimoto et al., 2008], iron [Liu et al., 2008], and nitrogen [Gouveia and Oliveria, 2009; Yeesang and Cheirsilp, 2011], have been reported to influence the growth and lipid content of algae. Nitrogen starvation especially affects the lipid accumulation in microalgal cells [Merzlyak et al., 2007]. However, to date, the studies on various modified and enhanced microalgal cultivation, lipid production, lipid extraction, and transesterification techniques are still in progress.

In this study, three microalgal species *I. galbana* LB987, *N. oculata* CCAP849/1, and *D. salina*, which have relatively higher biomass and lipid productivity, were cultivated under photoautotrophic, heterotrophic, and mixotrophic conditions to obtain higher biomass and total lipid content. Effects of various carbon sources and light intensity on growth, chlorophyll concentration, total lipid content, and fatty-acid composition under the different culture conditions were investigated.

Collection @ chosun

조선대학교
CHOSUN UNIVERSITY

2. Materials and methods

2-1. Microalgae and growth medium

Three marine microalgae, which accommodate high content of lipid in cells, were used in this study. *I. galbana* LB987 (obtained from UTEX Culture Collection of Algae at The University of Texas at Austin, Austin, TX, USA) and *N. oculata* CCAP849/1 (obtained from Culture Collection of Algae and Protozoa, UK) were cultured in f/2 medium [Guillard and Ryther, 1962], with the following composition (per liter of sea water): 75 mg $NaNO_3$, 5.65 mg $NaH_2PO_4 \cdot 2H_2O$, 4.16 mg Na_2·EDTA, 3.15 mg $FeCl_3 \cdot 6H_2O$, 0.01 mg $CuSO_4 \cdot 5H_2O$, 0.02 mg $ZnSO_4 \cdot 7H_2O$, 0.01 mg $CoCl_2 \cdot 6H_2O$, 0.18 mg $MnCl_2 \cdot 4H_2O$, 6 µg $Na_2MoO_4 \cdot 2H_2O$, 0.5 µg, cyanocobalamin (vitamin B_{12}), 0.1 mg thiamine-HCl (vitamin B_1), and 0.5 µg biotin. *D. salina* (a gift from Hanyang University, Seoul, Korea) was cultured in modified D medium [Castenholz, 1969], with the following composition (per liter of distilled water): 58.44 g NaCl, 4.84 g Tris, 0.51 g KNO_3, 0.92 g $MgCl_2 \cdot 6H_2O$, 0.12 g $MgSO_4 \cdot 7H_2O$, 0.04 g $CaCl_2$, 0.02 g K_2HPO_4, 0.55 mg $FeCl_3$, 2.45 mg EDTA, 0.31 mg H_3BO_3, 0.20 mg $MnCl_2 \cdot 4H_2O$, 0.02 mg $ZnSO_4 \cdot 5H_2O$, 0.01 mg $CuSO_4 \cdot 5H_2O$, 0.05 mg $NaMoO_4 \cdot 2H_2O$, 0.005 mg $CoCl_2 \cdot 6H_2O$, 0.03 mg $NaVO_3$, and 2.1 g $NaHCO_3$.

Collection @ chosun

조선대학교
CHOSUN UNIVERSITY

2-2. Microalgal culture conditions

Photoautotrophic batch cultivation of the three marine microalgae was performed in 1-L Erlenmeyer flasks containing a working volume of 0.3 L medium at pH 8.0 with cotton plugs that allow exchange with the atmosphere. Cells were cultivated at 25 °C. Cultures were illuminated with cool-white fluorescent lamps, which were fixed on the wall, and light intensity was attenuated by adjusting distance from lamps and was measured with an illuminance meter (LT Lutron LM-81LX; Lutron Electronic Enterprise, Co., Taipei, Taiwan). From our previous results of optimal growth conditions, light intensity was maintained at 80 μmol photon/m^2/s for *I. galbana* LB987 and *N. oculata* CCAP849/1 and at 100 μmol photon/m^2/s for *D. salina*, and the photoperiods were 12:12 h light/dark in all three microalgae. Their photoautotrophic cultivation period was 10 days.

To determine the optimal nitrogen concentration for maximal biomass and lipid productivity, each of *I. galbana* LB987 and *N. oculata* CCAP849/1 was cultivated in a modified f/2 medium containing different $NaNO_3$ concentrations ranging from 0.75 to 1.0 mM; *D. salina* was cultivated in a modified D medium containing various KNO_3 concentrations ranging from 1 to 10 mM.

For heterotrophic cultivation, the above two different culture media were supplemented with six different carbon sources: glucose, xylose, rhamnose, fructose, sucrose, and galactose (0.01 M). The influence of initial glucose concentration on microalgal growth was performed within arange of 0.01 to 0.05 M. Mixotrophic cultivation was evaluated with an initial glucose concentration of 0.02 M for *I. galbana* LB987 and *N. oculata* CCAP849/1 and 0.05 M for *D. salina*. The effect of light intensity on algal cell growth and total lipid content under mixotrophic cultivation was tested with different light intensities ranging from 0 to 200 μmol photon/m^2/s.

Collection @ chosun

조선대학교
CHOSUN UNIVERSITY

2-3. Determination of biomass production

Dry biomass was determined with 100 mL of microalgal culture, which was collected and filtered through a 0.8 μm glass membrane (Pall Corporation, Port Washington, NY, USA). The filtrate was dried at 105 °C for 8 h in an electric oven (Advantec FUW243PA; Advantec, Ehime, Japan) and then weighed by using an electronic balance (Ohaus Explorer EX623; Ohaus Corporation, Newark, NJ). All of the experiments were conducted in triplicate.

2-4. Measurement of reducing sugar concentration

Reducing sugar was quantitatively analyzed by DNS (3,5-dinitrosalicylic acid) assay method suggested by Miller [1959]. DNS reagent was prepared as follows: 0.25 g of DNS and 75 g of sodium potassium tartrate were dissolved in 250 mL of 0.4 M sodium hydroxide solution. Glucose with different concentrations, from 1.0 to 10.0 mg/mL, was used to create the calibration curve. To analyze the residual glucose concentration in the microalgal medium according to the cell growth, 500 μL of each medium sample was mixed with 5.0 mL of DNS reagent and heated at 100 °C for 10 min to develop the red-brown color. 8 mL of distilled water was added into the samples when temperature dropped to the room temperature. Then the samples were detected by UV–visible spectrophotometer (DU800; Beckman Coulter, Brea, CA, USA) at 540 nm. All of the tests were conducted in triplicate.

Collection @ chosun

조선대학교
CHOSUN UNIVERSITY

2-5. Determination of chlorophyll content

Chlorophylls in fresh microalgal cells were extracted with acetone. The concentration of chlorophylls in the extracted solution was determined by measuring the absorbance at 645 and 663 nm with a UV–visible spectrophotometer (DU800; Beckman Coulter, Brea, CA, USA) and then calculating with the following equation [Becker, 1994]:

$$\text{Chlorophylls (mg/L)} = 8.02 \times A663 + 20.21 \times A645 \quad \text{(Eq. 1)}$$

The chlorophyll contents in the microalgal cells (mg/g) were calculated by dividing the concentration of the chlorophylls (mg/L) by the dry weight (g/L) of microalgae.

2-6. Estimation of total lipid content

Microalgal cells were harvested by centrifugation at 5000 × g for 30 min. The cell pellets were frozen overnight at -30 °C and freeze-dried at -50 °C under vacuum (FD 8508 Bench-Top freeze-dryer; Ilshin BioBase, Co. Ltd., Gyeonggi-do, South Korea). One gram of dried cell biomass was blended with 200 mL of distilled water, and the cell mixture was disrupted by a sonicator (Sonifier 250; Branson Ultrasonics, Danbury, CT, USA) at a resonance of 10 kHz for 5 min. Lipid extraction was performed according to the modified method described by Folch et al. [1957]. Total lipid was extracted with a mixture of chloroform–methanol (2:1, v/v) for 1 h. The chloroform layer was removed by evaporation with rotary vacuum (Rotavapor R-205; Buchi Labortechnik, Flawill, Switzerland) and weighed.

Collection @ chosun

조선대학교
CHOSUN UNIVERSITY

2-7. Analysis of fatty acid composition

The extracted lipid was used to analyze fatty acid composition by a modified saponification and methylation procedure described by Metcalfe and Schmitz [1966]. The composition of each microalgal strain was determined by gas chromatography (GC-2010 Plus; Shimadzu Corporation, Kyoto, Japan), with an art-2560 capillary column (length 100 m, 0.25 mm inner diameter, 0.25 μm film thickness) and a flame ionization detector. Operation conditions were as follows: inlet temperature 260 °C, initial oven temperature 140 °C held for 5 min and then ramped by 4 °C per min and held for 15 min, and the detector temperature 260 °C. Fatty acids were identified by a comparison of their retention times with known standards.

Collection @ chosun

조선대학교
CHOSUN UNIVERSITY

3. Results

3-1. Effect of nitrogen concentration on photoautotrophic growth and total lipid content

To examine the effect of nitrogen on the biomass and total lipid production of the three microalgae under photoautotrophic cultivation (light intensity was maintained at 80 μmol photon/m^2/s for *I. galbana* LB987 and *N. oculata* CCAP849/1, and at 100 μmol photon/m^2/s for *D. salina*), different concentrations of nitrogen were supplemented to the modified culture media. As shown in Fig. 3-1, a low nitrogen concentration did not support cell growth but stimulated total lipid accumulation in cells. As nitrogen concentration increased, biomass production increased. High amounts of biomass from *I. galbana* LB987 (0.58 g biomass per liter) and *N. oculata* CCAP849/1 (0.56 g/L) were obtained at a concentration of 0.95 mM $NaNO_3$, whereas a biomass of 0.62 g/L was obtained from *D. salina* at 7.5 mM KNO_3. In contrast to biomass production, total lipid content decreased significantly in all three strains by increasing nitrogen concentration. In particular, total lipid content decreased >35% (w/w) in *D. salina* as nitrogen concentration increased from 1.0 to 10.0 mM.

Collection @ chosun

조선대학교
CHOSUN UNIVERSITY

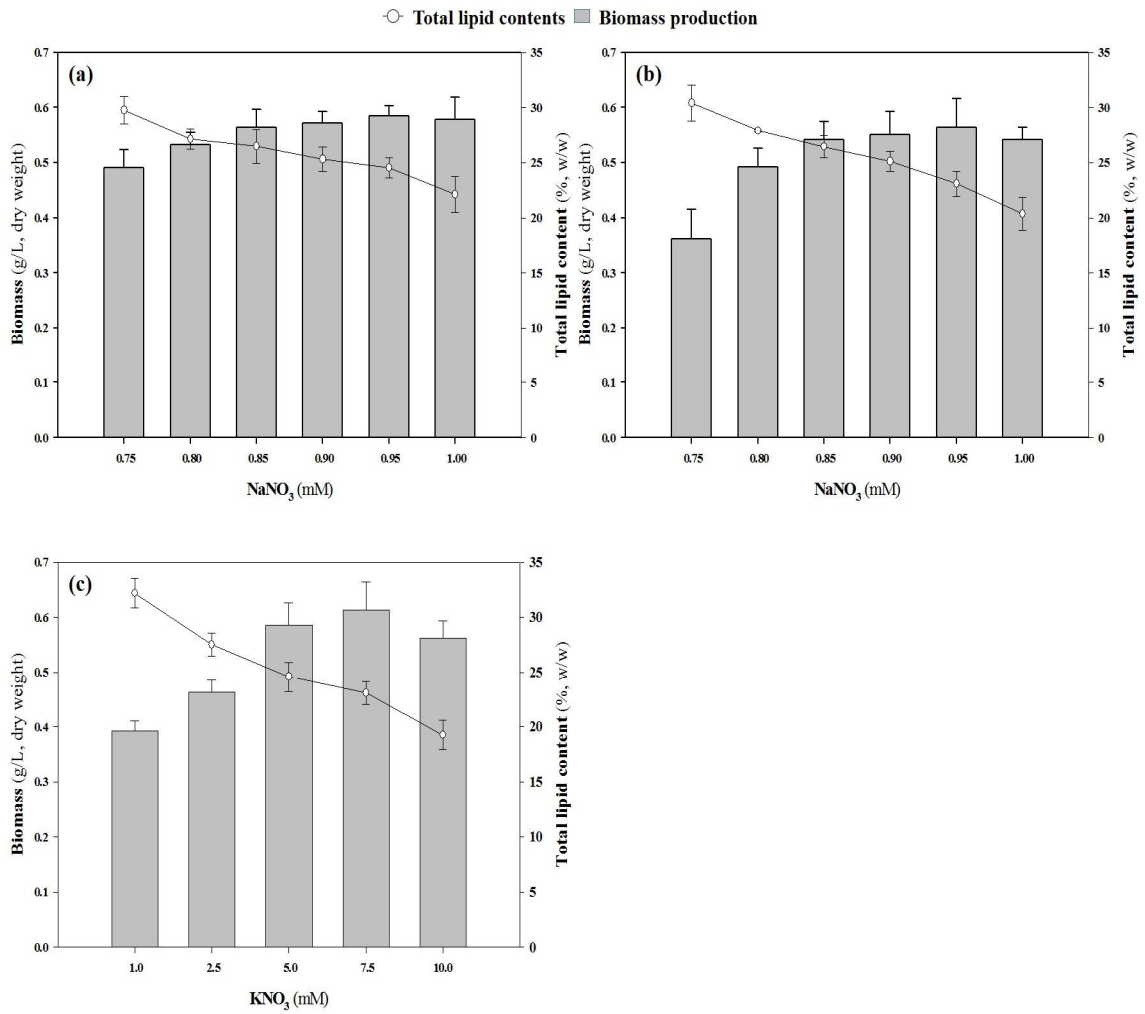

Fig. 3-1. Effect of nitrogen concentration on biomass and total lipid content under photoautotrophic condition: (a) *I. galbana* LB987; (b) *N. oculata* CCAP849/1; and (c) *D. salina*.

Collection @ chosun

조선대학교
CHOSUN UNIVERSITY

3-2. Effect of carbon source on heterotrophic growth

Fig. 3-2 shows the growth of the three microalgae under heterotrophic culture conditions with various carbon sources (0.01 M), such as glucose, galactose, fructose, xylose, rhamnose, and sucrose. The three microalgal species can use all of the carbon sources tested. However, among the carbon sources tested, glucose was the best, with maximal biomass of 0.75 g/L for *I. galbana* LB987, 1.40 g/L for *N. oculata* CCAP849/1, and 0.65 g/L for *D. salina*, respectively, during 10 days cultivation. Compared with photoautotrophic cultivation, heterotrophically cultured biomass increased remarkably; especially, that of *N. oculata* CCAP849/1 increased approximately three fold. On the other hand, poor biomass production was observed from *I. galban*a LB987 and *D. salina* when supplemented with sucrose and from *N. oculata* CCAP849/1 with galactose as the sole carbon source. It is obvious from the data shown in Fig. 3-2 that the total lipid contents in cells cultured in heterotrophic conditions were relatively low.

To learn about the effect of initial glucose concentration on cell growth, all three microalgae were cultured in different modified media supplemented with various glucose concentrations (0.01–0.05 M) for 10 days. The results are illustrated in Fig. 3-3. When 0.02 M glucose was supplemented, the highest amount of biomass was observed in *I. galban*a LB987 (0.79 g/L) and *N. oculata* CCAP849/1 (1.46 g/L). On the other hand, 0.90 g/L biomass was observed in *D. salina* with 0.05 M glucose. In addition, glucose consumption rates of three microalgae in different initial concentration were also determined as cells grew (Fig. 3-3). After 10 days incubation with 0.02 M glucose, the consumption rates of *I. galbana* LB987 and *N. oculata* CCAP849/1 were found to be 83.8 and 93.3%, respectively. In contrast, no more than 50% of glucose was utilized in higher concentrations (>0.04 M). Similarly, *D. salina* showed the highest consumption rate (97.3%) when grown on initial 0.05 M glucose concentration, but substrate inhibition was also happened at higher concentrations (data not shown). Moreover, the pH changes in the medium during cells growth were also monitored. Medium pH deceased from initial 8.0 to

Collection @ chosun

조선대학교
CHOSUN UNIVERSITY

final 6.8–7.2 for 10 days incubation in all three microalgae, but it did not inhibit cell growth significantly.

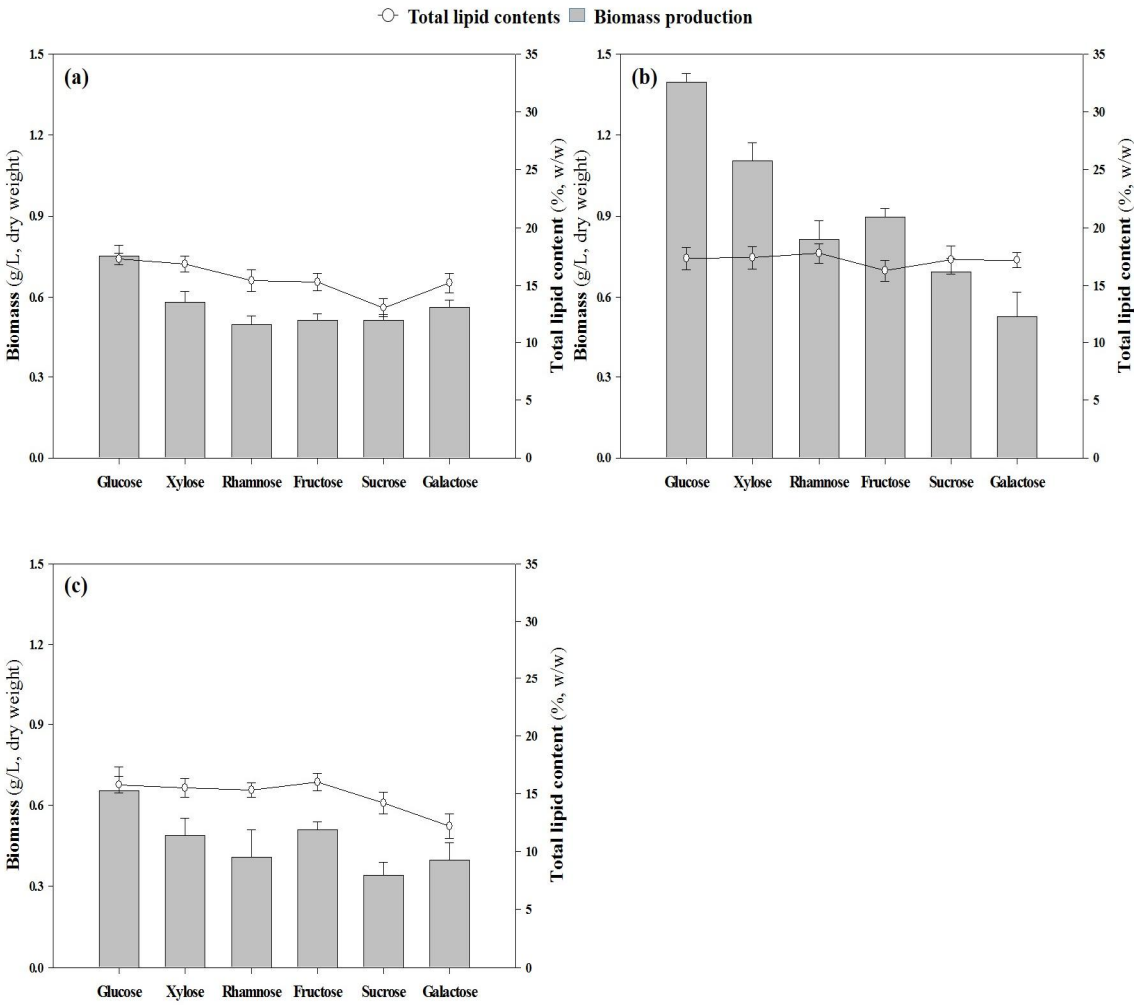

Fig. 3-2. Effect of six different carbon sources (0.01 M) on heterotrophic microalgal growth: (a) *I. galbana* LB987; (b) *N. oculata* CCAP849/1; and (c) *D. salina*.

Collection @ chosun

조선대학교
CHOSUN UNIVERSITY

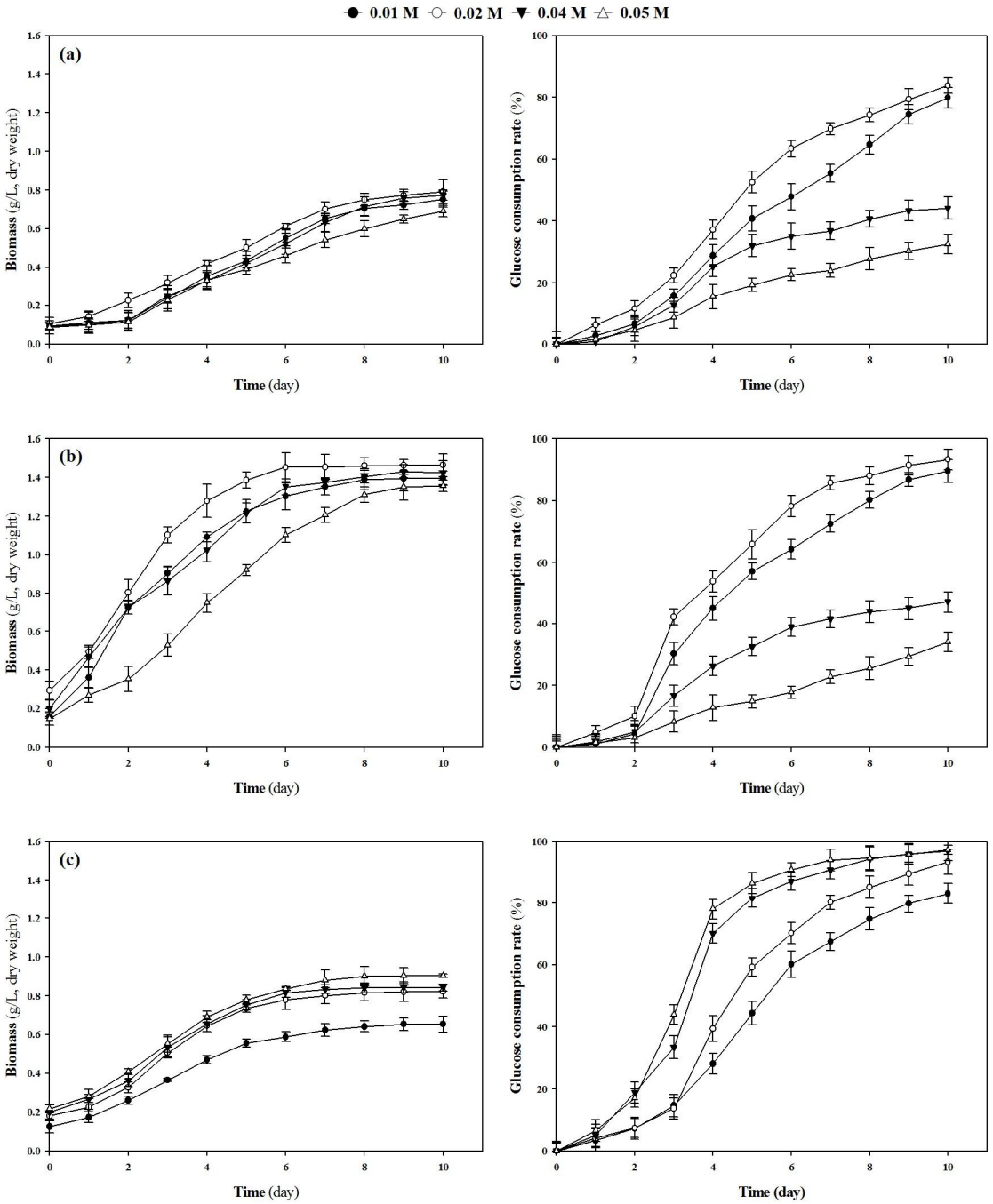

Fig. 3-3. Influence of glucose concentration (0.01-0.05 M) on microalgal growth under heterotrophic cultivation and glucose consumption rate according to cell growth: (a) *I. galbana* LB987; (b) *N. oculata* CCAP849/1; and (c) *D. salina*.

Collection @ chosun

조선대학교
CHOSUN UNIVERSITY

3-3. Biomass, total lipid, and chlorophyll content under different culture conditions

The effect of culture mode on biomass, chlorophyll, and total lipid content was investigated. For heterotrophic and mixotrophic cultivation, 0.02 M glucose for *I. galbana* LB987 and *N. oculata* CCAP849/1 and 0.05 M glucose for *D. salina* were supplemented to the media, and light intensity for mixotrophic conditions was the same as that for photoautotrophic conditions. As shown in Fig. 3-4, biomass production of all strains improved dramatically when they were grown under mixotrophic conditions. Biomass obtained under photoautotrophic, heterotrophic, and mixotrophic culture conditions were as follows: 0.56, 0.83, and 0.89 g/L for *I. galbana* LB987; 0.54, 1.46, and 1.69 g/L for *N. oculata* CCAP849/1; and 0.59, 0.90, and 1.16 g/L for *D. salina*, respectively.

As described above, microalgal cells grown under heterotrophic condition, which means dark conditions, maintained low-level chlorophyll and total lipid content. However, under mixotrophic conditions, light stimulated the production of chlorophyll and total lipid to the maximal level. Chlorophyll concentration in cells grown under photoautotrophic, heterotrophic, and mixotrophic cultivation were as follows: 32.3, 4.1, and 29.1 mg/g for *I. galbana* LB987; 41.9, 3.7, and 39.2 mg/g for *N. oculata* CCAP849/1; and 38.5, 2.6, and 35.2 mg/g for *D. salina*, respectively (Fig. 3-4). In addition, total lipid contents (%, w/w) in cells obtained from photoautotrophic, heterotrophic, and mixotrophic cultivation were as follows: 26.5, 17.4, and 30.1% (w/w) for *I. galbana* LB987; 26.5, 18.4, and 37.3% (w/w) for *N. oculata* CCAP849/1; and 24.6, 15.8, and 31.3% (w/w) for *D. salina,* respectively. The increase or decrease patterns for chlorophyll and total lipid production under different culture conditions were very similar.

It is known that light intensity directly influences microalgal cell growth and photosynthesis. Therefore, the effect of light intensity on biomass, total lipid, and chlorophyll concentrations was assessed under mixotrophic cultivation, with varying light

Collection @ chosun

조선대학교
CHOSUN UNIVERSITY

intensity ranging from 0 to 200 μmol photon/m^2/s and a constant photoperiod (12:12 h, light/dark cycle). It is noteworthy that light intensity did not have a significant impact on cell growth but stimulated chlorophyll synthesis and lipid production in cells remarkably (Fig. 3-5). Optimal range of light intensity for maximum total lipid production of all three strains was found to be from 80 to 150 μmol photon/m^2/s.

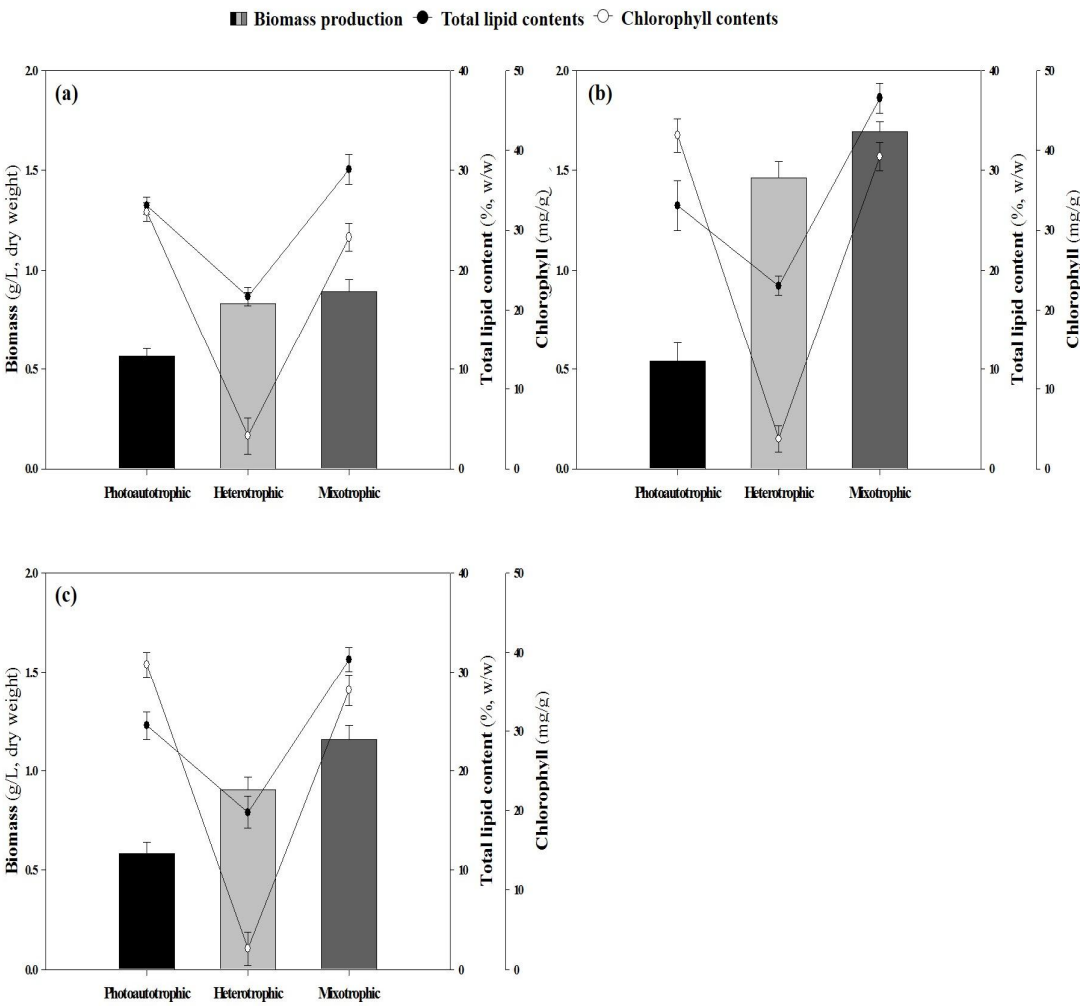

Fig. 3-4. Biomass, total lipid and chlorophyll content of three green microalgae grown photoautotrophic, heterotrophic, and mixotrophic culture conditions;: (a) *I. galbana* LB987; (b) *N. oculata* CCAP849/1; and (c) *D. salina*.

Collection @ chosun

조선대학교
CHOSUN UNIVERSITY

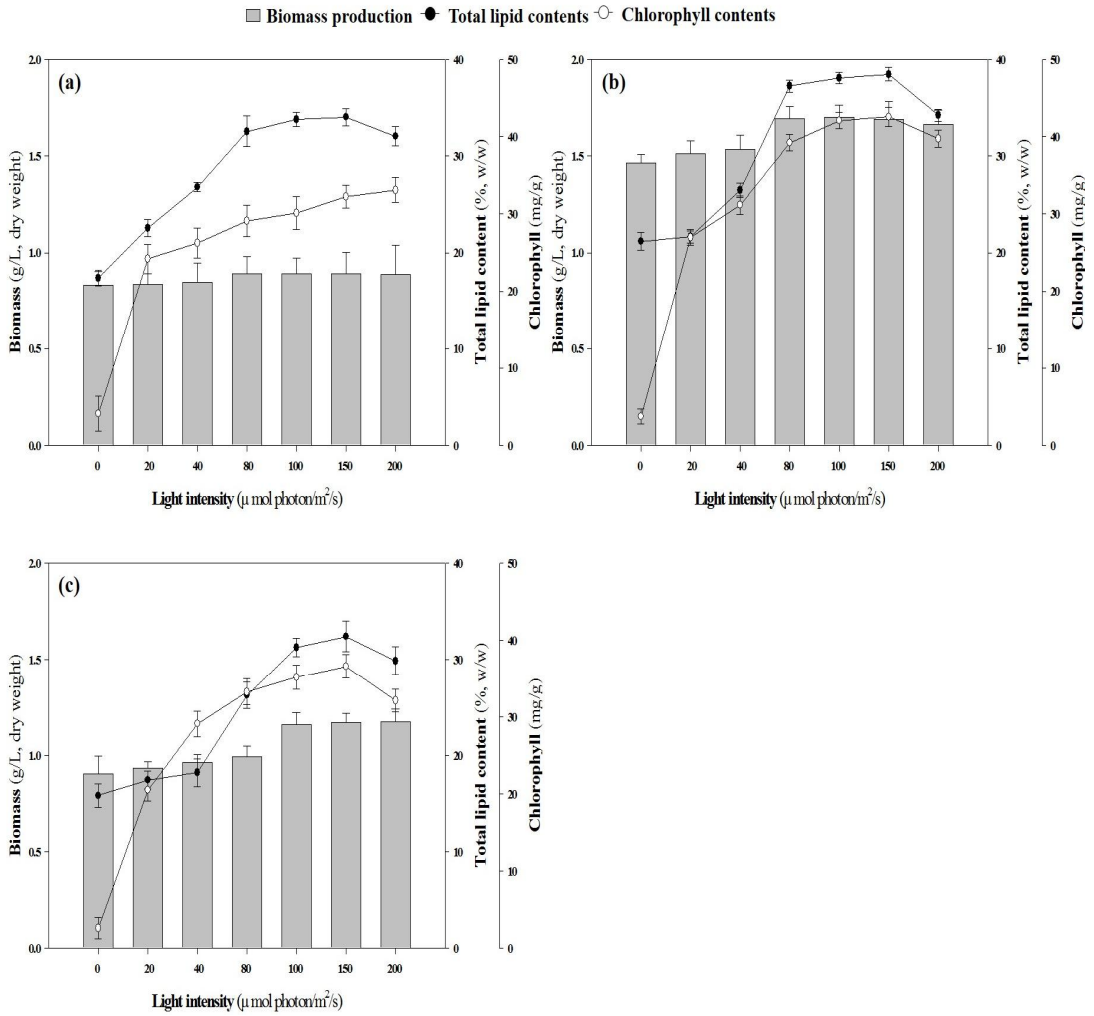

Fig. 3-5. Effect of light intensity on cell growth, total lipid content, and chlorophyll content under mixotrophic cultivation: (a) *I. galbana* LB987; (b) *N. oculata* CCAP849/1; and (c) *D. salina*.

Collection @ chosun

조선대학교
CHOSUN UNIVERSITY

3-4. Effect of light intensity on fatty acid composition

Effect of light intensity on total fatty acid concentration and composition of total lipid in all three strains was analyzed with different light intensities ranging from 0 to 200 μmol photon/m^2/s. Fatty acid composition was determined as palmitic acid (C16:0), palmitoleic acid (C16:1), stearic acid (C18:0), oleic acid (C18:1), linoleic acid (C18:2), and linolenic acid (C18:3) from extracted lipid to focus on the quality improvement of biodiesel. As light intensity increased up to 150 μmol photon/m^2/s, fatty acid concentrations in the three microalgae increased slightly (Fig. 3-6). *N. oculata* CCAP849/1 produced the highest amount of C16–C18 fatty acids among the three strains, 67.0 mg/mL with a light intensity of 150 μmol photon/m^2/s. Unlike *I. galbana* LB987 and *N. oculata* CCAP849/1, the concentration of C16–C18 fatty acids of *D. salina* increased remarkably according to the increase of light intensity up to 150 μmol photon/m^2/s, although its relative concentration level (approximately 20 mg/mL) was low. More than 40 mg/mL fatty acids were involved as forms of lignoceric acid (C24:0), docosahexaenoic acid (C22:6), and eicosapentaenoic acid (C20:5), in decreasing order.

Meanwhile, light intensity variations did not change C16–C18 fatty acids composition significantly in all three strains (Table 1). Regardless of light intensity, the major constituents of *I. galbana* LB987 were long-chain fatty acid of palmitic (C16:0) and oleic acid (C18:1), whereas those of *N. oculata* CCAP849/1 were palmitic (C16:0) and palmitoleic acid (C16:1). In the case of *D. salina*, linolenic (C18:3) and linoleic acids (C18:2) were found to be dominant in cells. It is noteworthy that all three strains contained a relatively low concentration of stearic acid (C18:0), a common fatty acid in microalgae.

Collection @ chosun

조선대학교
CHOSUN UNIVERSITY

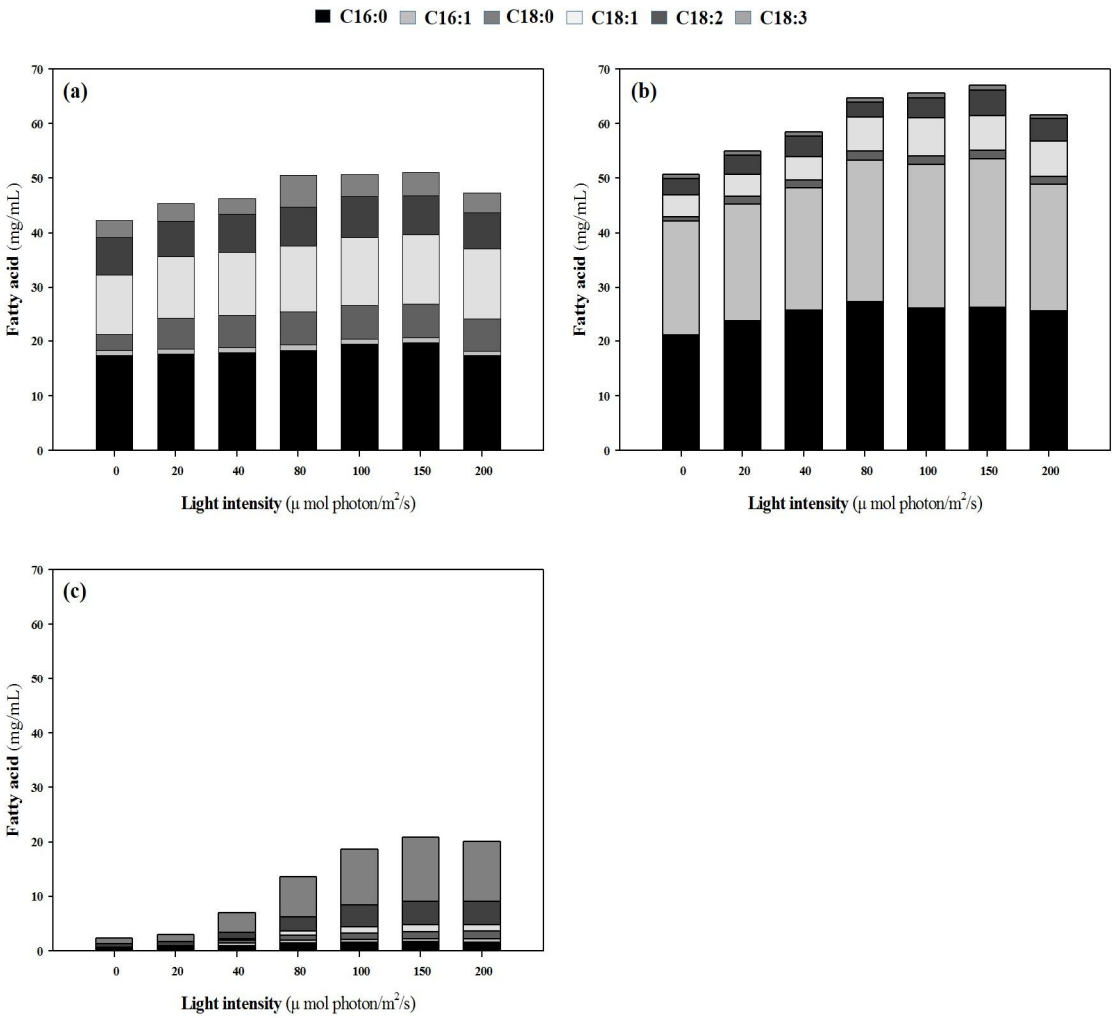

Fig. 3-6. Effect of light intensity on fatty acid composition under mixotrophic cultivation: (a) *I. galbana* LB987; (b) *N. oculata* CCAP849/1; and (c) *D. salina*.

Collection @ chosun

조선대학교
CHOSUN UNIVERSITY

Table 3-1. Relative fatty acid (C16-18) composition (%) of lipids in cells grown under mixotrophic condition with different light intensities

Microalgae	Light intensity (μmol photon/m^2/s)	Fatty acid compositions						
		C16:0	C16:1	C18:0	C18:1	C18:2	C18:3	total fatty acid
		mg/mL, (%)	mg/mL, (%)	mg/mL, (%)	mg/mL, (%)	mg/mL, (%)	mg/mL, (%)	mg/mL, (%)
I. galbana LB987	0	17.4, (41.2)	0.9, (2.0)	3.1, (7.3)	10.9, (25.8)	6.9, (16.3)	3.1, (7.3)	42.3, (100)
	20	17.6, (38.7)	0.9, (2.0)	5.9, (13.0)	11.2, (24.7)	6.5, (14.3)	3.3, (7.3)	45.4, (100)
	42	17.9, (38.8)	0.9, (2.0)	6.0, (13.0)	11.6, (25.1)	7.0, (15.1)	2.8, (6.1)	46.2, (100)
	80	18.3, (36.2)	1.0, (1.9)	6.3, (12.5)	12.0, (23.7)	7.1, (14.0)	5.9, (11.7)	50.6, (100)
	100	19.4, (38.3)	0.9, (1.8)	6.4, (12.6)	12.4, (24.4)	7.5, (14.8)	4.1, (8.0)	50.7, (100)
	150	19.7, (38.5)	1.0, (1.9)	6.4, (12.5)	12.6, (24.6)	7.2, (14.1)	4.3, (8.4)	51.1, (100)
	200	17.3, (41.9)	0.9, (1.9)	6.1, (12.9)	12.7, (26.8)	6.7, (14.2)	3.6, (7.6)	47.3, (100)
N. oculata CCAP849/1	0	21.3, (41.9)	20.8, (41.1)	0.8, (1.7)	4.1, (8.0)	3.0, (5.8)	0.8, (1.5)	50.7, (100)
	20	23.8, (43.3)	21.5, (39.0)	1.4, (2.5)	4.1, (7.5)	3.5, (6.3)	0.8, (1.4)	55.0, (100)
	40	25.8, (44.1)	22.5, (38.5)	1.4, (2.4)	4.3, (7.3)	3.7, (6.3)	0.8, (1.4)	58.5, (100)
	80	27.3, (42.3)	26.0, (40.2)	1.7, (2.6)	6.3, (9.7)	2.7, (4.1)	0.8, (1.2)	64.7, (100)
	100	26.2, (40.0)	26.4, (40.2)	1.5, (2.3)	6.9, (10.5)	3.7, (5.6)	0.9, (1.4)	65.6, (100)
	150	26.4, (39.4)	27.2, (40.6)	1.5, (2.2)	6.3, (9.4)	4.8, (7.1)	0.9, (1.3)	67.0, (100)
	200	25.7, (41.6)	23.2, (37.6)	1.4, (2.3)	6.6, (10.6)	4.1, (6.6)	0.8, (1.2)	61.6, (100)
D. salina.	0	0.2, (8.8)	0.2, (7.1)	0.2, (8.0)	0.1, (4.6)	0.6, (25.6)	1.1, (45.8)	2.4, (100)
	20	0.4, (11.7)	0.2, (6.7)	0.2, (7.0)	0.2, (5.0)	0.7, (24.8)	1.3, (44.6)	3.0, (100)
	40	0.9, (13.2)	0.4, (6.3)	0.6, (8.4)	0.3, (4.1)	1.2, (16.7)	3.6, (51.2)	7.0, (100)
	80	1.5, (10.8)	0.5, (3.7)	0.9, (6.9)	0.7, (4.8)	2.7, (19.6)	7.4, (54.3)	13.7, (100)
	100	1.6, (8.5)	0.5, (2.8)	1.1, (5.9)	1.2, (6.2)	4.0, (21.6)	10.3, (55.0)	18.6, (100)
	150	1.6, (7.8)	0.6, (2.7)	1.3, (6.5)	1.2, (6.0)	4.3, (20.8)	11.7, (56.3)	20.8, (100)
	200	1.6, (8.0)	0.6, (3.0)	1.4, (6.8)	1.2, (5.9)	4.4, (21.7)	11.0, (54.6)	20.1, (100)

Collection @ chosun

조선대학교
CHOSUN UNIVERSITY

4. Discussion

Nitrogen concentration in the culture medium is one of the vital factors that affect lipid synthesis of microalgae. It has been reported that lipid content in *Chlorella* could be doubled or even tripled under N-depletion conditions [Coverti et al., 2009; Scott et al., 2010], and a reciprocal relationship between nitrogen concentration and lipid content was also observed [Widjaja et al., 2009]. Under nitrogen starvation, the capacity for de novo lipid synthesis seems a characteristic of some algal species by converting excess of carbon and energy into triacylglycerols (TAG) [Thompson, 1996]. TAG consisted mainly of saturated and monounsaturated fatty acids can be efficiently stored in the cell and generate more energy than carbohydrates upon oxidation, thus forming the efficient carbon sink for rebuilding the cell after the stress. Although nitrogen starvation is well known to trigger a high amount of lipid accumulation, it can cause poor cell growth as well. Therefore, it is important to establish an appropriate concentration of nitrogen in culture medium to obtain maximal lipid productivity. This study shows that the total lipid content in cells decreased but cell growth improved with increasing nitrogen concentration (Fig. 3-1).

Some photoautotrophic microalgal cells can grow under mixotrophic conditions, with the addition of external organic carbon sources. This phenomenon exists in a number of microalgal genera and species distributed in major taxonomic divisions [Feuillade and Feuilade, 1989; Ukeles and Rose, 1976]. Most of the previous works have focused on the use of organic carbon as precursor for cell growth and for the accumulation of macromolecules, such as lipids, saccharides, proteins, and other active biochemicals under heterotrophic cultivation [Mata et al., 2010]. Heterotrophic cultivation has many advantages such as pure and high cell density culture without photolimitation effect and ease of harvesting. The use of carbon source is species-specific. In the present study, among the carbon sources tested, the supplementation of glucose led to a significant improvement of

Collection @ chosun

조선대학교
CHOSUN UNIVERSITY

growth in all three microalgal cells (Fig. 3-2). In general, glucose is the most commonly used carbon source in the heterotrophic cultivation of many microalgae. Based on the finding from Griffiths et al. [1960], we found that high biomass concentrations were obtained when glucose was added as the sole carbon source. Liang et al. [2009] showed that the highest biomass and a 14-fold higher lipid productivity of *C. vulgaris* were obtained under heterotrophic conditions in the presence of glucose. In addition, Liu et al. [2010] stated that glucose is the best carbon source for microalgal growth and lipid accumulation. This is mainly because the supplementation of glucose in the culture medium induces the membrane-bound H^+-glucose symport system [Haass and Tanner, 1973] and enhances the driving force of glucose uptake [Tanner, 1969]. The major metabolic pathways of glucose in algal cells are the glycolytic and pentose phosphate pathways. The reducing equivalents ($FADH_2$ and NADPH) are produced from glucose metabolism involved in ATP synthesis during oxidative phosphorylation. As a consequence, all of the produced ATPs are used for cell growth and lipid accumulation.

In our study, increasing growth trend was observed with increasing glucose concentrations; however, higher glucose concentrations provoked a decrease in biomass amount, which might be attributed to substrate inhibition (Fig. 3-3). In this case, excess glucose molecules would compete with the glucose molecules on the membrane-bound glucose permease.

The influence of three different culture modes on growth, chlorophyll, and total lipid content in three microalgae is presented in Fig. 3-4. Low biomass production occurred under photoautotrophic cultivation compared with heterotrophic or mixotrophic cultivation. The major reason for this outcome was that, in phototrophic conditions, only one factor acts as an energy source (light). Meanwhile, both light energy and organic carbon source were used for ATP production under mixotrophic conditions. In mixotrophic conditions, light energy is the major source for ATP production in the early stage of cell growth. Furthermore, in the presence of an organic carbon source, the concentration of photosynthetic pigments was low, and the formation of thylakoids was disturbed within the

Collection @ chosun

조선대학교
CHOSUN UNIVERSITY

cell. Yang et al. [2000] stated that total ATPs produced under photoautotrophic, heterotrophic, and mixotrophic conditions were 34.4, 19.4, and 27.4 mmol/g/h, respectively. However, the percentages of ATP consumption/production were 56.8, 18.2, and 36.3% during photoautotrophic, heterotrophic, and mixotrophic cultivation, respectively. A low ATP consumption during heterotrophic cultivation was attributed to the absence of the Calvin cycle (no light energy), and most of ATP was consumed only for glucose uptake and biomass synthesis. Among the three different culture mode operations, the highest total lipid content was observed under mixotrophic cultivation. This is because mixotrophic cultivation uses both light energy and carbon sources for cell growth and lipid accumulation.

The effect of light intensity on microalgal growth and total lipid content is depicted in Fig. 3-5. Our previous studies indicated that cell growth and total lipid production of freshwater green microalgal cells under mixotrophic conditions are notably affected by light intensity [Gim et al., 2014]. Cheirsilp and Torpee [2012] reported that the number of photosynthetic pigments (chlorophyll a and light-harvesting pigments such as chlorophyll c, phycobilins, and carotenoids) increases with increasing light intensity. In the present study, the total lipid content increases with increasing light intensity; this is because excessive light energy was converted into fatty acids. Under optimal growth conditions, light energy absorbed by antenna pigments is converted to ATP or NADPH, and this chemical energy is stored ultimately as starch and/or lipids by fixing CO_2 through the Calvin cycle and lipogenesis. Furthermore, when high light energy was supplied into the microalgal culture, the enzymes involved in fatty acid biosynthesis were very active, particularly acetyl-CoA carboxylase, desaturase, acyl-carrier protein synthase, ATP/citrate lyase, and membrane-bound glucose permease [Arroyo et al., 2011; Gim et al., 2014]. In contrast, photo-oxidative cell damage occurred when microalgal cells were grown under higher light intensity. Under these conditions, the light-harvesting chlorophyll molecules were converted to unstable forms, which in turn react with dissolved oxygen species. These reactive oxygen species then react with free fatty acids to make lipid peroxidase in inactive form, which reduces the fatty acid concentration. Furthermore, microalgal cells can

Collection @ chosun

조선대학교
CHOSUN UNIVERSITY

accumulate excessive light energy in the form of other macromolecules such as polysaccharides and proteins. Instead, low light intensity may increase the light reaction center pigments and light-harvesting (antenna) pigments to absorb maximal photons for normal cell growth. Moreover, a large volume of chloroplasts and a high density of thylakoid membranes lead to reduced lipid storage [Gim et al., 2014].

It has been shown that light intensity influences fatty acid composition of microalgal cells such as triglyceric acids, glycolipids, phospholipids, and polyunsaturated fatty acids (PUFA) [Yang et al., 2000]. Fatty acid composition plays an important role in the evaluation of biodiesel quality. The changes in fatty acid composition attributed to light intensity are highly species-specific. Furthermore, when the cells were grown at a higher light intensity, this led to an increased concentration of saturated fatty acids but a decrease in PUFA [Brown et al., 1996]. In contrast, low light intensity induces the formation of membrane polar lipids associated with chloroplasts. In this situation, more electron receptors were synthesized in thylakoids. Under low light intensity, the photosynthetic pigments and PUFA increased [Zhukova and Titlyanov, 2006]. It is noteworthy that Solovchenko et al. [2013] reported that the fatty acid composition of lipids in *Desmodesmus* sp. were most likely changed in chloroplasts accompanied by the dismantling of thylakoid membranes under very high light intensity.

In this study, the effect of light intensity on total amount and composition of fatty acid (C16–C18) of total lipid in three microalgal cells was investigated. As shown in Fig. 3-6 and Table 3-1, fatty acid concentration increased slightly with increasing light intensity up to 150 μmol photon/$m^{2/}$s, and the order of microalgal species containing high fatty acids (C16–C18) concentration was *N. oculata* CCAP849/1 > *I. galbana* LB987 > *D. salina*. However, relative fatty acid compositions of total lipid were not changed by the variation of light intensity. Regardless of light intensity, *I. galbana* LB987 contained approximately 40% palmitic (C16:0) and 25% oleic acids (C18:1) as major fatty acids but stearic (C18:0) and linoleic acids (C18:2) as minor fatty acids, whereas *N. oculata* CCAP849/1 contained >40% palmitic (C16:0) and >40% palmitoleic acids (C16:1) as major

Collection @ chosun

조선대학교
CHOSUN UNIVERSITY

fatty acids but oleic acid (C18:1) as minor fatty acid. In the case of *D. salina*, total fatty acid concentration was 62.1 mg/mL, however, C16–C18 concentration was found to be only 20 mg/mL. More than 40 mg/mL fatty acid was involved as forms of lignoceric (C24:0), docosahexaenoic (C22:6), and eicosapentaenoic acids (C20:5) in *D. salina*. From these results, we can expect that the species of *N. oculata* CCAP849/1 and *I. galbana* LB987 can be used as sources for biodiesel production, whereas *D. salina* species can be used as a source for omega-3 production, which is effective for human health benefits of cancer, cardiac disease, stroke, high blood pressure, and arrhythmia [Romieu et al., 2005; Vazhappilly and Chen, 1998].

Table 3-2 shows the comparative analysis of the biomass and lipid production in the three marine microalgae species with other related species under the different culture conditions. From this analysis, it was confirmed that mixotrophic cultivation is more efficient for lipid production than photoautotrophic culture in the same microalgal species and glucose can be used for growth as a better organic source. Among the microalgal species described in this Table 3-2, *N. oculata* CCAP849/1 was the best biomass- and lipid producing microalga under mixotrophic culture conditions with 0.02 M glucose and light intensity of 150 μmol photon/$m^{2/}$s. Maximal biomass and lipid productivities of this species were 169.4 and 63.1 mg/L/d, respectively.

Collection @ chosun

조선대학교
CHOSUN UNIVERSITY

Table 3-2. Relative fatty acid (C16-18) composition (%) of lipids in cells grown under mixotrophic condition with different light intensities

Microalgae	Reactor type	Culture conditions			Biomass		Lipid			Ref.
		Culture mode	Light intensity (μmol photon/m^2/s)	Carbon sources	Production (g/L)	Productivity (mg/L/d)	Content (%, w/w)	Production (g/L)	Productivity (mg/L/d)	
I. galbana	Circular cylindrical (20 L)	Photoautotrophic	36	-	0.57	24.9	23.2	-	-	Lee et al., 2011
I. galbana	Circular cylindrical (5 L)	Photoautotrophic	110	-	0.80	66.6	24.0	-	-	Ra et al., 2015
I. galbana LB987	Erlenmeyer flask (1 L)	Mixotrophic	150	0.02 M glucose	0.89	89.1	30.1	0.27	26.8	In this study
N. oculata	Circular cylindrical (20 L)	Photoautotrophic	36	-	0.57	20.4	8.2	-	-	Lee et al., 2011
N. oculata CCMP525	Circular cylindrical (5 L)	Photoautotrophic	110	-	0.51	47.5	17.0	-	-	Ra et al., 2015
N. oculata CCAP849/1	-	Mixotrophic	270	0.06 M glucose	0.61	-	-	0.16	14.0	Wan et al., 2011
D. tertiolecta	Erlenmeyer flask (1 L)	Mixotrophic	150	0.02 M glucose	1.69	169.4	38.5	0.63	63.1	In this study
D. slaina	Circular cylindrical (5 L)	Photoautotrophic	110	-	0.28	44.2	23.0	-	-	Ra et al., 2015
D. slaina FACHB435	Circular cylindrical (5 L)	Photoautotrophic	110	-	0.25	37.5	22.0	-	-	Ra et al., 2015
D. salina	-	Mixotrophic	270	0.08 M glucose	0.52	-	-	0.15	12.0	Wan et al., 2011

Collection @ chosun

조선대학교
CHOSUN UNIVERSITY

Chapter IV

Growth factors in oceanic sediment significantly stimulate the biomass and lipid production of two oleaginous microalgae

Collection @ chosun

조선대학교
CHOSUN UNIVERSITY

1. Introduction

Because of the shortage and increasing cost of conventional fossil fuels, the development of new technologies for renewable biofuel production is expected to become increasingly important [Concas et al., 2014]. Microalgae are considered a suitable energy resource through the photoautotrophic mechanism that can convert carbon dioxide into biomass, fatty acids, and lipids. Several oleaginous microalgae, such as *C. vulgaris*, *I. galbana*, *N. oculata*, *S. obliquus*, and *Tetraselmis suecica* were considered some of the most promising feedstock for biofuel production because of their rapid growth rate (cell doubling time of 1–10 days) and high intracellular lipid content (more than 50%, cell dry weight) [Yang et al., 2011]. In contrast, *B. braunii* and *P. tricornutum* have relatively high lipid content (maximum 57–75%), but require long cultivation times (approximately 20–30 days) and have low biomass productivities (0.02 and 0.003–1.9 g/L/d) [Mata et al., 2010]. Therefore, at present, these two microalgal strains were not considered to be suitable sources for biodiesel production.

Generally, it is known that soil extracts contain essential elements for microalgal growth, such as macronutrient elements (C, N, and P), trace metal ions (Fe^{3+}, Mg^{2+}, Ca^{2+}, Mn^{2+}, Zn^{2+}, Co^{2+}, Cu^{2+}, and Mo^{2+}, etc.), vitamins, chelators, and other carbon additives. In recent years, interest in the function of metal ions for microalgal biomass and lipid production has been growing. Metal ions are environmental factors that affect the metabolic growth and lipid accumulation processes of microalgae [Huang et al., 2014]. Iron is one of the most essential metal ions required by microalgae. Several studies have shown that increasing iron concentration in the culture medium promotes an increase in both growth rate and lipid content of microalgae [Liu et al., 2008; Ruangsomboon et al., 2013]. In addition, calcium and magnesium are also favorable for algal lipid accumulation [Gorain et al., 2013]. Most of these experiments were conducted under photoautotrophic conditions.

Collection @ chosun

조선대학교
CHOSUN UNIVERSITY

Humic substances (humic and fulvic acids) in soil extracts could serve multiple functions in biological systems [Petersen, 1991]. They influence phytoplankton via both direct (e.g., a nutrient source [Carlsson et al., 1999] or modifier of membrane characteristics [Petersen, 1991]) and indirect (e.g., light attenuation [Dera et al., 1978; Doering et al., 1994] and trace metal chelation [Sunda and Huntsman, 1995; Sunda et al., 1983]) mechanisms. Enhanced microalgal growth using soil extract has been primarily attributed to the chelating action of the humic substances, which reduce heavy metal ion toxicity or increase the bioavailability of trace metals, such as iron. Sweeney [Sweeney, 1954] used soil extract as an alternative for vitamin B_{12} and EDTA, which are commonly added to seawater medium. In natural seawater, dissolved organic carbon (DOC) and EDTA act as chelators. Steelink [1977] and Prakash and Rashid [1968] reported that the iron-humic substance complex in aquatic systems stimulated microalgal growth. Most macronutrients and major metal ions are generally highly soluble and non-toxic, but several micronutrients were toxic at high concentrations. For example, hydrous ferric oxide, one form of iron compounds, is an insoluble precipitate and unavailable to microalgae. In addition, the ferric precipitate adsorbed other essential metals and lowered their bioavailability. Because of these difficulties, providing adequate and non-toxic trace metal ions to microalgae in culture is very important. Initially, this problem was solved through the addition of oceanic sediments, which contains various kinds of trace metal ions along with complex mixtures of high molecular weight organic acids, such as humic acid.

In this study, the composition of oceanic sediment was analyzed and the mixing ratio between sediment extract and culture medium was optimized to obtain maximum biomass and lipid production of microalgae under the mixotrophic mode. The optimum concentrations of growth stimulators, such as metal ions, EDTA and humic substances, were investigated. Finally, biomass and lipid productions obtained from cells cultured in media containing different components of growth stimulators or oceanic sediment were compared.

Collection @ chosun

조선대학교
CHOSUN UNIVERSITY

2. Materials and Methods

2-1. Microalgal culture media and conditions

Two microalgae, which accommodate a high content of lipid in their cells, were used in this study. One freshwater microalgal species, *B. braunii* LB572, and another marine species, *P. tricornutum* B2089, were obtained from UTEX Culture Collection of Algae (The University of Texas at Austin, Austin, USA). The media used in this study were Jaworski's medium [Thompson et al., 1988] for *B. braunii* LB572, and f/2 medium [Guillard and Ryther, 1962] for *P. tricornutum* B2089. Microalgal cells obtained from culture collection were spread out on an agar surface and single colonies were isolated to avoid the bacterial contamination.

Pre-cultivation of the two microalgae was performed in a 500 mL Erlenmeyer flask containing a working volume of 250 mL of microalgal species-specific medium with cotton plugs that allow exchange with the atmosphere. Cells were cultivated at 25 °C under photoautotrophic culture conditions. Cultures were illuminated with cool-white fluorescent lamps, which were fixed on the wall, and light intensity was attenuated by adjusting the distance from lamps and was measured with an illuminance meter (LT Lutron LM-81LX; Lutron Electronic Enterprise, Co., Taipei, Taiwan). Based on our previous results of optimal growth conditions, light intensity was maintained at 95 μmol photon/m^2/s for *P. tricornutum* B2089 and at 100 μmol photon/m^2/s for *B. braunii* LB572. The photoperiods were 12:12 h (Light:Dark cycle). Each cultivation period for the two microalgal species was as follows: 20 days for *B. braunii* LB572 and 21 days for *P. tricornutum* B2089.

Collection @ chosun

조선대학교
CHOSUN UNIVERSITY

2-2. Preparation of oceanic sediment extract

Oceanic sediments were collected at six coastal areas in Jeollanam-do province, Republic of Korea. Sediment samples were collected at a depth of 10-20 cm and primarily leached through a no. 4–10 Sieve (opening diameter: 4.76–2 mm) and dried at 30 °C for 24 h. 35 g of dried sediment was placed in 1 L of distilled water and treated with 10 mL of 1 N-HNO_3 to adjust pH 2.0. The mixture was stirred for 6 h and then allowed to stand for 1 h. Then, the supernatant was filtered using a 0.2 μm membrane filter (Pall, USA) and the final pH of the extract was adjusted to 7.0–8.0.

2-3. Effect of oceanic sediments on cell growth and lipid production

As described in the introduction, oceanic sediment contains complex mixtures of high molecular mass organic acids, along with various types of trace metal ions. Among the multiple sediments collected from six areas at different periods, the samples collected from Yeosu-city (34°47'48.6"N 127°33'30.6"E) at summer season (from June to September, 2016) was the most nutritious and contained an appropriate ratio of dissolved organic carbon (DOC), T-N, T-P, and metal ions at approximately similar concentrations, so these samples was used in all subsequent experiments. Several effects of growth factors in these sediments on microalgal growth and lipid production under the mixotrophic culture modes were investigated as detailed below.

In experiment I, to determine the optimal mixing ratio for maximum biomass and lipid production, the culture medium and oceanic sediment extract were mixed with medium to sediment ratios of 10:0, 9:1, 8:2, 7:3, 6:4, and 5:5 (v/v). Microalgal cell cultivation was performed in 5L Erlenmeyer flasks containing 3 L of culture medium mixed with appropriate amount of oceanic sediment extract.

Collection @ chosun

조선대학교
CHOSUN UNIVERSITY

In experiment II, the availability of DOC in the oceanic sediment extract was tested as a carbon source. When the culture medium was mixed with sediment extract at a ratio of 6:4 (v/v), DOC concentration in the medium was 1.08 g/L. As a control, 1.0 g/L of glucose was added to each microalgal culture medium. During cell cultivation in different media, consumption of DOC and glucose in the media was determined and compared. In addition, concomitant biomass production was measured.

In experiment III, the effects of metal ions in the sediment on biomass and lipid production were investigated. First, the concentration of Fe^{3+}, Mg^{2+}, and Ca^{2+} in the mixture of culture medium with extractat a ratio of 6:4 (v/v) was determined. Next, each metal ion in a limited concentration range was added to the corresponding culture medium without oceanic sediment extract. After cell cultivation in different media, biomass and lipid production were determined and compared.

In experiment IV, the effects of EDTA or aquatic humic substances (AHSs) to reduce metal ion toxicity or increase bioavailability of metal ions was examined. Different concentrations of EDTA (0, 0.25, 0.5, 1.0, 2.0, 3.5, 7.0, 10.0, and 20.0 mg/L) were treated in each culture medium containing the optimal concentration of metal ion for cell growth. In addition, AHSs were extracted from oceanic sediment and added to the culture medium at different concentrations (0, 1.0, 5.0, 10.0, 20.0, 40.0, 80.0, and 100.0 mg/L). Extraction of AHSs from sediment was conducted using the method of Schnitzer and Vendette [1975]. A 50 g sample of dried sediment was added to 500 mL of 0.5 N-NaOH. The mixture was agitated for 24 h and centrifuged at 900 × *g* for 30 min. The supernatant was adjusted to pH2 with 6 N-HCl and centrifuged. To remove the salts, the supernatant (the crude fulvic acid extract) was dialyzed with distilled water using a dialysis sac (Thermo scientific, USA). The precipitate (the crude humic acid extract) was washed with distilled water three times, and then dried. The final concentrations of humic and fulvic acids were analyzed with TOC (TOC 5000, Shimadzu, Japan). After cell cultivation, the differences between initial and final concentrations of trace metal ions were determined to confirm the uptake of metal ions.

Collection @ chosun

조선대학교
CHOSUN UNIVERSITY

2-4. Analytical methods

Microalgal dry biomass was determined with 100 mL of microalgal culture, which was collected and harvested by centrifugation at 4500 × *g* for 15 min. Cell pellets were frozen immediately at -80 °C and later freeze dried at -45 °C under vacuum using a freeze-dryer (FD 8508 Bench-Top freeze-dryer, Ilshin BioBase, Republic of Korea). After drying, microalgal pellets were weighed using an electronic balance (Ohaus, Explorer EX623, USA).

For estimation of total lipid contents (%, w/w), 1 g of dried microalgal cells were blended with 200 mL of distilled water, and the cell mixture was disrupted by sonication (Sonifier 250, Branson, USA) at a resonance of 10 kHz for 5 min. Lipid extraction was performed according to a modification of the method described by Folch et al. [1957]. Total lipids were extracted with a mixture of chloroform-methanol (2:1, v/v) in a separatory funnel and shaken for 1 h. The lower part of the chloroform layer (containing lipid) was selected and removed by evaporation using a rotary evaporator (Rotavapor R-205, Buchi, Switzerland) and the extracted lipids were weighed. Metal ion concentration of oceanic sediment extract was analyzed with an ICP-MS (Elan DRCII, Perkin Elmer, USA) and DOC (also humic substances) was determined by TOC (TOC 5000, Shimadzu, Japan). The concentrations of total nitrogen (T-N) and total phosphorus (T-P) were determined by standard methods [APHA, 1995].

Collection @ chosun

조선대학교
CHOSUN UNIVERSITY

3. Results

3-1. Analysis of oceanic sediments composition

The concentrations of macronutrients and trace metal ions dissolved in the oceanic sediment extract used in this study are shown in Table 4-1. The concentrations of DOC, T-N, and T-P, were 2652.2, 15.0, and 0.7 mg/L, respectively. In addition, the concentration of Fe^{3+}, Mg^{2+}, and Ca^{2+} ions were 1.85, 9.92, and 13.80 mg/L, respectively.

Table 4-1. Compositions of macronutrients and metal ions in oceanic sediment extract used in this study

Macronutrients (mg/L)			**Trace metal ions** (mg/L)							
DOC	T-N	T-P	Mg^{2+}	Ca^{2+}	Fe^{3+}	Mn^{2+}	Zn^{2+}	Co^{2+}	Cu^{2+}	Mo^{2+}
2708.2	15.8	0.8	10.2	14.7	1.9	32.2	27.0	5.2	19.6	3.4

Collection @ chosun

조선대학교
CHOSUN UNIVERSITY

3-2. Optimization of mixing ratio between culture medium and oceanic sediment extract

To determine the optimal mixing ratio for maximum biomass and lipid production, microalgal culture medium and oceanic sediment extract were blended at ratios of 10:0, 9:1, 8:2, 7:3, 6:4, and 5:5 (v/v). Biomass and lipid production data for the two microalgae cultivated mixotrophically for 14 days with different mixing ratios are shown in Table 4-2. Overall, the maximum production of biomass and lipids in the microalgae was observed at a mixing ratio of 6:4 (v/v), and lipid contents increased 8-10% (w/w) as the amount of sediment increased. When compared with sediment-free medium, specific growth rates of *B. braunii* LB572 and *P. tricornutum* B2089 were enhanced 13.0 and 11.3 times, respectively. Because of increased growth rate, the cultivation time of both microalgae was reduced by at least 6 days. Under this condition, maximal biomass and lipid production of *B. braunii* LB572 was 5.54 and 3.09 g/L, and that of *P. tricornutum* B2089 was 6.41 and 3.61 g/L, respectively. These data suggested that oceanic sediment remarkably stimulated *B. braunii* LB572 and *P. tricornutum* B2089, resulting in the increase of biomass and lipid production at least 6- and 8-folds, respectively. Based on these results, the following experiment was conducted to determine the components in the oceanic sediment that promoted microalgal growth.

Collection @ chosun

조선대학교
CHOSUN UNIVERSITY

Table 4-2. Effect of mixing ratio between culture medium and oceanic sediments on the microalgal biomass and lipid production

Microalgae	Mixing ratio between culture medium and oceanic sediments (v/v)	Cultivation time (day)	Biomass		Lipid	
			Specific growth rate (day^{-1})	Production (g/L)	Content (%, w/w)	Production (g/L)
B. braunii LB572	10:0 (JM)	20	0.03	0.79	48.0	0.38
	9:1	14	0.09	1.36	47.2	0.64
	8:2	14	0.13	1.99	48.5	0.97
	7:3	14	0.22	3.22	51.3	1.65
	6:4	14	0.39	5.54	55.8	3.09
	5:5	14	0.21	3.00	50.2	1.51
P. tricornutum B2089	10:0 (f/2)	21	0.04	0.96	46.0	0.44
	9:1	14	0.10	1.49	46.5	0.69
	8:2	14	0.16	2.40	49.3	1.18
	7:3	14	0.26	3.76	51.5	1.94
	6:4	14	0.45	6.41	56.3	3.61
	5:5	14	0.29	4.18	49.2	2.06

* JM (Jaworski's medium), and f/2 medium

Collection @ chosun

조선대학교
CHOSUN UNIVERSITY

3-3. Effect of DOC on biomass and lipid production

As shown in Table 4-1, oceanic sediment extract contained 2708.2 mg/L of DOC. There is a possibility that the DOC could be utilized as a carbon source for mixotrophic growth of microalgal cells, although its concentration was relatively low. When culture medium was mixed with oceanic sediment extract at a ratio of 6:4 (v/v), DOC concentration in the mixture was approximately 1.0 g/L. If DOC was used as a carbon source, its consumption and concomitant algal growth patterns should be similar with those of glucose. Thus, 1.0 g/L of glucose (as a control group) or DOC in mixture was used in the carbon utilization test for *B. braunii* LB572 and *P. tricornutum* B2089 under mixotrophic culture mode with illumination at 95 μmol photon/m^2/s under a 12:12 h (light:dark) photoperiod. Compared to glucose, less DOC was consumed for 14 days, but at least 1.5 times higher cell mass and a concomitant 1.1 times higher lipid contents were achieved (Fig. 4-1). This indicated that small amounts of DOC was utilized as a carbon source for microalgal growth.

Collection @ chosun

조선대학교
CHOSUN UNIVERSITY

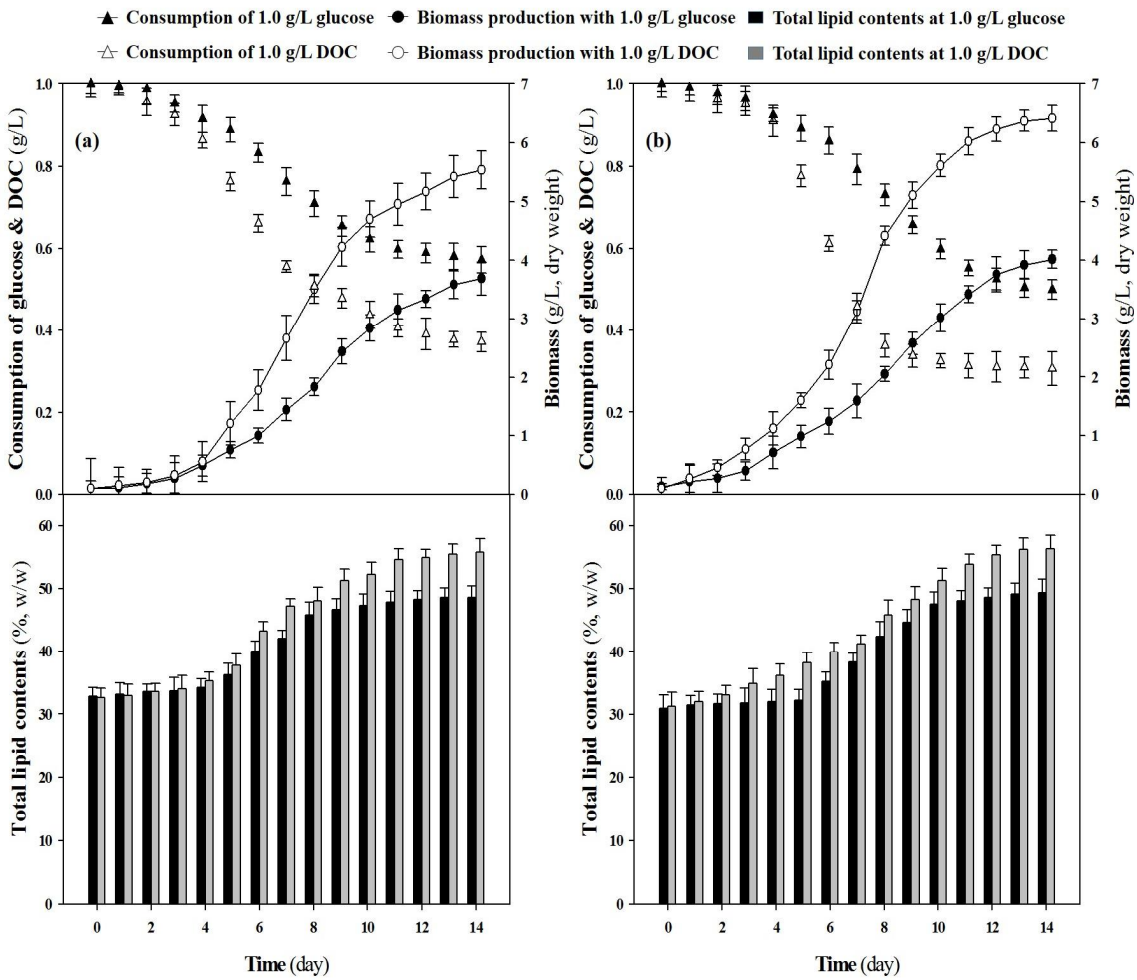

Fig. 4-1. Effect of glucose or DOC in oceanic sediment on biomass and lipid production of (a) *B. braunii* LB572 and (b) *P. tricornutum* B2089.

Collection @ chosun

조선대학교
CHOSUN UNIVERSITY

3-4. Effect of metal ions on microalgal growth and lipid production

As mentioned above, oceanic sediment included several metal ions, including 1.9 mg/L Fe^{3+}, 10.2 mg/L Mg^{2+}, and 14.7 mg/L Ca^{2+}. Next, experiments were conducted to investigate the optimum concentration of each metal ion to determine if the concentrations of metal ions in the sediment were sufficient to positively influence the growth and lipid production of microalgae. Each cell of *B. braunii* LB572 and *P. tricornutum* LB2089 was cultured on different medium (JM or f/2 medium), which was supplied with different concentrations of metal ions; the concentration ranges of Fe^{3+}, Mg^{2+}, and Ca^{2+} were 0–20, 0–10, and 0–20 mg/L, respectively. As shown in Fig. 4-2a and c, increasing the initial concentration of Fe^{3+} dramatically stimulated biomass and lipid productions, as well as lipid contentin both microalgae. When Fe^{3+} concentration reached 5.0 mg/L, the biomass and lipid productions of *B. braunii* LB572 and *P. tricornutum* B2089 increased more than 5.5 and 28 times, respectively, compared to those of the control (Fe^{3+}-free) group. In addition, lipid content of both microalgae was also improved (4–5 times higher than that of the control). However, at higher concentrations, their production was seriously inhibited. The effect of Ca^{2+} on growth and lipid production of microalgae was very similar to that of Fe^{3+}. As the initial concentrations of Ca^{2+} increased up to 10.0 mg/L for *B. braunii* LB572 and 5.0 mg/L for *P. tricornutum* B2089, the biomass and lipid production also highly increased (Fig. 4-2b and d). Compared with Fe^{3+} and Ca^{2+} produced less biomass but accumulated similar contents of lipids in cells. The stimulating effect of Mg^{2+} on microalgal biomass and lipid production was less than that of Fe^{3+} and Ca^{2+} ions (data not shown). However, biomass and lipid production tended to increase with increasing concentrations up to 5.0 mg/L in *B. braunii* LB572 and 2.5 mg/L in *P. tricornutum* B2089.

Consequently, the optimal concentrations of metal ions for photoautotrophic microalgal growth and lipid production were found to be as follows: 5.0 mg/L Fe^{3+}, 10.0 mg/L Ca^{2+}, and 5.0 mg/L Mg^{2+} for *B. braunii* LB572; and 5.0 mg/L Fe^{3+}, 5.0 mg/L Ca^{2+},

Collection @ chosun

조선대학교
CHOSUN UNIVERSITY

and 2.5 mg/L Mg^{2+} for *P. tricornutum* B2089. Under these optimal conditions, the biomass, lipid production, and lipid content of *B. braunii* LB572 were 4.06 g/L, 2.19 g/L, and 53.9% (w/w), respectively; those of *P. tricornutum* B2089 were 4.99 g/L, 2.80 g/L, and 56.1%, respectively. These values were 5-6 times higher than those obtained from cultures in JM or f/2 medium, but were lower than those obtained from cells grown on the medium mixed with oceanic sediment. Although the sediment mixed medium contained lower metal ions than the optimum concentrations, it produced more biomass and lipids. From these results, it is expected that some components in sediment may improve the bioavailability of metal ions to microalgae.

Collection @ chosun

조선대학교
CHOSUN UNIVERSITY

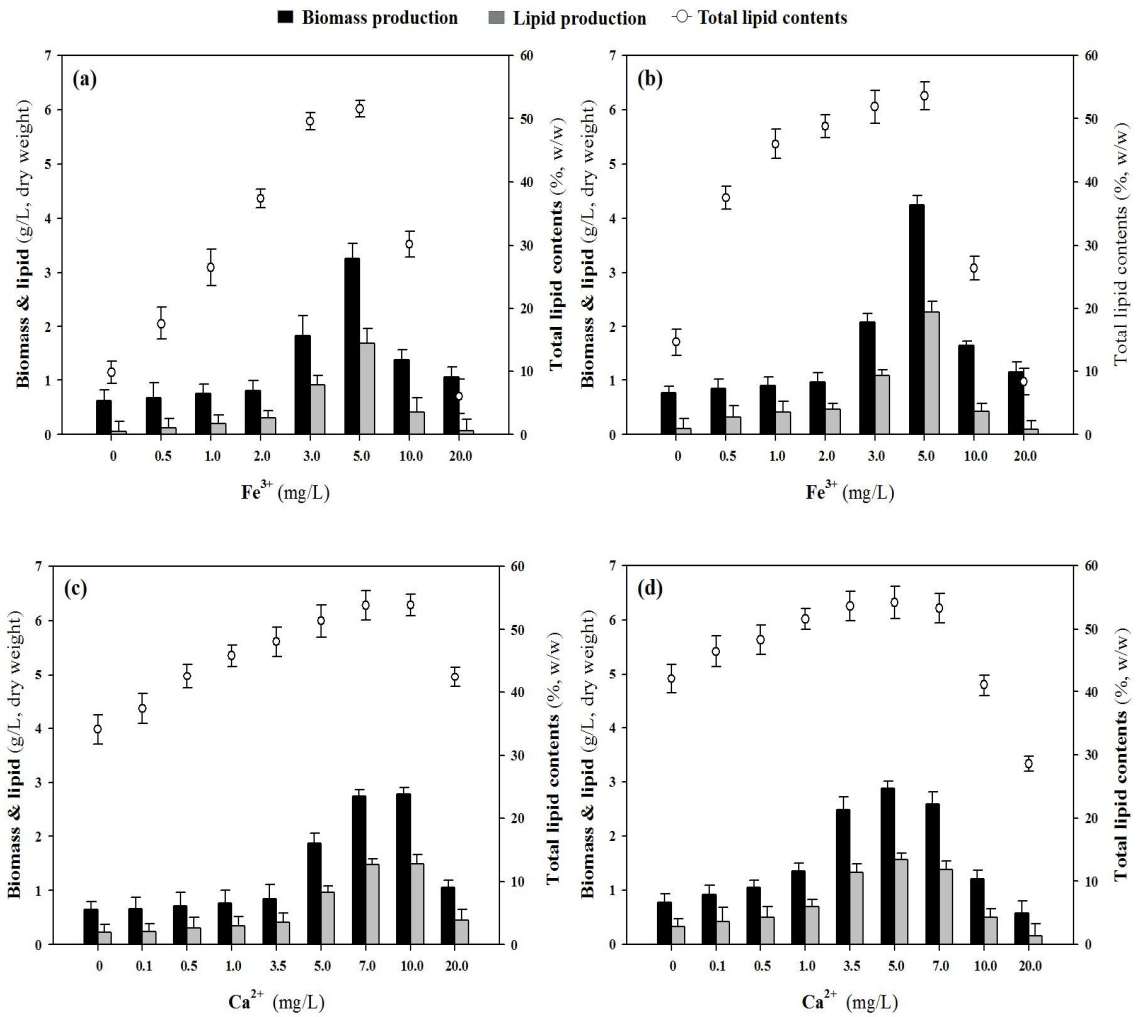

Fig. 4-2. Effect of $Fe^{3+}$and Ca^{2+}on the biomass and lipid production of *B. braunii* LB572 (a and b) and *P. tricornutum* B2089 (c and d).

Collection @ chosun

조선대학교
CHOSUN UNIVERSITY

3-5. Effect of EDTA or humic substances on bioavailability of metal ions to microalgae

The effect of EDTA, a non-specific complexing ligand, on the biomass and lipid accumulation of microalgal strains was studied at optimal concentrations of Fe^{3+}, Ca^{2+}, and Mg^{2+} ions. As shown in Fig. 4-3, biomass and lipid production significantly increased as the EDTA concentration increased up to 3.5 mg/L for *B. braunii* LB572 and 7.0 mg/L for *P. tricornutum* B2089. Under optimum EDTA concentration, biomass and lipid production of *B. braunii* LB572 were 4.4- and 6.7-fold higher and those of *P. tricornutum* B2089 were 5.8- and 11.3-fold higher than the control group grown on EDTA-free medium. When EDTA concentration was low, residual concentrations of Fe^{3+} and Ca^{2+} in the medium decreased along with the increase of EDTA concentration. This indicates that EDTA enhanced the solubility of Fe^{3+} and Ca^{2+}, and therefore improved the uptake of Fe^{3+} and Ca^{2+} into the microalgal cells [Jin et al., 2009; Yokoi et al., 2002]. However, high concentrations of EDTA severely inhibited the uptake of Fe^{3+} and Ca^{2+} and concomitantly hindered the growth and lipid accumulation of cells.

As described above, AHSs (humic and fulvic acid) are typically nonspecific organic ligands and generally constitute 30–80% of DOC [Jin et al., 2009]. In this study, 145 and 220 mg/L of humic and fulvic acids were extracted from 2708.2 mg/L of DOC in oceanic sediment. To evaluate the effect of AHSs on cell growth and lipid accumulation, 0–100 mg/L of the crude extracted humic and fulvic acids were applied to the culture medium, which contained optimal concentrations of Fe^{3+}, Ca^{2+}, and Mg^{2+} ions. Similar with EDTA effects, cell growth, lipid production and accumulation in both microalgae increased as the concentration of humic acid increased up to 80 mg/L, and concomitantly the residual concentrations of Fe^{3+} and Ca^{2+} in the medium decreased (Fig. 4-4). However, at higher concentrations than 100 mg/L, the uptake of Fe^{3+} and Ca^{2+} decreased and cell growth and lipid accumulation were inhibited significantly.

Collection @ chosun

조선대학교
CHOSUN UNIVERSITY

Fig. 4-5 shows the comparison of biomass, and lipid production and accumulation in microalgal cells grown on the media containing different compositions, such as oceanic sediments or optimized concentrations of metal ions, EDTA, and humic acid. The highest biomass and lipid production were obtained from the cells grown on appropriate culture medium (JM or f/2 medium) mixed with oceanic sediment at a ratio of 6:4 (v/v) for 14 days.

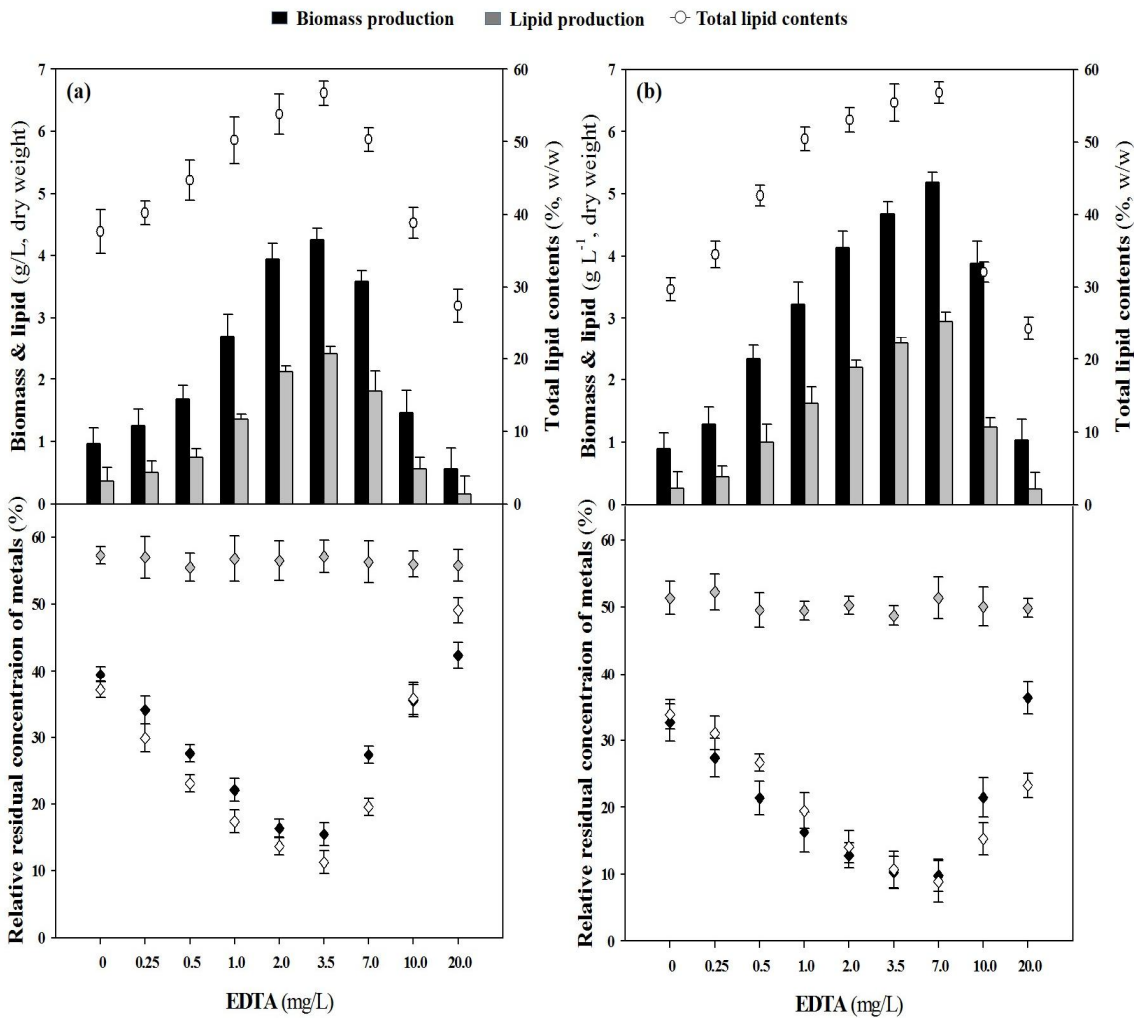

Fig. 4-3. Chelation effect of EDTA on the bioavailability of metal ions to (a) *B. braunii* LB572 and (b) *P. tricornutum* B2089.

Collection @ chosun

조선대학교
CHOSUN UNIVERSITY

4. Discussion

Based on the results that maximal biomass and lipid productions of the two microalgae were obtained from the cells cultivated in the culture medium containing sediment extract at a ratio of 6:4 (v/v), it was investigated which components in the sediment promoted microalgal growth. There have been many reports concerning the physiological function of metals for microalgal biomass and lipid production [Abd El Baky et al., 2012; Ben Amor-Ben Ayed et al., 2015; Gorain et al., 2013; Huang et al., 2014; Liu et al., 2008; Ren et al., 2014]. Trace metal ions are very important in the cellular mechanism of microalgae, including photosynthesis, cell division, respiration, and intracellular transportation, and protein and lipid biosynthesis. They also enhance biomass and lipid yields of microalgae [Wan et al., 2014].

In these experiments, the optimum concentrations of Fe^{3+}, Mg^{2+}, and Ca^{2+} for two microalgae were determined. As the initial concentration of Fe^{3+} increased up to 5.0 mg/L, biomass and lipid productions increased significantly (Fig. 4-2a and c). Abd El Baky et al. [2012] and Ren et al. [2014] described an increasing trend of cell growth and lipid accumulation of *Scenedesmus* sp. with an increasing of Fe^{3+} levels within appropriate concentration ranges under photoautotrophic or heterotrophic mode. Similar results were also found from *Monoraphidium* sp. [Che et al., 2015] and *C. vulgaris* [Liu et al. 2008]. Also, as shown in Fig. 4-2b and d, the initial concentrations of Ca^{2+} reached 5.0-10.0 mg/L, the biomass and lipid production highly increased. Becker [1994] stated that Ca^{2+} is likely to be involved in cell growth and lipid accumulation through mechanisms, such as the formation of the cell membrane and enhancement of photo chemical efficiency of photosystem II. Conversely, Gorain et al., [2013] reported that increased Ca^{2+} concentration in the growth medium had little effect on biomass yield of *C. vulgaris* and *S. obliquus*; however, lipid content increased under photoautotrophic cultivation. Although a remarkable

Collection @ chosun

조선대학교
CHOSUN UNIVERSITY

effect of Mg^{2+} on lipid production was not observed in the tested microalgae, it is certain that Mg^{2+} plays an important role in their growth because it could enhance the acetyl-CoA carboxylase (ACCase) activity [Livine and Sukenik, 1992]. ACCase exerted intense regulation on fatty acid synthesis.

Compared to the effect of metal ion concentration, metal speciation is very important for bioavailability [Stumm and Morgan, 1996]. AHSs universally exist in natural water and are typically non-specific complexing organic ligands. They have a significant influence on metal speciation, and thus on bioavailability of metals to microalgae. Herein, the effects of EDTA and AHSs on the bioavailability of metal ions to the tested microalgae were determined. As shown in Fig. 4-3, the fact that the residual concentrations of Fe^{3+} and Ca^{2+} in the medium decreased along with the increase of EDTA concentration indicates that EDTA promotes the bioavailability of Fe^{3+} and Ca^{2+} to microalgal cells. At the same time, maximal biomass and lipid production was attained at concentration ranges from 3.5 to 7.0 mg/L. Gerringa et al., [2000] stated that EDTA increases the solubility of ferric oxide, and thereby increases iron availability to algae when EDTA concentration is low, but it chelates iron strongly and may decrease iron availability to some algae when EDTA concentration is high. Conversely, the uptake of Mg^{2+} in both microalgae was not affected by the EDTA concentration. Ren et al., [2014] reported that Mg^{2+} concentration exhibited as light decline with the addition of EDTA, which implies that the effect of EDTA on the bioavailability of Mg^{2+} was negligible. Like EDTA, humic acid also increased the bioavailability of Fe^{3+} and Ca^{2+} to microalgal cells and improved biomass and lipid production (Fig. 4-4). Interestingly, humic acid had a higher effect on biomass and lipid production than fulvic acid, which also had a similar effect (data not shown). Droop [1962] found that the growth of *Skeletonema costatum* was enhanced when humic acid was applied to the culture medium and that humic acid was more active than fulvic acid. Conversely, the effect of humic and fulvic acids on Mg^{2+} uptake was negligible. There are many reports demonstrating that humic substances stimulate algal growth. The growth-stimulating activity of soil extract on *Gymnodinium* species was primarily caused by

Collection @ chosun

조선대학교
CHOSUN UNIVERSITY

the chelating action of the humic component, which resulted in a reduction of the toxicity or an increase in the bioavailability of trace metals [Prakash and Rashid, 1968]. Ohkubo et al., [1998] showed that a chelating substance, such as humic isolates, can stimulate the growth of *Microcystis aeruginosa* by reducing the toxicity of heavy metals. Granéli and Moreira [1990] demonstrated that *Prorocentrum minimum* responds to humic acid with an increase in growth rate. Koukal et al., [2003] and Pempkowiak and Kosakoeska [1998] showed that the presence of humic substances stimulated photosynthesis and growth in the green algae, *Pseudokirchneriella subcapitata* and *C. vulgaris* A1-76, by reducing the toxicity of heavy metals.

Collection @ chosun

조선대학교
CHOSUN UNIVERSITY

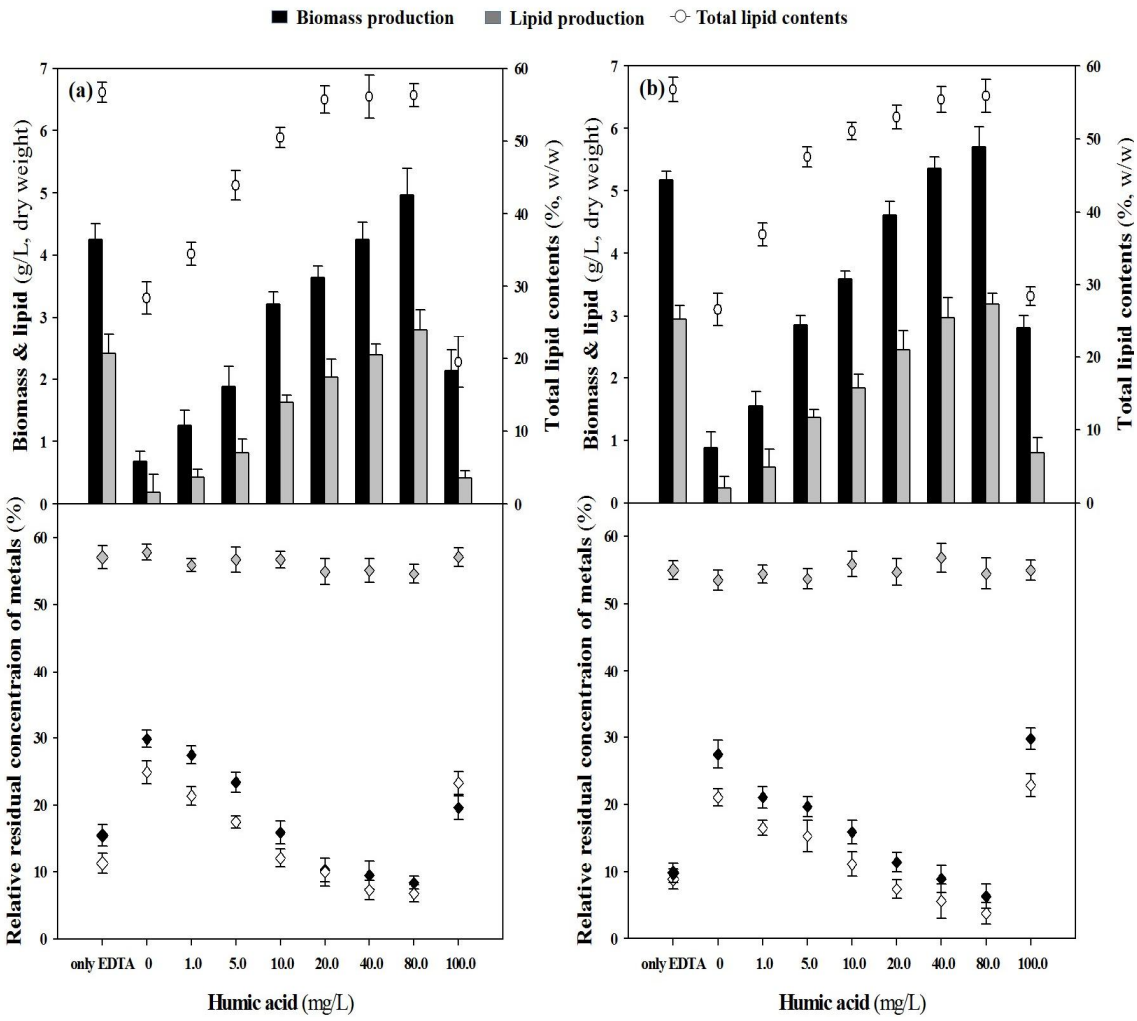

Fig. 4-4. Chelation effect of humic acid on the microalgal growth and bioavailability of metal ions to (a) *B. braunii* LB572 and (b) *P. tricornutum* B2089.

Collection @ chosun

조선대학교
CHOSUN UNIVERSITY

As stated above, the optimum concentrations of Fe^{3+}, Ca^{2+}, Mg^{2+}, EDTA, and humic acid for both algal growth were 5.0, 5.0–10.0, 2.5–5.0, 3.5–7.0, and 80.0 mg/L, respectively. Although concentrations of Fe^{3+}, Ca^{2+}, Mg^{2+}, and humic acid in the culture medium were relatively low, their concentrations increased to 1.86, 7.93, 7.04, and 80.0 mg/L in JM (*B. braunii* LB572) and 1.33, 5.88, 4.08, and 80.0 mg/L in f/2 medium (*P. tricornutum* B2089), respectively, when mixed with oceanic sediment at a ratio of 6:4 (v/v). From this comparison, it is expected that the oceanic sediment can supply and satisfy the optimal concentrations of several growth-stimulators for *B. braunii* LB572 and *P. tricornutum* B2089. Finally, the biomass and lipid productions of *B. braunii* LB572 and *P. tricornutum* B2089 cultured in a medium mixed with sediment were compared with those of other related microalgae grown on other carbon sources (Table 4-3). Consequently, the low cost of oceanic sediment would allow it to be easily utilized for microalgal cultivation for commercial purpose. In the near future, a large-scale cell cultivation will be conducted in 10 L tubular photobioreactors containing oceanic sediment medium.

Collection @ chosun

조선대학교
CHOSUN UNIVERSITY

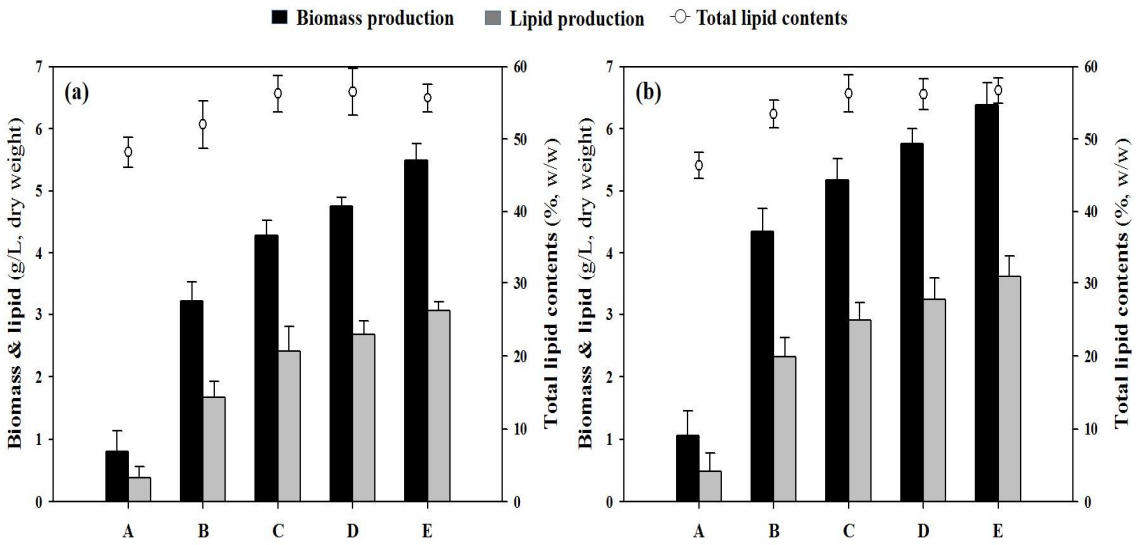

Fig. 4-5. Comparison of biomass and lipid production, and roral lipid contents of (a) *B. braunii* LB572 and (b) *P. tricornutum* B2089 cells cultivated on the corresponding medium containing different components: A algal medium (control); B optimized conc. of Fe^{3+}; C optimized conc. of metal ions (Fe^{3+}, Ca^{2+}, and Mg^{2+}); D optimized conc. of metal ions (Fe^{3+}, Ca^{2+}, and Mg^{2+}) plus humic acid; and E oceanic sediment extract (6:4, v/v).

Collection @ chosun

조선대학교
CHOSUN UNIVERSITY

Table 4-3. Comparison of biomass and lipid production of *B. braunii* and *P. tricornutum* with other related microalgae

Microalgae	Culture mode	Carbon sources (g/L)	Biomass production (g/L)	Total lipid contents (%, w/w)	Ref.
B. braunii TRG	mixotrophic	Glucose (5.0)	2.46	37.5	Yeesang and Cheirsilp, 2014
B. braunii FC124	mixotrophic	Glucose (5.0)	2.40	34.9	Gim et al., 2014
B. braunii LB572	mixotrophic	DOC in sediment (1.0)	5.54	55.8	This study
P. tricornutum UTEX-640	mixotrophic	Glycerol (9.2)	7.04	-	Cerón-García et al., 2006
P. tricornutum B2089	mixotrophic	DOC in sediment (1.0)	6.41	56.3	This study

Collection @ chosun

조선대학교
CHOSUN UNIVERSITY

Chapter V

Effect of light intensity and photoperiod on the cell growth, lipid accumulation and fatty acid composition in microalgal cells under mixo-trophic culture mode

Collection @ chosun

조선대학교
CHOSUN UNIVERSITY

1. Introduction

Microalgae is a 3rd-generation biodiesel feedstock and has been developed as one of the most promising alternative raw materials for biodiesel production because of its higher biomass production and energy conversion efficiency [Becker, 1994; Mata et al., 2010].

B. braunii is a colonial green microalga living in fresh water, such as lake and ponds [Wake and Hillen, 1980], and *P. tricornutum* is a marine diatom. These two microalgae strains contained a relatively high lipid content of about 30-60% (w/w), and were suitable for alternative source of energy production [Banerjee et al., 2002; Ruangsomboon, 2012]. It is known that biomass production of *B. braunii* and *P. tricornutum* were 3.5 g/L [Zhila et al., 2011] and 0.26 g/L [Song et al., 2013], respectively, under photoautotrophic culture mode. However, biomass production and lipid accumulation of *Botryococcus* species increased under mixotrophic culture condition, but total lipid content was still less than 40% (w/w) [Gim et al., 2014; Yeesang and Cheirsilp, 2014]. In addition, there are not so many researches on lipid production of *Phaeodactylum* strain under mixotrophic cultivation. Fortunately, it is possible to obtain high cell growth and lipid accumulation of both microalgal cells by mixotrophic cultivation with oceanic sediment extract.

Generally, various environment factors such as macronutrients, trace elements, temperature, and photo regimes are affecting the growth rates of microalgal cells. Especially light is the basic energy source for photosynthesis and essential for microalgal growth and assimilation metabolism [George, et al., 2014; Guihéneuf et al., 2009; He et al., 2015a and b; Khotimchenko and Yakovleva, 2005; Liu et al., 2012; Wahidin et al., 2013]. Photosynthesis and biomass productivity of microalgae are greatly improved in the appropriate light intensity. Light energy are generally used for biomass and cell membrane

Collection @ chosun

조선대학교
CHOSUN UNIVERSITY

formation by allocating energy into the photosynthetic complexes and chloroplast membrane matrix, respectively, under limited light energy [Khotimchenko and Yakovleva, 2005; Hu et al., 2008]. When light intensity is very high, ROS is remarkably increased, and microalgae are pressed to strong oxidative stress, which inhibit cell growth and photosynthesis activity. However, accumulation of lipid and triacylglyceride (TAG) tends to increase [Zhang et al., 2013].

Additionally, Downstream processes such as harvest-disruption-extraction, which require relatively high energy and high cost, are recognized as bottlenecks in microalgal biorefinery process [Günerken et al., 2015; Lee et al., 2015]. Microalgal cells walls are relatively thick, and globules such as polysaccharide and protein are trapped in cell membranes, making it very difficult to disrupt microalgae [Gerken et al., 2013; Günerken et al., 2015]. Therefore, it is not easy to extract various products from microalgal cells [Gerken et al., 2013]. As shown in Fig. 1-6, various methods can be used for the cell wall disruption of microorganisms such as microalgae. In generally, the disruption methods can be classified by mechanical and non-mechanical methods [Agerkvist and Enfors, 1990; Chen et al., 2009; Middelberg, 1995; Mutanda et al., 2011].

Therefore, the present work focussed to study the effect of different photo regimes (light intensity and photoperiods) on growth, lipid accumulation, fatty acid compositions of the oil-rich microalgae, *B. braunii* LB572 and *P. tricornutum* B2089 in the 10 L-scale tubular-photobioreactor. Moreover, the six physical and chemical disruption methods (autoclave, sonication, bead-beater, microwave, french-press, and osmotic shock) for efficient lipid extraction of *B. braunii* LB572 and *P. tricornutum* B2089 were optimized, and the optimum disruption method procedure was selected for each microalgae.

Collection @ chosun

조선대학교
CHOSUN UNIVERSITY

2. Materials and Methods

2-1. Microalgae and culture medium

A microalgal strains of *B. braunii* LB572 and *P. tricornutum* B2089 were obtained from UTEX Culture Collection of Algae (The University of Texas at Austin, Austin, USA). The media used in this study were Jaworski's medium [Thompson et al., 1988] for *B. braunii* LB572, and f/2 medium [Guilard and Ryther, 1962] for *P. tricornutum* B2089. Microalgal cells obtained from culture collection were spread out on an agar surface and single colonies were isolated to avoid bacterial contamination. In a previous study, it was found that the optimal mixing ratio between species-specific medium and oceanic sediments extracts for mixotrophic cultivation was 6:4 (v/v).

2-2. Preparation of oceanic sediment extract

Oceanic sediments were collected at six coastal areas in Jeollanam-do province, Republic of Korea. Sediment samples were collected at a depth of 10-20 cm and primarily leached through a no. 4-10 Sieve (opening diameter: 4.76-2 mm) and dried at 30 °C for 24 h. 35 g of dried sediment was placed in 1 L of distilled water and treated with 10 mL of 1 N-HNO_3 to adjust pH 2.0. The mixture was stirred for 6h and then allowed to stand for 1h. Then, the supernatant was filtered using a 0.2 μm membrane filter (Pall, USA) and the final pH of the extract was adjusted to 7.0–8.0.

Collection @ chosun

조선대학교
CHOSUN UNIVERSITY

2-3. Culture conditions

2-3-1. Pre-cultivation

Pre-cultivation of two oleaginous microalgae were performed in a 5 L Erlenmeyer flask containing a working volume of 3 L of mixed medium (JM or f/2 medium:oceanic sediments extract, 6:4 (v/v)) with cotton plugs that allow exchange with the atmosphere. Microalgal cells were cultivated at 25 °C under mixotrophic culture mode. Cultures were illuminated with cool-white fluorescent lamps, which attenuated by adjusting the distance from lamps and was controlled by an illuminance meter (LT Lutron LM-81LX; Lutron Electronic Enterprise, Co., Taipei, Taiwan). Based on our previous results of optimal growth conditions, light regimes was maintained at 95 μmol photon/$m^{2/}$s and 12:12 h (Light:Dark) cycle for *B. braunii* LB572 and *P. tricornutum* B2089. Batch cultivation period was 13 days.

2-3-2. Batch cultivation in a photobioreactor

B. braunii LB572 and *P. tricornutum* B2089 were cultured in a 12 L scale tubular-type photobioreactor (70 × Φ 15 cm) containing a working volume of 10 L medium (Fig. 5-1). The photobioreactor was made of Pyrex glass and was placed horizontally to broaden the surface area of medium. Several injection ports were made on the bottom of photobioreactor for the influx of air and air flow rate was controlled with a flow meter (Dwyer, USA). The optimal pHs of *B. braunii* LB572 and *P. tricornutum* B2089 were adjusted to 7.2 and 7.8, respectively. Cultivation temperature was maintained at 25 °C and light intensity was attenuated by adjusting the distance from lamps with an illuminance meter.

Collection @ chosun

조선대학교
CHOSUN UNIVERSITY

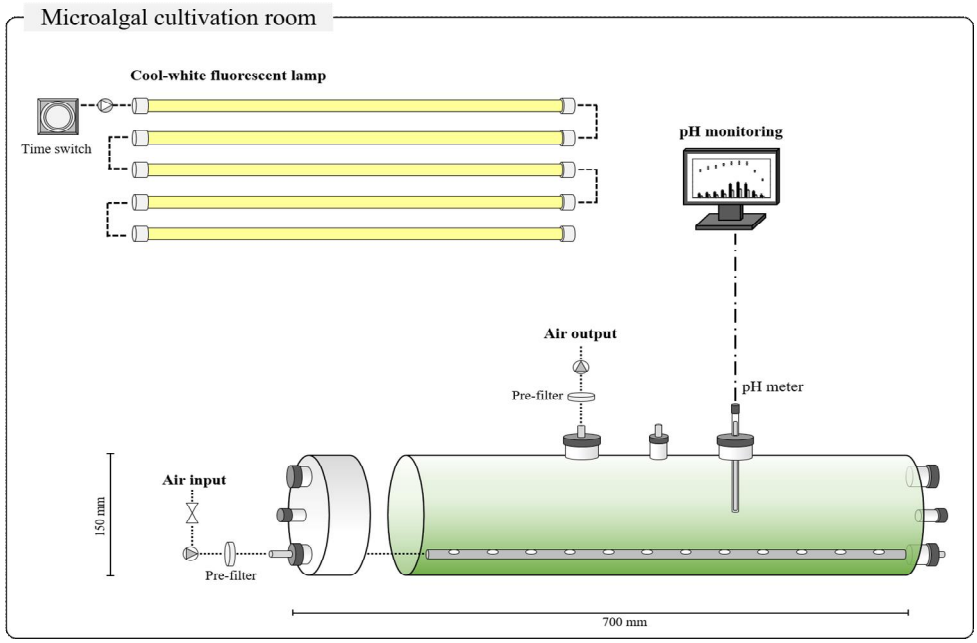

Fig. 5-1. Schematic diagram of the tubular-type photobioreactor.

2-4. Experimental conditions

Effect of photo regimes on microalgal growth, lipid accumulation, and fatty acid composition were investigated. To examine optimal light intensity and photoperiods for maximum growth and lipid accumulation of the microalgae, different light intensity (50, 95, 125, 150, 200, and 300 μmol photon/m^2/s) and photoperiod (24:0, 18:6, 12:12, and 6:18, h:h/Light:Dark cycle) were supplied. Under these different conditions, biomass production and lipid accumulation were investigated. In addition, the composition changes of fatty acid in cells was also observed.

Collection @ chosun

조선대학교
CHOSUN UNIVERSITY

2-5. Microalgal biomass and lipid contents

2-5-1. Microalgal biomass and lipid

To measure biomass and total lipid contents of microalgal cells, 500 mL of the cultured sample was collected and harvested by centrifugation at 4500 × *g* for 15 min. Then, microalgal cell pellet were frozen immediately at -80 °C and later freeze dried at -45 °C under vacuum by freeze-dryer (FD 8508 Bench-Top freeze-dryer, Ilshin BioBase, Republic of Korea). After frozen drying, the dried pellet samples were weighed using an electronic balance (Ohaus, Explorer EX623, USA) for measurements of microalgal biomass production (g/L, dry weight). Also, for estimation of total lipid contents (%, w/w), 1 g of dried pellet were washed with 200 mL of distilled water. And then the cell mixture was disrupted by microwave (Multiwave 3000, Anton Paar, Austria) at 1250 W and 2450 MHz at 150 °C for 20 min. Extraction of lipid from microalgal pellet was carried out according to a modification of the method described by Folch et al. [1957].

2-5-2. Analysis of fatty acid composition

The fatty acid composition from each microalgal strain was determined by gas chromatograph (Shimadzu GC-2010 plus, Japan). For saponification and methylation of microalgal extracted lipid was performed according to the modified procedure described by Metcalfe-Schmitz method [1966].

Collection @ chosun

조선대학교
CHOSUN UNIVERSITY

2-6. Optimization of microalgal cell disruption methods

Approximately 1 g of dried microalgal biomass was mixed with 100 mL of distilled water, and two microalgal samples were disrupted by the following various methods: autoclave (PPAC-1000, Lab house, Republic of Korea), sonication (Sonifier 250, Branson, USA), bead-beater (BioSpec Products, USA), microwave (Microwave 3000, Anton Paar, Austria), french-press (VS-4600P, Vision scientific, Republic of Korea), and osmotic shock. And the experimental conditions for the optimization of each cell disruption methods are shown in table 5-1. Moreover, the optimum disruption method of *B. braunii* LB572 and *P. tricornutum* B2089 were used to compare the efficiency of dry biomass and wet biomass of microalgae.

Table 5-1. Experimental conditions for optimization of five disruption method

Disruption methods	Conditions
Autoclave	for 5, 10, 15, 30, 60, and 90 min at 121 ℃
Sonication	resonance of 5, 10, 15, 30, and 60 kHz for 3, 5, 10, and 15 min
Bead-beater	bead diameter was 0.1, 0.5, 1.0, and 2.0 mm and high speed at 2000, 2500, 3000, and 3500 for 10 min
Microwave	power of 0, 50, 100, 500, 1000, 1200, and 1250 W for 0-25 min at 20-200 ℃ under 2450 MHz
French-press	at 500, 1000, 2000, 2500, and 3000 psi
Osmotic shock	using a 0, 0.1, 0.3, 0.5, 0.7, 1.0, and 2.0 M NaCl with a stirred for 1 min and maintained 48 h

Collection @ chosun

조선대학교
CHOSUN UNIVERSITY

3. Results and discussion

3-1. Optimization of microalgal cell disruption methods

Fig. 5-2 and table 5-2 show the lipid contents of two microalgae according to the optimal conditions of the various cell disruption methods. As a result of comparing the lipid extraction efficiency of the disruption method under optimum conditions, it was highly estimated in order to microwave, french-press, autoclave, bead-beater, and sonication. Already several researcher were investigated and compared according to various disruption methods for microalgal lipid extraction. As with this studies, microwave method showed to be effective disruption method for extracting lipid and vegetable oil [Lee et al., 2010; Mahesar et al., 2008; Prabakaran and Ravindran, 2011; Rakesh et al., 2015; Virot et al., 2008]. In this study, microwave, french press, and autoclave methods were found to be most effective among the various methods. However, the french press is difficult to treat large volumes of microalgal biomass because the amount of sample that can be processed is limited. Microwave and autoclave methods were most simple and easy systems, especially, microwave disruption methods the temperature and pressure at high speeds to create temperature and pressure gradients inside and outside the microalgal cell wall, so that the lipids can be extracted efficiently without damage [Uquiche et al., 2008; Virot et al., 2008]. For the high yield and economic efficiency of the biodiesel production process from microalgae, the lipid extraction efficiency is excellent and scale-up should be easy [Lee et al., 2010]. Therefore, microwave and autoclave are most effective for commercial application because it is easy to extract and operate with a relatively high productivity as shown in this study.

Collection @ chosun

조선대학교
CHOSUN UNIVERSITY

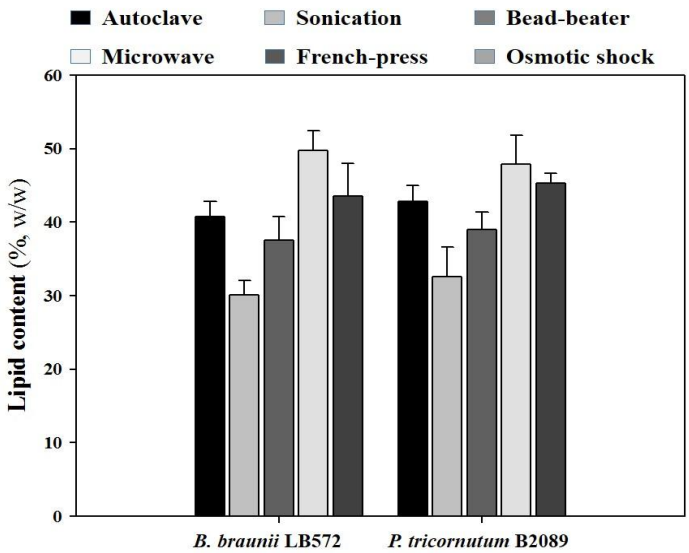

Fig. 5-2. Comparison of lipid contents of *B. braunii* LB572 and *P. tricornutum* B2089 under six optimum disruption methods.

Based on the optimized disruption conditions of previous studies, each microalgal lipid contents of dry and wet biomass were investigated respectively, and lipid extraction efficiency according to biomass condition was compared (Fig. 5-3). As a result of extracting lipids from microalgae using microwave optimal disruption method, the lipid production (lipid content, w/w) of wet biomass was estimated as follows: 0.51 g/L (44.9%, w/w) for *B. braunii* LB572 and 0.45 g/L (42.1%, w/w) *P. tricornutum* B2089, respectively. According to Fig. 5-3, compared to dry biomass, the lipid content and production of wet biomass was extracted to a level equivalent to approximately 80-90%. Guldhe et al. [2014], energy consumption by freeze-dry and dry oven was measured as 22.0 and 6 kW, respectively. It is expected that economical process will be possible through development of more effective disruption, extraction, and biodiesel conversion methods without drying process of wet biomass.

Collection @ chosun

조선대학교
CHOSUN UNIVERSITY

Table 5-2. Comparison of total lipid contents of six fresh and marine microalgae by each cell disruption methods

	Autoclave[a]	Sonication[b]	Bead-beater[c]	Microwave[d]	French-press[e]	Osmotic shock[e]
	Total lipid contents (%, w/w)					
B. braunii LB572	40.77	30.13	37.51	49.71	43.52	22.40
P. tricornutum B2089	42.80	32.57	39.00	47.91	45.28	17.70

[a] autoclaving at 121 ℃ with 1.5 MPa for 60 min

[b] sonication at a resonance of 30 kHz for 15 min

[c] bead diameter 0.1 mm at a high-speed of 3000 rpm for 10 min

[d] microwave oven at a 150 ℃ for 20 min with frequency of 1250 W and 2450 MHz

[e] press run at 3000 psi

[f] osmotic shock using a 2.0 M-NaCl with a stirred for 1 min and incubated 48 h

Collection @ chosun

조선대학교
CHOSUN UNIVERSITY

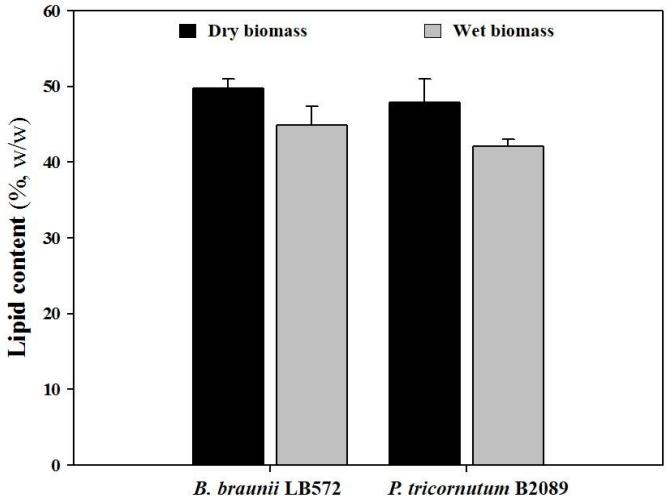

Fig. 5-3. Comparison of lipid contents of microalgal dry and wet biomass under optimum microwave method.

3-2. Cell growth and lipid content in different culture vessels

Table 5-2 shows the comparison of biomass and lipid productions of *B. braunii* LB572 and *P. tricornutum* B2089, which are cultured in different culture vessels. Microalgal species-specific medium was mixed with sediment extract at a ratio of 6:4 (v/v)), and the cells were cultured in a 5 L-Erlenmeyer flask or a 12 L photobioreactor. After 13 days incubation, specific growth rates of *B. braunii* LB572 and *P. tricornutum* B2089 in a photobioteactor increased by 1.4- and 2.1-times higher than those in a flask. Concomitantly, biomass and lipid productions of them in a photobioteactor were improved at similar ratios. Because mass culture of microalgae using photobioreactor is easy to control various culturing factors and is safe from external pollutants, it is possible to obtain maximal biomass and lipid of microalgae [Cogne et al., 2005; Ugwu et al., 2008].

Collection @ chosun

조선대학교
CHOSUN UNIVERSITY

3-3. Effect of light intensity and photoperiod on biomass production under mixotrophic cultivation mode

The effect of light intensity on the growth of *B. braunii* LB572 and *P. tricornutum* B2089 was shown in Fig. 5-4. Cell growth and lipid accumulation of *B. braunii* LB572 increased when light intensity increased up to 200 μmol photon/m^2/s. However, they dramatically decreased when light intensity reached to 300 μmol photon/m^2/s. In case of *P. tricornutum* B2089, biomass production increased as light intensity increased up to 150 μmol photon/m^2/s, but higher intensity gradually inhibited biomass production. Already, many literatures have mentioned that enough light intensity and duration time stimulated microalgal growth, however, excessive light regimes could decline cell growth [He et al., 2015a and b; Hu et al., 2008; Xiao et al., 2015]. In our previous study, we cultured the cells with light intensity of 95 μmol photon/m^2/s, then biomass production of two microalgae was as follows: 7.28 g/L for *B. braunii* LB572 and 12.6 g/L for *P. tricornutum* B2089, respectively. When they were cultured with light intensity of 200 or 150 μmol photon/m^2/s, respectively, their biomass production improved to 7.64 g/L for *B. braunii* LB572 and 13.4 g/L for *P. tricornutum* B2089, respectively. The increased microalgal growth and biomass production were due to the increased light intensity, and the similar patterns are observed in various microalgal strains such as *Ankistroedesmus fusiformis* H1 [He et al., 2015b], *Nannochloropsis* sp. [Wahidin et al., 2013], *Chlorella* sp. L1, *Monoraphidium* sp. [He et al., 2015a], *Scenedesmus* sp. [Liu et al., 2012], and *B. braunii* KMITL 2 [Ruangsomboon, 2012]. Biomass production increased as light intensity increased, but it tended to decrease at relatively high light intensity. Under high light conditions, the excited electrons of photosystem II exceed the transport capacity of the electron transport chain system so that they increase ROS (reactive oxygen species), which increase oxidative stress or inhibit photosynthesis activity. On the other

Collection @ chosun

조선대학교
CHOSUN UNIVERSITY

hand, excess light intensity strongly stimulated the accumulation of lipid and TAGs [Zhang et al., 2013].

The effect of four different photoperiods conditions (24:0, 18:6, 12:12, and 6:18, h:h/Light:Dark cycles) at different light intensity ranges (50-300 μmol photon/m^2/s) on the growth of *B. braunii* LB572 and *P. tricornutum* B2089 for 13 days cultivation is illustrated in Fig. 5-4. Maximum biomass of *B. braunii* LB572 and *P. tricornutum* B2089 were 9.05 g/L and 14.16 g/L, respectively, when they were exposed to light illumination of 18 h at 200 μmol photon/m^2/s for *B. braunii* LB572 and at 150 μmol photon/m^2/s for *P. tricornutum* B2089, respectively. On the other hand, longer light supply time than 18 h remarkably decreased biomass production in both microalgal species. Although it was possible to achieve a high growth rate with sufficient light supply, biomass production was reduced due to photo-inhibition [Wahidin et al., 2013]. Many researches reported that optimum photoperiod for the highest microalgal growth and lipid accumulation was 12:12 h or 18:6 h [Anderson, 2005; Khoeyi et al., 2012; Wahidin et al., 2013].

Collection @ chosun

조선대학교
CHOSUN UNIVERSITY

Table 5-3. Comparison of biomass and lipid productions of two oleaginous microalgal cells in different culture vessels

	3 L-Erlenmeyer flask						12 L-tubular photobioreactor					
	Light				Lipid		Light				Lipid	
	Intensity (μmol photon/m^2/s)	Periods (h:h/L:D)	Specific growth rate (d^{-1})	Biomass production (g/L)	Content (%, w/w)	Production (g/L)	Intensity (μmol photons/m^2/s)	Periods (h:h/L:D)	Specific growth rate (d^{-1})	Biomass production (g/L)	Content (%, w/w)	Production (g/L)
***B. braunii* LB572**	95	12:12	0.39	5.54	55.2	3.06	95	12:12	0.55	7.28	57.0	4.15
***P. tricornutum* B2089**	95	12:12	0.45	6.41	56.5	3.62	95	12:12	0.96	12.55	58.4	7.45

Collection @ chosun

조선대학교
CHOSUN UNIVERSITY

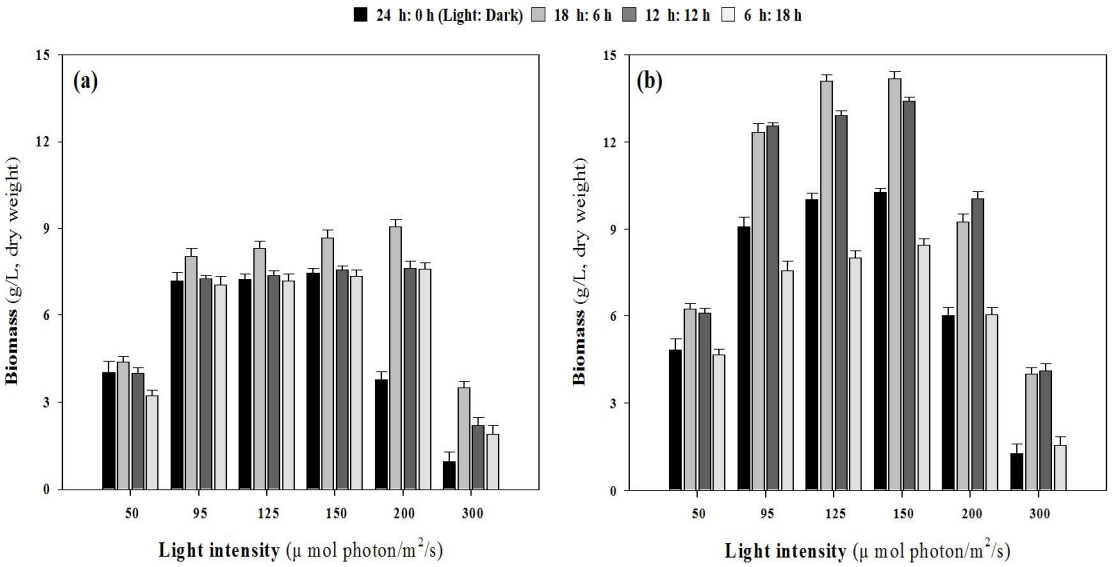

Fig. 5-4. Effect of light intensity and photoperiod on biomass production of (a) *B. braunii* LB572 and (b) *P. tricornutum* B2089.

3-4. Effect of light intensity and photoperiods on lipid content

Lipid content of *B. braunii* LB572 and *P. tricornutum* B2089 was varied depending on the light intensity and photoperiods. As shown in Fig. 5-5, lipid content increased with increasing light intensity and duration time. Previous studies have also reported that lipid accumulation in microalgal cells increase with increasing light intensity and light duration time up to 18 h [George et al., 2014; Ruangsomboon, 2012; Wahidin et al., 2013]. Also, lipid production of *B. braunii* LB572 and *P. tricornutum* B2089 was similar to biomass production, and the highest lipid production of two microalgae were as follows: 5.43 g/L for *B. braunii* LB572 at 200 μmol photon/m^2/s for 18 h light illumination and 9.02 g/L for *P. tricornutum* B2089 at 150 μmol photon/m^2/s for 18 h light, respectively (data not shown). Consequently, as light duration time increased from 12 h to 18 h, lipid content increased by 1-2% and lipid production increased by 1.1-1.2 times.

Collection @ chosun

조선대학교
CHOSUN UNIVERSITY

In this study, it was found that increasing light intensity and duration time had an positive effect on the lipid accumulation as well as microalgal growth. During photosynthesis, ATP and NADPH compounds are formed in the light dependent reactions, and metabolic molecules such as lipid are synthesized by using them in the light independent reactions (dark reaction). Therefore, an appropriate proportion of photoperiod shows a synergistic effect that is positive for the growth and lipid synthesis of microalgae, and can be attributed to high productivity and economical efficiency in the microalgae culture process [Bouterfas et al., 2002; Ugwu et al., 2007].

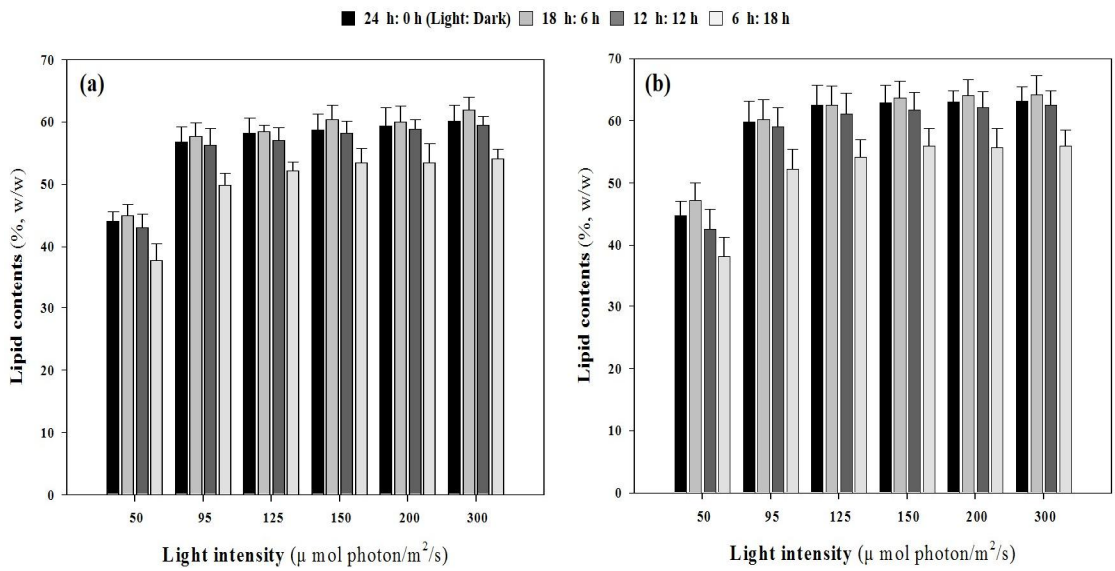

Fig. 5-5. Effect of light intensity and photoperiod on lipid content of (a) *B. braunii* LB572 and (b) *P. tricornutum* B2089.

Collection @ chosun

조선대학교
CHOSUN UNIVERSITY

3-5. Effect of light regimes on fatty acid composition

It is known that culture conditions of microalgae are important factors in the determination of quality and quantity of biodiesel through the changes of composition and content of each fatty acid [Khotimchenko and Yakovleva, 2005; Pratoomyot et al., 2005; Renaud et al., 1991]. The major fatty acids in high quality biodiesel are monounsaturated fatty acids (MUFAs) such as palmitoleic acid (C16:1) and oleic acid (C18:1) [He et al., 2015b; Knothe, 2009; Xiao et al., 2015]. As described in chapter 5, *B. braunii* LB572 and *P. tricornutum* B2089, which were cultivated photoautotrophically at 95 μmol photons/m^2/s for 12:12-h cycles, contained more than 50% of MUFAs. In addition, total fatty acid (TFA) content in cells of *B. braunii* LB572 and *P. tricornutum* B2089 cultivated mixotrophically in the sediment mixed medium was about 1.2 times higher than that in cells cultured in the species-specific medium (data not shown). Under the same illumination conditions as above, the main fatty acids contained in the two microalgae cultured mixotrophically were palmitic acid (14.9%), oleic acid (58.4%) and linolenic acid (23.6%) for *B. braunii* LB572, and palmitic acid (20.8%), palmitoleic acid (61.0%) and oleic acid (10.0%) for *P. tricornutum* B2089, respectively. Generally, as the light intensity and duration times increased, the content of SFAs and MUFAs tends to increase but PUFAs tends to decrease [Guihéneuf et al., 2009; He et al., 2015a and b; Xiao et al., 2015]. For *B. braunii* LB572, as light intensity increased from 95 to 300 μmol photon/m^2/s at photoperiod 12:12 h, the content of palmitic acid increased from 14.9 to 21.6%. And, as light intensity reached to 200 μmol photon/m^2/s, the content of oleic acid increased, but its content decreased at higher intensity. On the other hand, the content of linolenic acid (C18:3) decreased as light intensity increased. Namely, the highest content was found when light intensity was 50 μmol photon/m^2/s and illumination time was 6 h. The effect of light intensity and photoperiod on fatty acid composition in cells of *P. tricornutum* B2089 was similar with that in cells of *B. braunii* LB572. The content of palmitic acid steadily increased as light intensity increased up to 300 μmol photon/m^2/s, whereas that of

Collection @ chosun

조선대학교
CHOSUN UNIVERSITY

palmitoleic or oleic acid increased as light intensity increased up to 200 μmol photon/m^2/s. However, the content of linoleic acid (C18:2) decreased continuously as light intensity increased. Similary, as light illumination time increased from 12 to 24 h at any light intensity ranges, the content of SFAs and MUFAs slightly increased, however, that of PUFAs tended to decrease. In both microalgae, stearic acid (C18:0) content was observed at very low level regardless of light intensity and duration time.

Collection @ chosun

조선대학교
CHOSUN UNIVERSITY

Table 5-4. Fatty acid composition of *B. braunii* LB572 under various light regimes

Light regimes	Light intensity (μmol photon/m^2/s)																							
	50				95				125				150				200				300			
	Photoperiods (h:h, light:dark)																							
	6:18	12:12	18:6	24:0	6:18	12:12	18:6	24:0	6:18	12:12	18:6	24:0	6:18	12:12	18:6	24:0	6:18	12:12	18:6	24:0	6:18	12:12	18:6	24:0
	Fatty acid composition (%, total fatty acid)																							
C16:0	12.8	13.2	13.3	13.3	14.5	14.9	15.1	15.3	14.6	15.3	15.5	15.7	15.1	15.6	15.7	15.9	16.2	16.7	16.9	17.2	20.9	21.6	22.0	22.5
C16:1	0.6	0.7	0.8	1.0	0.5	0.7	0.8	1.2	0.6	0.8	1.0	1.1	0.9	0.9	1.0	1.3	1.0	1.2	1.3	1.5	2.2	3.5	3.7	4.0
C18:0	2.0	1.8	1.8	1.9	0.6	0.7	0.7	0.8	0.9	0.8	0.7	1.2	1.0	0.8	0.9	1.1	1.5	1.1	1.0	1.2	3.8	3.3	3.4	3.7
C18:1	40.0	50.2	50.8	51.4	55.3	58.4	59.0	59.6	56.0	59.2	61.1	61.9	59.4	62.3	63.1	**63.6**	58.8	62.5	63.2	**64.0**	56.0	56.5	57.1	57.4
C18:2	6.8	1.4	3.0	4.3	4.1	1.7	1.4	0.3	5.4	2.0	0.5	0.1	1.8	0.1	0.3	0.0	3.2	0.4	0.1	0.0	0.4	0.3	0.2	0.3
C18:3	37.8	32.7	30.3	28.1	25.0	23.6	23.0	22.8	22.5	21.9	21.2	20.0	21.8	20.3	19.0	18.1	19.3	18.1	17.5	16.1	16.7	14.8	13.6	12.1
SFA	14.8	15.0	15.1	15.2	15.1	15.6	15.8	16.1	15.5	16.1	16.2	16.9	16.1	16.4	16.6	17.0	17.7	17.8	17.9	18.4	24.7	24.9	25.4	26.2
MUFA	40.6	50.9	51.6	52.4	55.8	59.1	59.8	60.8	56.6	60.0	62.1	63.0	60.3	63.2	64.1	**64.9**	59.8	63.7	64.5	**65.5**	58.2	60.0	60.8	61.4
PUFA	44.6	34.1	33.3	32.4	29.1	25.3	24.4	23.1	27.9	23.9	21.7	20.1	23.6	20.4	19.3	18.1	22.5	18.5	17.6	16.1	17.1	15.4	13.8	12.4
Total	100																							

Collection @ chosun

조선대학교
CHOSUN UNIVERSITY

Table 5-5. Fatty acid composition of *P. tricornutum* B2089 under various light regimes

Light regimes	Light intensity (μmol photon/m^2/s)																							
	50				95				125				150				200				300			
	Photoperiods (h:h, light:dark)																							
	6:18	12:12	18:6	24:0	6:18	12:12	18:6	24:0	6:18	12:12	18:6	24:0	6:18	12:12	18:6	24:0	6:18	12:12	18:6	24:0	6:18	12:12	18:6	24:0
	Fatty acid composition (%, total fatty acid)																							
C16:0	17.9	19.3	19.7	20.0	20.2	20.8	20.7	21.0	21.0	21.3	21.4	21.6	21.3	21.8	22.1	22.3	21.8	22.7	23.3	22.8	22.2	23.6	23.7	24.1
C16:1	55.1	57.8	58.2	58.4	58.3	61.0	61.1	61.2	60.4	62.3	62.3	62.4	61.1	63.1	63.3	**63.6**	64.9	65.3	65.7	**65.9**	64.1	64.2	64.4	64.6
C18:0	3.1	2.7	2.4	2.2	1.9	0.2	0.2	0.3	0.4	0.2	0.2	0.2	0.4	0.3	0.3	0.6	0.5	0.4	0.3	0.7	0.8	0.2	0.4	1.2
C18:1	7.5	8.4	8.8	9.0	11.2	10.0	10.4	10.8	10.3	10.8	10.9	11.0	11.7	12.0	12.4	12.8	11.0	10.5	10.3	10.0	9.0	9.2	9.2	9.5
C18:2	9.8	8.0	8.9	9.3	8.2	7.8	7.4	6.4	7.8	5.2	5.0	4.5	5.4	2.7	1.9	0.7	1.7	0.9	0.4	0.6	3.9	2.7	2.1	0.6
C18:3	6.6	3.8	2.0	1.1	0.2	0.2	0.2	0.3	0.1	0.2	0.2	0.3	0.1	0.1	0.0	0.0	0.1	0.2	0.0	0.0	0.0	0.1	0.2	0.0
SFA	21.0	22.0	22.1	22.2	22.1	21.0	20.9	21.3	21.4	21.5	21.6	21.8	21.7	22.1	22.4	**22.9**	22.3	23.1	23.6	**23.5**	23.0	23.8	24.1	25.3
MUFA	62.6	66.2	67.0	67.4	69.5	71.0	71.5	72.0	70.7	73.1	73.2	73.4	72.8	75.1	75.7	76.4	76.9	75.8	76.0	75.9	73.1	73.4	73.6	74.1
PUFA	16.4	11.8	10.9	10.4	8.4	8.0	7.6	6.7	7.9	5.4	5.2	4.8	5.5	2.8	1.9	0.7	0.8	1.1	0.4	0.6	3.9	2.8	2.3	0.6
Total	100																							

Collection @ chosun

조선대학교
CHOSUN UNIVERSITY

Chapter VI

Repeated batch and continuous cultivation of two oleaginous microalgae in photobioreactor and direct-transesterification for biodiesel production

Collection @ chosun

조선대학교
CHOSUN UNIVERSITY

1. Introduction

The entire world is working hard to find solutions to the economic and strategic implications of producing alternative fuels from new biomass resources [Tang et al., 2012]. Microalgae have a very high potential as a biomass of bioenergy, and we can suggest possible solutions to this problem. However, commercial applications of microalgal mass production are very difficult because of the limitations of microalgal growth, lipid content, and cultivation techniques to date. Thus, development and selection of various reactors and culture types such as fed-batch, repeated-batch and continuous cultivation) are very important for mass cultivation of microalgae [Carvalho et al., 2006]. The culture type affects the microalgal growth and biochemicals as well as various growth factors [Han et al., 2013]. Until recently, various cultivation techniques have been studied for lipid synthesis and promotion of microalgal growth, however, most research and commercialization have been performed in most batch system [Gardner et al., 2011; Kitaya et al., 2008; Liu et al., 2011]. However, studies are underway on optimization and process development on various mass cultivation systems such as fed-batch [Cerón-García et al., 2013; McGinn et al., 2012; Mirón et al., 2002; Ruiz et al., 2013], repeated-batch [Kaewpintong et al., 2007; Radmann et al., 2007; Reinehr and Costa, 2006], semi-continuous [Ashokkumar et al., 2014; Cerón-García et al., 2013; Feng et al., 2014; Han et al., 2013; Rodolfi et al., 2009; Yoon et al., 2015], continuous culture system [Alonso et al., 2000; Ethier et al., 2011; McGinn et al., 2012]. The various cultivation types of the above microalgae could be accompanied by the economics of large-scale culture systems [Bezerra et al., 2011].

The process of extracting lipids from biomass of cultured microalgae is an essential and limited process in the biodiesel production process. In fact, many energy and chemicals are used to effectively extract lipids from microalgal cells, and it is nor easy to

Collection @ chosun

조선대학교
CHOSUN UNIVERSITY

apply them in the actual biodiesel field [Ehimen et al., 2010; Gerken et al., 2013; Günerken et al., 2015; Hidalgo et al., 2013]. Transesterification (or alcoholysis) is a reaction in which fatty acid methyl esters (FAMEs) and glycerol are produced through the reaction of triglyceride with alcohol such as methanol, and the reaction is promoted through the use of catalysts such as acids, bases, and enzymes [Chisti, 2007]. The biodiesel production process using microalgae has many obstacles such as high cost biomass production and biodiesel conversion process, and low-yield biodiesel conversion [Ehimen et al., 2010]. Therefore, the development of single lipid extraction-transesterification of microalgal biomass is an invaluable technology in biodiesel production facilities [Jin et al., 2014].

In this study, biomass and lipid production and productivity of *B. braunii* LB572 and *P. tricornutum* B2089 according to repeated-batch and continuous culture systems were compared in the 10 L-scale tubular-photobioreactor under optimal culture conditions and mixed media examined (Chapter IV and V). In addition, a single process of dry-diruption-extraction-transesterification process using the wet biomass of microalgae cultured and FAMEs yield and productivity of two microalgae were investigated.

Collection @ chosun

조선대학교
CHOSUN UNIVERSITY

2. Materials and Methods

2-1. Microalgae and culture medium

A microalgal strains of *B. braunii* LB572 (obtained from UTEX Culture Collection of Algae at The University of Texas at Austin, Austin, TX, USA) and *P. tricornutum* B2089 (obtained from Culture Collection of Algae and Protozoa, UK) were selected. In previous study, optimal mixing ratio was investigated for the preparation of mixed medium of microalgae species-specific medium and oceanic sediments extracts. The optimum ratio of mixed medium of *B. braunii* LB572 and *P. tricornutum* B2089 were 6:4 (v/v), respectively.

2-2. Pre-cultivation

Pre-cultivation of two oleaginous microalgae were performed in a 5 L Erlenmeyer flask containing a working volume of 3 L of mixed medium (JM and f/2: oceanic sediments extract, 6:4 (v/v)) with cotton plugs that allow exchange with the atmosphere. Microalgal cells were cultivated at 25 °C under mixotrophic culture mode. Cultures were illuminated with cool-white fluorescent lamps, which attenuated by adjusting the distance from lamps and was controlled by an illuminance meter (LT Lutron LM-81LX; Lutron Electronic Enterprise, Co., Taipei, Taiwan). Based on our previous results of optimal growth conditions and light regimes was maintained at 200 μmol photon/m^2/s and 18:6 h/Light:Dark cycle for *B. braunii* LB572 and 150 μmol photon/m^2/s and 18:6 h/Light:Dark cycle for *P. tricornutum* B2089. Each batch cultivation period for the two microalgal species were as follows: 13 days for *B. braunii* LB572 and *P. tricornutum* B2089.

Collection @ chosun

조선대학교
CHOSUN UNIVERSITY

2-3. Estimation of biomass and lipid production

To measure biomass and total lipid contents of microalgal cells, 500 mL of the cultured sample was collected and harvested by centrifugation at 4500 × *g* for 15 min. Then, microalgal cell pellet were frozen immediately at -80 °C and later freeze dried at -45 °C under vacuum by freeze-dryer (FD 8508 Bench-Top freeze-dryer, Ilshin BioBase, Republic of Korea).

After frozen drying, that dried pellet samples were weighed using an electronic balance (Ohaus, Explorer EX623, USA) for measurements of microalgal biomass production (g/L, dry weight). Also, for estimation of lipid contents (%, w/w), 1 g of dried pellet were washed with 200 mL of distilled water. And then the cell mixture was disrupted by microwave (Multiwave 3000, Anton Paar, Austria) at 150 ℃ for 20 min with radiation at 1250 W and 2450 MHz. Extracted lipid from microalgal pellet was carried out according to a modification of the method described by Folch et al. [1957]. The lipids contents were extracted with a mixture of chloroform-methanol (2:1, v/v) in a separatory funnel and shaken for 1 h. The chloroform layer (containing lipid) was selected and removed by evaporation using a rotary evaporator (Rotavapor R-205, Buchi, Switzerland) and the extracted lipids were weighed.

Collection @ chosun

조선대학교
CHOSUN UNIVERSITY

2-4. Determination of microalgal growth and dilution rate

Another method of measuring the microalgal growth was also used in this study, the specific growth rates, and the microalgal specific growth rates was calculated as follows:

$$\mu(d^{-1}) = (\ln B_2 - \ln B_1)/(T_2 - T_1) \quad \text{(Eq. 6-1)}$$

where B_2 and B_1 is the biomass productions at cultivation times T_2 and T_1, respectively. In this study, the specific growth rates was taken to be equivalent to the steady-state dilution rate (D, d^{-1}) for continuous cultivation of microalgae:

$$\mu(d^{-1}) = D(d^{-1}) \quad \text{(Eq. 6-2)}$$

Eq. 6-3 and 6-4 were used to calculate the two microalgal cultured biomass productivity in repeated batch and continuous culture systems [Feng et al., 2014; Griffiths and Harrison, 2009]:

$$BP_{repeated-batch} = (B_2 - B_1)/(T_2 - T_1) \quad \text{(Eq. 6-3)}$$

$$BP_{continuous} = (B_2 - B_1) \times D \quad \text{(Eq. 6-4)}$$

where B_2 and B_1 is the biomass productions on day T_2 and T_1, respectively. And where D is steady-state dilution rate (D, d^{-1}) for two microalgal continuous cultivation:

For microalgal lipid productivity for each culture mode was also estimation of

Collection @ chosun

조선대학교
CHOSUN UNIVERSITY

is as follows:

$$LP = (B_2 \times \frac{C_2}{100} - B_1 \times \frac{C_1}{100})/(T_2 - T_1) \quad \text{(Eq. 6-5)}$$

where B_2 and B_1 is the biomass productions and C_2 and C_1 is the lipid content on cultivation time T_2 and T_1, respectively.

2-5. Analytical methods

Metal ion concentration of oceanic sediment extract was analyzed with an ICP-MS (Elan DRCII, Perkin Elmer, USA) and TOC (also humic substances) was determined by TOC (TOC 5000, Shimadzu, Japan). The concentrations of total nitrogen (T-N) and total phosphorus (T-P) were determined by standard methods [APHA, 1995].

Collection @ chosun

조선대학교
CHOSUN UNIVERSITY

2-6. Repeated-batch and continuous cultivation in tubular-photobioreactor

B. braunii LB572 and *P. tricornutum* B2089 were repeated-batch and continuous cultivated in a designed 10 L scale tubular-photobioreactor (70 × Φ 15 cm) was used (Fig. 6-1). The photobioreactor was made of Pyrex glass and it was placed horizontally for microalgal cells incubation to broaden the surface area of medium supplied with air (containing carbon dioxide). Several injection ports were made on the bottom of photobioreactor for the influx of air and proper air flow rate controlled at 1.0 vv/m with a flow meter (Dwyer, USA). The optimal pH of *B. braunii* LB572 and *P. tricornutum* B2089 were 7.2 and 7.8, thus the pH in the photobioreactor was adjusted to the optimal pH for every day. repeated-batch and continuous culture using a tubular-photobioreactor of *B. braunii* LB572 and *P. tricornutum* B2089 were performed in the microalgal cultivation room. During the experiment, the cultivation room was maintained at 25 °C and each of light intensity and photoperiod was irradiated to each microalgal species using a cool-white fluorescent lamps. The light regimes of each microalgae were as follows. 200 μmol photon/m^2/s and 18:6 h/Light:Dark cycle for *B. braunii* LB572 and 150 μmol photon/m^2/s and 18:6 h/Light:Dark cycle for *P. tricornutum* B2089. Moreover, each of microalgal cultivation were used 10 L of JM: and f/2:oceanic sediments mixed medium (6:4, v/v).

Two microalgae cultures were performed for 13 days in batch culture system for specific growth rate and dilution rate. Based on the specific growth rate and dilution rate in batch culture, the optimum dilution rate was investigated by comparing the biomass productivity against each dilution rate of two microalgae in the continuous culture system. Also, the amount of feed to be recovered and fed was determined based on the optimum dilution rate in the case of repeated-batch culture. The two microalgal strains dilution rates were 0.1, 0.35, 0.5, 0.7, and 1.0 d^{-1}, respectively. The flow rate of the feed and harvest of medium to each dilution rate was controlled by peripatetic pump and operated continuously.

Collection @ chosun

조선대학교
CHOSUN UNIVERSITY

After the batch culture, the repeated-batch and continuous culture systems of *B. braunii* LB572 and *P. tricornutum* B2089 were continued for about 30 days, respectively. After batch culture, approximately 40% of algal culture was recovered, and fresh medium (microalgal species specific and oceanic sediment mixed medium, 6:4 (v/v)) of the same volume mixed medium was again supplied. In this culture mode was repeated 5 times in a cycles of 6 days.

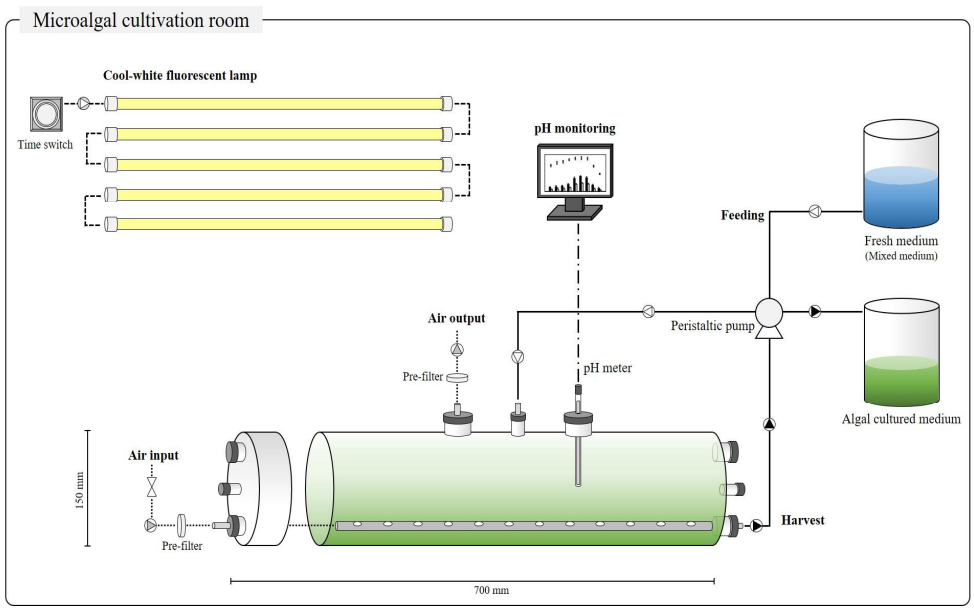

Fig. 6-1. Schematic diagram of the tubular-photobioreactor for repeated-batch and continuous cultivation systems.

Collection @ chosun

조선대학교
CHOSUN UNIVERSITY

2-7. Direct-transesterification

2-7-1. Optimization of transesterification

For the first time to optimize the transesterification process, each concentration of methanol (20, 35, 70, and 100 mL), sulfuric acid (1, 3, 6, and 10 mL, 98% purity), and chloroform (1, 4, 6, 8, and 10 mL) were optimized in about 10 g of dry microalgal biomass in the reactor of Fig. 6-2, the reaction performed at 100 ℃ for 120 min. After the optimum concentration of chemicals were investigated, the reaction temperature (50, 100, 150, 200, and 250 ℃) and reaction time (30, 60, 90, 120, and 240 min) of transesterification were optimized. At the same time, the pressure in the reactor according to reaction temperature was confirmed by pressure gauge located at the top of the reactor. After optimization, the efficiency of direct-transesterification process with dry and wet biomass were compared.

The reactor used in this reaction was a volume of 100 mL (working volume: about 80 mL), and it is possible to operate at 500 ℃ and 300 bar. The material of the reactor is 316 stainless steel (316SS) is austenitic chromium-nickel stainless rust resistant to chemical corrosion and heat-resistant steel (Fig. 6-2).

Collection @ chosun

조선대학교
CHOSUN UNIVERSITY

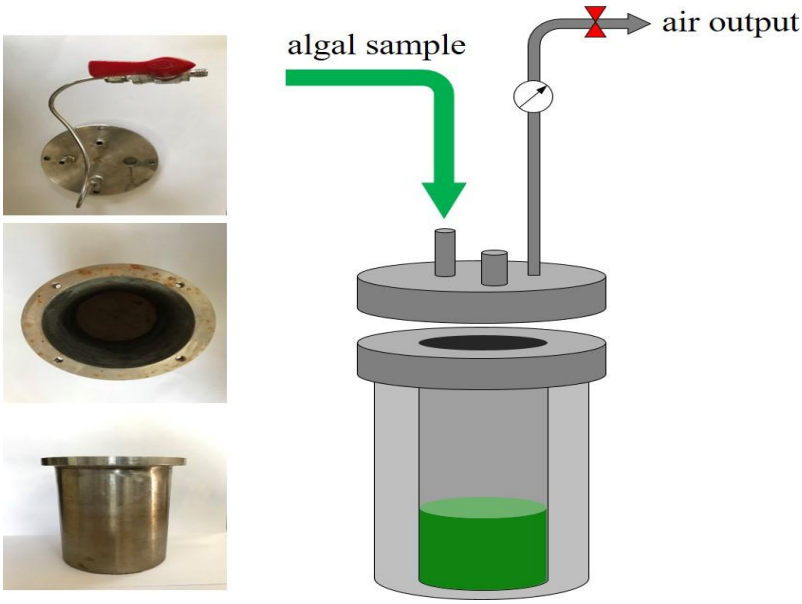

Fig. 6-2. Diagram of reactor for direct-transesterification reactor.

2-7-2. Analysis of FAME

The extracted lipid was used to analyze FAME composition by a modified saponification and methylation procedure described by Metcalfe and Schmitz [1966]. The composition of each microalgal strain was determined by gas chromatography (GC-2010 Plus; Shimadzu Corporation, Kyoto, Japan), with an art-2560 capillary column (length 100 m, 0.25 mm inner diameter, 0.25 μm film thickness) and a flame ionization detector. Operation conditions were as follows: inlet temperature 260 °C, initial oven temperature 140 °C held for 5 min and then ramped by 4 °C per min and held for 15 min, and the detector temperature 260 °C. Fatty acids were identified by a comparison of their retention times with known standards.

Collection @ chosun

조선대학교
CHOSUN UNIVERSITY

Moreover, the productivity of FAME was calculated (Eq. 6-6) as the productivity of microalgal biomass and the fatty acid content measurement by gas chromatography.

$$FAP\,(mg/L/d) = P_{biomass} \times FA\,(\%) \qquad \text{(Eq. 6-6)}$$

Additionally, The efficiency of the direct-transesterification was calculated by following equation:

$$FAME_{yield}\,(\%\,of\ microalgal\ lipid) = FAME\,(\%)/\,Lipid\,(\%) \times 100 \qquad \text{(Eq. 6-7)}$$

where FAME (%, w/w) is content by GC-FID of fatty acid methyl esters and lipid represent the content of gravimetric measurement.

Collection @ chosun

조선대학교
CHOSUN UNIVERSITY

3. Results and discussion

3-1. Microalgal growth rate and dilution rate

In the batch culture type, the specific growth rate were 0.33 d^{-1} for *B. braunii* LB572 and 0.37 d^{-1} for *P. tricornutum* B2089 in photobioreactor, and according to Eq. 2, the dilution rate was used as specific growth rate value, respectively. The biomass and lipid production of two microalgae were as follows (Fig. 6-3): 7.28 and 4.15 g/L for *B. braunii* LB572 and 12.80 and 7.45 g/L for *P. tricornutum* B2089, respectively.

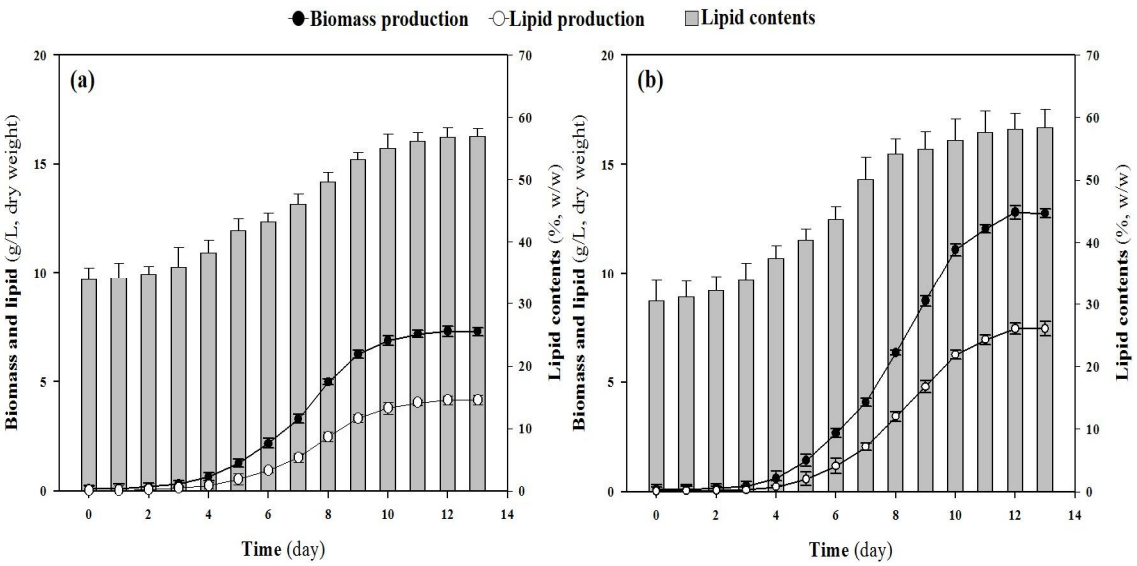

Fig. 6-3. Measurement of growth rate, biomass production, and lipid content of (a) *B. braunii* LB572 and (b) *P. tricornutum* B2089 in batch culture using tubular-photobiorector.

Collection @ chosun

조선대학교
CHOSUN UNIVERSITY

3-2. Continuous cultivation

As shown in Fig 6-4, the *B. braunii* LB572 and *P. tricornutum* B2089 were cultured for 13 days under batch culture type, and then continuous cultivation was carried out according to the respective dilution rate, the highest dilution rate of biomass production of the both microalgae was 0.1 d^{-1}. As the dilution rate increased, biomass production decreased gradually. however, at 0.1 d^{-1} with the highest biomass production, the biomass productivity of both microalgal strains were 0.77 and 1.29 g/L/d, approximately 3 times lower than the biomass productivity at 0.35 d^{-1}. Biomass productivity of two microalgae also declined as the dilution rate increased to over 0.35 d^{-1}. As a result of comparing biomass production with batch culture type of two microalgal species, in continuous culture type with a dilution rate of 0.35 d^{-1}, biomass production was slightly lower in both microalgae than in batch culture mode. On the other hand, the biomass and lipid productivity of *B. braunii* LB572 and *P. tricornutum* B2089 were about 4 times higher than the batch culture type in continuous cultivation at 0.35 d^{-1}. According to Tang et al., [2012], the dilution rate in continuous culture of *Chlorella minutissima* has a significant effect on the steady-state cell density and biomass production, and cell density and biomass production tend to decrease with increasing dilution rate. The biomass and lipid productivity of various microalgal species by continuous or semi-continuous culture type were compared with the results of this study. In particular, Cerón-García et al. [2013] reported that biomass production of *P. tricornutum* UTEX640 was 8.87 g/L and productivity was 1.49 g/L/d when cultivated in semi-continuous culture mode, the above results are about 1.4-3.0 times lower than biomass production and productivity of *P. tricornutum* B2089 (in this study) by continuous culture mode. As shown table 6-3, the biomass productivity of microalgae in continuous and repeated-batch cultivation types were lower than that of present study.

Collection @ chosun

조선대학교
CHOSUN UNIVERSITY

The concentration of nutrients and trace elements in the culture medium maintained a suitable concentration for microalgal growth during continuous cultivation of both microalgae, also the pH was maintained ar a constant pH range without significant changes (Fig. 6-5).

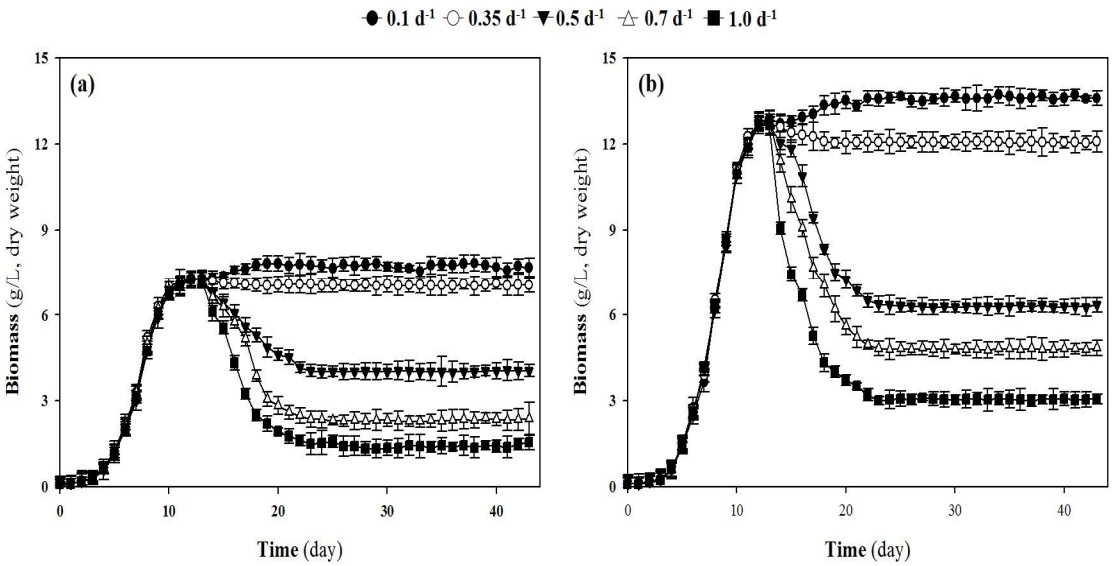

Fig. 6-4. Effect of dilution rate (d^{-1}) on biomass production of (a) *B. braunii* LB572 and (b) *P. tricornutum* B2089 in continuous cultivation under mixotrophic culture condition.

Collection @ chosun

조선대학교
CHOSUN UNIVERSITY

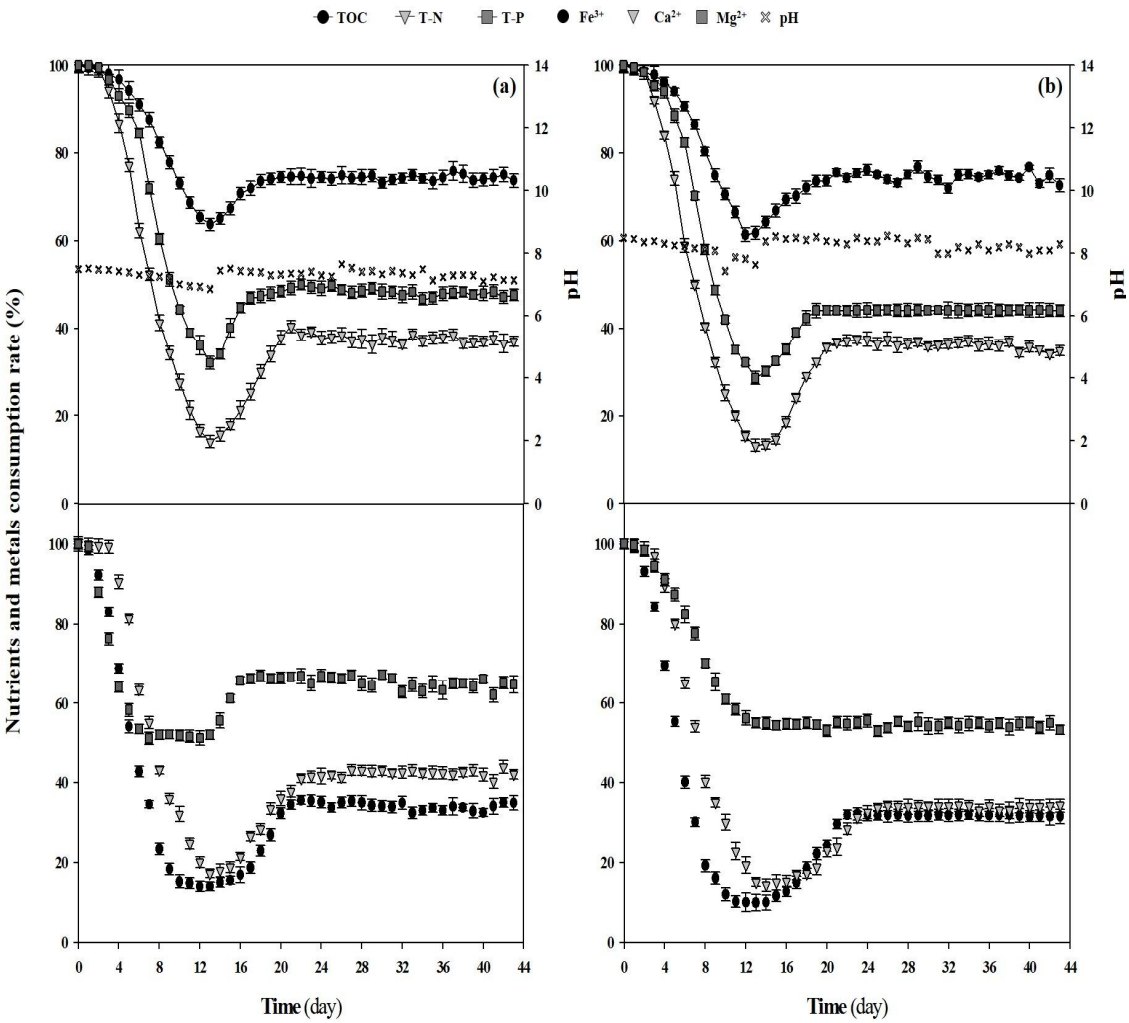

Fig. 6-5. Investigation of various nutrients (C, N, and P) and metal ions consumption rate (%) during the continuous cultivation (0.35 d^{-1}) of (a) *B. braunii* LB572 and (b) *P. tricornutum* B2089.

Collection @ chosun

조선대학교
CHOSUN UNIVERSITY

Table 6-1. Comparison of two microalgal biomass and lipid productivity in continuous culture mode

Microalgae	Dilution rate (d-1)	Biomass		Lipid		
		Production (g/L)	Productivity (g/L/d)	Content (%, w/w)	Production (g/L)	Productivity (g/L/d)
B. braunii LB572	Batch	7.28	0.55	57.0	4.15	0.32
	0.1	7.71	0.77	57.2	4.41	0.44
	0.35	7.07	2.47	56.8	4.02	1.41
	0.5	4.44	2.22	50.3	2.23	1.12
	0.7	2.92	1.46	41.2	1.20	0.84
	1.0	1.98	0.99	33.8	0.67	0.67
P. tricornutum B2089	Batch	12.75	0.97	58.4	7.45	0.57
	0.1	12.88	1.29	58.0	7.47	0.75
	0.35	12.11	4.24	57.8	7.00	2.45
	0.5	7.10	3.55	52.4	3.72	1.86
	0.7	5.61	2.80	43.9	2.46	1.72
	1.0	3.71	1.86	30.5	1.13	1.13

Collection @ chosun

조선대학교
CHOSUN UNIVERSITY

3-3. Repeated-batch cultivation

After batch cultured for 13 day, *B. braunii* LB572 and *P. tricornutum* B2089 were repeated batch cultured 5 times (every 6 days) in 10 L-scale tubular-photobioreactor. As shown Fig. 6-6 and 6-7, biomass and lipid production of *B. braunii* LB572 and *P. tricornutum* B2089 increased gradually, but lipid content did not show any significant difference in both microalgae. Biomass and lipid production in both microalgae tended to increase by about 1.1 times as the batch culture was repeated. In the 5^{th} repeated batch cultivation, biomass and lipid production of two microalgae were 13.65 and 7.96 g/L for *B. braunii* LB572 and 18.71 and 11.54 g/L for *P. tricornutum* B2089, respectively. As a result of comparing the biomass and lipid productivity of *B. braunii* LB572 and *P. tricornutum* B2089 according to repeated-batch and continuous culture type, repeated-batch cultivation type was biomass and lipid production by 1.5-2.0 times, lipid productivity by 2.5-3.4 times, and lipid content by 2-4%, respectively, higher than continuous culture type. However, there was no significant difference in biomass productivity between the both culture types. *Spirulina platensis* was able to continuously increase or maintain the biomass productivity and growth rate by repeated-batch culture type for about 50 days and this study found that cost of mass cultivation of *S. platensis* for commercialization could be reduced [Radmann et al., 2007].

Until now, there has not been much studies on the use of microalgal repeated-batch cultivation type for biodiesel production, but this study shows that the biomass and lipid productivity of *B. braunii* LB572 and *P. tricornutum* B2089 in repeated-batch cultivation were significantly higher than other researches.

Collection @ chosun

조선대학교
CHOSUN UNIVERSITY

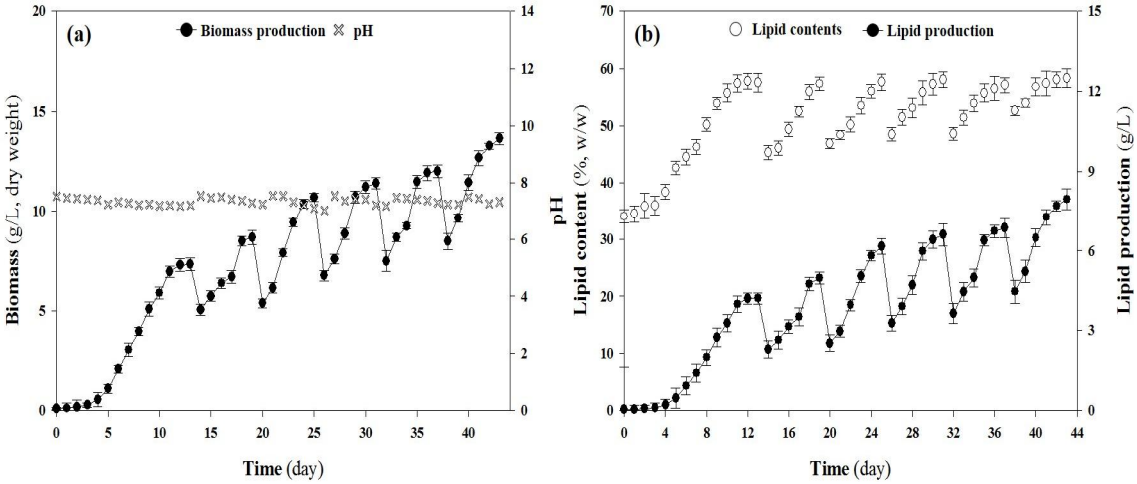

Fig. 6-6. Mixotrophic cultivation of *B. braunii* LB572 in repeated fed-batch cultivation system using tubular-photobiorector: (a) biomass production and pH and (b) lipid contents and lipid production.

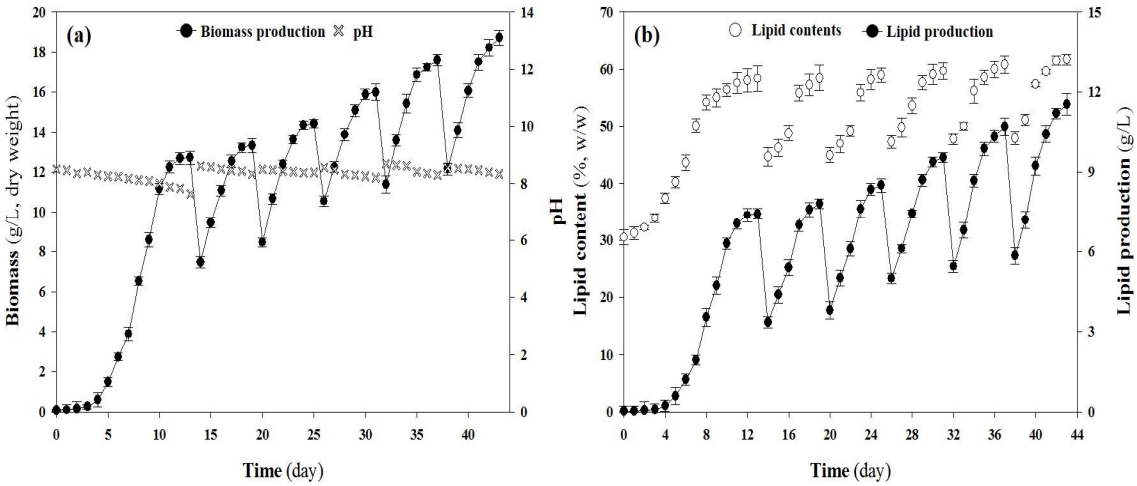

Fig. 6-7. Mixotrophic cultivation of *P. tricornutum* B2089 in repeated fed-batch cultivation system using tubular-photobiorector: (a) biomass production and pH and (b) lipid contents and lipid production.

Collection @ chosun

조선대학교
CHOSUN UNIVERSITY

Table 6-2. Comparison of two microalgal biomass and lipid productivity in repeated batch culture mode

Microalgae	Times of repeated	Biomass		Lipid		
		Production (g/L)	Productivity (g/L/d)	Content (%, w/w)	Production (g/L)	Productivity (g/L/d)
B. braunii LB572	Batch	7.32	0.56	57.5	4.21	0.32
	1st	8.68	1.72	57.3	4.97	4.64
	2nd	10.70	2.12	57.6	6.16	4.70
	3rd	11.40	2.26	58.0	6.61	4.78
	4th	12.02	2.38	57.1	6.86	4.60
	5th	13.65	2.71	58.3	7.96	4.84
P. tricornutum B2089	Batch	12.72	0.97	58.4	7.42	0.57
	1st	13.35	2.66	58.5	7.81	5.60
	2nd	14.42	2.87	59.0	8.51	5.70
	3rd	15.89	3.18	59.7	9.56	5.84
	4th	17.60	3.50	60.8	10.70	6.06
	5th	18.71	3.72	61.7	11.54	6.24

Collection @ chosun

조선대학교
CHOSUN UNIVERSITY

Table 6-3. Comparison of microalgal biomass and lipid productivity according to each culture modes

Microalgae	Culture mode	Biomass		Lipid			Ref.
		Production (g/L)	Productivity (g/L/d)	Content (%, w/w)	Production (g/L)	Productivity (g/L/d)	
N. oleoabundans	Semi-continuous	-	0.052	-	-	-	Yoon et al., 2015
Chlorella pyrenoidosa FACHB9	Semi-continuous	-	-	-	-	0.12	Han et al., 2013
S. obliquus	Semi-continuous	4.45	0.54	49.6	-	0.20	Feng et al., 2014
Spirulina platensis	Semi-continuous	4.39	1.32	-	-	-	Bezerra et al., 2011
Scenedesmus sp.	Continuous	0.31	0.23	-	-	-	Mcginn et al., 2012
P. tricornutum UTEX640	Semi-continuous	8.87	1.49	-	-	-	Cerón García et al., 2013
B. braunii TN101	Semi-continuous	33.8	-	51.5	-	-	Ashokkumar et al., 2014
Schizochytrium limacinum SR21	Fed batch	37.9	3.25	-	-	-	Ethier et al., 2011
Schizochytrium limacinum SR21	Continuous	11.8	3.48	-	-	-	Ethier et al., 2011
C. minutissima UTEX2219	Continuous	0.73	0.14	-	-	-	Tang et al., 2012
S. obliquus SAG276-10	Continuous	-	0.27	-	-	0.11	Ruiz et al., 2013
Spirulina platensis	Repeated batch	-	0.05	-	-	-	Radmann et al., 2007
B. braunii LB572	Continuous	7.07	2.47	56.8	4.02	1.41	in this study
P. tricornutum B2089	Continuous	12.11	4.24	57.8	7.00	2.45	in this study
B. braunii LB572	Repeated batch	13.65	2.71	58.3	7.96	4.84	in this study
P. tricornutum B2089	Repeated batch	18.71	3.72	61.7	11.54	6.24	in this study

Collection @ chosun

조선대학교
CHOSUN UNIVERSITY

3-4. Optimization of Driect-transesterification

In this study, the direct-transesterification was optimized for biodiesel production from the microalgal biomass, and the FAME yield of *B. braunii* LB572 and *P. tricornutum* B2089 were investigated in the optimal direct-transesterification. In order to optimize the direct-transesterification, the addition amount of methanol, sulfuric acid, and chloroform and reaction temperature and time were optimized, respectively (Fig. 6-8). The samples used were non-disrupted dry biomass, and the control of this experiment was a disrupted dry microalgal biomass.

The results of optimization of direct-transesterification from microalgal biomass was as follows: 70 mL of methanol, 6.0 mL of sulfuric acid, 8.0 mL of chloroform, 200 ℃, and 60 min for *B. braunii* LB572 and 35 mL of methanol, 6.0 mL of sulfuric acid, 8.0 mL of chloroform, 200 ℃, and 60 min for *P. tricornutum* B2089, respectively, also the pressure inside the reactor for transesterification was measured to be about 75 bar at the optimum esterified temperature of 200 ℃. FAME yield (from non-disrupted biomass) of *B. braunii* LB572 and *P. tricornutum* B2089 in the above optimized transesterification were 95.6 and 96.2%, respectively, moreover, 2-3% higher than the disrupted microalgal biomass. The above results show that dry biomass could be transesterification to more than 90% of FAME yield from extracted lipid from non-disruption process of microalgal biomass.

By controlling the dewatering and drying process of microalgal biomass, it is possible to reduce the cost of the biodiesel production [Johnson and Wen, 2009]. Direct-transesterification was carried out without drying to investigated the FAME yield of wet microalgal biomass cultured in photobioreactor. As a results, the FAME yield of wet biomass was not significantly different from that of dried microalgal biomass, however increased about 1-2% over the FAME yield of lipids extracted from dry biomass. According to table 6-4, the content of FAME contained in microalgal lipids was about 55%, and through this optimized direct-transesterification, the recovery of FAME from the

Collection @ chosun

조선대학교
CHOSUN UNIVERSITY

lipids of *B. braunii* LB572 and *P. tricornutum* B2089 were over 96%. Finally, from the wet biomass of *B. braunii* LB572 and *P. tricornutum* B2089 were cultivated 5th repeatedly, the FAME productivity were expected to be 0.26 g/L/d and 0.37 g/L/d, respectively.

Collection @ chosun

조선대학교
CHOSUN UNIVERSITY

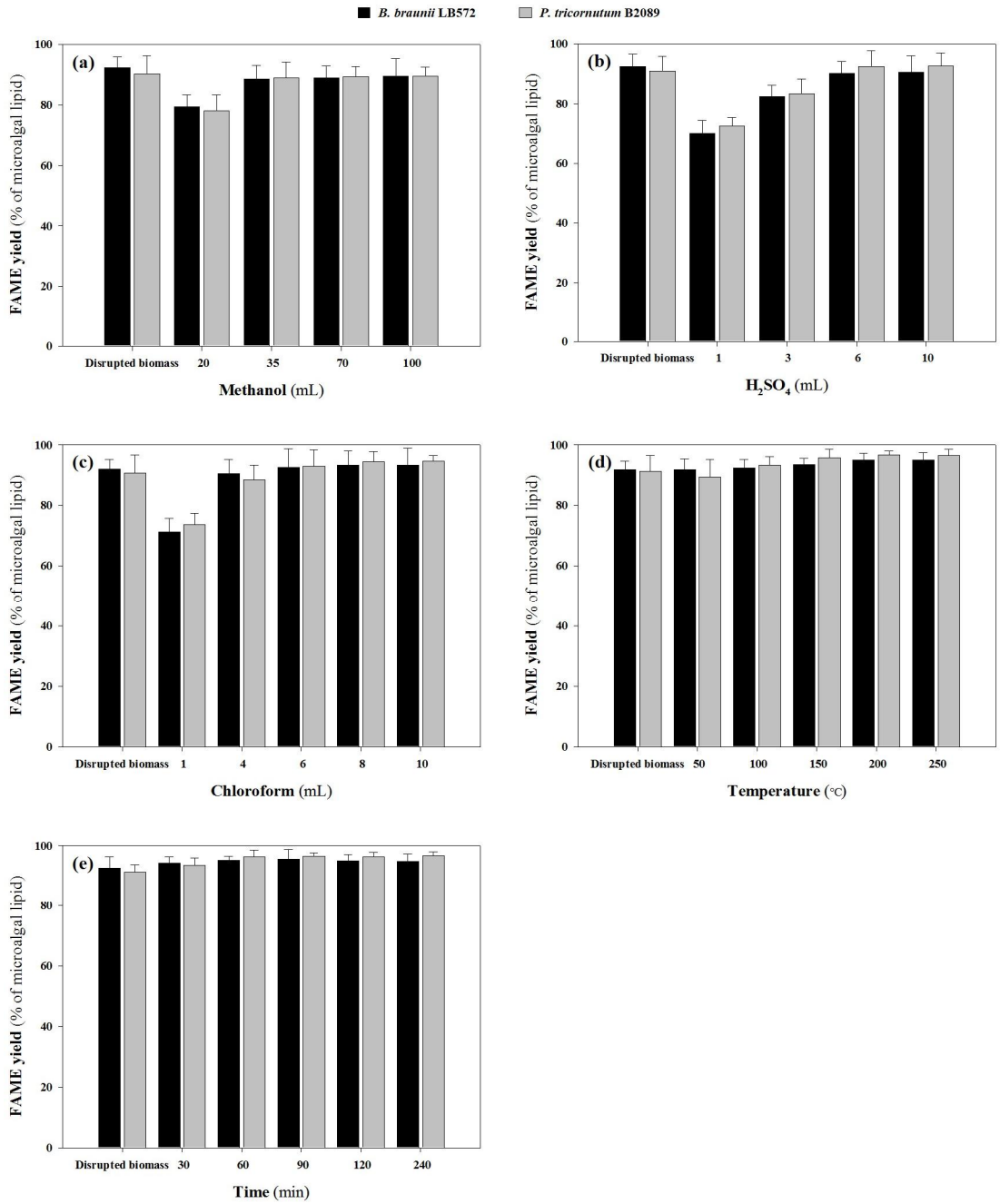

Fig. 6-8. Optimization of (a) methanol, (b) sulfuric acid, (c) chloroform, (d) temperature, and (e) reaction time for transesterification.

Collection @ chosun

조선대학교
CHOSUN UNIVERSITY

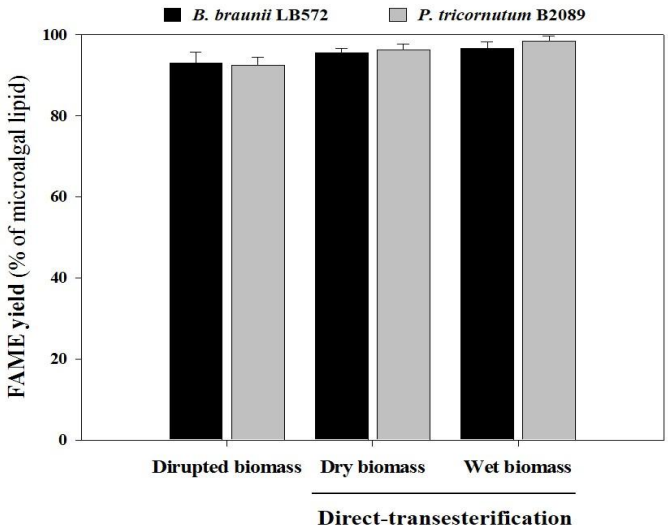

Fig. 6-9. Comparison of FAME yields of dry and wet biomass by direct-transesterification.

Collection @ chosun

조선대학교
CHOSUN UNIVERSITY

Table 6-4. Comparison of FAME yield of two microalgal wet and dry biomass using optimized direct-transesterification in the repeated-batch culture mode

	B. braunii LB572			*P. tricornutum* B2089		
	Disrupted biomass	Direct-transesterification		Disrupted biomass	Direct-transesterification	
		Dry biomass	Wet biomass		Dry biomass	Wet biomass
Lipid content (%, w/w)	57.3	57.2	51.0	58.6	58.8	54.1
FAME content (% of lipid)	53.29	54.8	55.4	54.2	56.4	57.7
FAME yield (% of lipid)	93.0	95.6	96.7	92.5	96.2	98.4
FAME productivity (g/L/d)[a]	0.25	0.26	0.26	0.34	0.36	0.37

[a] using biomass cultured in 5th repeated batch culture

Collection @ chosun

조선대학교
CHOSUN UNIVERSITY

Reference

Abd El Baky, H.H., El Baroty, G.S., Bouaid, A., Martinez, M., Aracil, J., 2012. Enhancement of lipid accumulation in *Scenedesmus obliquus* by optimizing CO_2 and Fe^{3+} levels for biodiesel production, Bioresour. Technol. 119, 429-432.

Abd El Baky, H.H., El Baroty, G.S., Bouaid, A., 2014. Lipid induction in *Dunaliella salina* culture aerated with various levels CO_2 and its biodiesel production. J. Aquacult. Res. Dev. 5, http://dx.doi.org/10.4172/2155-9546.1000223.

Agerkvist, I., Enfors, S.O., 1990. Characterization of *E. coli* cell disintegrates from a bead mill and high pressure homogenizers. Biotechnol. Bioeng. 36, 1083–1089.

Akkerman, I., Janssen, M., Rocha, J., Wijffels, R.H., 2002. Photobiological hydrogen production: photochemical efficiency and bioreactor design. Int. J. Hydrogen Energy 27, 1195-1208.

Alonso, D.L., Belarbi, E.-H., Fernández-Sevilla, J..M., Rodríguez-Ruiz, J., Molina Grima, E., 2000. Acyl lipid composition variation related to culture age and nitrogen concentration in continuous culture of the microalga *Phaeodactylum tricornutum*. Phytochemistry 54, 461-471.

Collection @ chosun

조선대학교
CHOSUN UNIVERSITY

Anderson, R.A., 2005. Algal culturing techniques. Academic Press Publication, West Boothbay Harbor.

APHA (American Public Health Association), 1995. Standard Methods for the Examination of Water and Wastewater, 19th ed., Washington, D.C., USA.

Arroyo, T.H., Wei, W., Ruan, R., Hu, B., 2011. Mixotrophic cultivation of *Chlorella vulgaris* and its potential application for oil accumulation from non-sugar materials. Biomass Bioenergy 35, 2245-2253.

Aslan, S., Kapdan, I.K. 2006. Batch kinetics of nitrogen and phosphorus removal from synthetic wastewater by algae. Ecological. Eng. 28, 64-70.

Ashokkumar, V., Agila, E., Sivakumar, P., Salam, Z., Rengasamy, R., Ani, F.N., 2014. Optimization and characterization of biodiesel production from microalgae *Botrycoccus* grown at semi-continuous system. Energy Convers. Manage. 88, 936-946.

Banerjee, A., Sharma, R., Chisti, Y., Banerjee, U.C., 2002. *Botryococcus braunii*: a renewable source of hydrocarbons and other chemicals. Crit. Rev. Biotechnol. 22, 245-279.

Collection @ chosun

조선대학교
CHOSUN UNIVERSITY

Barbosa, M.J., Zijffers, W.J., Nisworo, A., Vaes, W., Schoonhoven, V.J., Wijffels, R.H., 2005. Optimization of biomass, vitamins, and carotenoid yield on light energy in a flat-panel reactor using the A-stat technique. Biotechnol. Bioeng. 89, 233–242.

Barnwal, B.K., Sharma, M.P., 2005. Prospects of biodiesel production from vegetables oils in India. Renew. Sustain. Energy. Rev. 9, 363-378.

Barsanti, L., Gualtieri, P., 2006. Algae: Anatomy, Biochemistry, and Biotechnology. CRC Press, p. 167.

Becker, E.W., 1994. Microalgae: Biotechnology and Microbiology, Cambridge University Press, UK.

Ben Amor-Ben Ayed, H., Taidi, B., Ayadi, H., Pareau, D., Stambouli, M., 2015. Effect of magnesium ion concentration in autotrophic culture of *Chlorella vulgaris*, Algal Res. 9, 291-269.

Ben-Amotz, A., Shaish, A., Avron, M., 1991. The biotechnology of cultivation *Dunaliella* for production of β-carotene rich algae. Bioresol. Technol. 38, 233-235.

Collection @ chosun

조선대학교
CHOSUN UNIVERSITY

Bezerra, R.P., Montoya, E.Y.O., Sato, S., Perego, P. de Carvalho, J.C.M., Converti, A., 2011. Effects of light intensity and dilution rate on the semicontinuous cultivation of *Arthrospira* (*spirulina*) *platensis*. A kinetic Monod-type approach. Bioresour. Technol. 102, 3215-3219.

Bold, H.C., 1949. The morphology of *Chlamydomonas* sp. nov. Bull Torrey Bot Club 76, 101-8.

Borowitzka, M.A., Borowitzka, L.J., 1988. *Dunaliella*. In: Borowitzka, M.A., Borowitzka, L.J. (Eds.) Microalgal Biotechnology. Cambridge University Press, New York, US.

Bouterfas, K.C.D., Belkoura, M., Dauta, A., 2002. Light and temperature effects on the growth rate of three fresh water algae isolated from eutrophic lake. Hydrobiologia 489, 207-217.

Bringezu, S., Ramesohl, S., Arnold, K., Fischedick, M., Von Geibler, J., Liedtke, C., Schutz, H., 2007. Towards a sustainable biomass strategy: What we know and what we should know. Wuppertal 163, pp.1-50.

British Petroleum (BP), 2016. BP Statistical Review of World Energy 2015. BP, London, UK.

Collection @ chosun

조선대학교
CHOSUN UNIVERSITY

Brown, M.R., Dunstan, G.A., Norwood, S.J., Miller, K.A., 1996. Effects of harvest stage and light on the biochemical composition of the diatom *Thalassiosira pseudinana*. J. phycol. 32, 64-73.

Cantrell, K.B., Ducey, T., Ro, K.S., Hunt, P.G., 2008. Livestock waste-to-bioenergy generation opportunities. Bioresour. Technol. 99, 7941-7953.

Carlsson, P., Granéli, E., Segatto, A.Z., 1999. Cycling of biologically available nitrogen in riverine humic substances between marine bacteria, a heterotrophic nan nanoflagellate and photosynthetic dinoflagellate, Aquat. Microb. Ecol. 18, 23-36.

Carvalho, A.P., Meireles, L.A., Malcata, F.X., 2006. Microalgal reactors: A review of enclosed system designs and performances. Biotechnol. Prog. 22, 1490-1506.

Castenholz, R.W., 1969. Thermophilic blue-green algae and the thermal environment. Bact. Rev. 33, 476-504.

Cerón-García, M.C., Fernández-Sevilla, J.M., Sánchez-Mirón, A., García-Camacho, F., Contreras-Gómez, A., Molina-Grima, E., 2013. Mixotrophic growth of *Phaeodactylum tricornutum* on fructose and glycerol in fed-batch and semi-continuous modes. Bioresour. Technol. 147, 569-576.

Collection @ chosun

조선대학교
CHOSUN UNIVERSITY

Cerón-García, M.C., García-Camacho, F., Sánchez-Mirón, A., Fernández-Sevilla, J.M., Chisti, Y., Molina-Grima, E., 2006. Mixotrophic production of marine microalga *Phaeodactylum tricornutum* on various carbon sources, J. Microbiol. Bitechnol. 16, 689-694.

Che, R., Huang, L., Yu, X., 2015. Enhanced biomass production, lipid yield and sedimentation efficiency by iron ion, Bioresour. Technol. 192, 795-798.

Cheirsilp, B., Torpee, S., 2012. Enhanced growth and lipid production of microalgae under mixotrophic culture condition: Effect of light intensity, glucose concentration and fed-batch cultivation. Bioresour. Technol. 110, 510-516.

Chen, P., Min, M., Chen, Y., Wang, L., Li, Y., Chen, Q., Wang, C., Wan, Y., Wang, X., Cheng, Y., Deng, S., Hennessy, K., Lin, X., Liu, Y., Wang, Y., Martinez, B., Ruan, R., 2009. Review of the biological and engineering aspects of algae to fuels approach. Int. J. Agric. Biol. Eng. 2, 1-30.

Chen, Y.H., Walker, T.H., 2011. Biomass and lipid production of heterotrophic microalgae *Chlorella protothecoides* by using biodiesel-derived crude glycerol. Biotechnol. Lett. 33, 1973-1983.

Cheng, Y., Zhou, W.G., Gao, C.F., Lan, K., Gao, Y., Wu, Q.Y., 2009 Biodiesel production from Jerusalem artichoke (Helianthus Tuberosus L.) tuber by heterotrophic microalgae *Chlorella protothecoides*. J. Chem. Technol. Biotechnol. 84, 777-781.

Collection @ chosun

조선대학교
CHOSUN UNIVERSITY

Chisti, Y., 2007. Biodiesel frommicroalgae. Biotechnol. Adv. 25, 294-306.

Chojnacka, K., Marquez-Rocha, F.-J., 2004. Kinetic and stoichiometric relationships of the energy and carbon metabolism in the culture of microalgae. 3, 21-34.

Cho, S., Ji, S.C., Hur, S., Bae, J., Park, I.S., Song, Y.C. 2007 Optimum temperature and salinity conditions for growth of green algae *Chlorella ellipsoidea* and *Nannochloris oculata*. Fish. Sci. 73, 1050-1056.

Chu, S.P., 1942, The influence of the mineral composition of the medium on the growth of planktonic algae: patt I. Methods and culture media. J. Ecol. 30 (2), 284-325.

Church, J., Hwang, J.H., Kim, K.T., Mclean, R., Oh, Y.K., Nam, B., J, J.C., Lee, W.H., 2017. Effect o salt type and concentration on the growth and lipid contetn of *Chlorella vulgaris* in synthetic saline wastewater for biofuel production. 243, 147-153.

Cogne, G., Cornet, J.F., Gross, J.B., 2005. Design, operation, and modeling of a membrane photobioreactor to study the growth of the cyanobacterium *Arthrospira platensis* in space conditions. Biotechnol. Prog. 21, 741-750.

Collection @ chosun

조선대학교
CHOSUN UNIVERSITY

Concas, A., Steriti, A., Pisu, M., Cao, G., 2014. Comprehensive modeling and investigation of the effect of iron on the growth rate and lipid accumulation of *Chlorella vulgaris* cultured in batch photobioreactors, Bioresour. Technol. 153, 340-350.

Converti, A., Casazza, A.A., Ortiz, E.Y., Perego, P., Del Borghi, M., 2009. Effect of temperature and nitrogen concentration on the growth and lipid content of *Nannochloropsis oculata* and *Chlorella vulgaris* for biodiesel production. Chem. Eng. Process 48, 1146-1151.

Das, P., Lei, W., Aziz, S.S., Obbard, J.P., 2011. Enhanced algal growth in both phototrophic and mixotrophic culture under blue light. Bioresour. Technol. 102, 3883-3887.

de Martino, A., Meichenin, A., Shi, J,. Pan, K.H., Bowler, C., 2007. Genetic and phenotypic characterization of *Phaeodactylum tricornutum* (Bacillariophyceae) accessions. J. Phycol. 43, 992-1009

Demirbas, A., 2005. Biodiesel production from vegetable oils via catalytic and non-catalytic supercritical methanol transesterification methods. Pror. Energy. Combust. Sci. 31 (5–6), 466-487.

Collection @ chosun

조선대학교
CHOSUN UNIVERSITY

Dera, J., Gohs, L., Wozniak, B., 1978. Experimental study of the composite parts of the light-beam attenuation process in waters of the Gulf of Gdańsk, Oceanol. 10, 5-26.

Dismukes, G.C., Carrieri, D., Bennette, N., Ananyev, G.M., Posewitz, M.C., 2008. Aquatic phototrophs: efficient alternatives to land-based crops for biofuels. Curr. Opin. Biotechnol. 19, 235-240.

Doan, T.T.Y., Sivaloganathan, B., Obbard, J.P. 2011. Screening of marine microalgae for biodiesel feedstock. Biomass Bioenergy 35, 2534-2544.

Doering, P.H., Oviatt, C.A., McKenna, J.H., Reed, L.W., 1994. Mixing behavior of dissolved organic carbon and its potential biological significance in the Pawcatuck River Estuary, Estuaries 17, 521-536.

Doran, P.M., 1995. Bioprocess engineering principles. Published by Academic Press.

Dragone, G., Fernandes, B.,Vicente, A.A., Teixeira, J.A., 2010. Third generation biofuels from microalgae. In: Vilas, A.M., (Eds), Current Research, Technology and Education Topics in Applied Microbiology and Microbial Biotechnology, vol. 2, Formatex Research Center, Badajoz, pp. 1355-1366.

Droop, M.R., 1974. Heterotrophy of carbon, In: Stewart, W.D.P. (Eds), Algal Physiology Biochemistry Blackwell Scientific, Oxford, UK, pp. 530-559.

Droop, M.R., 1962. On cultivating *Skeletonema costatum*: some problems, in: A. Pirson (Eds.), Fisher, Stuttgart, pp.77-82.

Collection @ chosun

조선대학교
CHOSUN UNIVERSITY

Dunahay, T.G., Jarvis, E.E., Dais, S.S., Roessler, P.G., 1996. Manipulation of microalgal lipid production using genetic engineering. Appl. Biochem. Biotechnol. 57-58, 223-31.

Ehimen, E., Sun, Z., Carrington, C., 2010. Variables affecting the in situ transesterification of microalgae lipids. Fuel 89, 677-684.

Eisentraut, A., 2010. Sustainable production of second-generation biofuels potential and perspectives in major reconomies and developing countries. Int. Energy Agency (IEA), 7-8.

Ethier, S., Woisard, K., Vaughan, D., Wen, Z., 2011. Continuous culture of the microalgae *Schizochytrium limacinum* on biodiesel-derived crude glycerol for producing docosahexaenoic acid. Bioresour. Technol. 102, 88-93.

Fatih, B., 2015. World energy outlook 2015, International Energy Agency, London, UK.

Fedorov, A.S., Kosourov, S., Ghirardi, M.L., Seibert, M., 2005. Continuous H_2 photoproduction by *Chlamydomonas reinhardtii* using a novel two-stage, sulfate-limited chemostat system. Appl. Biochem. Biotechnol. 121124, 403-412.

Felizardo, P., Correia, M.J.N., Raposo, I., Mendes, J.F., Berkemeier, R., Bordado, J.M., 2006. Production of biodiesel from waste frying oil. Waste Manag. 26, 487-494.

Collection @ chosun

조선대학교
CHOSUN UNIVERSITY

Feng, P., Yang, K., Xu, Z., Wang, Z., Fan, L., Zin, L., Zhu, S., Shang, C., Chai, P., Yuan, Z., Hu, L., 2014. Growth and lipid accumulation characteristics of *Scenedesmus obliquus* in semi-continuous cultivation outdoors for biodiesel feddstock. Bioresour. Technol. 173, 406-414.

Feuillade, M., Feuillade, J., 1989. Heterotrophic capabilities of blue–green alga *Oscillatoria rubescens*. Arch. Hydrobiol. 117, 61-76.

Fernandez, F.G.A., Sevilla, J.M.F., Perez, J.A.S., Grima, E.M., Chisti, Y., 2001. Airlift driven external loop tubular photobioreactors for outdoor production of microalgae: assessment of design and performance. Chem. Eng. Sci. 56, 2721–2732.

Folch, J., Lees, M., Stanley, G.H.S., 1957. A simple method for the isolation and purification of total lipids from animal tissues, J. Biol. Chem. 226, 497-509.

Fukuda, H., Kondo, A., Noda, H., 2001. Biodiesel fuel production by transesterification of oils. J. Biosci. Bioeng. 92, 405-416.

Collection @ chosun

조선대학교
CHOSUN UNIVERSITY

Gardner, D.R., Cooksey, K.E., Mus, F., Macur, R., Moll, K., Eustance, E., Calson, R.P., Gerlach, R., Fields, M.W., Peyton, B.M., 2012. Use od sodium bicarbonate to stimulate triacylglycerol accumulation in the chlorophyte *Scenedesmus* sp., and the diatom *Phaodactylum tricornutum*. J. Appl. Phycol. 24, 1311-1320.

Gardner, R., Peters, P., Peyton, B., Cooksey, K.E., 2011. Medium pH and nitrate concentration effects on accumulation of triacylglycerol in two members of the chlorophyta. J. Appl. Phycol. 23, 1005-1016.

George, B., Pancha, I., Desai, C., Chokshi, K., Paliwal, C., Ghosh, T., Mishra, S., 2014. Effects of different media composition, light intensity and photoperiod on morphology and physiology of freshwater microalgae *Ankistrodesmus falcatus*-A potential strain for bio-fuel production. Bioresour. Technol. 171, 367-374.

Gerken, H.G., Donohoe, B., Knoshaug, E.P., 2013. Enzymatic cell wall degradation of Chlorella vulgaris and other microalgae for biofuels production. Planta. 237, 239-253.

Gerringa, L.J.A., De Baar, H.J.W., Timmermans, K.R., 2000. A comparison of iron limitation of phytoplankton in natural oceanic waters and laboratory media conditioned with EDTA, Mar. Chem. 68, 335-346.

Ghirardi, M.L., Zhang, J.P., Lee, J.W., Flynn, T., Seibert, M., Greenbaum, E., Melis, A., 2000. Microalgae: a green source of renewable H_2. Trends Biotechnol. 18, 506-511.

Collection @ chosun

조선대학교
CHOSUN UNIVERSITY

Gim, G.H., Kim, J.K., Kim, H.S., Kathiravan, M.N., Yang, H., Jeong, S.H., Kim, S.W. 2014. Comparison of biomass production and total lipid content of freshwater green microalgae cultivated under various culture conditions. Bioprocess. Biosyst. Eng. 37, 99-106.

Gim, G.H., Ryu, J., Kim, M.J., Kim, P.I., Kim S.W., 2016. Effects of carbon sources and light intensity on the growth and total lipid production of three microalgae under different culture conditions. J. Ind. Microbiol. 43, 605-616.

Giridhar Babu, A., Wu, X., Kabra, A.N., Kim, D.P., 2017. Cultivation of an indigenous Chlorella sorokiniana with phytohormones for biomass and lipid production under N-limitation. Agal Res. 23, 178-185.

Gordillo, F.J.L., Goutx, M., Figueroa, F.L., Niell, F.X. 1998. Effects of light intensity, CO_2 and nitrogen supply on lipid class composition of *Dunaliella viridis*. J. Appl. Phycol. 10, 135-144.

Gorain, P.C., Bagchi, S.K., Mallick, N., 2013. Effect of calcium, magnesium and sodium chloride in enhancing lipid accumulation in two green microalgae, Environ. Technol. 34, 1887-1894.

Gouveia, L., Oliveira, A.C., 2009. Microalgae as raw material for biofuels production. J. Ind. Microbiol. Biotechnol. 36, 269-274.

Collection @ chosun

조선대학교
CHOSUN UNIVERSITY

Granéli, E., Moreira, M.O., 1990. Effects of river water of different origin on the growth of marine dinoflagellates and diatoms in laboratory cultures, J. Exp. Mar. Biol. Ecol. 136, 89-106.

Griffiths, J.S., Harrison, S.T.L., 2009. Lipid productivity as a key characteristic for choosing algal species for biodiesel production, J. Appl. Phycol. 21, 493-507.

Griffiths, D.J., Thresher, C.L., Street, H.E., 1960. The heterotrophic nutrition of *Chlorella vulgaris*. Ann. Bot. 24, 1-11.

Grobbelaar, J.U., 2004. Algal nutrition. In: Richmond A, editor. Handbook of microalgal culture: biotechnology and applied phycology. Blackwell, pp. 97-115.

Guihéneuf, F., Mimouni, V., Ulmann, L., Tremblin, G., 2009 Combined effects of irradiance level and carbon source on fatty acid and lipid class composition in the microalgae *pavlova lutheri* commonly used in mariculture. J. Experiment. Marine. Biol. Ecol. 369, 136-143.

Guillard, R.R.L., Ryther, J.H., 1962. Studies of marine planktonic diatoms I. *Cyclotella nana* Hustedt and *Detonula confervaceae* (Cleve) Gran, Can. J. Microbiol. 8, 229-239.

Guldhe, A., Singh, B., Rawat, I., Ramluckan, K., Bux, F., 2014. Efficacy of drying and cell disruption techniques on lipid recovery from microalgae for biodiesel production. Fuel 128, 46-52.

Collection @ chosun

조선대학교
CHOSUN UNIVERSITY

Günerken, E., D'Hondt, E., Eppink, M.H., Garcia-Gonzalez, L., Elst, K., Wijffels, R.H., 2015. Cell disruption for microalgae biorefineries. Biotechnol. Adv. 33, 243-260.

Haass, D., Tanner, W., 1973. Regulation of hexose transport in *Chlorella vulgaris*. Plant Physiol. 53, 14-20.

Han, F., Huang, J., Li, Y., Wang, W., Wan, M., Shen, G., Wang, J., 2013. Enhanced lipid productivity of *Chlorella pyrenoidosa* through the culture strategy of semi-continuous cultivation with nitrogen limitation and pH control by CO_2. Bioresour. Technol. 136, 418-424.

Hannon, M., Gimpel, J., Trana, M., Rasalaa, B., Mayfieldb, S., 2014. Biofuels from algae: challenges and potential. Biofuels 1, 763-784.

Harris, E.H., 1989. The *Chlamydomonas* source book: a comprehensive guide to biology and laboratory use, Academic Press, San diego, USA, pp. 780.

Harrison, S.T.L., 1991. Bacterial cell disruption: a key unit operation in the recovery of intracellular products. Biotechnol. Adv. 9, 217-240.

Collection @ chosun

조선대학교
CHOSUN UNIVERSITY

He, Q., Yang, H., Wu, L., Hu, C., 2015a. Effects of light intensity on physiological changes, carbon allocation and neutral lipid accumulation in oleaginous microalgae. Bioresour. Technol. 191, 219-228.

He, Q., Yang, H., Hu, C., 2015b. Optimizing light regimes on growth and lipid accumulation in *Ankistrodesmus fusiformis* H1 for biodiesel production. Bioresour. Technol. 198, 876-883.

Hibberd, D.J., 1981. Notes on the taxonomy and nomenclature on the algal classes Eustigmatophyceae and Tribophyceae (synonym Xanthophyceae). Bot. J. Linn. Soc. 82, 93-119.

Hidalgo, P., Toro, C., Ciudad, G., Navia, R., 2013. Advances in direct transesterification of microalgal biomass for biodiesel production. Rev. Environ. Sci. Biotechnol. 12, 179-199.

Ho, S.H., Lu, W.B., Chang, J.S. 2012. Photobioreactor strategies for improving the CO_2 fixation effiency of indigenous *Scenedesmus obliquus* CNW-N: Statistical optimization of CO_2 feeding. Bioresour. Technol. 105, 106-113.

Hongjin, Q., Guangce, W., 2009 Effect of carbon source on growth and lipid accumulation in *Chlorella sorokiniana* GXNN01. Chinese J. Oceanol. Limnol. 27, 762-768.

Collection @ chosun

조선대학교
CHOSUN UNIVERSITY

Hosoglu, M.I., Gultepe, I., Elibol, M. 2012. Optimization of carbon and nitrogen sources for biomass and lipid production by *Chlorella saccharophila* under heterotrophic conditions and development of Nile red fluorescence based method for quantification of its neutral lipid content. Biochem. Eng. J. 61, 11-19.

Hu, Q., Sommerfeld, M., Jarvis, E., Ghirardi, M., Posewitz, M., Seibert, M., Darzins, A. 2008. Microalgal triacylglycerols as feedstocks for biofuel production: perspectives and advances. Plant J. 54, 621-639.

Huang, G.H., Chen, F., Wei, D., Zhang, X.W., Chen, G., 2010. Biodiesel production by microalgal biotechnology. Appl. Energy 87, 38-46.

Huang, L., Xu, J., Li, T., Wang, L., Deng, T., Yu, X., 2014. Effect of additional Mg^{2+} on the growth, lipid production, and fatty acid composition of *Monoraphidium* sp. FXY-10 under different culture conditions, Ann. Microbiol. 64, 1247-1256.

Imamoglu, E., Sukan, F.V., Dalay, M.C., 2007. Effect of different culture media and light intensities on growth of *Haematococcus pluvialis*. Int. J Natural. Eng. Sci. 1, 5-9.

Jin, B., Duan, P., Xu, Y., Wang, B., Wang, F., Zhang, L., 2014. Lewis acid-catalyzed in situ transesterification/esterification of microalgae in supercritical ethanol. Bioresour. Technol. 162, 341-349.

Collection @ chosun

조선대학교
CHOSUN UNIVERSITY

Jin, X., Chu, Z., Yan, F., Zeng, Q., 2009. Effects of lanthanum (III) and EDTA on the growth and competition of *Microcystis aeruginosa* and *Scenedesmus quadricauda*, Limnologica 39, 86-93.

Johnson, M.B., Wen, Z., 2009. Production of biodiesel fuel from the microalga Schizochytrium limacinum by direct transesterification of algal biomass. Energy Fuels 23, 5179-5183.

Jung, K.A., Lim, S.R., Kim, Y., Park, J.M., 2012. Potentials of macroalgae as feedstocks for biorefinery. Bioresour. Technol. 135, 182-190.

Kaewpintong, K., Shotipruk, A., Powtongsook, S., Pavasant, P., 2007. Photoautotrophic high-density cultivation of vegetative cells of *Haematococcus pluvialis* in airlift bioreactor. Bioresour. Technol. 98, 288-295.

Kalacheva, G.S., Zhila, N.O., Volova, T.G., 2002a. Lipid and hydrocarbon competition of a collection strain and awild sample of the green microalga *Botryococcus*. Aquat. Ecol. 36, 317-330.

Kalacheva, G.S., Zhila, N.O., Volova, T.G., 2002b. Lipid of the green alga *Botryococcus* cultured in a batch mode. Microbiol. 70, 256-62.

Kalplan, D., Cohen, Z., Abeliovich, A., 1986. Optimal growth conditions for *Isochrysis galbana*. Biomass 9, 37-48.

Collection @ chosun

조선대학교
CHOSUN UNIVERSITY

Kapdan, I.K., Kargi, F., 2006. Bio-hydrogen production from waste materials. Enzyme Microb. Technol. 38, 569-582.

Khotimchenko, S.V., Yakovleva, I.M. 2005. Lipid composition of the red alga *Tichocarpus crinitus* exposed to different levels of photon irradiance. Phytochemistry 66, 73-79.

Kim, W., Park, J.M., Gim, G.H., Jeong, S., Kang, C.M., Kim, D., Kim, S.W., 2012 Optimization of culture conditions and comparison of biomass productivity of three green algae. Bioprocess Biosyst. Eng. 35, 19-27.

Kitaya, Y., Xiao, L., Masuda, A., Ozawa, T., Tsuda, M., Omasa, K.. 2008. Effects of temperature, photosynthetic photon flux density, photoperiod and O_2 and CO_2 concentrations on growth rates of the symbiotic dinoflagel-late, *Amphidinium* sp. J. Appl. Phycol. 20, 737742.

Knothe, G., 2009. Improving biodiesel fuel properties by modifying fatty ester composition. Enengy Environ. Sci. 2, 759-766.

Knothe, G., Dunn, R.O., Bagby, M.O., 1997. Biodiesel: the use of vegetable oils and their derivatives as alternative diesel fuels. ACS Symp. Ser. 666, 172-208.

Kobayashi, M., Kakizono, T., Yamaguchi, K., Nishio, N., Nagai, S., 1992. Growth and astaxanthin formation of *Haematococcus pluvialis* in heterotrohpic and micotrophic conditions. J. Ferment. Bioeng. 74, 17-20.

Collection @ chosun

조선대학교
CHOSUN UNIVERSITY

Khoeyi, Z.A., Seyfabadi, J., Ramezanpour, Z., 2012. Effect of light intensity and photoperiod on biomass and fattya cid composition of the microalgae, *Chlorella vulgaris*. Aquacult. Int. 20, 41-49.

Kong, W.B., Yang, H., Cao, Y.T., Song, H., Hua, S.F., Xia, C.G., 2013. Effect of glycerol and glucose on the enhancement of biomass, lipid and soluble carbohydrate production by *Chlorella vulgaris* in mixotrophic culture. Food Technol. Biotechnol. 51, 62-69.

Koukal, B., Guéguen, C., Pardos, M., Dominik, J., 2003. Influence of humic substances on the toxic effects of cadmium and zinc to the green alga *Pseudokirchneriella subcapitata*, Chemosphere 53, 953-961.

Kulkarni, M.G., Dalai, A.K., 2006. Waste cooking oil-an economical source for biodiesel: A review. Inds. Eng. Chem. Res. 6 (45), 2901-2913.

Kumar, K., Dasgupta, C.N., Nayak, B., Lindblad, P., Das, D., 2011. Development of suitable photobioreactors for CO_2 sequestration addressing global warming using green algae and cyanobacteria. Bioresour. Technol. 102, 4945-4953.

Lee, J.Y., Yoo, C.Y., Jun, S.Y., Ahn, C.Y., Oh, H.M., 2010. Comparison of several methods for effective lipid extraction from microalgae. Bioresour. Technol. 101, S75-S77.

Lee, K., Lee, C. 2002 Nitrogen removal from wastewaters by microalgae without consuming organic carbon sources. J. Microbiol. Biotechnol. 12, 979-985.

Collection @ chosun

조선대학교
CHOSUN UNIVERSITY

Lee, S.j., Go, S., Jeong, G.T., Kim, S.K., 2011. Oil production from five marine microalgae for the production of biodiesel. Biotechnol. Bioprocess. Eng. 16, 561-556.

Lee, Y.C., Lee, K., Oh, Y.K., 2015. Recent nanoparticle engineering advances in microalgal cultivation and harvesting processes of biodiesel production: a review. Bioresour. Technol. 184, 63-72.

Leesing, R., Nontaso, N. 2010. Microalgal oil production by green microalgae under heterotrophic cultivation. KKU Res. J. 15, 787-793.

Li, X.F., Xu, H., Wu, Q.Y., 2007. Large-scale biodiesel production from microalga *Chlorella protothecoides* through heterotrophic cultivation in bioreactors. Biotechnol. Bioeng. 98, 764-771.

Li, Y., Wang, B., Wu, N., Lan, C.Q., 2008. Effects of nitrogen sources on cell growth and lipid production of *Neochloris oleoabundans*. Appl. Microbiol. Biotechnol. 81, 629-636.

Liang, Y., Sarkany, N., Cui, Y., 2009 Biomass and lipid productivities of *Chlorella vulgaris* under autotrophic, heterotrophic and mixotrophic growth conditions. Biotechnol. Lett. 31, 1043-1049.

Liu, J., Hung, J., Fan, K.W., Jiang, Y., Zhong, Y., Sun, Z., Chen, F., 2010. Production potential of *Chlorella zofingienesis* as a feedstock for biodiesel. Bioresour. Technol. 101, 8658-8663.

Collection @ chosun

조선대학교
CHOSUN UNIVERSITY

Liu, J., Huang, J.C., Sun, Z., Zhong, Y.J., Jiang, Y., Chen, F., 2011. Differential lipid and fatty acid profiles of photoautotrophic and heterotrophic *Chlorella zofingiensis*: Assessment of algal oils for biodiesel production. Bioresour. Technol. 102, 106-110.

Liu, J., Yuan, C., Hu, G., Li, F., 2012. Effects of light intensity on the growth and lipid accumulation of microalga *Scenedesmus* sp. 11-1 under nitrogen limitation. Appl. Biochem. Biotechnol. 166, 2127-2137.

Liu, Z., Wang, G., 2014. Effect of Fe^{3+} on the growth and lipid content of *Isochrysis galbana*. Chin. J. Oceanol. Limnol. 32, 47-53.

Liu, Z.Y., Wang, G.-C., Zhou, B.-C., 2008. Effect of iron on growth and lipid accumulation in *Chlorella vulgaris,* Bioresour. Technol. 99, 4717-4722.

Livne, A., Sukenik, A., 1992. Lipid synthesis and abundance of acetyl CoA carboxylase in *Isochrysis galbana* (Prymnesiophyceae) following nitrogen starvation, Plant Cell Physiol. 33, 1175-1181.

Loubiere, K., Olivo, E., Bougaran, G., Pruvost, J., Robert, R., Legrand, J., 2009. A new photobioreactor for continuous microalgal production in hatcheries based on external-loop airlift and swirling flow. Biotechnol. Bioeng. 102, 132-147.

Lürling, M., 1998. Effect of grazing-associated infochemicals on growth and morphological development in *Scenedesmus acutus* Meyen (Chlorophyceae). J. Phycol. 34, 578–586.

Collection @ chosun

조선대학교
CHOSUN UNIVERSITY

Mahesar, S.A., Sherazi, T.H., Abro, K., Kandhro, A., Bhanger, M.I., Van de Voort, F.R., Sedman, J., 2008. Application of microwave heating for the fast extraction of fat content from the poultry feeds. Talanta. 75, 1240-1244.

Mandal, M., Ghosh, A., Tiwari, O.N., Gayen, K., Das, P., Mandal, M.K., Halder, G., 2017. Influence of carbon sources and light intensity on biomass and lipid production of *Chlorella sorokiniana* BTA 9031 isolated from coalfield under various nutritional modes. Energy Convers. Manag. 145, 247-254.

Mandal, S., Mallick, N., 2009. Microalga *Scenedesmus obliquus* as a potential source for biodiesel production. Appl. Microbiol. Biotechnol. 84, 281-291.

Mata, T.M., Martins, A.A., Caetano, N.S., 2010. Microalgae for biodiesel production and other application: review. Renew. Sustain. Energy. Rev. 14, 217-232.

McGinn, P.J., Dickinson, K.E., Park, K.C., Whithey, C.G., Macquarrie, S.P., Black, F.J., Frigon, J.-C., Guiot, S.R., O'Leary, S.J.B., 2012. Assessment of the bioenergy and bioremediation potentials of the microalga *Scenedesmus* sp. AMDD cultivated in municipal wastewater effluent in batch and continuous mode. Algal Res. 1, 155-165.

Meher, L.C., Vidya Sagar, D., Naik, S.N., 2006. Technical aspects of biodiesel production by transesterification-a review. Renew. Sustain. Energy. Rev. 10, 248-268.

Melis, A., 2002. Green alga hydrogen production: progress, challenges and prospects. Int. J. Hydrogen Energy 27, 1217-1228.

Collection @ chosun

조선대학교
CHOSUN UNIVERSITY

Merzlyak, M.N., Chivkunova, O.B., Gorelova, O.A., Reshetnikova, I.V., Solovchenko, A.E., Khozin-Goldberg, I., Cohen, Z., 2007. Effect of nitrogen starvation on optical properties, pigments, and arachidonic acid content of the unicellular green alga *Parietochloris incise* (Trebouxiophyceae, Chlorophyta). J. Phycol. 43, 833-843.

Metcalfe, L.D., Schmitz, A.A., Pelka, J.R. 1966. Rapid preparation of fatty acid esters from lipids for gas chromatographic analysis. Anal. Chem. 38, 514-515.

Metting, F.B., 1996. Biodiversity and application of microalgae. J. Ind. Microbiol. 17 (5–6), 477-489.

Metzger, P., Largeau, C., 2005. *Botryococcus braunii*: a rich source for hydrocarbons and related ether lipids. Appl. Microbiol. Biotechnol. 66, 486-496.

Miao, X., Wu, Q., 2006. Biodiesel production from heterotrophic microalgal oil. Bioresour. Technol. 97, 841-846.

Middelberg, A.P.J., 1995. Process-scale disruption of microorganisms. Biotechnol. Adv. 13, 491-551.

Miller, G.L., 1959. Use of dinitrosalicylic acid reagent for determination of reducing sugar. Anal. Chem. 31, 426-428.

Collection @ chosun

조선대학교
CHOSUN UNIVERSITY

Mirón, A.S., Garcia, M.C.C., Camacho, F.G., Grima, E.M., Chisti, Y., 2002. Growth and biochemical characterization of microalgal biomass produced in bubble column and airlift photobioreactors: studies in fed-batch culture. Enzyme Microb. Technol. 31, 1015-1023.

Mitra, D., Leeuwen, J., Lamsal, B., 2012. Heterotrophic/mixotrophic cultivation of oleaginous *Chlorella vulgaris* on industrial co-products. Algal Res. 1, 40-48.

Mock, T., Kroon, B.M.A., 2002. Photosynthetic energy conversion under extreme conditions-II: the significance of lipids under light limited growth in antractic sea ice diatoms. Phytochemistry 61, 53-60.

Mohd-Sahib, A.-A., Lim, J.-W., Lam, M.-K., Uemura, Y., Isa, M.H., Ho, C.-D., Kutty, S.R.M., Wong, C.-Y., Rosli, S.-S., 2017. Lipid for biodiesel production from attached growth *Chlorella vulgaris* biomass cultivating in fluidized bed bioreactor packed with polyurethane foam material. Bioresour. Technol. 239, 127-136.

Morais, M.G., Costa, J.A.V., 2007. Carbon dioxide fixation by *Chlorella kessleri, C. vulgaris, Scenedesmus obli*
quus and *Spirulina* sp. cultivated in flasks and vertical tubular photobioreactors. Biotechnol. Lett. 29, 1349-1352.

Morita, M., Watanabe, Y., Okawa, T., Saiki, H., 2001. Photosynthetic productivity of conical helical tubular photobioreactors incorporating *Chlorella* sp. Under various culture medium flow conditions. Biotechnol. Bioeng. 74, 137-144.

Collection @ chosun

조선대학교
CHOSUN UNIVERSITY

Mutanda, T., Ramesh, D., Karthikeyan, S., Kumari, S., Anandraj, A., Bux, F., 2011. Bioprospecting for hyper-lipid producing microalgal strains for sustainable biofuel production. Bioresour. Technol. 102, 57-70.

Neilson, A.H., Lewin, R.A., 1974. The uptake and utilization of organic carbon by algae: an essay in comparative biochemistry. Phycologia. 13, 227-264.

Ohkubo, N., Yagi, O., Okada, M., 1998. Effect of humic acid and fulvic acids on the growth of *Microcystis aeruginosa*, Environ. Technol. 19, 611-617.

Pal, D., Goldberg, I.K., Cohen, Z., Boussiba, S., 2011. The effect of light, salinity, and nitrogen availability on lipid production by *Nannochloropsis* sp.. Appl. Microbiol. Biotechnol. 90, 1429-1441.

Pempkowiak, J., Kosakoeska, A., 1998. Accumulation of cadmium by green algae *Chlorella vulgaris* in the presence of marine humic substances, Environ. Int. 24, 583-588.

Petersen Jr, R.C., 1991. The contradictory biological behavior of humic substances in the aquatic environment, in: Allard, B., Borén, H., Grimvall, A., (Eds.), Humic Substances in the Aquatic and Terrestrial Environments, Springer-Verlag, Berlin, pp. 367-390.

Prabakaran, P., Ravindran, A.D., 2011. Acomparative study on effective cell disruption methods for lipid extraction from microalgae. Lett. Appl. microbiol. 53, 150-154.

Prakash, A., Rashid, M.A., 1968. Influence of humic substances on the growth of marine phytoplankton: dinoflagellates, Limnol. Oceanogr. 13, 598-606.

Collection @ chosun

조선대학교
CHOSUN UNIVERSITY

Pratoomyot, J., Srivilas, P., Noiraksar, T. 2005. Fatty acids composition of 10 microalgal species. Songklanakarin J. Sci. Technol. 27(6), 1179-1187.

Qin, J., 2005. Bio-hydrocarbons from algae-impacts of temperature, light and salinity on algae growth. Barton, Australia: Rural Industries Research and Development Corporation.

Ra, C.H., Kang, C.H., Kim, N.K., Lee, C.G., Kim, S.K., 2015. Cultivation of four microalgae for biomass and oil production using a two-stage culture strategy with salt stress. Renew. Energy. 80, 117-122.

Radmann, E.M., Reinhr, C.O., Costa, J.A.V., 2007. Optimization of the repeated batch cultivation of microalga *Spirulina platensis* in open raceway ponds. Aquaculture 265, 118-126.

Rammus, J., 1990. A form-function analysis of photon captures for seaweeds. Hydrobiologia 204, 65-71.

Rakesh, S., Dhar, D.W., Prasanna, R., Saxena, A.K., Saha, S., Shukla, M., Sharma, K., 2015. Cell disruption methods for improving liipid extraction efficiency in unicellular microalgae. Eng. Life Sci. 15, 443-447.

Ratledge, C., Kanagachandran, K., Anderson, A.J., Gr antham, D.J., Stephenson, J.C., 2001. Production of docosahexaenoic acid by *Crypthecodinium cohnii* grown in a pH-auxostat culture with acetic acid as principal carbon source. Lipids 36, 12410-12416.

Collection @ chosun

조선대학교
CHOSUN UNIVERSITY

Reinehr, C.O., Costa, J.A.V., 2006. Repeated batch cultivation of the microalga *Spirulina platensis*. World J. Microb. Biot. 22, 937-943.

REN21 (Reneable Energy Policy Network for the 21st Century), 2016. Renewables 2016 Global Status Report, Paris, France.

Ren, H.Y., Liu, B.F., Kong, F., Zhao, L., Xie, G.J., Ren, N.Q., 2014. Enhanced lipid accumulation of green microalga *Scenedesmus* sp. by metal ions and EDTA addition, Bioresour. Technol. 169, 763-767.

Ren, H.Y., Liu, B.F., Ma, C., Zhao, L., Ren, N.Q., 2013. A new lipid-rich microalga *Scenedesmus* sp. strain R-16 isolated using Nile red staining: effects of carbon and nitrogen sources and initial pH on the biomass and lipid production. Biotechnol. Biofuels 6, 143.

Renaud, S.M., Parry, D.L., Luong-Van, T., Kuo, C., Padovan, A., Sammy, N., 1991. Effect of light intensity on the proximate biochemical and fatty acid composition of *Isochrysis* sp. and *Nannochloropsis oculata* for use in tropical aquaculture. J. Appl. Phycol. 3, 43-53.

Renaud, S.M., Thinh, L.V., Parry, D.L. 1999. The gross chemical composition and fatty acid composition of 18 species of tropical Australian microalgae for possible use in mariculture. Aquaculture 170, 147-159.

Richmond, A., 2004. Handbook of microalgal culture: biotechnology and applied phycology. Blackwell Science Ltd.

Collection @ chosun

조선대학교
CHOSUN UNIVERSITY

Richmond, A., Hu, Q., 2013. Handbook of Microalgal Culture: Applied phycology and biotechnology. Second Ed. Jhon Wiley and Sons Ltd, Oxford, UK.

Rodolfi, L., Zittelli, G.C., Bassi, N., Padovani, G., Biondi, N., Bonini, M., Tredici, M.R., 2009. Microalgae for oil: strain selection, induction of lipid synthesis and outdoor mass cultivation in a low-cost photobioreactor. Biotechnol. Bioeng. 102, 100-112.

Roesijadi, G., Jones, S.B., Snowden-Swan, L.J., Zhu, Y., 2010. Macroalgae as a Biomass Feedstock: a Preliminary Analysis. Pacific Northwest National Laboratory, Richland, WA.

Romieu, I., Tellez Rojo, M.M., Lazo, M., Manzano Patino, A., Cortez Lugo, M., Julien, P., Belanger, M.C., Hernandez Avila, M., Holguin, F., 2005. Omega-3 fatty acid prevents heart rate variability reductions associated with particulate matter. Am. J. Respir. Crit. Care. Med. 12, 1534-1540.

Rosillo-Calle, F., 2016. A review of biomass energy- shortcomings and concerns. J. Chem. Technol. Biotechnol. 91, 1933-1945.

Rosenberg, J.N., Kobayashi, N., Barnes, A., Noel, E.A., Betenbaugh, M.J., Oyler, G.A., 2014. Comparative analyses of three *Chlorella* species in response to light and sugar reveal distinctive lipid accumulation patterns in the microalga *C. sorokiniana*. PLos ONE 4, 11-13.

Collection @ chosun

조선대학교
CHOSUN UNIVERSITY

Ruangsomboon, S., 2012. Effect of light, nutrient, cultivation time and salinity on lipid production of newly isolated strain of the green microalga, *Botryococcus braunii* KMITL 2. Bioresour. Technol. 109, 261-265.

Ruangsomboon, S., Ganmanee, M., Choochote, S., 2013. Effects of different nitrogen, phosphorus, and iron concentrations and salinity on lipid production in newly isolated strain of the tropical green microalga, *Scenedesmus dimorphus* KMITL, J. Appl. Phycol. 25, 867-874.

Ruiz, J., Álvarez-Díaz, P.D., Arbib, A., Garrido-Pérez, C., Barragán, J., Perales, J.A., 2013. Performance of a flat panel reactor in the continuous culture of microalgae in urban wastewater: Prediction from a batch experiment. Bioresour. Technol. 127, 456-463.

Sauer, A., Heise, K.P., 1984. Regulation of acetyl-coenzyme A carboxylase and acetyl-coenzyme A synthetase in spinach chloroplasts. Z Naturforsch. 39, 268-275.

Savin, L.J., 2012. Renewables. Global status report. REN21 Secretariat, Paris, France.

Sawayama, S., Inoue, S., Dote, Y., Yokoyama, S.Y. 1995. CO_2 fixation and oil production through microalga. Energy Convers. Manag. 136, 729-731.

Scott, S.A., Davey, M.P., Dennis, J.S., Horst, I., Howe, C.J., Lea-Smith, D.J., Smith, A.G., 2010. Biodiesel from algae: challenges and prospects. Curr. Opinion. Biotechnol. 21, 277-286.

Collection @ chosun

조선대학교
CHOSUN UNIVERSITY

Schenk, P., Thomas-Hall, S., Stephens, E., Marx, U., Mussgnug, J., Posten, C., Kruse, O., Hankamer, B., 2008. Second generation biofuels: high-efficiency microalgae for biodiesel production. Bioenerg. Res. 1, 20-43.

Schnitzer, M., Vendette, E., 1975. Chemistry of humic substances extracted from an arctic soil, Can. J. Soil Sci. 55, 93-103.

Searchinger, T., Heimlich, R., Houghton, R.A., Dong, F., Elobeid, A., Fabiosa, J., Tokgoz, S., Hayes, D., Yu, T.-H., 2008. Use of U.S. croplands for biofuels increases greenhouse gases through emissions from land-use change. Science 319 (5867), 1238-1240.

Sheehan, J., Dunahay, T., Benemann, J., Roessler, P., 1998. A look back at the U.S. Department of Energy's Aquatic Species program: Biodiesel from Algae. Report NREL/TP-580-24190.

Shi, X.M., Liu, H.J., Zhang, X.W., Chen, F., 1999. Production of biomass and lutein by *Chlorella protothecoides* at various glucose concentrations in heterotrophic cultures. Process Biochem. 34, 341-347.

Solovchenko, A.E., Chivkunova, O.B., Semenova, L.R., Selyakh, I.O., Shcherbakov, P.N., Karpova, E.A., Lobakova, E.S., 2013. Stress-induced changes in pigment and fatty acid content in the microalga *Desmodesmus* sp. isolated from a white sea hydroid. Russ. J. Plant. Physiol. 60, 313-321.

Collection @ chosun

조선대학교
CHOSUN UNIVERSITY

Song, M., Pei, H., Hu, W., Ma, G., 2013. Evaluation of the potential of 10 microalgal strains for biodiesel production. Bioresour. Technol. 141, 245-251.

Spolaore, P., Joannis Cassan, C., Duran, E., Isambert, A., 2006. Commercial applications of microalgae. J. Biosci. Bioeng. 101, 87-96.

Stanier, R.Y., Kunisawa, R., Mandel, M., Cohen Bazire, G., 1971. Purification and properties of unicellular blue-green algae (order Chroococcales). Bacteriol. Rev. 35, 171-205.

Steelink, C., 1977. Humates and other natural organic substances in the aquatic environment, J. Chem. Educ. 54, 599-603.

Stumm, W., Morgan, J.J., 1996. Aquatic Chemistry: Chemical equilibria and rates in natural waters, John Wiley and Sons, New York, USA.

Sugimoto, K., Midorikawa, T., Tsuzuki, M., Sato, N., 2008. Upregulation of PG synthesis on sulfur-starvation for PS I in *Chlamydomonas*. Biochem. Biophys. Res. Commun. 369, 660-665.

Sukenik, A., Carmell, Y., Berner, T., 1989 Regulation of fatty acid composition by irradiance level in the eustigmatophyte *Nannochloropsis* sp.. J. Phycol. 25, 686-692.

Sunda, W.G., Huntsman, S.A., 1995. Iron uptake and growth limitation in oceanic and coastal phytoplankton, Mar. Chem. 50, 189-206.

Collection @ chosun

조선대학교
CHOSUN UNIVERSITY

Sunda, W.G., Huntsman, S.A., Harvey, G.R., 1983. Photoreduction of manganese oxides in seawater and its geochemical and biological implications, Nature 301, 234-236.

Sweeney, B.M., 1954. *Gymnodinium splendens*, a marine dinoflagellate requiring vitamin B_{12}, Am. J. Bot. 41, 821-824.

Sydney, E.B., Sturm, W., Carvalho, J.C., Soccol, V.T., Larroche, C., Pandey, A., Soccol, C.R., 2010. Potential carbon dioxide fixation by industrially important microalgae. Bioresour. Technol. 10, 5892-5896.

Tan, C.K., Johns, M.R., 1991. Fatty acid production by heterotrophic *Chlorella saccharophila*. Hydrobiologia 215, 13-19.

Tang, H., Chen, M., Simon Ng, K.Y., Salley, S.O., 2012. Continuous microalgae cultivation in a photobioreactor. Biotechnol. Bioeng. 109, 2468-2474.

Tang, H., Abunasser, N., Garcia, M.E.D., Chen, M., Ng, K.Y.S., Salley, S.O., 2011, Potential of microalgae oil from *Dunaliella tertiolecta* as a feedstock for biodiesel. Appl. Energy 88, 3330.

Tanner, W., 1969. Light-driven active uptake of 3-O-methylglucose via an inducible hexose uptake system of *Chlorella*. Biochem. Biophys. Res. Commun. 36, 278-283.

Collection @ chosun

조선대학교
CHOSUN UNIVERSITY

Tansakul, P., Savaddirakasa, Y., Prasertsan, P., Tongurai, C., 2005. Cultivation of the hydrocarbon-rich alga, *Botryococcus braunii* in secondary treated effluent from a sea food processing plant. Thai. J. Agric. Sci. 38, 71-76.

Tasić, M.B., Pinto, L.F.R., Klein, B.C., Veljković, V.B., Filho, R.M., 2016. *Botryococcus braunii* for biodiesel production. Renew. Sustain. Energy Rev. 64, 260-270.

Terry, K.L., Raymond, L.P., 1985. System design for the autotrophic production of microalgae. Enzyme Microb. Technol. 7, 474-487.

Thomas, W.H., Dodson, A.N., 1968. Effects of phosphate concentration on cell division rates and yield of a tropical oceanic diatom. Biol. Bull. 134, 199-208.

Thompson, A.S., Rhodes, J.C., Pettman, I., 1988. Natural environmental research council culture collection of algae and protozoa: catalogue of strains, Freshwater Biological Association, Ambleside, UK.

Thompson, G.A., Jr. 1996. Lipids and membrane function in green algae. Biochim. Biophys. Acta. 1302, 17-45.

Tian-Yuan, Z., Yin-hu, w., Lin-Lan, Z., Xiao-Xiong, W., Hong-Ying, H., 2014. Screening heterotrophic microalgal strain by using the biolog method for biofuel production from organic wastewater. Algal Res. 6, 175-179.

Tredici, M.R., Zittelli, G.C., 1998. Efficiency of sunlight utilization: tubular versus flat photobioreactors. Biotechnol. Bioeng. 57, 187-197.

Collection @ chosun

조선대학교
CHOSUN UNIVERSITY

Ugwu, C.U., Aoyagi, H., Uchiyama, H., 2007. Influence of irradiance, dissolved oxygen concentration, and temperature on the growth of Chlorella sorokiniana. Photosynthetica 45, 309-311.

Ugwu, C.U., Aoyagi, H., Uchiyama, H., 2008. Photobioreactors for mass cultivation of algae. Bioresour. Technol. 99, 4021-4028.

Ukeles, R., Rose, W.E., 1976. Observations on organic carbon utilisation by photosynthetic marine microalgae. Marine Biol. 7, 11-28.

Uquiche, E., Jerez, M., Ortiz, J., 2008. Effect of pretreatment with microwaves on mechanical extraction yield and quality of vegetable oil from Chlilean hazelnuts (*Gevuina avellana* Mol). Innov. Food Sci. Emerg. Technol. 9, 495-500.

Van Gerpen, J., 2005. Biodiesel processing and production. Fuel Process Technol. 86, 1097-1107.

Vazhappilly, R., Chen, F., 1998. Eicosapentaenoic acid and docosahexaenoic acid production potential of microalgae and their heterotrophic growth. J. Am. Oil Chem. Soc. 75, 393-397.

Valenzuela, J., Carlson, R.P., Gerlach, R., Cooksey, K., Peyton, B.M., Bothner, B., Fields, M.W., 2013. Nutrient resupplementation arrests bio-oil accumulation in *Phaeodactylum tricornutum*. Appl. Microbiol. Biotechnol. 97, 7049-7059.

Collection @ chosun

조선대학교
CHOSUN UNIVERSITY

Valenzuela, J., Mazurie, A., Carlson, R.P., Gerlach, R., Cooksey, K.E., Peyton, B.M., Fields, M.W., 2012. Potential role of multiple carbon fixation pathways during lipid accumulation in *Phaeodactylum tricornutum*. Biotechnol. Biofuels 5, 40.

Virot, M., Tomao, V., Ginies, C., Visinoni, F., Chemat, F., 2008. Microwave-integrated extraction of total fats and oils. J. Chromatogr. A 1196-1197, 57-64.

Wahidin, S., Idris, A., Shaleh, S.R.M., 2013. The influence of light intensity and photoperiod on the growth and lipid content of microalgae *Nannochloropsis* sp.. Bioresour. Technol. 129, 7-11.

Wake, L.V., Hillen, L.W., 1980. Study of a "bloom" of the oil-rich alga *Botryococcus braunii* in the Darwin river. Biotechnol. Bioeng. 22, 1637-1656.

Wan, M., Jin, X., Xia, J., Rosenberg, J.N., Yu, G., Nie, Z., Oyler, G.A., Betenbaugh, M.J., 2014. The effect of iron on growth, lipid accumulation, and gene expression profile of the freshwater microalga *Chlorella sorokiniana*, Appl. Microbiol. Biotechnol. 98, 9473-9481.

Wan, M., Liu, P., Xia, J., Rosenberg, J.N., Oyler, G.A., Betenbaugh, M.J., Nie, Z., Qiu, G., 2011. The effect of mixotrophy on microalgal growth, lipid content, and expression levels of three pathway genes in *Chlorella sorokiniana*. Appl. Microbiol. 91, 835-844.

Wang, H., Xiong, H., Zeng, X., 2012. Mixotrophic cultivation of *Chlorella pyrenoidosa* with diluted primary piggery wastewater to produce lipids. Bioresour, Technol. 104, 215-220.

Collection @ chosun

조선대학교
CHOSUN UNIVERSITY

Widjaja, A., Chien, C.C., Ju, Y.H., 2009. Study of increasing lipid production from fresh water Microalgae *Chlorella vulgaris*. J. Taiwan Institute Chem. Eng. 40, 13-20.

Wolf, F.R., Nemethy, E.K., Blanding, J.H., Bassham, J.A., 1985. Biosynthesis of unusual acyclic isoprenoids in the alga *Botryococcus braunii*. Phytochemistry 24, 733-737.

Wong, Y.K., Ho, Y.K., Ho, K.C., Leung, H.M., Yung, K.K.L., 2017. Maximization of cell growth and lipid production of freshwater microalga *Chlorella vulgaris* by environment technique for biodiesel production. Envrion. Sci. Pollut. Re. 24, 9089-9101.

Xia, L., Ge, H., Zhou, X., Zhang, D., Hu, C., 2013. Photoautotrophic outdoor two-stage cultivation for oleaginous microalgae *Scenendesmus obtusus* XJ-15. Bioresour. Technol. 144, 261-267.

Xiao, Y., Zhang, J., Cui, J., Yao, X., Sun, Z., Feng, Y., Cui, Q., 2015. Simultaneous accumulation of neutral lipids and biomass in *Nannochloropsis oceanica* IMET1 under high light intensity and nitrogen replete conditions. Algal Res. 11, 55-62.

Xin, L., Hong ying, H., Ke, G., Ying xue, S., 2010. Effects of different nitrogen and phosphorus concentrations on the growth, nutrient uptake, and lipid accumulation of a freshwater microalga *Scenedesmus* sp. Bioresour. Technol. 101, 5494-5500.

Xu, H., Miao, X.L., Wu, Q.Y., 2006. High quality biodiesel production from a microalga *Chlorella protothecoides* by heterotrophic growth in fermenters. J. Biotechnol. 126, 499-507.

Collection @ chosun

조선대학교
CHOSUN UNIVERSITY

Yang, C., Hua, Q., Shimizu, K., 2000. Energetics and carbon metabolism during growth of microalgal cells under photoautotrophic, mixotrophic and cyclic light-autotrophic/dark-heterotrophic conditions. Biochem. Eng. J. 6, 87-102.

Yang, J., Xu, M., Zhang, X., Hu, Q., Sommerfeld, M., Chen, Y., 2011. Life-cycle analysis on biodiesel production from microalgae: water footprint and nutrients balance, Bioresour. Technol. 102, 159-165.

Yeesang, C., Cheirsilp, B., 2011. Effect of nitrogen, salt, and iron content in the growth medium and light intensity on lipid production by microalgae isolated from freshwater sources in Thailand. Bioresour. Technol. 102, 3034-3040.

Yeesang, C., Cheirsilp, B., 2014. Low-cost production of green microalga *Botryococcus braunii* biomass with high lipid content through mixotrophic and photoautotrophic cultivation, Appl. Biochem. Biotechnol. 174, 116-129.

Yeh, K.L., Chang, J.S., Chen, Y.M., 2010. Effect of light supply and carbon source on cell growth and cellular composition of a newly isolated microalga *Chlorella vulgaris* ESP-31. Eng. Life Sci. 10, 201-208.

Yokoi, H., Maki, R., Hirose, R., Hayashi, S., 2002. Microbial production of hydrogen from starch-manufacturing wastes, Biomass Bioenergy 22, 389-395.

Yokota, A., Harada, A., Kitaoka, S., 1989. Characterization of ribulose 1,5-bisphosphate carboxylase/oxygenase from *Euglena gracilis* Z. J. Biochem. 105, 400-405.

Collection @ chosun

조선대학교
CHOSUN UNIVERSITY

Yoo, C., Jun, S.Y., Lee, J.Y., Ahn, C.Y., Oh, H.M., 2010. Selection of microalgae for lipid production under high levels carbon dioxide. Bioresour. Technol. 101, S71-S74.

Yoon, S.Y., Hong, M.E., Chang, W.S., Sim, S.J., 2015. Enhanced biodiesel production in Neochloris oleoabundans by a semi-continuous process in two-stage photobioreactors. Bioprocess Biosyst. Eng. 38, 1415-1421.

Zervos, A., 2016. Renewables 2016 Global Status Report, REN21 Paris, Secretariat, Paris, France.

Zhang, K., Miyachi, S., Kurano, N., 2001. Evaluation of a vertical flat-plate photobioreactor for outdoor biomass production and carbon dioxide biofixation: effects of reactor dimensions, irradiation and cell concentration on the biomass productivity and irradiation utilization efficiency. Appl. Microbiol. Biotechnol. 55, 428-433.

Zhang, H., Wang, W., Li, Y., Yang, W., Shen, G., 2011. Mixotrophic cultivationi of *Botryococcus braunii*. Biomass Bioenergy 35, 1710-1715.

Zhang, T.Y., Wu, Y.H., Zhu, S.f., Li, F.M., Hu, H.Y., 2013. Isolation and heterotrophic cultivation of mixotrophic microalgae strains for domestic wastewater treatment and lipid production under dark condition. Biresour. Technol. 149, 586-589.

Zhila, N.O., Kalacheva, G.S., Volova, T.G., 2011. Effect of salinity on the biochemical composition of the alga *Botryococcus braunii* Kütz IPPAS H-252. J. Appl. Phycol. 23, 47-52.

Collection @ chosun

조선대학교
CHOSUN UNIVERSITY

Zhukova, N.V., Titlyanov, E.A., 2006. Effect of light intensity on the fatty acid composition of dinoflagellates symbiotic with hermatypic corals. Bot. Mar. 49, 339-346.

Zou, S., Wu, Y., Yang, M., Li, C., Tong, J., 2009. Thermochemical catalytic liquefaction of the marine microalgae *Dunaliella tertiolecta* and characterization of bio-oils. Energ. Fuel. 23, 3753-3758.

Collection @ chosun

조선대학교
CHOSUN UNIVERSITY

Overall conclusion

In the present study, four green microalgal growth and total lipid contents were compared in three different modes of cultivations. Comparing to photoautotrophic cultivation, higher biomass productionwas observed in heterotrophic cultivation. Among the various carbon sources tested, glucose was the best carbon source for four microalgal growths, and 1 % glucose was optimum for higher biomass production in three microalgal species except *S. obliquus* R8 (2 % glucose). The *B. braunii* FC124 was found to be a best lipid producing microalga under 80 µmol photons/m^2/s of light intensity, 1 %of glucose and 20 days incubation. Lipid accumulation increased with increasing light intensity in the mixotrophic cultivation. Total lipid content was lesser in the heterotrophic mode when compared with other two modes. Nevertheless, no significant variations in the biomass production was noted between heterotrophic and mixotrophic cultivations. These algal species can be used for the industrial scale-up of lipid production.

In this study, the improvement of biomass and total lipid production of three microalgal species under different culture modes was investigated. Nitrogen starvation under photoautotrophic conditions could increase lipid synthesis of microalgae. Cells cultivated under mixotrophic condition with 0.02 M glucose and light intensity of 150 µmol photons/m^2/s showed the maximal biomass and lipid productivities. Light intensity stimulated chlorophyll synthesis and lipid production in cells significantly, but did not increase cell growth. Meanwhile, light intensity variations did not change C16–C18 fatty acids composition significantly in all three strains. *N. oculata* CCAP849/1 used in this study can be applicable for industrial level lipid production.

The effect of growth stimulators in oceanic sediment on the biomass and lipid production of *B. braunii* LB572 and *P. tricornutum* B2089 was investigated. The optimal mixing ratio between culture medium and oceanic sediments extract for maximal production

Collection @ chosun

조선대학교
CHOSUN UNIVERSITY

was 6:4 (v/v). Among the components in sediment, Fe^{3+} and Ca^{2+} significantly improved biomass and lipid production and humic acid increased the uptake of metal ions to the microalgae. The fact that concentrations of metal ions and humic acid in the culture medium containing sediment were within the optimum ranges indicates oceanic sediment can supply sufficient growth factors required for microalgal growth.

Under mixotrophic culture mode, the lipid content of *B. braunii* LB572 and *P. tricornutum* B2089 increased steadily as the light intensity and duration time. However, biomass production decreased significantly at high light intensity, as more than 200 μmol photons/m^2/s for *B. braunii* LB572 and 150 μmol photons/m^2/s for *P. tricornutum* B2089. The effect of photoperiod was also similar to that of light intensity. Also, the MUFA content tended to increased with light intensity and duration time, but PUFA decreased.

The lipid extract efficiency of *B. braunii* LB572 and *P. tricornutum* B2089 according to optimized six disruption methods was high in order of microwave, french-press, autoclave, bead-beater, sonication, and osmotic shock. In the optimal microwave method (icrowave oven at 150 ℃ for 20 min with frequency of 1250 W and 2450 MHz), the lipid content of *B. braunii* LB572 and *P. tricornutum* B2089 were 49.71 and 47.91% (w/w), respectively. Moreover, the lipid extraction efficiency of dry and wet microalgal biomass using the above disruption method was about 10% lower than dry biomass.

In the batch culture type, the specific growth rate, biomass and lipid production of the cultivated above microalgal strains in the 10 L tubular-photobioreactor using the optimized light regimes and developed mixed medium studied in this study were as follows: 0.33 d^{-1}, 7.28 and 4.15 g/L for *B. braunii* LB572 and 0.37 d^{-1}, 12.80 and 7.45 g/L for *P. tricornutum* B2089, respectively. In the continuous culture type, the two microalgae were examined with the highest biomass and lipid productivity at a dilution of 0.35 d^{-1}, which was about 3 times higher than the batch culture type. However, biomass and lipid production have been diluted with increasing dilution rates. In addition, when the batch culture type was repeated 5 times, the biomass and lipid production of the both

Collection @ chosun

조선대학교
CHOSUN UNIVERSITY

microalgae increase 1.1 times at each repeated culture cycle. The biomass and lipid production of two microalgae finally produced were as follows: 13.65 and 7.96 g/L for *B. braunii* LB572 and 18.71 and 11.54 g/L for *P. tricornutum* B2089, respectively. There was no significant difference in biomass productivity between continuous and repeated-batch culture type, but the lipid productivity in the repeated-batch type was about three times higher than the continuous culture type.

The conversion yield of FAME (% of microalgal lipid) under direct-ransesterification from non-disrupted biomass of *B. braunii* LB572 and *P. tricornutum* B2089 was about 95%, and there was no significant difference in the yield of FAME of disrupted biomass of both microalgae. The FAME yield esterified from wet biomass were found to be 96.7% for *B. braunii* LB572 and 98.4% for *P. tricornutum* B2089, respectively, which was 1-2% higher than FAME yield of dry biomass. Finally, the FAME productivity of each microalgae cultured in repeated-batch culture type by optimized direct-transesterification was measured as follows: 0.26 g/L/d for *B. braunii* LB572 and 0.37 g/L/d for *P. tricornutum* B2089, respectively.

Collection @ chosun

조선대학교
CHOSUN UNIVERSITY

요 약 문

다양한 배양조건에 따라 담수 (*Chlorella* sp., *C. vulgaris* CCAP211/1B, *B. braunii* FC124, 그리고 *S. obliquus* R8) 및 해양 미세조류 (*I. galbana* LB987, *N. oculata* CCAP849/1, 그리고 *D. salina*)의 성장 및 지질 함량을 조사하였다. 광독립영양배양조건 (photoautotrophic culture mode)과 달리 종속영양 (Heterotrophic) 또는 혼합영양배양조건 (Mixotrophic culture mode)에서 배양할 경우 해당 미세조류의 성장이 향상되었다. 한편, 광독립영양배양조건과 혼합영양배양조건에서 미세조류 세포 내의 지질 축적량이 증가하였다. 그러나, 혼합영양배양조건에서, 빛은 담수 미세조류의 성장과 지질 축적 증진에 영향을 미쳤다. 그리고, 해양 미세조류의 바이오매스 생산에 큰 영향을 미치지 못했으나, 클로로필과 지질 함량은 빛의 세기가 증가함에 따라 급격하게 증가하는 경향을 보였다. 또한, 광독립영양배양조건에서 *I. galbana* LB987, *N. oculata* CCAP849/1, 그리고 *D. salina*는 낮은 질소 (NO_3^-)의 농도에서 지질의 생산이 촉진되었으나, 질소의 농도가 증가함에 따라 바이오매스의 생산량은 증가하며 지질 함량은 감소하였다.

또한, 미세조류의 높은 지질 함량을 유지하고 성장 증가를 위해, 혼합영양배양조건에서 미세조류의 생장 촉진제인 해양 퇴적물 (oceanic sediments)가 *B. braunii* LB572와 *P. tricornutum* B2089의 바이오매스 및 지질의 생산에 미치는 영향을 조사하였다. 미세조류의 각 배양 배지와 해양 퇴적물을 혼합한 최적 혼합 비율은 6:4 (v/v)로 *B. braunii* LB572와 *P. tricornutum* B2089의 specific growth rate가 약 각각 13.0과 11.3 배 증가하였다. 그리고, 최적 혼합비율의 혼합배지에서 두 미세조류의 바이오매스와 지질의 생산량의 경우, *B. braunii* LB572는 5.54 및 3.09 g/L 그리고 *P. tricornutum* B2089는 6.41 및 3.61 g/L로 각각 조사되었다. 해양 퇴적물 내 두 미세조류의 생장과 지질 축적량 증진에 미치는 영향인자를 확인한 결과, Fe^{3+} 와 Ca^{2+}는 두 미세조류의 바이오매스 및 지질 생산을 촉진하였으나 Mg^{2+}의 경우 큰 영향을 미치지 못했다. 또한, 해양 퇴적물로부터 추출한 부식산 (humic acid)은 금속이온들의 생체 이용률

Collection @ chosun

조선대학교
CHOSUN UNIVERSITY

(bioavailability)을 증가시켜 해당 미세조류의 생장 및 지질 추출을 극대화하였다. 따라서, 해양 퇴적물을 이용한 미세조류 배양 배지 조제를 통해 미세조류의 바이오매스와 지질의 대량생산을 위한 저비용의 공급이 가능할 것으로 판단된다.

본 연구에서는, 해양 퇴적물의 혼합배지를 이용한 혼합영양배양조건에서 oleaginous 미세조류인 *B. braunii* LB572와 *P. tricornutum* B2089를 10 L 규모의 관형-광생물반응기 (10 L-Scale tubular-photobioreactor)를 이용하여 빛의 세기 및 주기에 따른 성장, 지질 축적, 및 지방산 조성에 미치는 영향을 조사하였다. 빛의 세기가 *B. braunii* LB572는 200 μmol photons/m^2/s 그리고 *P. tricornutum* B2089는 150 μmol photons/m^2/s까지 증가함에 따라 바이오매스 생산량은 점차적으로 증가하였으며, 빛의 세기가 최대 300 μmol photons/m^2/s 까지 증가함에 따라 두 미세조류 모두 지질 생산량은 증가하는 경향을 나타내었다. 또한, 빛 주기의 경우 빛 세기와 비슷한 결과가 조사되었다. 두 종 미세조류 모두 18:6시간/명반응:암반응의 주기에서 가장 높은 바이오매스 및 지질의 생산량이 조사되었으며, 빛의 세기의 경우 *B. braunii* LB572는 200 μmol photons/m^2/s 그리고 *P. tricornutum* B2089는 150 μmol photons/m^2/s로 각각 조사되었다. 다양한 빛의 조건에 따라 미세조류의 지질 내 지방산 (C16-C18)의 함량 및 조성의 변화를 나타내었다. 미세조류를 이용한 바이오디젤 생산에 필수적인 지방산인 C16-C18의 지방산 중 빛의 세기 및 공급시간이 증가함에 따라 포화지방산 (saturated fatty acid)과 단일 불포화지방산 (monounsaturated fatty acid)의 함량이 증가하였으나, 다중 불포화지방산 (polyunsaturated fatty acid)의 함량은 점차적으로 감소하는 양상을 보였다.

배양된 미세조류의 바이오매스로부터 효과적인 지질 추출을 위해 적합한 파쇄방법의 선택 및 최적화를 수행하였다. 본 연구에서 이용한 파쇄방법은 6가지의 물리적 혹은 화학적 방법 (autoclave, sonication, bead-beater, microwave, french-press, 그리고 osmotic shock)을 각각 이용하여 *B. braunii* LB572와 *P. tricornutum* B2089의 최적 파쇄방법을 조사한 결과, 두 종 미세조류 모두 microwave 방법으로 확인되었다. 본 연구에서 조사된 microwave의 최적 파쇄 조건은 오븐의 온도를 150 ℃에서 1250 W와 2450 MHz의 세기에서 20분 동안 각 미세조류의 시료를 파쇄 하였으며, 위 최적 파쇄 조건에서 *B. braunii* LB572와 *P. tricornutum* B2089의 지질 함량은 49.71과

Collection @ chosun

조선대학교
CHOSUN UNIVERSITY

47.91% (w/w)로 각각 조사되었다.

선행연구 결과를 기반으로 하여, 연속 배양 (continuous culture)과 반복-회분 (repeated-batch culture)을 수행하면서 *B. braunii* LB572와 *P. tricornutum* B2089의 바이오매스와 지질 생산성을 비교하였다. 두 미세조류를 12 L 관형-광생물반응기 (working volume 10 L)에서 13일 동안 각각 회분배양한 후, 약 30일 동안 연속배양 또는 반복-회분배양하였다. 회분배양에서 *B. braunii* LB572와 *P. tricornutum* B2089의 specific growth rate를 조사한 결과 *B. braunii* LB572는 0.33 그리고 *P. tricornutum* B2089는 0.37 d^{-1}로 각각 조사되었다. 연속배양에서 신선한 배지를 2.4 mL/min의 속도로 주입하고 역시 동일한 속도로 균체가 생장한 배양액을 회수하였다. 0.35 d^{-1}의 희석률에서 가장 높은 바이오매스 및 지질의 생산성을 나타내었으며, 이 때 *B. braunii* LB572의 바이오매스 및 지질의 생산성은 2.47 및 1.41 g/L/d이었고, *P. tricornutum* B2089의 바이오매스 및 지질의 생산성은 4.24 및 2.45 g/L/d이었다. 이 결과는 두 미세조류의 회분배양에서 얻은 생산성보다 약 4배 증가한 것이다. 또한, 미세조류를 반복-회분배양하기 위해 6일을 주기로 하여 10 L 배양액 중 4 L의 균체 배양액을 일시에 회수하고 역시 동일한 양의 신선한 배지를 일시에 공급하면서 30일 동안 총 5번을 반복적으로 회분배양하였다. 두 미세조류 모두 회분배양이 반복됨에 따라 지질 함량은 큰 변화를 보이지 않았으나, 바이오매스와 지질의 생산량 및 생산성은 일정하게 증가하였다. 최종적으로 5번째 회분배양이 반복되었을 때 바이오매스 및 지질의 생산성은 *B. braunii* LB572의 경우, 2.71 및 4.84 g/L/d 그리고 *P. tricornutum* B2089의 경우, 3.72 및 6.24 g/L/d로 각각 조사되었다. 이러한 결과는 바이오매스와 지질 생산에 있어서 연속배양 보다 반복-회분배양이 더 효율적이라는 것을 의미한다.

본 연구에서 생산된 미세조류 바이오매스를 이용한 바이오디젤 생산을 위해 직접-에스테르 교환반응 조건을 최적화하였다. 또한 최적화된 직접-에스테르 교환반응 (Direct-transeterification)을 통해 *B. braunii* LB572와 *P. tricornutum* B2089의 FAME yield 및 생산성을 각각 조사하였다. 이 때 직접-에스테르 교환반응의 최적조건은 다음과 같다. 기본적으로 6.0 mL sulfuric acid와 8.0 mL chloroform을 각각 10 g의 바이오매스에 첨가한 후 200 ℃ 에서 60 분간 처리하되, *B. braunii* LB572에는 70 mL methanol을, *P. tricornutum* B2089에는 35 mL methanol을 첨가하였다. 반응기 내부

Collection @ chosun

조선대학교
CHOSUN UNIVERSITY

온도가 200 ℃ 일 때, 반응기 내 압력은 약 75 bar로 측정되었다. 건조시키지 않은 바이오매스를 직접-에스테르 교환반응을 통해 얻은 각 FAME yield는 *B. braunii* LB572가 95.6%, *P. tricornutum* B2089가 96.2%이었다. 이 때 *B. braunii* LB572와 *P. tricornutum* B2089의 FAME 생산성은 0.26 및 0.37 g/L/d로 각각 조사되었다.

Collection @ chosun

조선대학교
CHOSUN UNIVERSITY

Publication list

Bioprocess Biosyst Eng (2012) 35:19–27
DOI 10.1007/s00449-011-0612-1

ORIGINAL PAPER

Optimization of culture conditions and comparison of biomass productivity of three green algae

Wonduck Kim · Jang Min Park · Geun Ho Gim · Sang-Hwa Jeong · Chang Min Kang · Duk-Jin Kim · Si Wouk Kim

Received: 30 May 2011 / Accepted: 14 July 2011 / Published online: 10 September 2011
© Springer-Verlag 2011

Abstract Culture conditions for the mass production of three green algae, *Chlorella* sp., *Dunaliella salina* DCCBC2 and *Dunaliella* sp., were optimized using a response surface methodology (RSM). A central composite design was applied to investigate the effects of initial pH, nitrogen and phosphate concentrations on the cultivation of microalgae. The optimal growth conditions estimated from the design are as follows: *Chlorella* sp. (initial pH 7.2, ammonium 17 mM, phosphate 1.2 mM), *D. salina* DCCBC2 (initial pH 8.0, nitrate 3.3 mM, phosphate 0.0375 mM) and *Dunaliella* sp. (initial pH 8.0, nitrate 3.7 mM, phosphate 0.17 mM). Culturing the microalgae with the optimized conditions confirmed that the maximum growth rates were attained for these parameters. The optimum CO_2 concentrations of *Chlorella* sp., *D. salina* DCCBC2 and *Dunaliella* sp. were 1.0, 3.0 and 1.0% (v/v), respectively. The specific growth rates (μ) of *Chlorella* sp., *D. salina* DCCBC2 and *Dunaliella* sp. were 0.58, 0.78 and 0.56 day^{-1}, respectively, and the biomass productivities were 0.28, 0.54 and 0.30 g dry cell wt l^{-1} day^{-1}, respectively. The CO_2 fixation rates of *Chlorella* sp., *D. salina* DCCBC2 and *Dunaliella* sp. were 42.8, 90.9 and 45.5 mg l^{-1} day^{-1}, respectively. Mixotrophic cultivation of *Chlorella* sp. with glucose increased biomass productivity from 0.28 to 0.51 g dry cell wt l^{-1} day^{-1}. However, *D. salina* DCCBC2 and *Dunaliella* sp. were not stimulated by several organic compounds tested.

Keywords Green algae · Response surface methodology · Biomass productivity · CO_2 fixation · Mixotrophic cultivation

W. Kim · J. M. Park · G. H. Gim · S. W. Kim (✉)
Department of Environmental Engineering and Pioneer Research Center for Controlling of HAB, Chosun University, Gwangju 501-759, South Korea
e-mail: swkim@chosun.ac.kr

W. Kim
e-mail: wonduck@chosun.ac.kr

S.-H. Jeong
Department of Mechanical Engineering, Chosun University, Gwangju 501-759, South Korea
e-mail: shjoeng@chosun.ac.kr

C. M. Kang
Department of Environment and Health, Chodang University, Jeonnam 534-701, South Korea
e-mail: cmkang@chodang.ac.kr

D.-J. Kim
Department of Water Supply and Sewage, Korea Environment Corporation, Incheon 404-708, South Korea
e-mail: duk-jin@keco.or.kr

Introduction

Microalgae have been utilized as valuable sources in various industry fields. Recently, microalgae have emerged as an alternative source of energy that could be a substitute for fossil fuels. It has been reported that biofuel production from microalgae is more advantageous than that from plants due to their rapid growth rates [1], relatively simple genetic system [2] and limited effect on the food supply [3]. Presently, studies to identify microalgae species containing high levels of fatty acids and the development of improved oil extraction techniques are being performed extensively [4]. In addition, some microalgae species are capable of producing high-value compounds. The microalgae *Spirulina*, *Dunaliella*, *Chlorella*, *Schizochytrium*, and *Euglena* are sources of carotenoid, phycocyanin, lipids (EPA), vitamins (biotin, vitamin C, vitamin E), cosmetics,

Collection @ chosun

조선대학교
CHOSUN UNIVERSITY

antioxidants, medicine and healthy food [5]. Thus, the development of efficient mass production of microalgae and purification of the produced compounds is critical to industrialization.

Carbon dioxide in the air and water can be converted into organic compounds using the Calvin–Benson cycle of the photosynthesis pathway in microalgae species. Previous reports estimated that microalgae might be responsible for ~50% of total global CO_2 fixation [6]. CO_2 fixation by microalgae is also crucial for nutrient cycling in the aqueous ecosystems, and it is one of the effective methods that could mitigate atmospheric CO_2 buildup. Weissman and Tillett [7] reported that microalgae could convert up to 99% of CO_2 in solution. Biological CO_2 fixation by microalgae is cost-effective compared to other chemical CO_2 fixation techniques because it can occur using only sunlight and water at ambient temperature and pressure. In addition, CO_2 exhausted from industrial facilities can be fixed directly by microalgae and the subsequent biomass can be recycled as animal feed and clean fuel. Thus, this fixation method can contribute to the mitigation of atmospheric CO_2 that causes global warming [8].

Optimization of high-density cell cultivation conditions is crucial for maximizing industrial productivity of microalgae. During the optimization process, culture conditions for the maximal growth rate are determined by repeating experiments. The process can be facilitated by a response surface methodology (RSM), which can determine the optimized values with a limited number of experiments and less time. Additionally, correlation among the variables can be evaluated from the methodology [9, 10]. The aim of this study is the investigation of influences of various culture factors, such as nitrogen, phosphate, pH, temperature, light intensity, CO_2 and organic compounds, on the growths of one freshwater green alga, *Chlorella* sp., and two seawater green algae, *Dunaliella salina* DCCBC2 [11] and *Dunaliella* sp. [12]. The optimized values for nitrogen, phosphate and pH for growth were determined by a RSM, and the effects of CO_2 and organic compounds on the cultivations were also studied. In this study, *Chlorella* sp. served as a control species, and the biomass productivities of the two seawater green algae were compared.

Methods and materials

Microalgae, media and cultivation conditions

Chlorella sp., *D. salina* DCCBC2 and *Dunaliella* sp. were obtained from Prof. EonSeon Jin of Hanyang University, Seoul, Korea. Tris–Acetate–Phosphate (TAP) medium [13] was used for cultivations of *Chlorella* sp., and D medium was used for both of *D. salina* DCCBC2 and *Dunaliella* sp. TAP medium is composed of (per liter): 0.8 g NH_4Cl, 0.1 g $CaCl_2{\cdot}2H_2O$, 0.2 g $MgSO_4{\cdot}7H_2O$, 0.3 g K_2HPO_4, 0.05 g EDTA·$2H_2O$, 0.005 g $FeSO_4{\cdot}7H_2O$, 0.022 g $ZnSO_4{\cdot}7H_2O$, 0.005228 g H_3BO_3, 0.0051 g $MnCl_2{\cdot}4H_2O$, 0.0011 g $CuCl_2{\cdot}2H_2O$, 0.0026 g $Na_2MoO{\cdot}2H_2O$, 0.0016 g $CoCl_2{\cdot}6H_2O$. D medium is composed of (per liter): 58.44 g NaCl, 4.844 g Tris, 0.5055 g KNO_3, 0.91576 g $MgCl_2{\cdot}6H_2O$, 0.12325 g $MgSO_4{\cdot}7H_2O$, 0.0441 g $CaCl_2$, 0.0228 g K_2HPO_4, 0.00055 g $FeCl_3$, 0.00245 g EDTA, 0.000305 g H_3BO_3, 0.000198 g $MnCl_2{\cdot}4H_2O$, 0.000023 g $ZnSO_4{\cdot}5H_2O$, 0.00001 g $CuSO_4{\cdot}5H_2O$, 0.000048 g $NaMoO_4{\cdot}2H_2O$, 0.000005 g $CoCl_2{\cdot}6H_2O$, 0.000027 g $NaVO_3$, 2.1 g $NaHCO_3$. The growth experiments for optimizing culture conditions were performed for 11 days. During the incubation, 12-h cycles of light and dark were repeated. In this study, the microalgae were grown in flasks, but for the incubation with an influx of CO_2, a specially designed tubular photobioreactor (70 × Φ15 cm, total volume 12 l) was used (Fig. 1). The reactor was made of Pyrex glass and it was placed horizontally for microalgae incubation to broaden the surface area of medium supplied with CO_2 gas. In this study, the photobioreactor system consisted of three separate reactors to perform three different experiments. Depending on the experimental purpose, they can be connected together. Several injection ports were made on the bottom of each bioreactor for the influx of CO_2 gas from a gas cylinder and a constant CO_2 concentration was controlled with a flow meter (Dwyer, USA). The specific CO_2 concentrations were prepared by mixing 100% N_2 and 15% CO_2 from each gas cylinder. The reactors contained 10 l culture broth that had been inoculated with 100 ml of pre-culture. To determine the optimal nitrogen concentration for maximum biomass productivity, *Chlorella* sp., *D. salina* DCCBC2 and *Dunaliella* sp. were cultivated with media containing 15, 20, 25 and 30 mM NH_4Cl or 1, 3, 5 and 7 mM KNO_3, respectively. To determine the phosphate concentration for maximum biomass productivity, 2, 4, 6 and 8 mM K_2HPO_4 or 0.025, 0.1, 0.2 and 0.4 mM K_2HPO_4, respectively, were added into the media. To find optimal pH values for growth, each of the medium was prepared to have pH 6.0, 7.0, 8.0, and 9.0, respectively. The temperature range for growth was 23–29 °C. To examine the effect of light intensity on growth, 40, 60, 80 and 100 μE m^{-2} s^{-1} light from fluorescence lamps was illuminated into the culture broths. Each microalgae sample (1 ml) grown under different pH, temperature, and light intensities was collected, and biomass was estimated from optical density values of the samples at 682 nm.

Measurement of cell density and biomass

The number of microalgal cell was estimated with haemocytometer (Superior, Germany) enumeration. The counting

Collection @ chosun

조선대학교
CHOSUN UNIVERSITY

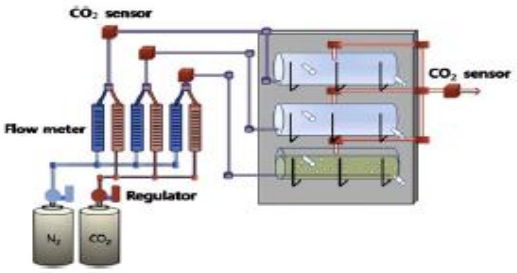

Fig. 1 Schematic diagram of a tubular photobioreactor system for mass production of microalgae

was performed three times to attain standard deviation values. To estimate dry weights of the microalgae, 100 ml of stationary microalgal cultures were centrifuged, and the resulting pellets of microalgae were washed three times with 0.9% NaCl (*Chlorella* sp.) or 3% NaCl solution (*D. salina* DCCBC2 and *Dunaliella* sp.). After washing, the pellet fraction was filtered through a 0.8-μm glass membrane (Pall, USA), dried in an electric oven (Advantec FUW243PA, Japan) for 8 h at 105 °C, and then weighed.

Response surface methodology

The culture conditions for biomass production were optimized by a RSM based on the 2^n factorial central composite design (CCD). The three growth experiments were performed independently for *Chlorella* sp., *D. salina* DCCBC2 and *Dunaliella* sp. The experiment was based on a 2^3 factorial central composite experimental plan with three conditions (i.e., pH, nitrogen source and phosphate). The range and levels of the experimental variables investigated in this study are given in Table 1. A set of 20 experiments was conducted with three variables, and each variable was studied at five levels ($\alpha = 2.0$). The Y_x represents the biomass production as dependent variables. For statistical calculations including the solutions of the second-order polynomial model equation, the Design Expert (version 8.0.2, Stat-Ease Inc., Minneapolis, USA) software package was used.

The equation was:

$$Y_x = a_0 + a_1X_1 + a_2X_2 + a_3X_3 + a_{12}X_1X_2 + a_{13}X_1X_3 + a_{23}X_2X_3 + a_{11}X_1^2 + a_{22}X_2^2 + +a_{33}X_3^2 + a_{123}X_1X_2X_3$$

where X_1, X_2 and X_3 represent coded levels of the independent variables; a_0 is the intercept term; a_1, a_2 and a_3 are linear terms; a_{11}, a_{22} and a_{33} are quadric terms; a_{12}, a_{13}, a_{23} and a_{123} are interaction terms.

Measurement of CO_2 fixation rate

To measure CO_2 fixation rates of the algae, gas injection into the 12-l photobioreactor was blocked and a Tedlar gas-sampling bag was connected to collect 1 ml gas in the reactor with a syringe. The CO_2 concentration in the collected samples was quantified with gas chromatography (Shimadzu, GC-17A, Japan) equipped with a Porapak Q 80/100 column (mesh 2 m × 3 mm I.D.) and a thermal conductivity detector (TCD). The temperatures of the oven and injector were set to 40 °C and that of the detector was set to 100 °C. Nitrogen gas was used as a carrier gas and the flow rate for the column was 30 ml/min. The formula used for calculating the CO_2 fixation rate was:

$$R_{CO_2} = \frac{[(P_0 + \rho gh)y_{CO_{2in}}P_o y_{CO_{2out}}]M_{wCO_2}}{8.314TV_{culture}}$$

Table 1 Levels of biomass production of *Chlorella* sp., *Dunaliella salina* DCCBC2 and *Dunaliella* sp. for various conditions in the experimental design

Variable	Symbol code	Range and levels				
		−2	−1	0	1	2
Chlorella sp.						
Initial pH	X_1	5	6	7	8	9
Ammonium (mM)	X_2	5	10	15	20	25
Phosphate (mM)	X_3	0.2	0.6	1	1.4	1.8
Dunaliella salina						
Initial pH	X_1	6	7	8	9	10
Nitrate (mM)	X_2	1	2	3	4	5
Phosphate (mM)	X_3	0.005	0.015	0.025	0.035	0.045
Dunaliella sp.						
Initial pH	X_1	6	7	8	9	10
Nitrate (mM)	X_2	1	2	3	4	5
Phosphate (mM)	X_3	0.1	0.15	0.2	0.25	0.3

Collection @ chosun

조선대학교
CHOSUN UNIVERSITY

where y_{CO_2in} and y_{CO_2out} are the CO_2 molar fractions in the inlet and outlet gas phases, P_0 is the atmospheric pressure (Pa), ρ is the density of liquid (kg m^{-3}) CO_2, h is the vertical distance of culture medium (m), M_{wCO_2} is the molecular weight of CO_2 (g mol^{-1}), T is the ambient absolute temperature (K) and V is the volume of culture medium (l).

The cultures for the above experiments were incubated for 6 days.

Mixotrophic cultivation

To study the effect of an organic compound as the carbon source on the mixotrophic growths, six different organic compounds (glucose, xylose, rhamnose, fructose, sucrose and galactose) were separately supplemented into the cultivation media. The concentration of each carbohydrate for the cultivation was 10 mM.

Measurement of N and P concentrations in culture media

The indophenol method for NH_4Cl measurement [14] and the UV absorption method for KNO_3 measurement were used to estimate the nitrogen concentration in the culture media. The phosphate concentration was determined by the ascorbic acid reduction method [15].

Results and discussion

Optimization of culture conditions of three green algae

Three green algae were cultivated in the presence of different nitrogen sources and it was found that *Chlorella* sp. utilized NH_4Cl as a main nitrogen source, but *D. salina* DCCBC2 and *Dunaliella* sp. preferred KNO_3. Maximal biomass productivity (1.0 g l^{-1}) of *Chlorella* sp. was achieved with 20 mM NH_4Cl, whereas for *D. salina* DCCBC2 (2.7 g l^{-1}) and *Dunaliella* sp. (1.2 g l^{-1}), 3 mM KNO_3 was optimal (Fig. 2).

The phosphate source for cultivation of the microalgae was K_2HPO_4. Maximal productivity for *Chlorella* sp. (1.0 g l^{-1}), *D. salina* DCCBC2 (2.8 g l^{-1}) and *Dunaliella* sp. (1.1 g l^{-1}) was obtained from 2, 0.025 and 0.4 mM K_2HPO_4, respectively (Fig. 3). These data indicate that *D. salina* DCCBC2 metabolizes phosphate more efficiently in a low concentration than the other microalgae. As shown in Figs. 2 and 3, *D. salina* DCCBC2 showed the highest growth rate and biomass productivity at all of the attempted nitrate and phosphate concentrations, indicating that it has

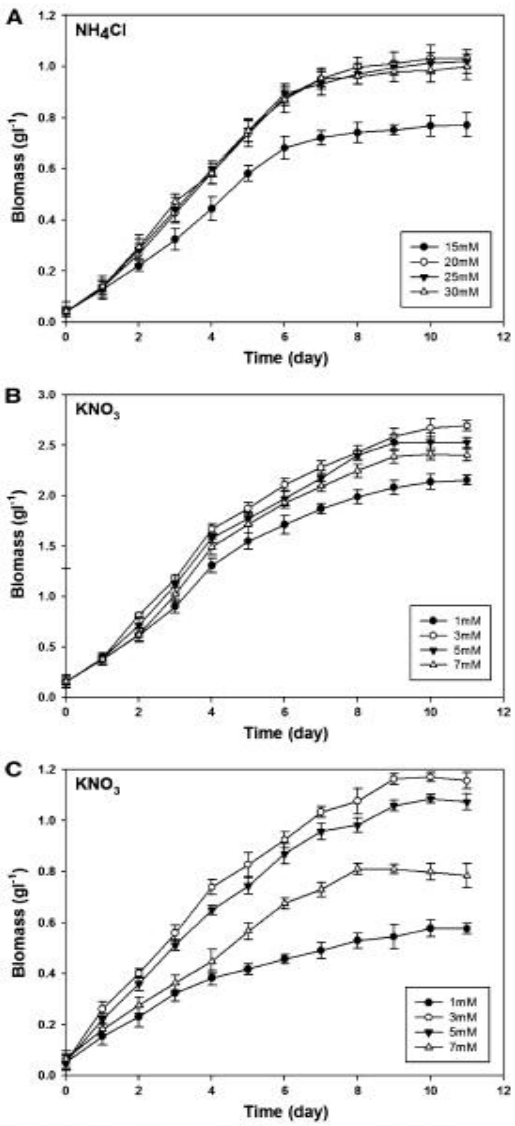

Fig. 2 Effect of nitrogen concentration on the growth of three green algae. **a** *Chlorella* sp., **b** *Dunaliella salina* DCCBC2, **c** *Dunaliella* sp.

Collection @ chosun

조선대학교
CHOSUN UNIVERSITY

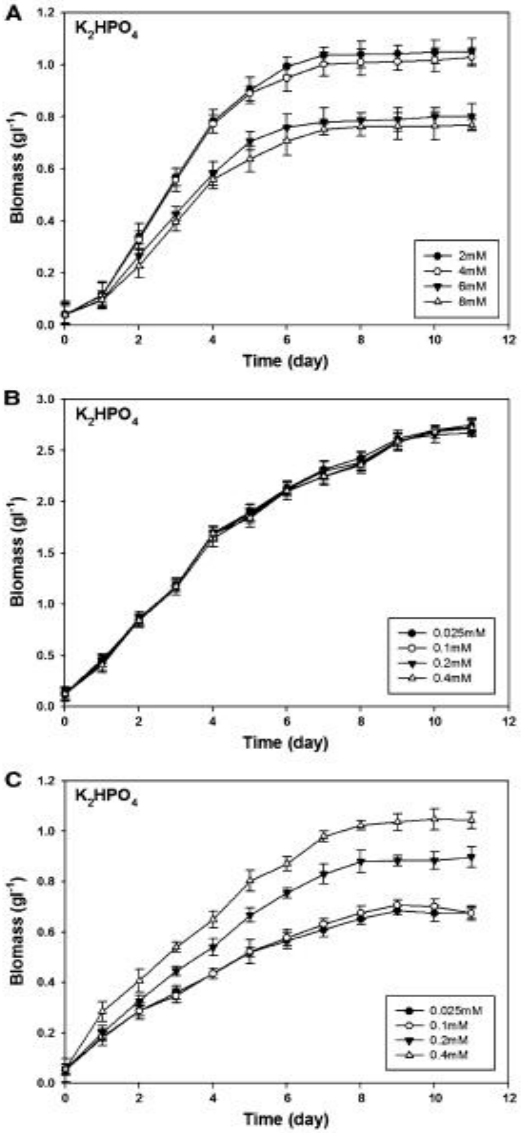

Fig. 3 Effect of phosphate concentration on biomass production. **a** *Chlorella* sp. **b** *Dunaliella salina* DCCBC2, **c** *Dunaliella* sp.

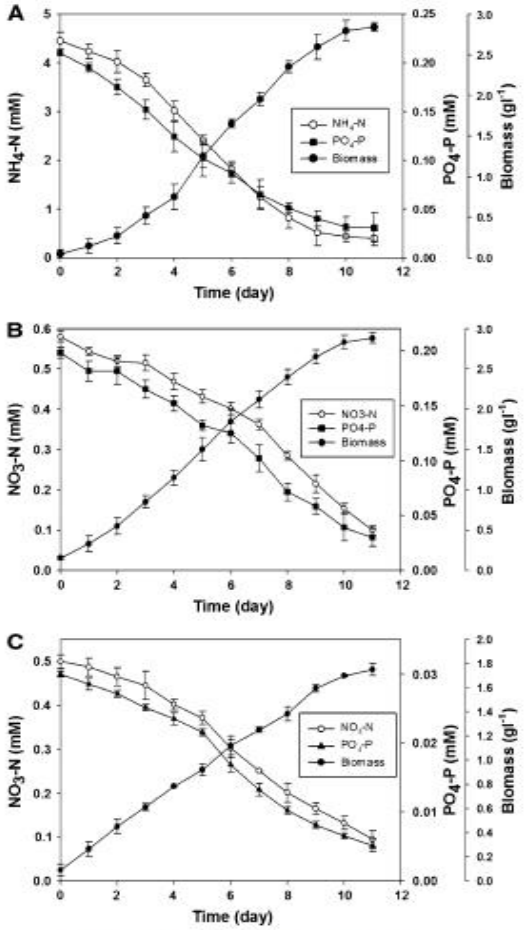

Fig. 4 Relationship between N-, P-concentration and biomass production. **a** *Chlorella* sp., **b** *Dunaliella salina* DCCBC2, **c** *Dunaliella* sp.

the most efficient system for utilization of nitrate and phosphate among the three green microalgae.

To investigate the influences of nitrogen and phosphate ions on the growth of the microalgae, the remaining ion concentration in the medium were sequentially determined during the cultivation. As shown in Fig. 4a, the concentrations of NH_4Cl and K_2HPO_4 in the medium for

Collection @ chosun

조선대학교
CHOSUN UNIVERSITY

Chlorella sp. drastically decreased in proportion to the cell growth. Similar reduction patterns of KNO_3 and K_2HPO_4 concentrations were also observed in the media for *Dunaliella* species (Fig. 4b, c). The drastic decrease period of the nitrogen and phosphate ion concentrations coincided with the rapid cell growth period, indicating that the ions are essential nutrients for microalgae to sustain optimal growths. Considering these results, the microalgae might be good candidates for disposal process of wastewater, which efficiently reduces the nitrogen and phosphate ions during cultivation of microalgae in the water [16, 17].

The optimum pH for growth of *Chlorella* sp. was 7.0, whereas 8.0 was optimum for *D. salina* DCCBC2 and *Dunaliella* sp. (Fig. 5). These results matched with pHs of the microalgal habitats; *Chlorella* sp. was isolated from fresh water, and *D. salina* DCCBC2 and *Dunaliella* sp. were isolated from sea water.

Microalgae are sensitive to temperature changes, thus maintaining constant temperature is important for stable long-term cultivation. Our study revealed that the optimum temperature conditions for growths of *Chlorella* sp. and the *Dunaliella* strains were 25 and 27 °C, respectively.

Light intensity is one of the most important factors for photosynthesis in microalgae and it affects biomass productivity. The optimum light intensities for maximum productivity were 100 μE m^{-2} s^{-1} for *Chlorella* sp. and 80 μE m^{-2} s^{-1} for *Dunaliella* strains.

Optimization of growth conditions by response surface methodology

To investigate the optimum culture conditions for maximum biomass production, experiments were performed according to a central composite design experimental plan (Table 2). The initial ranges were selected based on our preliminary work. The mathematical model, which represents a second-order polynomial, is given by Eqs. 1–3, where the variables take coded values. Y_1, Y_2 and Y_3 represent the responses that are dependent variables. The experiments were performed independently. A_{1-3} are the coded values of the independent variables: pH, ammonium and phosphate, in a medium, respectively. B_{1-3} and C_{1-3} are the coded values of the independent variables: pH, nitrate and phosphate, respectively.

Chlorella sp.: pH 7.2, ammonium 17 mM, phosphate 1.2 mM

$$Y_1 = 1.26 + 0.061A_1 + 0.12A_2 + 0.092A_3 + 0.011A_1A_2 + 0.013A_1A_3 + 0.026A_2A_3 - 0.21A_1^2 - 0.15A_2^2 - 0.12A_3^2 + 0.034A_1A_2A_3 \quad (1)$$

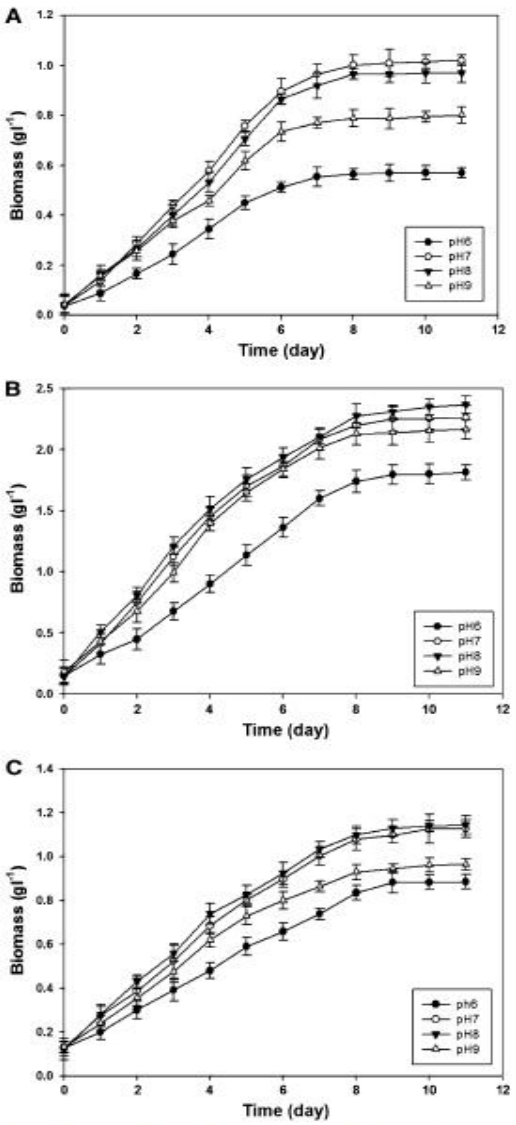

Fig. 5 Effect of pH on biomass production. **a** *Chlor ella* sp., **b** *Dunaliella salina* DCCBC2, **c** *Dunaliella* sp.

Collection @ chosun

조선대학교
CHOSUN UNIVERSITY

Table 2 Analysis of variance for quadratic models of *Chlorella* sp., *Dunaliella salina* DCCBC2 and *Dunaliella* sp.

Source	SS	DF	MS	*F* value	Prob > *F*
Chlorella sp.					
Model	1.87	10	0.19	27.12	<0.0001
Residual (error)	0.062	9	6.905E−003		
Lack of Fit	0.061	4	0.015	50.66	0.0003
Pure Error	1.497E−003	5	2.993E−004		
Total	1.93	19			
$R^2 = 0.9679$; CV = 9.44%; Adj. $R^2 = 0.9322$					
Dunaliella salina					
Model	13.29	10	1.33	21.76	<0.0001
Residual (error)	0.55	9	0.061		
Lack of fit	0.52	4	0.13	21.45	0.0024
Pure error	0.030	5	6.052E−003		
Total	13.84	19			
$R^2 = 0.9603$; CV = 12.91%; Adj. $R^2 = 0.9161$					
Dunaliella sp.					
Model	2.55	10	0.25	14.31	0.0002
Residual (error)	0.16	9	0.018		
Lack of fit	0.16	4	0.040	703.69	<0.0001
Pure error	2.843E−004	5	5.685E−005		
Total	2.71	19			
$R^2 = 0.9408$; CV = 13.04%; Adj. $R^2 = 0.8751$					

SS sum of squares, *DF* degrees of freedom, *MS* mean squares

D. salina DCCBC2: pH 8.0, nitrate 3.3 mM, phosphate 0.0375 mM

$$Y_2 = 2.95 + 0.028B_1 + 0.16B_2 + 0.33B_3 - 0.020B_1B_2 - 0.086B_1B_3 - 0.048B_2B_3 - 0.54B_1^2 - 0.47B_2^2 - 0.29B_3^2 - 0.087B_1B_2B_3 \quad (2)$$

Dunaliella sp.: pH 8.0, nitrate 3.7 mM, phosphate 0.17 mM

$$Y_3 = 1.44 + 0.052C_1 + 0.14C_2 + 0.15C_3 - 3.913E-003C_1C_2 + 0.012C_1C_3 + 0.049C_2C_3 - 0.20C_1^2 - 0.21C_2^2 - 0.11C_3^2 - 0.022C_1C_2C_3 \quad (3)$$

The statistical significance of the second-order model equations was checked using the *F* test analysis of variance (ANOVA, Table 2). The fitness of the model was expressed by the coefficient of determination, R^2, which was found to be 0.9679, 0.9603 and 0.9408 for the production of biomass for *Chlorella* sp., *D. salina* DCCBC2 and *Dunaliella* sp., respectively. The closer the R^2 value is to 1, the better the prediction of the response. The values for the adjusted determination coefficient (Adj R^2) (0.9322, 0.9161 and 0.8751) were also high, demonstrating the significance of each model, with the predicted R^2 value in reasonable agreement with the Adj R^2. This signifies a good agreement between experimental and predicted values of biomass production in each experiment.

The optimum conditions obtained from the growth experiments, in which nitrogen, phosphate, pH, temperature and light intensity are independent factors, were as follows: *Chlorella* sp.(ammonium 20 mM, phosphate 2 mM, pH 7.0, 27 °C, and 100 μE m^{-2} s^{-1}); *D. salina* DCCBC2 (nitrate 3 mM, phosphate 0.025 mM, pH 8.0, 27 °C, and 80 μE m^{-2} s^{-1}); and *Dunaliella* sp.(nitrate 3 mM, phosphate 0.4 mM, pH 8.0, 25 °C, and 100 μE m^{-2} s^{-1}). The optimal conditions from interactions of nitrogen, phosphate and pH by the central composite design were: *Chlorella* sp. (ammonium 17 mM, phosphate 2 mM, and pH 7.0); *D. salina* DCCBC2 (nitrate 3.3 mM, phosphate 0.0375 mM, and pH 8.0); and *Dunaliella* sp. (nitrate 3.7 mM, phosphate 0.17 mM, and pH 8.0). Under these conditions, the total biomass of *Chlorella* sp. increased from 1.0 to 1.2 g l^{-1} and those of *D. salina* DCCBC2 and *Dunaliella* sp. also increased from 2.5 to 2.9 g l^{-1} and from 1.2 to 1.4 g l^{-1}, respectively. The biomasses predicted by RSM analysis for *Chlorella* sp., *D. salina* DCCBC2 and *Dunaliella* sp. were 1.3, 3.1 and 1.4 g l^{-1}, respectively. These indicate good agreement between the experimental and predicted values for culture conditions.

Effect of CO_2 on the growth of microalgae

It is known that the photosynthesis rate of microalgae is significantly affected by CO_2 concentrations in a

Collection @ chosun

조선대학교
CHOSUN UNIVERSITY

Table 3 Specific growth rate, biomass productivity and CO_2 fixation rate for CO_2 concentration of *Chlorella* sp., *Dunaliella salina* DCCBC2 and *Dunaliella* sp.

Microalgae	CO_2 concentration (%)	Growth rate (μ, day^{-1})	Biomass productivity ($g\ l^{-1}\ day^{-1}$)	CO_2 fixation rate ($mg\ l^{-1}\ day^{-1}$)
Chlorella sp.	0.04	0.50	0.24	19.9
	0.5	0.57	0.26	40.5
	1.0	0.58	0.28	42.8
	3.0	0.44	0.18	15.2
	5.0	0.38	0.09	7.2
	10.0	–	–	–
	15.0	–	–	–
Dunaliella salina	0.04	0.72	0.475	38.5
	0.5	0.73	0.487	41.7
	1.0	0.74	0.50	50.5
	3.0	0.78	0.54	90.9
	5.0	0.59	0.39	23.2
	10.0	0.42	0.13	8.2
	15.0	–	–	–
Dunaliella sp.	0.04	0.49	0.26	22.5
	0.5	0.50	0.27	25.9
	1.0	0.56	0.30	45.5
	3.0	0.40	0.17	12.7
	5.0	0.25	0.12	10.4
	10.0	–	–	–
	15.0	–	–	–

photobioreactor [18]. Determinations of optimum CO_2 concentrations for growth of microalgae were performed in 12 l tubular photobioreactors. Optimum CO_2 concentrations of *Chlorella* sp., *D. salina* DCCBC2 and *Dunaliella* sp. were 1.0, 3.0 and 1.0% (v/v), respectively (Table 3). When the microalgae were cultivated under optimal CO_2 growth conditions, the biomass productivities of *Chlorella* sp., *D. salina* DCCBC2 and *Dunaliella* sp. were 0.28, 0.54 and 0.30 $g\ l^{-1}\ day^{-1}$, respectively. Generally the biomass productivity range of *Chlorella* strains is 0.18–0.34 $g\ l^{-1}\ day^{-1}$ and the optimum CO_2 concentration is 5–18% [18, 19]. The biomass productivity of *Dunaliella tertiolecta* UTCC 420 is 0.37 $g\ l^{-1}\ day^{-1}$ [20]. This indicates that *D. salina* DCCBC2 used in this study is the best strain for biomass production. In addition, the maximum CO_2 fixation rates for *Chlorella* sp. and *Dunaliella* sp. were 42.8 and 45.5 $mg\ l^{-1}\ day^{-1}$ under 1.0% CO_2 concentration, respectively, whereas that of *D. salina* DCCBC2 was 90.9 $mg\ l^{-1}\ day^{-1}$ at a 3.0% CO_2 concentration (Table 3).

Effect of organic compounds on the growth of microalgae

Microalgae are usually cultivated under autotrophic conditions, but their growth in photobioreactors is not efficient because high-density cultivation causes self-shading and lowers penetrating light intensity into the reactor [21]. To enhance biomass productivity in the reactor, mixotrophic cultivation in which a carbohydrate can be used as the carbon source was performed. In our study, six different carbohydrates were tested for their ability to increase the biomass production of the microalgae, and only glucose was able to stimulate the growth of *Chlorella* sp. When 0.5% (w/v) glucose was added to the medium, the biomass amount and productivity of *Chlorella* sp. significantly increased from 1.5 to 2.84 $g\ l^{-1}$ and from 0.22 to 0.41 $g\ l^{-1}\ day^{-1}$, respectively. However, at concentrations higher than 0.5% glucose, biomass productivity was sharply reduced (data not shown). The other carbohydrates did not affect biomass production of *Chlorella* sp. In contrast, glucose did not affect the growths of the two seawater algae and, reversibly, other carbon compounds inhibited the growths of them (data not shown). This data suggest that there are effective glucose metabolism pathways in *Chlorella* sp. [22].

Conclusion

To optimize culture conditions for seawater green microalgae, *D. salina* DCCBC2 and *Dunaliella* sp., growth experiments were performed separately with a control

Collection @ chosun

조선대학교
CHOSUN UNIVERSITY

species, *Chlorella* sp., in which independent factors (ammonium, nitrate, phosphate, pH, temperature and light intensity) served as limiting factors. The three culture conditions (N, P and pH) for the microalgae were again optimized by analysis of the central composite design using the RSM. The modified culture conditions significantly increased biomass production of the microalgae, indicating that the analysis was useful for optimization. Biomass productivity of the microalgae was more enhanced when the microalgae were cultivated with optimal CO_2 concentrations. During mixotrophic cultivations of the microalgae, only glucose was capable of stimulating the growth of *Chlorella* sp., whereas none of the carbohydrates tested influenced the growth of *D. salina* DCCBC2 and *Dunaliella* sp. Microalgal cell growth was largely dependent on nitrogen and phosphate concentration, indicating that these are crucial nutrients for efficient biomass production. Consequently, *D. salina* DCCBC2 would be the best strain for mass production of algal biomass.

Acknowledgments This work was supported by the grant of New & Renewable Energy Program of the Korea Institute of Energy Technology Evaluation and Planning (KETEP) funded by the Ministry of Knowledge Economy, Korea (20103020090020).

References

1. Chisti Y (2007) Biodiesel from microalgae. Biotechnol Adv 25:294–306
2. Leon-Banares R, Gonzalez-Ballester D, Galvan A, Fernandez E (2004) Transgenic as green cell-factories. Trends Biotechnol 22:45–52
3. Koh LP, Ghazoul J (2008) Biofuels, biodiversity, and people: Understanding the conflicts and finding opportunities. Biol Conserv 141:2450–2460
4. Mata TM, Martins AA, Caetano NS (2010) Microalgae for biodiesel production and other applications: A review. Renew Sustain Energ Rev 14:217–232
5. Pulz O, Gross W (2004) Valuable products from biotechnology of microalgae. Appl Microbiol Biot 65:635–648
6. Field CB (1998) Primary production of the biosphere: integrating terrestrial and oceanic compounds. Science 281:237–240
7. Weissman JC, Tillett DT (1992) Design and operation of an outdoor microalgae test facility: Large-scale system results. In: Brown LM, Sprague S (eds) Aquatic species project report. National Renewable Energy Laboratory, Golden, pp 32–56
8. Kumar AS, Ergas XY, Sahu A, Zhang Q, Dewulf J, Malcata FX, Langenhove H (2010) Enhanced CO_2 fixation and biofuel production via microalgae: recent developments and future directions. Trends Biotechnol 28:371–380
9. Myers RH, Montgomery DC (2002) Response surface methodology; process and product optimization using designed experiments, 2nd edn. Wiley, New York
10. Kim H, Eom HJ, Lee JS, Han JS, Han NS (2004) Statistical optimization of medium composition for growth of *Leuconostoc citreum*. Biotechnol Bioproc E 9:278–284
11. Polle JE, Struwe L, Jin E (2008) Identification and characterization of a new strain of the unicellular green alga *Dunaliella salina* (Teod.) from Korea. J Microbiol Biotechnol 18:821–827
12. Park S, Polle JE, Mellis A, Lee TK, Jin E (2006) Up-regulation of photoprotection and PSII-repair gene expression by irradiance in the unicellular green alga *Dunaliella salina*. Mar Biotechnol 8:120–128
13. Gorman DS, Levine RP (1965) Cytochrome f and plastocyanin: their sequence in the photosynthetic electron transport chain of *Chlamydomonas reinhardi*. PNAS 54:1665–1669
14. Dora S (1976) Determination of ammonia and kjeldahl nitrogen by indophenols method. Water Res 10:31–36
15. Towns TG (1986) Determination of aqueous phosphate by ascorbic acid reduction of phosphomolybdic acid. Anal Chem 58:223–229
16. Gonzalez LE, Canizars RO, Baena S (1997) Efficiency of ammonia and phosphorus removal from a Colombian agroindustrial wastewater by the microalgae *Chlorella vulgaris* and *Scenedesmus dimorphus*. Bioresource Technol 60:259–262
17. Chevalier P, Noue J (1985) Wastewater nutrient removal with microalgae immobilized in Carrageenan. Enzyme Microb Technol 7:621–624
18. Ryu HJ, Oh KK, Kim YS (2009) Optimization of the influential factors for the improvement of CO_2 utilization efficiency and CO_2 mass transfer rate. J Ind Eng Chem 15:471–475
19. de Greque MM, Costa JAV (2007) Carbon dioxide fixation by *Chlorella kessleri*, *C. vulgaris*, *Scenedesmus obliquus* and *Spirulina* sp. cultivated in flasks and vertical tubular photobioreactors. Biotechnol Lett 29:1349–1352
20. Francisco EC, Neves DB, Jacob-Lopesb E, Franco TT (2010) Microalgae as feedstock for biodiesel production: carbon dioxide sequestration, lipid production and biofuel quality. J Chem Technol Biotechnol 85:395–403
21. Ceron Garcia MC, Garcia Camacho F, Sanchez Miron A, Fernandez Sevilla JM, Chisti Y, Molina Grima E (2006) Mixotrophic production of marine microalga *Phaeodactylum tricornutum* on various carbon sources. J Microbiol Biotechnol 16:689–694
22. Ukeles R, Rose WE (1976) Observation on organic carbon utilization by photosynthetic marine microalgae. Mar Biol 37:11–28

Collection @ chosun

조선대학교
CHOSUN UNIVERSITY

Journal of Biotechnology 164 (2012) 179–187

Contents lists available at SciVerse ScienceDirect

Journal of Biotechnology

journal homepage: www.elsevier.com/locate/jbiotec

Enhanced indirubin production in recombinant *Escherichia coli* harboring a flavin-containing monooxygenase gene by cysteine supplementation

Gui Hwan Han, Geun Ho Gim, Wonduck Kim, Sun Il Seo, Si Wouk Kim*

Department of Environmental Engineering, BK21 Team for Biohydrogen Production, and Pioneer Research Center for Controlling of Harmful Algal Bloom, Chosun University, Gwangju 501-759, Republic of Korea

ARTICLE INFO

Article history:
Received 25 July 2012
Received in revised form 10 August 2012
Accepted 15 August 2012
Available online 30 August 2012

Keywords:
Indirubin
Indigo
Indole
Tryptophan
Flavin-containing monooxygenase

ABSTRACT

In our previous study, a batch fermentation of recombinant *Escherichia coli* DH5α cells harboring the *fmo* gene from *Methylophaga aminisulfidivorans* MP^T produced indirubin (5.0 mg/L) and indigo (920 mg/L) in a 5 L fermenter containing tryptophan medium (2 g/L tryptophan, 5 g/L yeast extract, 10 g/L NaCl). In this study, it was found that indirubin production greatly increased when 0.36 g/L cysteine was added to the tryptophan medium, although cysteine inhibited the growth of the recombinant *E. coli* harboring the *fmo* gene. However, the addition of cysteine did not inhibit the expression level and activity of FMO in the cell. Indigo was synthesized by the dimerization of two 3-hydroxyindole molecules under the non-enzymatic reaction. Cysteine influenced the regioselectivity of FMO and enhanced the synthesis of 2-hydroxyindole instead of 3-hydroxyindole, which might function to increase indirubin production. The optimal culture conditions for indirubin production in tryptophan medium were determined from the response surface methodology analysis: 2 g/L tryptophan, 5 g/L yeast extract, 10 g/L NaCl, 0.36 g/L (3 mM) cysteine, pH 8.0 at 35 °C. Under these conditions, the recombinant *E. coli* cells were capable of producing 223.6 mg/L of indirubin from 2 g/L of tryptophan. The intracellular accumulation of the indirubin crystals might stress the cell, which may be a main reason for the poor growth of the recombinant *E. coli* pBlue 1.7.

© 2012 Elsevier B.V. All rights reserved.

1. Introduction

Indigoid compounds such as indirubin and indigo have been employed as natural drugs and dyes since ancient times (Kohda et al., 1990; Xia and Zenk, 1992). Traditionally, Danggui Longhui wan, which contains indirubin, has been used for the treatment of numerous chronic diseases including chronic granulocytic leukemia (Han, 1994; Nam et al., 2005; Tang and Eisenbrand, 1992). Recently, indirubin was found to be a potent inhibitor of cyclin dependent kinases (CDKs) and glycogen synthase kinase-3β (GSK-3β), which suggests that indirubin may play an important role in the treatments of leukemia and Alzheimer's disease (Bradford, 1976; Hoessel et al., 1999; Leclerc et al., 2001).

In general, indirubin and indigo compounds are extracted from the plant cell cultures of *Indigofera tinctoria*, *Isatis tinctoria*, *Polygonum tinctorium*, and *Lonchocarpus cyanescens* (Ensley et al., 1983; Fitzhugh et al., 1997; Seldes et al., 1999). Recently, several investigations have reported that indirubin and indigo can be produced from recombinant micro organisms expressing oxygenase (Doukyu et al., 2002; Ensley et al., 1983; Madsen and Bollag, 1988; McClay et al., 2005; Murdock et al., 1993; Rui et al., 2005). Rui et al. reported that they convert 0.5 mM indole to 0.2 mM indirubin and 0.1 mM indigo in Tris–HCl buffer using *Escherichia coli* TG1cells harboring a toluene *ortho*-monooxygenase gene of *Burkholderia cepacia* G4. Our previous studies showed that recombinant *E. coli* DH5α cells harboring a flavin-containing monooxygenase (FMO) gene from *Methylophaga aminisulfidivorans* MP^T (Choi et al., 2003) produced indirubin (≤5 mg/L) and indigo (920 mg/L) in a 5 L fermenter containing tryptophan (2 g/L) medium (Han et al., 2008, 2011).

FMOs belong to a family of FAD, NADPH, and molecular oxygen-dependent enzymes. FMOs are involved in a wide range of oxidative biological processes, including drug detoxification and the biodegradation of aromatic compounds by the catalyzation of the oxygenation of many nitrogen-, sulfur-, phosphorous-, selenium-, and other nucleophilic heteroatom containing chemicals and drugs (Krueger and Williams, 2005). In addition to cytochrome P450s (CYPs), FMOs are considered to be important monooxygenase enzymes for metabolism in both prokaryotes and eukaryotes (Zhou and Shephard, 2006).

It is known that recombinant *E. coli* harboring oxygenases can produce indigoid compounds from glucose or indole. Glucose is readily available, but its metabolic pathway is so complicated that

* Corresponding author at: Department of Environmental Engineering, Chosun University, 309 Pilmun-daero, Dong-gu, Gwangju 501-759, Republic of Korea. Tel.: +82 62 230 6649; fax: +82 62 225 6040.
E-mail address: swkim@chosun.ac.kr (S.W. Kim).

0168-1656/$ – see front matter © 2012 Elsevier B.V. All rights reserved.
http://dx.doi.org/10.1016/j.jbiotec.2012.08.015

Collection @ chosun

조선대학교
CHOSUN UNIVERSITY

the efficiency of the indigoid compound production is low (Berry et al., 2002). Indole (>1–6 mM) inhibits the growth of *E. coli*, thus the indole concentration in the culture medium must be maintained at a low level to avoid toxicity (Chant and Summers, 2007). Therefore, tryptophan was used in this study as an alternative substrate for indirubin synthesis to overcome the aforementioned problems.

A modified synthetic pathway for several indigoid compounds in the recombinant *E. coli* containing FMO (AF494423) is represented in Fig. 1. In a tryptophan rich condition, extracellular tryptophan is transported into the cell by tryptophan permease and thereafter converted into indole, pyruvate, and ammonia by tryptophanase (TnaA; EC 4.1.99.1) (Newton and Snell, 1965). FMO catalyzes the hydroxylation of indole to 2-hydroxyindole and 3-hydroxyindole by using the reducing power of NADPH in the presence of oxygen (Choi et al., 2003; Eaton and Chapman, 1995; Maugard et al., 2002). In the non-enzymatic reaction, indigo is produced from the combination of two 3-hydroxyindole molecules, whereas indirubin is made from the dimerization of 2-hydroxyindole and 3-hydroxyindole (Berry et al., 2002; Cho et al., 2011; Choi et al., 2003; Eaton and Chapman, 1995; Maugard et al., 2002; McClay et al., 2005). Currently, it is thought that the disproportional production of indigo and indirubin is due to random combinations of the various hydroxyindole molecules under different conditions, but any enzyme activity in the combination reaction has not been discovered yet.

Herein we reported that the enhanced production of indirubin through the supplementation of cysteine in tryptophan medium for the growth of recombinant *E. coli* DH5α cells harboring the *fmo* gene. In addition, the effects of cysteine on the growth of *E. coli* and the FMO activity were investigated. Finally, the optimal conditions for maximum production of indirubin was analyzed using response surface methodology (RSM).

2. Materials and methods

2.1. Bacterial strains and chemicals

A restricted facultatively methylotrophic marine bacterium, *M. aminisulfidivorans* MP^T (KCTC 12909^T = JCM 14647^T), was isolated in our lab and was cultivated in a standard mineral base (SMB) medium containing 3% (w/v) sodium chloride and 1% (w/v) methanol, at 30 °C (Choi et al., 2003; Kim et al., 2007). Flavin-containing monooxygenase gene (*fmo*) was cloned from *M. aminisulfidivorans* MP^T and sequenced (GenBank No. AF494423). *E. coli* DH5α was used for the cloning and expression studies. Recombinant *E. coli* pBlue 1.7 harboring pBluescriptSKII(+) (Fermentas, Glen Burnie, MD, USA) that contains a *fmo* gene was cultivated in LB medium containing 50 μg/mL ampicillin at 30 °C. Tryptophan medium (0.2% tryptophan, 0.5% yeast extract, 1.0% sodium chloride (w/v), and 50 μg/mL ampicillin) was used for the production of indigoid derivatives. Dimethyl sulfoxide (DMSO), isatin, indole, 2-oxindole, 3-hydroxylacetate, and indigo were purchased from Sigma–Aldrich (St. Louis, MO, USA), and indirubin standard was from Biomol (Biomol Research Laboratories, Plymouth Meeting, PA, USA). All other chemicals were of analytical grade.

2.2. Cloning, expression, and purification of FMO

The *fmo* from *M. aminisulfidivorans* MP^T was subcloned into the *Nde*I and *Xho*I restriction sites of the expression vector pET30a(+). The expression of *fmo* was induced by the addition of 0.2 mM isopropyl-D-1-thiogalactopyranoside (IPTG) to the bacterial culture medium and incubation at 18 °C for 20 h. The cells were harvested (10,000 × *g*), disrupted by French Press (30,000 psi, French Pressure Cells 40k, Thermo Electron Corporation, Needham, MA, USA) and centrifuged at 12,000 × *g*. Then, the recombinant FMO protein in the supernatant fraction was purified through Ni-NTA affinity column chromatography (Qiagen GmbH, Hilden, Germany) and Superdex G-200 gel filtration column chromatography (GE Healthcare, Piscataway, NJ, USA). The purity of the FMO was determined by SDS-PAGE analysis, and the purified protein was concentrated to 45 mg/mL in 40 mM Tris–HCl (pH 8.0) by centrifugal ultrafiltration (100,000 Da, Vivaspin, Satourius Stedim, Germany) and stored at −20 °C for further study.

2.3. Enzyme assay and Western blot analysis of FMO

FMO activity was determined spectrophotometrically by the use of indole as substrates. The assay mixture (1 mL) contained 0.1 mM EDTA and 0.1 mM NADPH dissolved in 0.1 M Tricine/KOH buffer (pH 8.5), and an aliquot of the purified FMO solution was added to the mixture. The reaction rates of the enzyme were monitored by following NADPH oxidation at 340 nm. Protein concentrations were determined by the Bradford method (Bradford, 1976).

For Western blot analysis, harvested cells (1×10^9) were resuspended in 300 μL SDS gel-loading buffer (50 mM Tris–HCl [pH 6.8], 100 mM dithiothreitol, 2% (w/v) SDS, 0.1% (w/v) bromophenol blue, 10% (v/v) glycerol, and 8 mM $MgCl_2$) and placed in boiling water for 3 min. The resulting crude cell lysate (10 μL) was loaded into 8% polyacrylamide gels and electrophoresed, and Western blotting was performed as described in the manual (Sambrook and Russell, 2001). The antibody against FMO was prepared and provided by Abfrontier Co. (South Korea).

2.4. Determination of tryptophan and cysteine concentrations

For the quantitative analyses of tryptophan and cysteine were performed using the Waters Associates PICO-TAG methods (Bidlingmeyer et al., 1984), high performance liquid chromatography (HPLC) with a Pico-tag column (4 μm, 3.9 mm × 300 mm, Waters) was performed. The HPLC pump (Waters 510, Milford, MA, USA) was used for the time-dependent mixing of the mobile phases of solvent A (140 mM sodium acetate and 6% acetonitrile) and solvent B (60% acetonitrile). The gradient program consisted of two solvent mixtures: 0–9 min, 100% solvent A and 0% solvent B; 9–9.2 min, 86% A and 14% B; 9.2–17.5 min, 80% A and 20% B; 17.5–17.7 min, 54% A and 46% B; 17.7–21.0 min, 100% B; 21.0–30.0 min, 100% A. The flow rate was 1.0 mL/min. All solvents used for the mobile phase in HPLC were filtered through a 0.45 μm cellulose membrane filter (Life Sciences, Inc., Newtown, PA, USA) and degassed in the ultrasonic bath. The peak responses from each chemical were monitored at 254 nm by a variable wavelength photodiode UV detector (Waters 2487 UV, Milford, MA, USA).

2.5. Effect of reducing agents and amino acids on indirubin synthesis

To examine the effect of the reducing agents and amino acids on indirubin biosynthesis, variable concentrations (0–5 mM) of cysteine, methionine, serine, tyrosine, phenyalanine, arginine, aspartic acid, glutathione, dithiothreitol, ascorbic acid, thioglycolic acid, and isatin were added to the tryptophan medium.

2.6. Indigoid compound analysis

The 3-hydroxyindole formation was detected by a luminescence spectrometer (excitation at 365 nm and emission at 470 nm, Perkin Elmer LS 45, Perkin Elmer, Santa Clara, CA, USA) (Woo et al., 2000). The *in vitro* assay was performed in a 100 mM Tricine–KOH buffer (pH 8.5) containing various concentrations of cysteine,

Collection @ chosun

조선대학교
CHOSUN UNIVERSITY

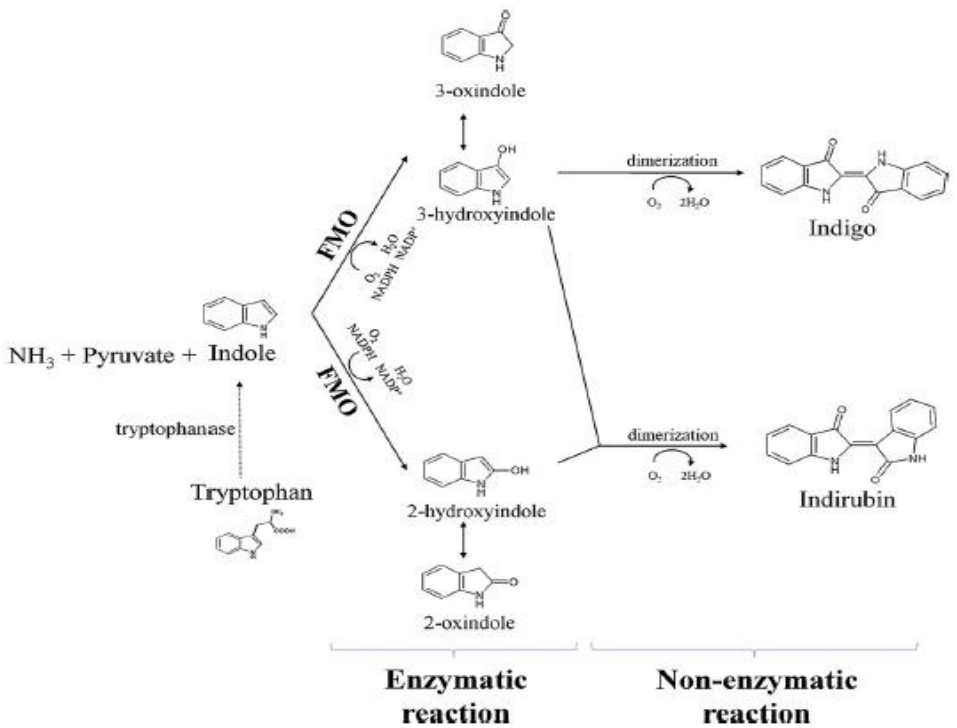

Fig. 1. Modified biosynthetic pathways of indigoid compounds from tryptophan by FMO in recombinant *E. coli* (Meyer et al., 2002; Rui et al., 2005).

0.1 mM NADPH, 10 mM indole, and the purified FMO (5 μg) at room temperature. For the *in vivo* assay, the concentrations of 2- or 3-hydroxyindole were measured by HPLC (Agilent 1200 HPLC, Santa Clara, CA, USA). The compounds were separated on a reverse-phase C_{18} column (5 μm, 4.5 mm × 150 mm, YMC, Milford, MA, USA) and detected with a diode array detector. Solvent A (0.1% formic acid) and solvent B (50% methanol and 50% acetonitrile) were applied as the mobile phase according to the following timetable: 0–8 min, 85% solvent A and 15% solvent B, flow rate of 1 mL/min; 8–10 min, 65% A and 35% B, flow rate of 2 mL/min; 10–15 min, 65% A and 35% B, flow rate of 2 mL/min. For the HPLC analysis, commercially available standards for isatin (6.67 min), 2-oxindole (9.24 min), and indole (13.60 min) were purchased and synthetic 3-hydroxyindole (13.91 min) was prepared by dephosphorylating 3-hydroxyindole phosphate with alkaline phosphatase under anaerobic conditions (Meyer et al., 2002).

Concentrations of indigo and indirubin were determined by HPLC analysis. Each cell culture broth from flasks or fermenters was centrifuged at 10,000 × *g* for 1 min to precipitate a dark pellet that was then washed twice with distilled water. The precipitants were resuspended in 10 mL of DMSO and then were subjected to repeated 1 min sonication (Branson, Danbury, CT, USA) with a microprobe. The amount of indirubin or indigo in the supernatant was determined by comparison to each standard indigoid solution dissolved in DMSO. The HPLC procedure was conducted with a photodiode array detector (Agilent 1200 HPLC, Santa Clara, CA, USA) and an effluent flow rate of 1 mL/min; indirubin sample was monitored at 540 and indigo was at 620 nm, respectively. For the analysis, an isocratic elution system of methanol and water (80:20, v/v) was applied and the YMC-pack ODS-A (C_{18}, 250 mm × 4.6 mm) column was used (Perpete et al., 2006).

2.7. Indirubin production

To produce the seed culture of recombinant *E. coli* DH5α, a single colony from tryptophan solid medium was used to inoculate 100 mL tryptophan medium, and incubation was continued for 16 h at 30 °C. The fermentation was carried out in a 10 L fermenter (Bioflow 3000 Model, New Brunswick, Enfield, CT, USA) with a 5 L working volume of tryptophan medium containing 0.36 g/L (3 mM) cysteine at 35 °C, pH 8.0, and at an agitation speed of 180 rpm. To investigate the effect of oxygen on the indirubin production, three different cultivations were conducted with different oxygen levels. For anoxic cultivation, air in the fermenter was replaced with nitrogen gas three times and the cells were cultured without agitation for 70 h. To prepare a sequential partial aerobic and anoxic condition, air (3 vvm) was supplied to the reactor for the initial 12 h cultivation, and then the oxygen in the fermenter was replaced with nitrogen gas three times and the cells were cultured without agitation for 58 h. For aerobic cultivation, air (3 vvm) was supplied

Collection @ chosun

조선대학교
CHOSUN UNIVERSITY

Table 1
Effect of various agents on biological synthesis of indirubin and indigo.

	Reaction condition	Product composition	
		Indigo (mg/L)	Indirubin (mg/L)
Biological synthesis	[a]TM	920 ± 0.86	5 ± 3.9
	TM + 0.06 g/L cysteine	478 ± 21.2	75.6 ± 6.4
	TM + 0.36 g/L cysteine	6.8 ± 4.5	223.6 ± 11.0
	TM + 0.46 g/L DTT	[b]ND	ND
	TM + 0.44 g/L isatin	ND	ND

[a] Tryptophan medium: 2.0 g/L of tryptophan, 5.0 g/L of yeast extract, and 10.0 g/L of sodium chloride.
[b] ND, not detected.

continuously to the medium with an agitation speed of 180 rpm during the growth.

2.8. Optimization of medium composition and culture conditions for indirubin production

The indirubin production conditions were optimized using a response surface methodology (RSM) based on the 2^n factorial central composite design. The first experiment was based on a 2^3 factorial central composite experimental plan with three medium components; cysteine, tryptophan, and yeast extract. The ranges and levels of the experimental variables investigated in this study are given in Table 1. A set of 20 experiments was carried out with three variables, and each variable was studied at five levels ($\alpha = 2.0$). The second experimental design was a 2^2 factorial central composite experimental plan with two culture conditions: pH and temperature. A set of 13 experiments was conducted with two variables, and each variable was studied at five levels ($\alpha = 2.0$) (Table 1). For statistical calculations, including the solutions of the second-order polynomial model equation (Raymond and Douglas, 2002), the Design Expert (Version 8.0, Stat-Ease Inc., Minneapolis, MN, USA) software package was used.

2.9. Electron microscopic observation of indigoid compounds in cells

To observe the biosynthesis and accumulation of indigoid compounds in the cells, cells were taken from two different culture media (with or without cysteine) time-dependently. The morphologies of the cells were observed by transmission electron microscopy (TEM, JEM-1400, JEOL Ltd., Tokyo, Japan) and scanning electron microscopy (SEM, S-4800, Hitachi, Tokyo, Japan).

3. Results and discussion

3.1. Effect of reducing agents on indirubin synthesis

In our previous batch fermentation study, it was found that recombinant *E. coli* pBlue 1.7 cells harboring the *fmo* gene produced indigo and indirubin by utilizing tryptophan as a substrate under high oxygen level (3 vvm of air supply) (Han et al., 2011). Under this condition, the major product (>99%) was indigo and a small amount of indirubin was produced (Table 1). Interestingly, when the indigo fermentation was performed in an aerobic condition for 12 h to cultivate the cells and then an anoxic condition, it was observed that some of the blue indigo compound that was produced in the medium turned into pink indirubin. Based on the above result, we expected the possibility that any other reducing agents, including amino acids, could increase the indirubin synthesis in the recombinant *E. coli*. Cysteine, methionine, serine, tyrosine, phenylalanine, arginine, aspartic acid, glutathione, dithiothreitol, ascorbic acid, thioglycolic acid, and isatin were added to the tryptophan medium. Among the various reducing agents tested, only 0.36 g/L (3 mM) cysteine was responsible for enhancing biological indirubin production (Table 1).

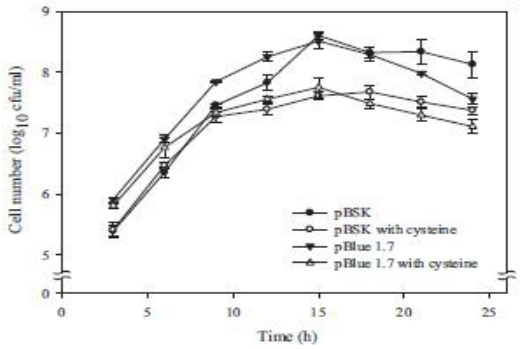

Fig. 2. Effects of cysteine on the growths of different types of recombinant *E. coli* cells. Symbols: (●) *E. coli* harboring pBSK grown on tryptophan medium, (▼) *E. coli* harboring pBlue 1.7 grown on tryptophan medium, (○) *E. coli* harboring pBSK grown on tryptophan medium containing 0.36 g/L cysteine, (△) *E. coli* harboring pBlue 1.7 grown on tryptophan medium containing 0.36 g/L cysteine.

3.2. Effect of cysteine on the growth of E. coli and fmo expression

To investigate whether cysteine supplementation influences the growth of recombinant *E. coli*, the cell numbers of the control *E. coli* DH5α and the recombinant *E. coli* DH5α at different growth phases were compared. For a control strain, the *E. coli* harboring pBSK that contains no inserted gene was used. Fig. 2 showed that addition of cysteine inhibited the growth of both the control and the recombinant strains. The cell numbers of the recombinant *E. coli* pBlue 1.7 cultured in tryptophan media with and without 0.36 g/L cysteine after 15 h cultivation at 35 °C were $(4.11 \pm 1.25) \times 10^7$ and $(4.05 \pm 1.58) \times 10^8$, respectively. And the numbers of cells of the control *E. coli* strains with and without cysteine at the same incubation time were $(4.12 \pm 1.16) \times 10^7$ and $(3.28 \pm 1.31) \times 10^8$, respectively. These experiments showed that cysteine significantly inhibited the growth of *E. coli* (Harris, 1981) (Table 2).

The Western blot analysis was performed to investigate the effect of cysteine on the expression of *fmo*. A comparison of the band intensities from the samples indicated that the expression level of FMO was not significantly reduced by the supplemented cysteine in the recombinant *E. coli* (data not shown). The enzyme assays with purified FMO also showed that the cysteine did not affect the activity of FMO, however, the higher concentration inhibited indirubin

Table 2
Experimental design (range, levels, and response) to assess the effects of medium composition (Experiment 1), pH, and temperature (Experiment 2).

Variable	Symbol code	Range and levels				
		−2	−1	0	1	2
Experiment 1 (medium composition)						
Cysteine (mM)	M_1	1	2	3	4	5
Tryptophan (g/L)	M_2	1.0	1.5	2	2.5	3.0
YE (g/L)	M_3	3	4	5	6	7
Experiment 2 (culture conditions)						
pH	C_1	6	7	8	9	10
Temperature (°C)	C_2	31	33	35	37	39

Collection @ chosun

조선대학교
CHOSUN UNIVERSITY

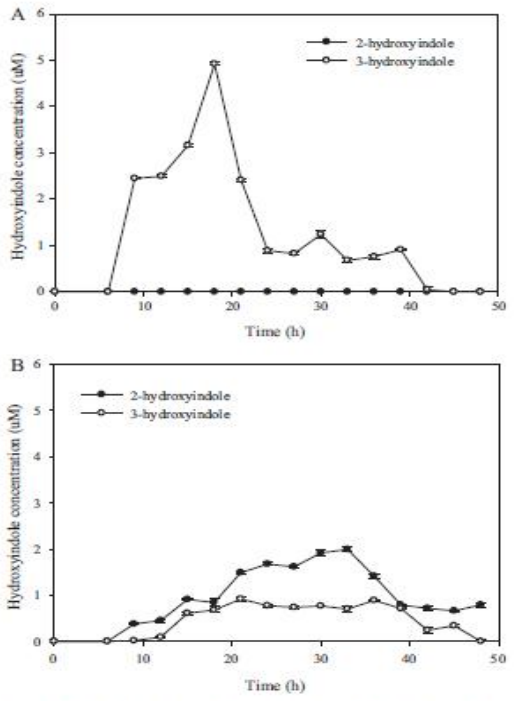

Fig. 3. Effect of cysteine on the hydroxylation level of indole to 2- and 3-hydroxyindole in *E. coli* cells. The time-dependent 2- and 3-hydroxyindole concentrations in the cells grown on tryptophan medium without (A) and with (B) cysteine were determined.

production. The minimum concentration of cysteine required for indirubin production was 0.06 g/L in the tryptophan medium.

3.3. *In vivo hydroxyindole formation*

To investigate the modified processes of indigo and indirubin biosynthesis after cysteine supplementation, different hydroxyindole formations were determined by *in vivo* assays. The same numbers (1.7×10^3) of recombinant *E. coli* cells were grown on tryptophan medium with or without cysteine, and the concentrations of 2- or 3-hydroxyindole synthesized in the cells were compared. In the cells grown on tryptophan medium without cysteine, 3-hydroxyindole concentration increased for 18 h, but thereafter it decreased significantly (Fig. 3(A)). During the incubation time, 2-hydroxyindole was not detected and the indigo concentration was maximal because indigo synthesis is proportional to the concentration of 3-hydroxyindole. However, when cysteine was added to the medium, relatively higher levels of 2-hydroxyindole than 3-hydroxyindole were synthesized from indole for 50 h, but isatin was not detected (Fig. 3(B)). As described above, both 2- and 3-hydroxyindole are essential for the dimerization process to produce indirubin. Based on these data, it is concluded that cysteine influences both the regioselectivity of FMO and hydroxylation level of indole to 2- or 3-hydroxyindole using a NADPH.

Table 3
Analysis of variance with coded values for the effects of medium composition (Experiment 1), pH, and temperature (Experiment 2).

Source	SS	DF	MS	*F*-value	Prob (*P*) > *F*
Experiment 1 (medium composition)					
Model	2038.08	9	226.45	19.60	<0.0001
Residual (error)	115.52	10	11.55		
Lack of fit	62.76	5	12.55	1.19	0.4268
Pure error	52.76	5	10.55		
Total	2153.60	19			
R-squared	0.9463				
Adj *R*-squared	0.8980				
Experiment 2 (culture condition)					
Model	287.45	8	35.93	40.15	<0.0015
Pure error	3.58	4	0.89		
Total	291.02	12			
R-squared	0.9877				
Adj *R*-squared	0.9631				

SS, sum of squares; DF, degrees of freedom; MS, mean squares.

A higher concentration of 2-hydroxyindole than 3-hydroxyindole stimulated the production of indirubin as a major product (Fig. 4). Therefore, it is possible to produce a high concentration of indirubin in a tryptophan medium by controlling the addition of cysteine.

3.4. *Optimization of medium and culture conditions for indirubin production*

Using the response surface methodology (RSM), the interaction between two variables and their optimum levels can be easily understood and located. Fig. 5(A) shows the interaction between cysteine (M_1) and tryptophan (M_2), and cysteine (M_1) and yeast extract (M_3), and tryptophan (M_2) and yeast extract (M_3). Fig. 5(B) shows the responses and curves for plots of the pH (C_1) and temperature (C_2). The optimum points for the maximum production of indirubin are near the center point of the pH and temperature ranges. To calculate indirubin production, the numerical quarterly equation given by Myers and Montgomery was used to solve Eqs. (1) and (2) (Raymond and Douglas, 2002).

$$\text{Indirubin concentration (mg/L)} = 48.983 + 0.250M_1 + 0.626M_2 - 0.623M_3 - 1.571M_1M_2 - 3.096M_1M_3 + 1.411M_2M_3 - 8.863M_1^2 - 2.172M_2^2 - 0.774M_3^2 \quad (1)$$

$$\text{Indirubin concentration (mg/L)} = 49.07 - 0.24C_1 + 0.90C_2 - 0.17C_1C_2 - 2.74C_1^2 - 2.71C_2^2 - 0.54C_1^2C_2 - 1.25C_1C_2^2 - 1.07C_1^2C_2^2 \quad (2)$$

The optimal values of the medium composition test variables in the coded units were: $M_1 = 0.22$, $M_2 = -0.26$, and $M_3 = -0.10$. The natural values were obtained by putting the respective values of M_i into Eq. (1) (Table 3). The optimal values of the culture condition test variables in the coded units were: $C_1 = -0.05$ and $C_2 = 0.17$. The natural values were obtained by putting the respective values of C_i into Eq. (2).

The fit of the models was expressed by the coefficients of determination, R^2, which were 0.9464 and 0.9877, respectively. The closer the R^2 value is to 1, the stronger the model and the better the prediction of the response. The values of the adjusted determination coefficient (Adj R^2) (0.8981 and 0.9631) were also high in reasonable agreement with the Adj R^2. In addition, the statistical significance of the second-order model equations was assessed using the *F*-test analysis of variance (ANOVA), which can indicate

Collection @ chosun

조선대학교
CHOSUN UNIVERSITY

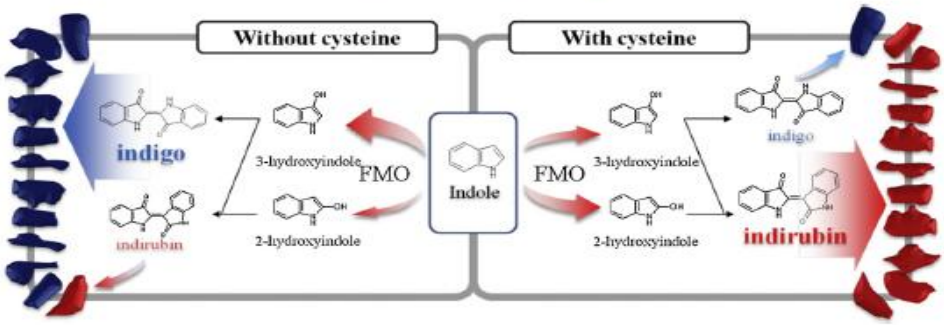

Fig. 4. Proposed biosynthetic mechanism of indigoid compounds from indole by FMO with and without cysteine.

a good agreement between the experimental and predicted values for the medium composition and culture conditions. The RSM analysis showed that cysteine concentration was a critical factor for indirubin production. The RSM data shown in "Eqs. (1) and (2)" were obtained from the tryptophan medium containing 0.36 g/L cysteine for which the initial pH was adjusted. The analysis determined that tryptophan concentration was another important factor in indirubin production. The RSM result showed that the tryptophan concentration for the highest indirubin production was 2.0 g/L. In addition, the optimal temperature and initial pH for the indirubin production were 35 °C and 8.0, respectively. The experimental results indicated that even a slight change in pH value greatly influence the indirubin production. The RSM model was confirmed experimentally. The maximum production of indirubin from the cells grown in modified tryptophan medium (tryptophan 2 g/L, yeast extract 5 g/L, sodium chloride 10 g/L, and cysteine 0.36 g/L) in a 300 mL flask was 93.1 mg/L. The initial pH for 48 h cultivation was pH 8.0 and the temperature was set to 35 °C, which was in close agreement with the prediction of model (data not shown).

3.5. Indirubin fermentation

To study the effect of oxygen concentration on indirubin production, three different fermentation processes in a 10 L fermenter were conducted. The estimated indirubin concentrations produced from different oxygen levels were: 82.5 mg/L (anoxic condition), 153.0 mg/L (sequentially partial aerobic–anoxic condition), and 223.6 mg/L (aerobic condition) (Fig. 6). These results indicated that the oxygen is essential for cell growth and indirubin synthesis just as it is for indigo synthesis. Under the partial aerobic–anoxic condition, indirubin production increased for 12 h (aerobic cultivation), but afterwards the production rate slowly decreased in the absence of oxygen. The maximal indirubin production occurred after aerobic fermentation for 48 h.

Fig. 7 shows the relationship between tryptophan and cysteine consumption and indirubin synthesis during cell growth in a 10 L fermenter with a 3 vvm air supply. As the tryptophan concentration decreased time-dependently, indirubin accumulated in the medium for 48 h. The recombinant *E. coli* converted 1.61 g/L tryp-

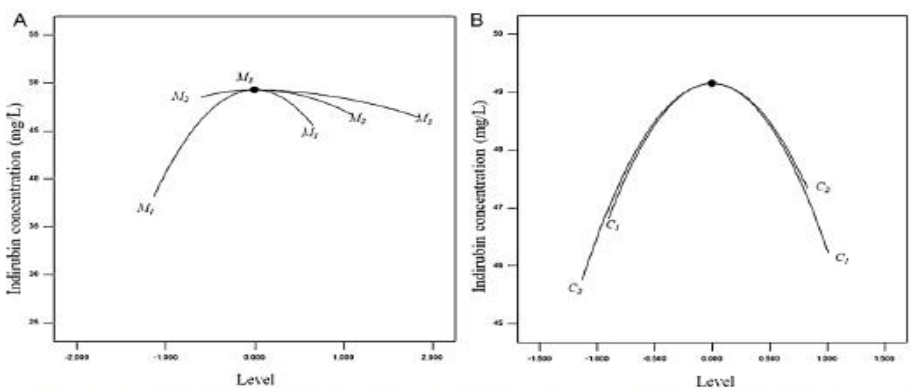

Fig. 5. Response surface plot shows the effect of (A) medium composition (tryptophan, yeast extract, and cysteine) and (B) culture conditions (pH and temperature) on the production of indirubin. The optimal coded units were: M_3 (tryptophan) = 0.22, M_2 (yeast extract) = −0.26, M_3 (cysteine) = −0.10, C_1 (pH) = −0.05, and C_2 (temperature) = 0.17.

Collection @ chosun

조선대학교
CHOSUN UNIVERSITY

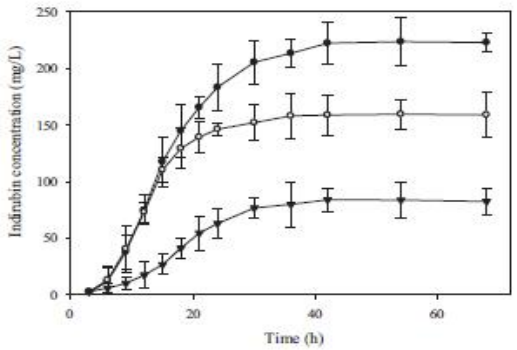

Fig. 6. Effect of aeration mode on indirubin production in the recombinant *E. coli* cells. Aeration was performed with a flow rate of 3 vvm. Symbols: (●) continuously aerobic; (○) sequentially partial aerobic–anoxic; (▾) anoxic fermentations.

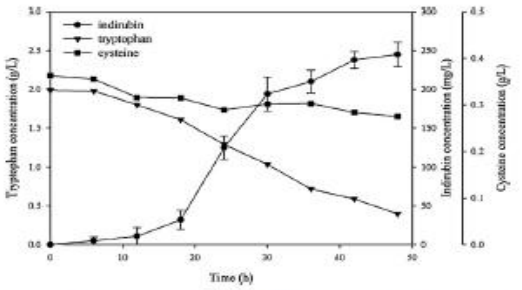

Fig. 7. Relationship between tryptophan and cysteine consumption and indirubin synthesis during cell growth in a 10 L fermenter with a 3 vvm air supply. Symbols: (●) indirubin; (▾) tryptophan; (■) cysteine.

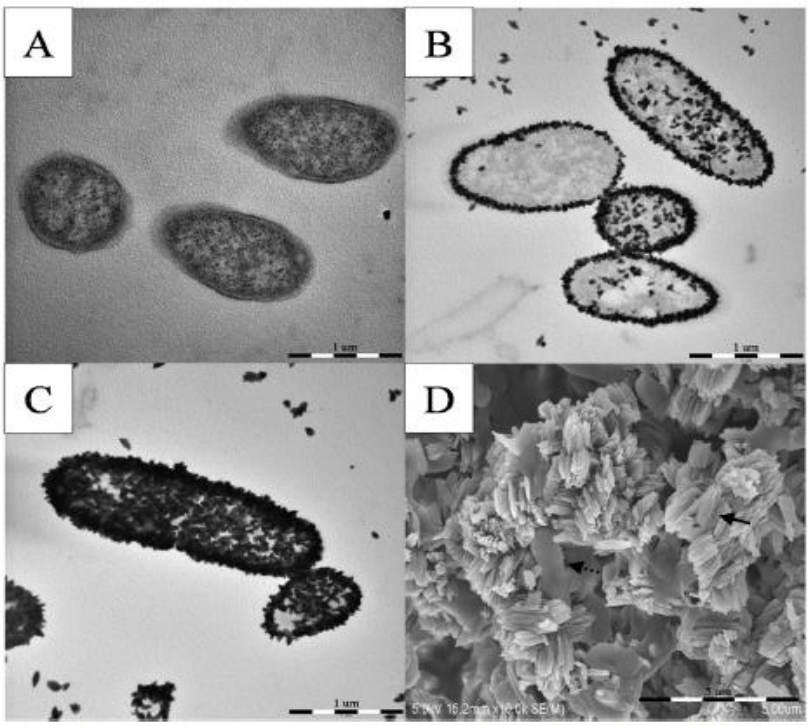

Fig. 8. TEM and SEM images showing the distribution of the synthesized indirubin compounds in the *E. coli* cells. (A) Cells cultured for 12 h in a tryptophan medium containing 0.36 g/L cysteine (40k×); (B) indirubin crystals were distributed around the cellular membrane after 24 h cultivation (40k×); (C) indirubin crystals were distributed around the cellular membrane after 48 h cultivation (40k×); (D) SEM images showing indirubin crystals secreted by the disruption of cells of *E. coli* pBlue 1.7 (10k×). Symbol: crystals of indirubin (↘) and *E. coli* (↘). Length scale is indicated by bars.

Collection @ chosun

조선대학교
CHOSUN UNIVERSITY

tophan to 0.25 g/L indirubin within 48 h by consuming 0.09 g/L cysteine. Interestingly, it was found that the minimum and optimum cysteine concentrations in this process are 0.06 g/L and 0.36 g/L, respectively, however, the cysteine concentration consumed during fermentation is no more than 0.1 g/L. It is not understood why such a high cysteine concentration in the medium was required for the indirubin production process.

3.6. TEM and SEM observations

Fig. 8 shows the accumulation process of synthesized indirubin in the recombinant *E. coli* cells. In the initial growth stage, the synthesized indirubin compounds were distributed around the cellular membrane, and thereafter they slowly accumulated inside the cells (Fig. 8(A)–(C)). Most of the cells were disrupted due to the indirubin toxicity, and the compounds were secreted and accumulated in the medium (Fig. 8(D)). This result indicated that none of the membrane transporters in the *E. coli* strain pumps out the indirubin compounds. The intracellular accumulation of the indirubin crystals might stress the cell, which may be a main reason for the poor growth of the recombinant *E. coli* pBlue 1.7. Additionally, a comparison of the growth implied that indirubin may be more toxic than indigo to the *E. coli* strain (Fig. 2). However, the identification and overexpression of a proper transporter that expels the indirubin compounds into the medium may improve the growth of the recombinant *E. coli* in the future.

4. Conclusions

In this study, an efficient indirubin production process was developed using recombinant *E. coli* DH5α harboring an *fmo* gene. Among the various reducing agents analyzed, cysteine shows higher indirubin production. When 0.36 g/L cysteine was added to the tryptophan medium, cells significantly increased the production of indirubin. The addition of cysteine did not influence the expression level or activity of FMO in the cell. However, cysteine was found to inhibit the cell growth of recombinant *E. coli* and affect the regioselectivity of FMO and the synthetic pathway of 2- and 3-hydroxyindole from indole, which might function to increase indirubin production. The recombinant *E. coli* cells were capable of producing 223.6 mg/L of indirubin under the following optimum culture conditions: 2 g/L tryptophan, 5 g/L yeast extract, 10 g/L NaCl, 0.36 g/L cysteine, and pH 8.0 at 35 °C. The synthesized indirubin compounds accumulated inside the cells and thereafter were released due to the disruption of the cells by the toxicity of the accumulated indirubin compounds. This study demonstrates that it is possible to produce an expensive indirubin in a large amount by simple fermentation with recombinant *E. coli* cells.

Acknowledgments

This work was supported by the 21C Frontier Microbial Genomics and Applications Center Program (Grant 11-2008-18-006-00), Ministry of Education, Science & Technology, Republic of Korea. This work was also partly supported by the Human Resources Development Program of the KETEP (No. 2011401010090).

References

Berry, A., Dodge, T.C., Pepsin, M., Weyler, W., 2002. Application of metabolic engineering to improve both the production and use of biotech indigo. Journal of Industrial Microbiology and Biotechnology 28, 127–133.
Bidlingmeyer, B.A., Cohen, S.A., Tarvin, T.L., 1984. Rapid analysis of amino acids using pre-column derivatization. Journal of Chromatography B: Biomedical Sciences and Applications 336, 93–104.
Bradford, M.M., 1976. A rapid and sensitive method for the quantitation of microgram quantities of protein utilizing the principle of protein-dye binding. Analytical Biochemistry 72, 248–254.
Chant, E.L., Summers, D.K., 2007. Indole signalling contributes to the stable maintenance of *Escherichia coli* multicopy plasmids. Molecular Microbiology 63, 35–43.
Cho, H.J., Cho, H.Y., Kim, K.J., Kim, M.H., Kim, S.W., Kang, B.S., 2011. Structural and functional analysis of bacterial flavin-containing monooxygenase reveals its ping-pong-type reaction mechanism. Journal of Structural Biology 175, 39–48.
Choi, H.S., Kim, J.K., Cho, E.H., Kim, Y.C., Kim, J.I., Kim, S.W., 2003. A novel flavin-containing monooxygenase from *Methylophaga* sp. strain SK1 and its indigo synthesis in *Escherichia coli*. Biochemical and Biophysical Research Communications 306, 930–936.
Doukyu, N., Nakano, T., Okuyama, Y., Aono, R., 2002. Isolation of an *Acinetobacter* sp. ST-550 which produces a high level of indigo in a water-organic solvent two-phase system containing high levels of indole. Applied Microbiology and Biotechnology 58, 543–546.
Eaton, R.W., Chapman, P.J., 1995. Formation of indigo and related compounds from indolecarboxylic acids by aromatic acid-degrading bacteria: chromogenic reactions for cloning genes encoding dioxygenases that act on aromatic acids. Journal of Bacteriology 177, 6983–6988.
Ensley, B.D., Ratzkin, B.J., Osslund, T.D., Simon, M.J., Wackett, L.P., Gibson, D.T., 1983. Expression of naphthalene oxidation genes in *Escherichia coli* results in the biosynthesis of indigo. Science 222, 167–169.
Fitzhugh, E.W., Feller, R.L., Roy, A., 1997. Artists' Pigments: A Handbook of Their History & Characteristics, 3rd ed. Oxford University Press, Oxford.
Han, G.H., Bang, S.E., Babu, B.K., Chang, M., Shin, H.-J., Kim, S.W., 2011. Bio-indigo production in two different fermentation systems using recombinant *Escherichia coli* cells harboring a flavin-containing monooxygenase gene (*fmo*). Process Biochemistry 46, 788–791.
Han, G.H., Shin, H.-J., Kim, S.W., 2008. Optimization of bio-indigo production by recombinant *E. coli* harboring *fmo* gene. Enzyme and Microbial Technology 42, 617–623.
Han, R., 1994. Highlight on the studies of anticancer drugs derived from plants in china. Stem Cells 12, 53–63.
Harris, C.L., 1981. Cysteine and growth inhibition of *Escherichia coli*: threonine deaminase as the target enzyme. Journal of Bacteriology 145, 1031–1035.
Hoessel, R., Leclerc, S., Endicott, J.A., Nobel, M.E.M., Lawrie, A., Tunnah, P., Leost, M., Damiens, E., Marie, D., Marko, D., Niederberger, E., Tang, W., Eisenbrand, G., Meijer, L., 1999. Indirubin, the active constituent of a Chinese antileukaemia medicine, inhibits cyclin-dependent kinases. Nature Cell Biology 1, 60–67.
Kim, H.G., Doronina, N.V., Trotsenko, Y.A., Kim, S.W., 2007. *Methylophaga aminisulfidivorans* sp. nov., a restricted facultatively methylotrophic marine bacterium. International Journal of Systematic and Evolutionary Microbiology 57, 2096–2101.
Kohda, H., Niwa, A., Nakamoto, Y., Takeda, O., 1990. Flavonoid glucosides from *Polygonum tinctorium*. Chemical and Pharmaceutical Bulletin 38, 523–524.
Krueger, S.K., Williams, D.E., 2005. Mammalian flavin-containing monooxygenases: structure/function, genetic polymorphisms and role in drug metabolism. Pharmacology and Therapeutics 106, 357–387.
Leclerc, S., Garnier, M., Hoessel, R., Marko, D., Bibb, J.A., Snyder, G.L., Greengard, P., Biernat, J., Wu, Y.-Z., Mandelkow, E.-M., Eisenbrand, G., Meijer, L., 2001. Indirubins inhibit glycogen synthase kinase-3 and CDK5/P25, two protein kinases involved in abnormal Tau phosphorylation in Alzheimer's Disease. Journal of Biological Chemistry 276, 251–260.
Madsen, E.L., Bollag, J.-M., 1988. Pathway of indole metabolism by a denitrifying microbial community. Archives of Microbiology 151, 71–76.
Maugard, T., Enaud, E., Sayette, A.D.L., Choisy, P., Legoy, M.D., 2002. β-Glucosidase-catalyzed hydrolysis of indican from leaves of *Polygonum tinctorium*. Biotechnology Progress 18, 1104–1108.
McClay, K., Boss, C., Keresztes, I., Steffan, R.J., 2005. Mutations of toluene-4-monooxygenase that alter regiospecificity of indole oxidation and lead to production of novel indigoid pigments. Applied Microbiology and Biotechnology 71, 5476–5483.
Meyer, A., Würsten, M., Schmid, A., Kohler, H.-P.E., Witholt, B., 2002. Hydroxylation of indole by laboratory-evolved 2-hydroxybiphenyl 3-monooxygenase. Journal of Biological Chemistry 277, 34161–34167.
Murdock, D., Ensley, B.D., Serdar, C., Thalen, M., 1993. Construction of metabolic operons catalyzing the *de novo* biosynthesis of indigo in *Escherichia coli*. Nature Biotechnology 11, 381–386.
Nam, S., Buettner, R., Turkson, J., Kim, D., Cheng, J.Q., Muehlbeyer, S., Hippe, F., Vatter, S., Merz, K.-H., Eisenbrand, G., Jove, R., 2005. Indirubin derivatives inhibit Stat3 signaling and induce apoptosis in human cancer cells. Proceedings of the National Academy of Sciences 102, 5998–6003.
Newton, W.A., Snell, E.E., 1965. Formation and interrelationships of tryptophanase and tryptophan synthetases in *Escherichia coli*. Journal of Bacteriology 89, 355–364.
Perpete, E.A., Preat, J., Andre, J.-M., Jacquemin, D., 2006. An ab initio study of the absorption spectra of indirubin isoindigo, and related derivatives. The Journal of Physical Chemistry A 110, 5629–5635.
Raymond, H.M., Douglas, M., 2002. Response Surface Methodology: Process and Product Optimization Using Designed Experiments, 2nd edition. A Wiley-Interscience Publication, New York.
Rui, L., Reardon, K.F., Wood, T.K., 2005. Protein engineering of toluene ortho-monooxygenase of *Burkholderia cepacia* G4 for regiospecific hydroxylation of indole to form various indigoid compounds. Applied Microbiology and Biotechnology 66, 422–429.

Collection @ chosun

조선대학교
CHOSUN UNIVERSITY

Sambrook, J., Russell, D.W., 2001. Molecular Cloning: A Laboratory Manual, 3rd ed. Cold Spring Harbor Laboratory Press, Cold Spring Harbor, NY.
Seldes, A.M., Burucúa, J.E., Maier, M.S., Abad, G., Jáuregui, A., Siracusano, G., 1999. Blue pigments in South American painting (1610–1780). Journal of the American Institute for Conservation 38, 100–123.
Tang, W., Eisenbrand, G., 1992. Chinese Drugs of Plant Origin: Chemistry, Pharmacology and Use in Traditional and Modern Medicine, 1st ed. Springer, Berlin, Heidelberg, New York.
Woo, H.-j., Sanseverino, J., Cox, C.D., Robinson, K.G., Sayler, G.S., 2000. The measurement of toluene dioxygenase activity in biofilm culture of *Pseudomonas putida* F1. Journal of Microbiological Methods 40, 181–191.
Xia, Z.Q., Zenk, M.H., 1992. Biosynthesis of indigo precursors in higher plants. Phytochemistry 31, 2695–2697.
Zhou, J., Shephard, E.A., 2006. Mutation, polymorphism and perspectives for the future of human flavin-containing monooxygenase 3. Mutation Research/Reviews in Mutation Research 612, 165–171.

Collection @ chosun

조선대학교
CHOSUN UNIVERSITY

Bioprocess Biosyst Eng (2014) 37:2149–2162
DOI 10.1007/s00449-014-1192-7

ORIGINAL PAPER

Biodegradation of Methyl Orange by alginate-immobilized *Aeromonas* sp. in a packed bed reactor: external mass transfer modeling

Mathur Nadarajan Kathiravan · Siluvai Antony Praveen · Geun Ho Gim · Gui Hawn Han · Si Wouk Kim

Received: 29 October 2013 / Accepted: 10 April 2014 / Published online: 9 May 2014
© Springer-Verlag Berlin Heidelberg 2014

Abstract Azo dyes are recalcitrant and xenobiotic nature makes these compounds a challenging task for continuous biodegradation up to satisfactorily levels in large-scale. In the present report, the biodegradation efficiency of alginate immobilized indigenous *Aeromonas* sp. MNK1 on Methyl Orange (MO) in a packed bed reactor was explored. The experimental results were used to determine the external mass transfer model. Complete MO degradation and COD removal were observed at 0.20 cm bead size and 120 ml/h flow rate at 300 mg/l of initial dye concentration. The degradation of MO decreased with increasing bead sizes and flow rates, which may be attributed to the decrease in surface of the beads and higher flux of MO, respectively. The experimental rate constants (k_{ps}) for various beads sizes and flow rates were calculated and compared with theoretically obtained rate constants using external film diffusion models. From the experimental data, the external mass transfer effect was correlated with a model $J_D = K\,Re^{-(1-n)}$. The model was tested with K value (5.7) and the Colburn factor correlation model for 0.20, 0.40 and 0.60 bead sizes were $J_D = 5.7\,Re^{-0.15}$, $J_D = 5.7\,Re^{-0.36}$ and $J_D = 5.7\,Re^{-0.48}$, respectively. Based on the results, the Colburn factor correlation models were found to predict the experimental data accurately. The proposed model was constructive to design and direct industrial applications in packed bed reactors within acceptable limits.

Keywords Immobilization · MO degradation · External mass transfer · COD · Bed reactor · Colburn factor

List of symbols

$[COD]_i$	Initial COD of dye solution (mg/l)
$[COD]_o$	Observed COD of dye solution (mg/l) at time t (min)
$[MO]_I$	Initial dye concentration (mg/l)
$[MO]_o$	Observed dye concentration (mg/l) at time t (min)
A	Parameter given by Eq. (22)
a_m	Surface area per unit weight of immobilized particles available for mass transfer ($cm^2\ mg^{-1}$)
MO_b	Substrate concentration at the bulk liquid
MO_s	Dye concentration at the surface of the immobilized particle ($mg\ l^{-1}$)
D_f	Substrate (chromium) effective diffusivity ($cm^2\ s^{-1}$)
dC/dz	Concentration gradient along the column length ($mg\ l^{-1}\ cm^{-1}$)
d_p	Particle diameter (cm)
G	Mass flux of chromium solution ($g\ cm^{-2}\ h^{-1}$)
H	Height of the column (cm)
J_D	Colburn factor
K	Constant

M. N. Kathiravan (✉) · G. H. Gim · G. H. Han · S. W. Kim (✉)
Department of Environmental Engineering, Pioneer Research Center for Controlling of Harmful Algal Bloom, Chosun University, 375 Seosuk-dong, Dong-gu, Gwangju 501-759, Republic of Korea
e-mail: mnkathir2025@gmail.com

S. W. Kim
e-mail: swkim@chosun.ac.kr

G. H. Gim
e-mail: ma.geunho@gmail.com

G. H. Han
e-mail: jeney69@gmail.com

S. A. Praveen
Environmental Materials Division, National Environmental Engineering Research Institute (NEERI), Nagpur 440020, India
e-mail: sa_praveen@neeri.res.in

Collection @ chosun

조선대학교
CHOSUN UNIVERSITY

k	Intrinsic first-order reduction rate constant (ml g^{-1} h^{-1})
k_m	External mass transfer coefficient (cm h^{-1})
k_p	Apparent first-order reaction rate constant (l g^{-1} h^{-1})
k_s	Surface first-order reaction rate constant (cm h^{-1})
N_{Re}	Reynolds number
Q	Volumetric flow rate (ml min^{-1})
R	Degradation rate (mg g^{-1} h^{-1})
r_m	External mass transfer rate (mg g^{-1} h^{-1})
MO_1	Concentration of dye (mg/l) in the reservoir
MO_2	Concentration (mg/l) at the outlet of the packed bed reactor to be circulated back to the reservoir
MO_{in}	Inlet MO concentration (mg/l)
MO_{out}	Column outlet MO concentration (mg/l)
V_{res}	Volume of the reacting solution in the reservoir (ml)
W	Amount of immobilized organism used (g)
E	Voidage
ρ_p	Density of the particle (g cm^{-3})
τ	Residence time (min) in the reservoir (V_{res}/Q)

Introduction

The extensive use of azo dyes in industries such as textiles, food, cosmetics, plastic, laboratories, leather, paper printing, color photography, pharmaceutical and pigment manufacturing has resulted in the releasing of large quantities of dyes containing industrial effluents into the environment. The Azo dyes, which are characterized by aromatic compounds with one or more (R–N=N–R) groups, are the most important and largest class of synthetic dyes used in commercial applications. They constitute a major class of environmental pollutants, accounting for 60–70 % of all the dyes and pigments used [1]. Presence of such dangerous colored compounds in the industrial wastewater creates serious environmental and health concerns [2, 3]. Currently, many conventional methods are available for decolorization of textile dyes such as chemical precipitation, membrane filtration, coagulation, adsorption and electrochemical degradation [4]. Aforementioned methods are effective for color removal; however, they consume more energy, enormous chemicals, involve high cost and produce large amounts of secondary pollutants [5]. Therefore, an effective, economical and eco-friendly method of treatment has become a necessity for clean production technology in textile dye industries.

Several microorganisms have been found to be able to decolorize azo dyes including bacteria, fungi and yeasts. Among these, an extensive study on the bacterial degradation of azo dyes by free cell cultures has been reported in the literature [6–16]. However, free cells used for industrial scale purposes has some operational problems such as cell toxicity, shear force, cell stability in agitated conditions and biomass-effluent separation. These problems may be overcome with immobilized bacterial cells. In recent years, researchers have paid more attention towards introducing novel technology like immobilized cells for textile dye degradation. The immobilized cells has many advantages such as high stability, regeneration, reuse, easier separation, accelerated reaction rates, increased cell metabolism, no cell wash-out and better control. Many immobilized cell systems have been developed and widely used for the complete degradation of textile dyes such as Direct Blue 1 and Direct Red 128 [17], Malachite Green [18], Reactive Blue 172 [19], Reactive Black 5 [20], Amaranth [21], reactive yellow 42 and reactive red 45 [22], Anthraquinone and indigoid [23], Remazol Brilliant Blue R [24], Reactive Blue 4 [25] and Basic Blue 41 and Reactive Black 5 [26].

Many researchers have reported using of immobilized bioreactors such as packed bed, airlift, membrane, trickle bed, fluidized bed, rotating biological contactor and tapered bed for continuous decolouration of textile dyes. Among the various reactors, the packed-bed reactors are commonly preferred for effective industrial wastewater treatment applications [27–29]. Recirculated packed bed batch reactor (RPBR) with single column or multicolumn packed bed has also been used to treat textile dye effluents [30–32]. In immobilized RPBR operations, the internal and external mass transfer limitations play a vital role in the reaction kinetics and its study is essential to scale-up. The influence of external mass transfer limitations in immobilized packed bed reactors was widely studied for various purposes such as chromium reduction [33], removal of carbohydrate and protein [34], hydrolysis of Jatropha oil [35], removal of phenol [36], phenolic effluents treatment [37], wastewater treatment [38], penicillin G deasylation [39] and biodegradation of phenol [40]. The mass transfer effects on immobilized packed bed reactor systems were performed by Murty et al. [41] and they concluded that the reaction kinetics was limited by internal and external mass transfer resistances. Mudliar et al. [42] developed a steady-state model for the evaluation of external liquid film diffusion and internal pore diffusion effects in an immobilized biofilm system under continuous mode. Development of mathematical models for the diffusional restriction and the operating parameters which affect this restriction in immobilized packed bed reactor are not only useful for model systems but also advantageous for direct industrial applications and scale-up. All the aforesaid studies involved only single bead diameter external mass transfer correlations in RPBR. To

Collection @ chosun

조선대학교
CHOSUN UNIVERSITY

the best of our knowledge, no research reports are available on the external mass transfer correlations of different bead diameters.

In the present investigation, an attempt was made to determine the external mass transfer limits on continuous degradation of Methyl Orange (MO) using alginate immobilized *Aeromonas* sp. in a recirculated packed bed reactor. The effect of various bead sizes and MO flow rates on external mass transfer limitations was analyzed and a correlation model was developed. The mass transfer coefficient at different scales and various operating parameters were used to predict the reactor performance as well as scale-up.

Materials and methods

Isolation and culture of microorganisms

Soil samples were collected (spade from the top 5–15 cm) aseptically in 50 ml screwcap sterile plastic tubes from three different locations of soil contaminated with textile dye effluents from textile dyeing industry area Karur, India. The soil samples were mixed properly and homogenized by sieving (2 mm mesh size) and stored at 4 °C until further use. Bacterial strains were isolated from soil by enriched growth medium according to the modified method of Li et al. [43]. The enrichment medium used in this study consisted of (g/l) glucose-10 g, yeast extract-0.5 g, peptone-5 g, NaCl-5 g %, $(NH_4)_2SO_3$-10 g, K_2HPO_4-0.2 g, KH_2PO_4-5 g % and $MgSO_4.7H_2O$-5 g, amended with 75 mg/l of the MO dye for adaptation of the microorganisms. The isolation procedure is as follows: one gram of the soil sample was added to 100 ml of enriched medium containing 75 mg/l of MO in 250 ml Erlenmeyer flask and incubated at 37 °C under shaking conditions at 150 rpm for 24 h. After incubation, 1 ml of the culture was serially diluted and 0.1 ml of aliquot was withdrawn from the 10^{-6} dilution. The diluted samples were inoculated in agar plates enriched with 100 mg/l MO. After incubation at 37 °C for 48 h, the individual colonies developed in the plates were screened according to the decolorization ability (clear zones around the colonies) and the distinct colony morphology. The colonies were picked and subcultured again in fresh nutrient broth and these isolates were used for further identification and characterization. The isolated bacterial species were identified based on the colony morphology, cell morphology and biochemical tests. The biochemical tests were performed according to the Hensyl Bergey's manual of systematic bacteriology [44]. The 16srRNA sequence analysis was performed as described by Kathiravan et al. [45]; these sequence was used to construct phylogenetic relatedness exploration and named as *Aeromonas* sp., MNK1.

Acclimatisation

In order to improvise the decolorizing efficiency, the isolated bacterial species was gradually exposed to the increasing concentration of MO dye to acclimatize. After the complete decoloration, the biomass was collected and used for successive transfers into fresh culture medium containing various dye concentrations (100–400 mg/l) and incubated at optimum conditions. This acclimatized microorganism was used further for all studies.

Immobilization of *Aeromonas* sp.

The acclimatized *Aeromonas* sp. was inoculated in a nutrient broth enriched with 300 mg/l of MO and incubated at 37 °C, with the agitation speed of 150 rpm for 48 h. The well-grown culture was harvested and centrifuged at 8,000 rpm for 10 min. The collected biomass was washed thrice with saline (0.85 % NaCl) solution. The bacterial biomass (1.58 g of biomass in 100 ml of alginate) was added to sterilized 3 % sodium alginate under sterile conditions. The alginate-cell mixture was dripped into sterile, cold 3 % $CaCl_2$ solution through different sizes of nozzles to get different bead diameters. The resultant alginate beads were allowed to harden by resuspending it into fresh sterile 0.01 M $CaCl_2$ solution for 24 h at 4 °C. The excess calcium ion was removed by washing the beads with double-distilled water.

Continuous MO degradation in packed bed reactor

For continuous MO degradation, the column used in this study was a cylindrical packed bed reactor (internal diameter—2.0 cm and length—35 cm) made up of Pyrex glass. Various sizes of alginate immobilized *Aeromonas* sp. beads were packed in the reactor up to the desired height. The total volume of packed bed reactor was 100.53 cm^3 and the bed volume was maintained at 86.85 cm^3 for different beads sizes. The enriched medium containing 300 mg/l of dye was passed through the column at various flow rates (120, 300 and 600 ml/h) in upflow mode and the flow rates were regulated with peristalic pump. At flow rates of 120, 300 and 600 ml/h, the hydraulic retention time was arrived as 21.5, 8.5 and 4.3 min, respectively. The column was operated for 72 h with each bead size. The effluent samples were collected at regular time intervals and centrifuged at 6,000 rpm for 5 min. The supernatant was used to determine the residual MO concentration.

Collection @ chosun

조선대학교
CHOSUN UNIVERSITY

Phytotoxicity assay

The toxicity effects of degraded and untreated methyl orange dye on the plant growth were determined by the procedure described by Purushothaman et al. [46] with slight modification. The uniform sized seeds of *Cicer arietinum* L. and *Dolichos lablab* L. were selected and surface sterilized with 1.2 % sodium hypochlorite for 5 min and thoroughly washed with DDW. The seeds were planted in Petri dishes with bunch filter-paper discs containing 300 mg/l of MO dye solution (untreated) and the degraded dye samples collected from the column were centrifuged and the supernatant was used as a treated sample. The planted seeds were germinated for 2 days at 30 ± 2 °C under darkness in an incubator. The Petri plates also contained streptomycin at a final concentration of 25 μg/l to suppress microbial growth. The germinated seeds were then exposed to 12 ± 2 h light–dark cycles at 30 ± 2 °C for 15 days. Phytotoxicity experiments were performed in triplicate and each replicate was carried out on 25 seeds for germination and growth measurements. Control experiments were performed with double-distilled water for seed germination. At the end of experimental period, the radical and hypocotyl lengths were recorded.

Analytical methods

Dye decolourization was measured spectrophotometrically at maximum absorbance ($\lambda_{max} = 466$ nm) using calibration curve. The percentage removal of dye was estimated by the following equation:

$$R_{color}\,\% = \left[\frac{[MO]_i - [MO]_o}{[MO]_i}\right] \times 100, \quad (1)$$

where $[MO]_i$ is the initial dye concentration (mg/l) and $[MO]_o$ is the observed dye concentration (mg/l) at time t (min).

COD analysis

Aliquots were withdrawn at regular intervals (3 h intervals) and analyzed for chemical oxygen demand (COD) by open reflux method [47]:

$$R_{COD}\,\% = \left[\frac{[COD]_i - [COD]_o}{[COD]_i}\right] \times 100, \quad (2)$$

where $[COD]_i$ is the initial COD of dye solution (mg/l) and $[COD]_o$ is the observed COD of dye solution (mg/l) at time t (min).

Model development

Immobilized cell systems cause extra diffusional limitations as compared to free cells. The presence and significance of diffusional limitations depends on the relative rate of bioconversions and diffusion [48]. Two transport processes are generally known to occur in a packed bed reactor containing organisms immobilized in a porous matrix. The first process is transfer of substrate from bulk liquid phase to immobilized biocatalyst surface, while the second process is simultaneous diffusion and reaction of the substrate within the biocatalyst. According to the film theory, there is a presence of a fictitious laminar film adjacent to the surface of any particle in contact with a flowing fluid. The substrate needs to be transported through this laminar boundary region, which is around the exterior of the catalyst. This transport occurs primarily by molecular diffusion and is called external mass transfer. In order to fabricate effective encapsulated systems, it is essential to gain understanding of the liquid mass transfer process.

In the present study, a relevant mass transfer model was developed as described by Aksu and Bulbul [49]. A few assumptions that have been made during the development of this model are (1) the reaction follows first order, (2) the immobilized cell particles are spherical, (3) the packed bed has a steady-state plug flow with no axial dispersion and (4) the activity of the cells throughout the particle is uniform.

Methyl Orange degradation rate constant

The material balance for MO in the recirculated packed bed column is given as

$$\left(\frac{HQ}{W}\right)\frac{dC}{dZ} \times 6 \times 10^{-2} = -r, \quad (3)$$

where r is the degradation rate (mg g^{-1} h^{-1}), Q is the volumetric flow rate (ml min^{-1}), H is the height of the column (cm), W is the amount of immobilized organism used (g) and dC/dz is the concentration gradient along the column length (mg l^{-1} cm^{-1}). Eq. (3) relates the apparent reaction rate and the bulk MO concentration in the column. Assuming first-order reaction, the reaction rate and bulk MO concentration in the column are related as given below:

$$r = k_p C, \quad (4)$$

where k_p is the apparent first-order reaction rate constant ($l\ g^{-1}\ h^{-1}$) and C is the bulk substrate concentration (mg l^{-1}). Substitution of Eq. (4) in Eq. (3) gives the following:

$$\left(\frac{HQ}{W}\right)\frac{dC}{dz} \times 6 \times 10^{-2} = -k_p C \quad (5)$$

Equation (4) is obtained by integrating Eq. (5) using boundary conditions at $z = 0$, $C = MO_{in}$ and at $z = H$, $C = MO_{out}$, the equation obtained is given as

Collection @ chosun

조선대학교
CHOSUN UNIVERSITY

$$\ln\left(\frac{MO_{in}}{MO_{out}}\right) = \frac{W}{Q}k_p \cdot \left(\frac{10^3}{60}\right), \quad (6)$$

where MO_{in} is the inlet MO concentration (mg/l) and MO_{out} is the column outlet MO concentration (mg/l). The outlet concentration of the recirculated packed bed reactor is given by the following expression:

$$MO_{out} = MO_{in}e^{-N} \quad (7)$$

$$\text{where } N = \frac{W}{Q}k_p \cdot \left(\frac{10^3}{60}\right) \quad (8)$$

Total mass balance

The packed bed reactor system was operated in recycle mode. Hence, the inlet concentration to the column changes for every cycle. Therefore, an overall mass balance for an RPBR as developed by Mutlu and Gökmen [50] was used in the present study. The assumption of reservoir as a perfectly mixed tank gives the overall mass balance as

$$\frac{dV_{res}}{dt} = 0, \quad (9)$$

where V_{res} is the volume of the reacting solution in the reservoir (ml). The component balance in the reservoir gives

$$\frac{dMO_1}{dt} = -\left(\frac{MO_2 - MO_1}{\tau}\right), \quad (10)$$

where τ is the residence time (min) in the reservoir (V_{res}/Q), MO_1 is the concentration of dye (mg/l) in the reservoir and MO_2 is the concentration (mg/l) at the outlet of the packed bed reactor to be circulated back to the reservoir. Based on Eq. (7), MO_2 is given as

$$MO_2 = MO_1e^{-N} \quad (11)$$

Substitution Eq. (11) into (10) gives the following equation:

$$\frac{dMO_1}{dt} = -\left(\frac{MO_1e^{-N} - MO_1}{\tau}\right) \quad (12)$$

The change of MO concentration in the reservoir with time is obtained by integrating Eq. (12) using boundary conditions of $V_{res} = V_{res}$ and $MO_1 = MO_0$ at $t = 0$; which gives

$$MO_1 = MO_0 \exp\left[-(e^{-N} - 1)\frac{t}{\tau}\right] \quad (13)$$

From the slope of the plot between ln (MO_1/MO_0) and time (Eq. 13), the k_p values of each flow rate can be determined.

Combined mass transfer and MO reduction

Mass transfer rate of MO from the bulk liquid to the surface of the immobilized beads is proportional to the external mass transfer coefficient, area of mass transfer and the driving force.

$$r_m = k_m a_m(MO_b - MO_s) \quad (14)$$

where r_m is the external mass transfer rate (mg g^{-1} h^{-1}), k_m is the external mass transfer coefficient (cm h^{-1}), a_m is the surface area per unit weight of immobilized particles available for mass transfer (cm^2 mg^{-1}), MO_b is the dye concentration at the bulk liquid and MO_s is the dye concentration at the surface of the immobilized particle (mg l^{-1}). The value of a_m can be determined using the following relation:

$$a_m = \frac{6(1-\varepsilon)}{\rho_p d_p}, \quad (15)$$

where d_p is the particle diameter (cm), ρ_p is the density of the particle (g cm^{-3}) and ε is the voidage.

The first-order reaction rate at the surface of the immobilized particle is given as follows:

$$r = k_s a_m MO_s \quad (16)$$

where k_s is the surface first-order reaction rates constant (cm h^{-1}). At steady state, the external mass transfer rate is equal to reaction rate and hence Eqs. (14) and (16) are equated and rearranged to give

$$MO_s = \frac{k_m MO_b}{k_s + k_m} \quad (17)$$

Substituting Eq. (17) into Eq. (16) and equating with $r = k_p C$ yields the following expression:

$$k_p = \frac{k_s k_m a_m}{k_s + k_m} \quad (18)$$

Rearranging the above equation and solving for k_m, the following equation was obtained:

$$k_m = \frac{k_p k_s}{(k_s a_m - k_p)} \quad (19)$$

Empirical model

The external mass transfer coefficient, k_m changes with parameters such as flow rate, reactor diameter and fluid properties, which in turn influence the apparent reaction rate.

$$\left[J_D = \frac{k_m \rho}{G}\left(\frac{\mu}{\rho D_f}\right)^{2/3} = K(Re)^{n-1}\right], \quad (20)$$

Collection @ chosun

조선대학교
CHOSUN UNIVERSITY

where J_D is the Colburn factor, defined in terms of Schmidt number and Reynolds number.

The values of n are affected by mass transfer conditions and n varies from 0.1 to 1.0. From Eq. (20), the expression for mass transfer coefficient obtained is given as

$$k_m = \left(\frac{K}{\rho}\right)\left(\frac{\mu}{\rho D_f}\right)^{-2/3}\left(\frac{d_P}{\mu}\right)^{n-1} G^n \quad (21)$$

$$k_m = AG^n \quad (22)$$

$$\text{where } A = \left(\frac{K}{\rho}\right)\left(\frac{\mu}{\rho D_f}\right)^{-2/3}\left(\frac{d_P}{\mu}\right)^{n-1} \quad (23)$$

Substitution of Eq. (22) into Eq. (18) gives the following equation:

$$\left(\frac{1}{k_p}\right) = \left(\frac{1}{Aa_m}\right)\left(\frac{1}{G^n}\right) + \left(\frac{1}{k_s a_m}\right) \quad (24)$$

Thus, the plot $1/k_p$ versus $1/G^n$ for different values of n yields a straight line with slope $1/Aa_m$ and intercept $1/k_s a_m$. Assuming values for K and n, the value of a_m was determined and compared with experimental a_m. The K and n values which predicted the experimental a_m value accurately were used to propose the mass transfer correlation for MO degradation using immobilized *Aeromonas* sp.

Results and discussion

Microorganism

Initially, a total of 37 bacterial isolates were obtained using enriched samples of soil collected from textile dye-contaminated sites. From the preliminary studies, it was observed that all isolates possessed the capacity of MO degradation at lesser concentration. From the acclimatization studies, higher MO degrading isolate was chosen as the best strain for further studies. The isolate *Aeromonas* sp. was Gram-negative rods with motile. It exhibited oxidases and catalase activities and produce N_2 gas from nitrate. This strain produces acids from various carbon sources such as glucose, maltose and sucrose. No acid production was obtained in galactose and lactose. It could not hydrolyze urea and did not show H_2S production. Positive results were observed in indole production. These characteristics indicated that the isolated strain belongs to *Aeromonas* sp.

The phylogenetic tree was constructed based on the 16SrRNA sequence and the sequence similarity was retrieved from the reference and type strains available in the public databases GenBank using the BLASTn sequence match routines. The sequences were aligned using the CLUSTALX program and analyzed with MEGA 4.1 (Beta) software. The evolutionary history was inferred using the neighbor-joining method. Codon positions included were 1st + 2nd + 3rd + noncoding. All positions containing gaps and missing data were eliminated from the dataset (complete deletion option). There were a total of 1,346 positions in the final dataset. Phylogenetic analysis were conducted using aforementioned tool and the tree was drawn to scale, with branch lengths (below the branches) in the same units as those of the evolutionary distances used to infer the phylogenetic tree and represented in Fig. 1. The isolated bacterial species had 97–98 % homologous sequence similarity with *Aeromonas* sp. FM (HM560619), *Aeromonas* sp. AC-1E (FJ231173) and *Aeromonas* sp. Fars89D3b (JF313416). Based on the colony morphology, biochemical tests and phylogenetic tree results, the organism was identified and named as *Aeromonas* sp. MNK1.

MO degradation by immobilized *Aeromonas* sp.

The size of alginate immobilized bacterial cell beads has a significant effect on the rate of degradation of MO. Moreover, the bead size determines the suitability for reactor configuration. In situations where the substrate has to be transported from the bulk solution to the outer surface of the matrix, both the intra-particular diffusion and the external mass transfer should be taken into consideration.

The effect of alginate bead size on dye removal efficiency was investigated by varying the bead size from 0.20 to 0.60 cm and the influence of different flow rates (120–600 ml/h) on MO degradation in packed bed reactor was estimated at optimum operating conditions and the results are shown in Figs. 2, 3, 4. For 0.20 cm bead size, the % of degradation was obtained as 99.56, 94.5 and 85.60 % for flow rates of 120, 300 and 600 ml/h, respectively. The results led to the conclusion that the alginate-immobilized *Aeromonas* sp. showed maximum MO degradation efficiency at 0.20 cm bead size with 120 ml/h flow rate in 72 h of incubation with lower diffusional limitations. Even though further increase in flow rate eliminates the thin laminar liquid layer formed around the beads, there is a decrease in the percentage degradation due to short contact time between the beads and MO solution. Mahmoud and Rachida [51] reported that the increase in flow rate significantly affected the degradation rate due to poor mass transfer, diffusional limitations and short residence time. As can be seen from Fig. 3, the percentage of MO degradation in 0.40 cm bead size particles was 92.02, 86.31 and 77.5 % for 120, 300 and 600 ml/h liquid flow rate, respectively. However, further increase in bead size (0.60 cm) significantly affects degradation rate and the degradation percentage was observed as 90.31, 78.50 and 64.21 % for 120, 300 and 600 ml/h flow rate, respectively

Collection @ chosun

조선대학교
CHOSUN UNIVERSITY

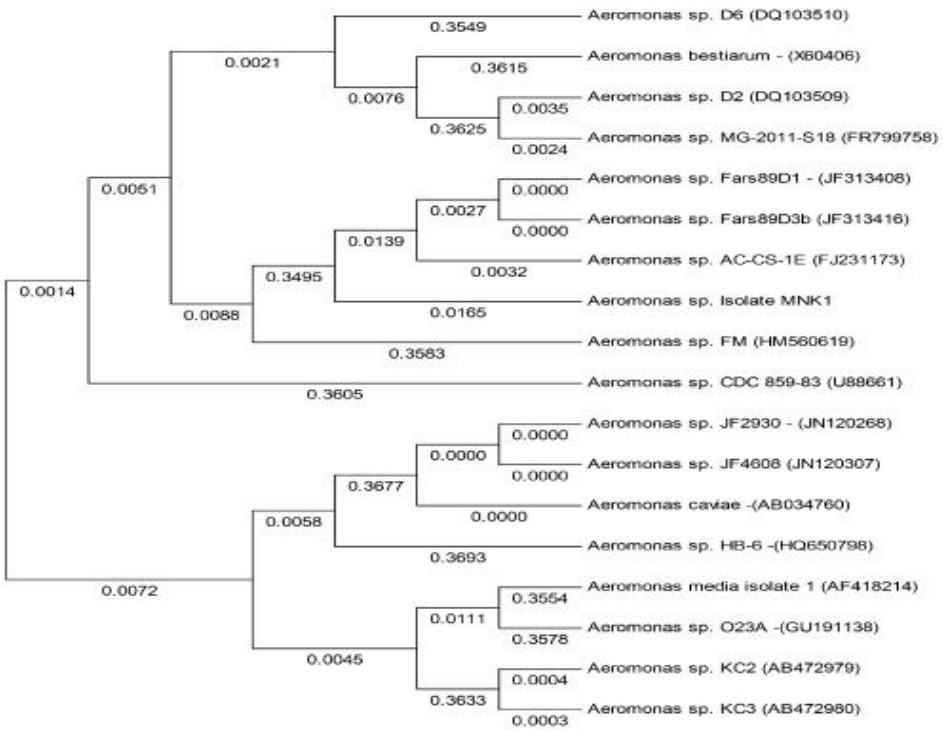

Fig. 1 Phylogenetic relationship analysis of the isolated bacteria *Aeromonas* sp. MNK1 by a neighbor-joining analysis of 16S rRNA sequences; the *scale* represents the evolutionary branch length and the accession number of the close relatives given in the *parentheses*

(Fig. 4). The control experiment shows negligible degradation of MO. From the effect of bead size on dye degradation studies, it was revealed that the percentage degradation decreased with increasing bead size. The smaller bead size particles has negligible mass transfer resistance and smaller bead diameter led to maximum MO degradation due to an increase in the surface to volume ratio.

COD removal

The % COD removal profiles during biodegradation of 300 mg/l of MO by alginate-immobilized *Aeromonas* sp. with different bead sizes (0.20–0.40 cm) and various flow rates (120–600 ml/h) are shown in Fig. 5. The %COD removal decreased with increasing bead size as well as flow rates. Maximum of 99.57 % of COD removal was observed at 0.20 cm of bead size and 120 ml/h flow rate. Approximately 7.6 and 15.6 % of lesser COD removal was observed for 0.40 and 0.60 cm beads, respectively, when compared with 0.20 cm bead particles. Figure 5, shows that the 4 and 14.03 % of lower COD removal was observed for 300 and 600 ml/h flow rate, respectively, and more than 66 % COD removal was obtained in other flow rates and bead sizes. The control experiments did not show any significant COD removal. Srinivasan et al. [12] reported that the enzymes produced by the bacterial species are responsible for the conversion of dye into various metabolites and that this process simultaneously reduces the color and COD.

Phytotoxicity tests

Untreated textile dye wastewater disposal by the various industries into the agricultural lands may have a direct impact on soil fertility and agricultural productivity.

Collection @ chosun

조선대학교
CHOSUN UNIVERSITY

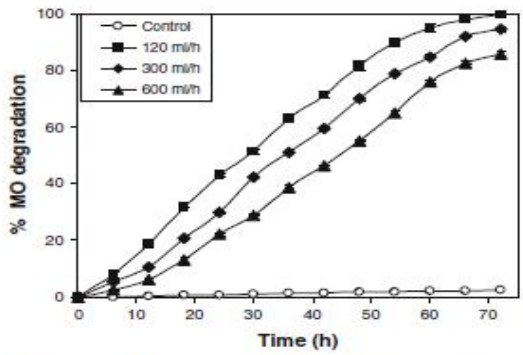

Fig. 2 Effect of flow rate on MO degradation by immobilized *Aeromonas* sp. in a packed bed reactor (conditions: MO concentration—300 mg/l; pH—7.0; temperature—37 °C; bead size—0.20 cm)

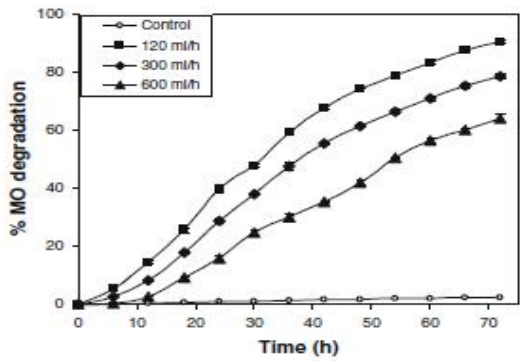

Fig. 4 Effect of flow rate on MO degradation by immobilized *Aeromonas* sp. in a packed bed reactor (conditions: MO concentration—300 mg/l; pH—7.0; temperature—37 °C; bead size—0.60 cm)

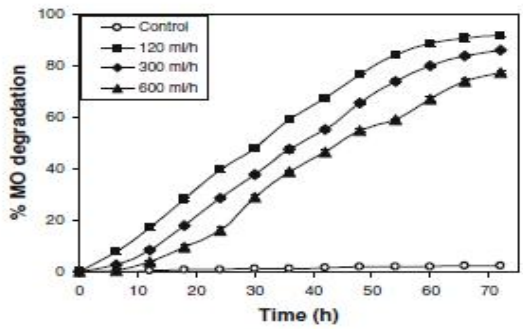

Fig. 3 Effect of flow rate on MO degradation by immobilized *Aeromonas* sp. in a packed bed reactor (conditions: MO concentration—300 mg/l; pH—7.0; temperature—37 °C; bead size—0.40 cm)

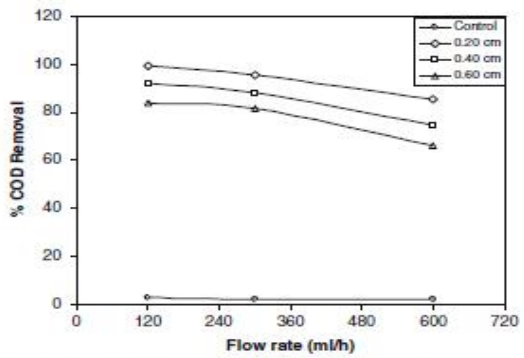

Fig. 5 Effect of flow rate and various bead sizes on % COD removal during MO degradation by *Aeromonas* sp. in a packed bed reactor (conditions: MO concentration—300 mg/l; pH—7.0; temperature—37 °C)

Hence, it was important to measure the phytotoxicity effects of the dyes before and after degradation (bead size—0.20 cm, initial MO concentration—300 mg/L, pH—7.0, temperature—37 °C and flow rate—120 ml/h treated dye solution) as environmental safety demands both in terms of pollutant removal and their detoxification. In order to study the phytotoxicity effects of the treated and untreated MO dye on the seed germination percentage, radical length and hypocotyl length of two different plant species were observed and the results are shown in Table 1. The results indicate that the seed germination (%) percentage, radical and hypocotyls length were significantly inhibited by the raw effluent treated seeds, when compared to that of control experiments. However, more than 88.24 % higher seed germination; increased radical length (82.69 %) and hypocotyl length (72.55 %) were observed in the seeds treated with degraded dye solution for *C. arietinum* plant. The same trend was observed in *D. lablab* which possessed 86.42 % higher seed germination, enhanced radical length (87.39 %) and hypocotyl length (77.78 %). From the study of phytotoxicity effects, the non-toxic nature of the degraded MO by *Aeromonas* sp. was investigated and it revealed that the degraded metabolites had less toxicity effects on seed germination rate,

Collection @ chosun

조선대학교
CHOSUN UNIVERSITY

Table 1 Phytotoxicity effects of untreated and treated MO samples on the seed germination, radical length and hypocotyl length of two different plants

Parameters	*Cicer arietinum* L.			*Dolichos lablab* L.		
	DDW	Untreated dye	Treated dye	DDW	Untreated dye	Treated dye
Seed germination %	100	12	98	100	14	97
Radical length (cm)	7.71 ± 0.12	2.32 ± 0.09	7.46 ± 0.14	6.54 ± 0.11	2.09 ± 0.008	6.03 ± 0.12
Hypocotyls length (cm)	9.32 ± 0.53	3.07 ± 0.10	8.94 ± 0.26	7.87 ± 0.13	3.06 ± 0.14	7.26 ± 0.19

Table 2 Experimentally observed values of first-order rate constant ($k_p s$) for MO degradation by immobilized *Aeromonas* sp. in a packed bed reactor

Q (cm^3 h^{-1})	k_{p1} (lg^{-1} h^{-1})[a]	k_{p2} (lg^{-1} h^{-1})[a]	k_{p3} (lg^{-1} h^{-1})[a]
120	0.5921	0.4541	0.3639
300	0.7793	0.6463	0.5551
600	0.8878	0.7972	0.7511

[a] k_{p1}, k_{p2}, k_{p3}—value of experimentally observed k_p values for bead size 0.2, 0.4 and 0.6 cm, respectively

radical formation and hypocotyl development in both the plants. This investigation also suggests that the treated dye solutions possess less toxicity than the untreated dye solutions towards plant seedling and growth.

External mass transfer

The experimental degradation rate constant (k_{ps}) of the MO dye by immobilized *Aeromonas* sp. was analyzed with varying bead sizes (0.20, 0.40 and 0.60 cm) and varying flow rates (120, 300 and 600 cm^3/h) and the values obtained are presented in Table 2. From the experimental results, it was observed that the k_p values increased with an increase in flow rate. This is due to the fact that the high flow rates provide higher turbulence and reduce the boundary layer effects, which eliminates the diffusion resistances and in turn increases k_p. However, the degradation rate was found to decrease with increasing bead size at the same flow rate. This is due to higher mass transfer limitations occurs in the beads. This can be attributed to the degradation in surface area to volume ratio with an increase in bead size, which limits the transfer of substrate and hence limits the overall rate constant. Further, the experimental results showed the MO degradation decreased with an increase in flow rate. Our previous studies revealed that the low residence time at high flow rates affects the diffusion of solute into the pores of the particles [33]. The same trend was observed at different flow rate and bead sizes. Dursun and Tepe [52] suggested that the diffusion resistances can be eliminated by using small size beads. For maximum degradation rates, the particle size should be as small as possible within the constraints of particle integrity, resistance to compression and the nature of the particle recovery systems.

To determine the influence of external mass transfer effects, the values of G and $1/G^n$ $(0 < n < 1)$ for the immobilized packed bed reactor were calculated and presented in Table 3. The flux G is the amount of MO passing through the cross section of the bed in unit time. Initially at a constant flow rate, the amount of MO entering the cross section of the bed remained the same for various bead sizes. Thus, the same value of G was obtained for various bead sizes at a given flow rate. On varying the flow rate, the amount of dye passing the cross section of the bed varies and consequently the G value changes. The relevant dimensionless numbers and mass fluxes were calculated using $\mu = 27.359$ g/cm/h, $\rho = 0.978$ g/cm^3, $D_t = 1.656 \times 10^{-4}$ cm^2/h and $\varepsilon = 0.5$. The trial and error procedure was repeated to determine the n value (0.1–1.0). For each bead size with different flow rates $1/k_p$ vs. $1/G^n$ was plotted. For various bead size immobilized particles, for 0.20 cm $(n < 0.2)$, 0.40 cm $(n < 0.3)$ and 0.60 cm $(n < 0.4)$, negative intercepts were obtained and consequently not considered for further calculations. The slope and intercept values obtained from these plots for various values of n are tabulated in Tables 5, 6, 7. The slope and intercept values increased with an increase in the n values. All n values were found to give a satisfactory straight line fit. However, all n values did not predict experimental a_m satisfactorily. Further analysis was carried out with K value 5.7 [33, 36, 53] and n values were varied between 0.3 and 1.0 for 0.2, 0.4 and 0.6 cm bead size particles. The values of A obtained using Eq. (23) were used to calculate a_m values from the slope obtained from $1/k_p$ vs. $1/G^n$ plots. A model plot for each bead size particles has been shown in Fig. 6a–c. For bead sizes 0.2, 0.4 and 0.6, the n values that accurately predicted the a_m and k_p were 0.85, 0.64 and 0.52, respectively. The values A, a_m and k_s obtained for different n values with various bead size particles are presented in Tables 2, 3, 4. From the results, it can be seen that the value of a_m obtained for $K = 5.7$ and $n = 0.85$ was equal to experimental a_m (15.276 cm^2/g) for 0.2 cm bead size particles, $K = 5.7$ and $n = 0.64$ was equal to the

Collection @ chosun

조선대학교
CHOSUN UNIVERSITY

Table 3 Calculated values of mass flux and various parameters for MO degradation by immobilized *Aeromonas* sp. in a packed bed reactor

Q ($cm^3\ h^{-1}$)	u ($cm\ h^{-1}$)	G ($g\ cm^{-2}\ h^{-1}$)	$1/G^{0.2}$	$1/G^{0.4}$	$1/G^{0.52}$	$1/G^{0.64}$	$1/G^{0.85}$
120	0.637	37.376	0.4847	0.2349	0.1521	0.0985	0.0461
300	1.592	93.395	0.4035	0.1629	0.0945	0.0548	0.0211
600	3.185	186.879	0.3513	0.1234	0.0659	0.0352	0.0117

Table 4 Slope and intercept of the plot $1/k_p$ vs. $1/G^n$ for various values of n for 0.2 cm bead size (experimental a_m value 15.276 $cm^2\ g^{-1}$)

n	Slope ($g^{(n+1)}\ cm^{-(2n+3)}\ h^{(1-n)}$)	Intercept ($g\ h\ l^{-1}$)	A ($g^{-n}\ cm^{(2n+1)}\ h^{(n-1)}$)	a_m ($cm^2\ g^{-1}$)	k_x ($cm\ h^{-1}$)
0.1	–	Negative	–	–	–
0.2	–	Negative	–	–	–
0.3	4.421	0.184	0.06	3.792	1.431
0.4	5.116	0.477	0.036	5.359	0.391
0.52	6.596	0.679	0.02	7.499	0.196
0.64	8.946	0.804	0.011	9.976	0.125
0.7	10.553	0.85	0.008	11.361	0.104
0.85	16.364	0.936	0.004	15.321	0.07
0.9	19.061	0.958	0.003	16.821	0.062
1	26.049	0.994	0.002	20.129	0.05

Table 5 Slope and intercept of the plot $1/k_p$ vs. $1/G^n$ for various values of n for 0.4 cm bead size (experimental a_m value 7.638 $cm^2\ g^{-1}$)

n	Slope ($g^{(n+1)}\ cm^{-(2n+3)}\ h^{(1-n)}$)	Intercept ($g\ h\ l^{-1}$)	A ($g^{-n}\ cm^{(2n+1)}\ h^{(n-1)}$)	a_m ($cm^2\ g^{-1}$)	k_x ($cm\ h^{-1}$)
0.1	–	Negative	–	–	–
0.2	–	Negative	–	–	–
0.3	–	Negative	–	–	–
0.4	8.567	0.179	0.024	4.85	1.149
0.52	11.038	0.518	0.014	6.25	0.309
0.64	14.959	0.728	0.011	7.657	0.179
0.7	17.639	0.805	0.007	8.368	0.148
0.85	27.327	0.949	0.004	10.18	0.104
0.9	31.821	0.986	0.003	10.799	0.094
1	43.462	1.048	0.002	12.064	0.079

Table 6 Slope and intercept of the plot $1/k_p$ vs. $1/G^n$ for various values of n for 0.6 cm bead size (experimental a_m value 5.092 $cm^2\ g^{-1}$)

n	Slope ($g^{(n+1)}\ cm^{-(2n+3)}\ h^{(1-n)}$)	Intercept ($g\ h\ l^{-1}$)	A ($g^{-n}\ cm^{(2n+1)}\ h^{(n-1)}$)	a_m ($cm^2\ g^{-1}$)	k_x ($cm\ h^{-1}$)
0.1	–	Negative	–	–	–
0.2	–	Negative	–	–	–
0.3	–	Negative	–	–	–
0.4	–	Negative	–	–	–
0.52	16.424	0.25	0.020	5.103	0.785
0.64	22.246	0.563	0.008	5.958	0.298
0.7	26.223	0.678	0.006	6.357	0.232
0.85	40.598	0.892	0.003	7.282	0.154
0.9	47.264	0.947	0.003	7.571	0.139
1	64.526	1.04	0.002	8.126	0.118

experimental a_m (7.657 cm^2/g) for 0.4 cm bead size particles and $K = 5.7$ and $n = 0.52$ was equal to experimental a_m (5.103 cm^2/g) for 0.6 bead size. The value of a_m decreases with an increase in particle size, which is mainly due to the decrease in surface area available for mass transfer per unit weight of the immobilized cells.

Collection @ chosun

조선대학교
CHOSUN UNIVERSITY

The calculated a_m, n and K values were used to determine the rate constant (k_s) from the intercept ($1/k_s a_m$) and the results are tabulated in Tables 4, 5, 6. The mass transfer coefficient (k_{m1}, k_{m2} and k_{m3}) values were calculated using Eq. (19) and given in Table 8. From Eq. (22), it can be seen that the plot ln k_m vs. ln G yields intercept as ln A and slope as n (Fig. 7a–c). Thus, for bead sizes 0.2, 0.4 and 0.6 cm, the slopes were 0.85, 0.64 and 0.52; and the intercepts were −5.5085, −4.4869 and −3.899, respectively. The values of A obtained are 0.004 $g^{-0.85}$ $cm^{2.7}$ $h^{-0.15}$, 0.011 $g^{-0.64}$ $cm^{2.28}$ $h^{-0.36}$ and 0.020 $g^{-0.52}$ $cm^{2.04}$ $h^{-0.48}$, respectively. These values are similar to those obtained from the intercept values for the corresponding n and k_s values. From these results it can be confirmed that the proposed model perfectly predicts the external mass transfer influence during MO degradation using immobilized cell packed bed reactor. The experimental k_{p1}, k_{p2} and k_{p3} values and the calculated k_p values for various bead sizes and different n values are presented in Table 8. A significant difference in k_p values for $n > 0.85$ suggests that n values greater than 0.85 did not represent the present system for smaller bead size (0.2 cm). The intermediate bead size (0.4 cm) k_{p2} values for $n > 0.64$ indicate that n values greater than 0.64 did not represent the system. Also, for larger bead size (0.6 cm) the k_{p2} values for $n > 0.52$ did not represent the system.

Therefore, the mass transfer correlations $J_D = 5.7\ Re^{-0.15}$ (for 0.2 cm bead size), $J_D = 5.7\ Re^{-0.36}$ (for 0.4 cm bead size) and $J_D = 5.7\ Re^{-0.48}$ (for 0.6 cm bead size) were found to accurately predict the experimental data for the degradation of MO using immobilized *Aeromonas* sp. in a packed bed batch reactor. The J_D factor correlations can be physically interpreted to understand the nature of diffusion and flow behavior at various flow rates and particle diameters [54, 55]. While analyzing the J_D

Table 7 Calculated values of external mass transfer coefficient values (k_ms) at various mass velocity G for various bead size

Q (cm^3 h^{-1})	G (g cm^{-2} h^{-1})	k_{m1} (cm h^{-1})[a]	k_{m2} (cm h^{-1})[a]	k_{m3} (cm h^{-1})[a]
20	37.376	0.087	0.114	0.133
300	93.395	0.189	0.204	0.214
600	186.879	0.34	0.319	0.307

[a] k_{m1}, k_{m2}, k_{m3}—calculated values of external mass transfer coefficient values at 0.20, 0.40 and 0.60 cm of bead, respectively

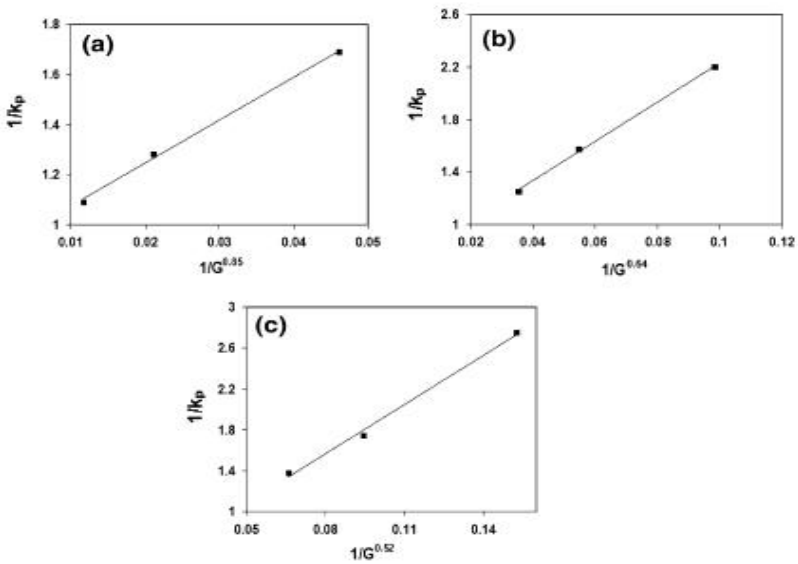

Fig. 6 Plot between $1/k_p$ and $1/G^n$ (**a** $n = 0.85$ for 0.20 cm bead size, **b** $n = 0.64$ for 0.40 cm bead size and **a** $n = 0.52$ for 0.60 cm bead size)

Collection @ chosun

조선대학교
CHOSUN UNIVERSITY

Table 8 Comparison of experimental k_{fs}s values with the calculated K_p values for various values of flow rates, n and bead size

N	k_{f1} (lg^{-1} h^{-1}) for 0.2 cm bead size with various Q in (cm^3 h^{-1})			k_{f2} (lg^{-1} h^{-1}) for 0.4 cm bead size with various Q in (cm^3 h^{-1})			k_{f3} (lg^{-1} h^{-1}) for 0.6 cm bead size with various Q in (cm^3 h^{-1})		
	$Q1$	$Q2$	$Q3$	$Q1$	$Q2$	$Q3$	$Q1$	$Q2$	$Q3$
0.3	0.766	0.822	0.859	–	–	–	–	–	–
0.4	0.737	0.815	0.865	0.499	0.62	0.715	–	–	–
0.52	0.7	0.806	0.871	0.476	0.633	0.756	0.364	0.555	0.752
0.64	0.662	0.797	0.877	0.454	0.645	0.797	0.356	0.598	0.861
0.7	0.642	0.792	0.88	0.443	0.652	0.817	0.352	0.62	0.92
0.85	0.591	0.780	0.887	0.416	0.668	0.866	0.343	0.679	1.08
0.9	0.574	0.776	0.889	0.407	0.673	0.882	0.339	0.7	1.136
1	0.54	0.768	0.894	0.39	0.684	0.913	0.333	0.742	1.256
Exp k_{fs} (lg^{-1} h^{-1})	0.592	0.779	0.887	0.454	0.646	0.797	0.364	0.555	0.751

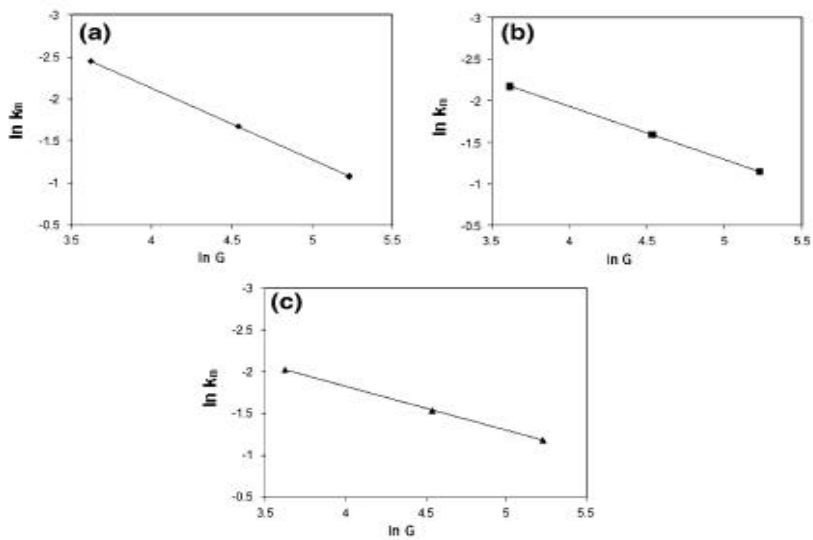

Fig. 7 Plot between calculated values of mass transfer coefficient (k_m) and superficial mass velocity (G)

factor correlations, it was revealed that the J_D values decreases with an increase in flow rate or particle size. At a given D_p, increasing the flow rate leads to turbulence and reduces the hydrodynamic boundary layer, which reduces the Schmidt number and consequently decreases J_D. Also at a given D_p, increasing the flow rate increases the flux G but decreases the residence time of MO in the reactor, which may lead to reduced mass transfer and hence a decrease in J_D is noticed. For a given Q, on increasing the D_p, the surface available for mass transfer decreases and consequently the J_D value decreases. Therefore, the external mass transfer effects are significant during biological degradation of MO and must be considered during scale up.

Conclusion

Methyl Orange degradation by alginate-immobilized *Aeromonas* sp. in a packed bed reactor was carried out. The percentage of MO degradation and COD removal was found to decrease with increasing bead size and flow rate of dye solution. The smaller bead particles have higher surface to volume ratio and led to maximum MO degradation.

Collection @ chosun

조선대학교
CHOSUN UNIVERSITY

Phytotoxicity toxicity studies using two different plants shows nontoxic products were produced.

Furthermore, external mass transfer correlation model in terms of dimensionless numbers was developed to facilitate the design and simulation of reactor performance. Colburn factor correlation model was proposed and the results obtained from this study for 0.20, 0.40 and 0.60 bead sizes were $J_D = 5.7\ Re^{-0.15}$, $J_D = 5.7\ Re^{-0.36}$ and $J_D = 5.7\ Re^{-0.48}$, respectively, and were found to satisfactorily predict the experimental data for the degradation of MO dye in a recirculated packed bed reactor.

Therefore, MO degradation using alginate-immobilized *Aeromonas* sp. is a promising candidature. From the external mass transfer studies, it was concluded that increasing the fluid flow rate leads to turbulence and reduces the hydrodynamic boundary layer, which consequently reduces the Schmidt number and J_D and that smaller bead size particles have negligible mass transfer resistance.

Acknowledgments This research was supported by the Pioneer Research Centre Program through the national Research Program of Korea funded by the Ministry of Education, Science and Technology (Grant No. 2008-2000122).

References

1. Manu B, Chaudhari S (2002) Anaerobic decolorisation of simulated textile wastewater containing azo dyes. Bioresource Technol 82:225–231
2. Montan GOJ, Domenech X, Garcia-Hortal JA, Torrades F, Peral J (2007) The testing of several biological and chemical coupled treatments for cibacorn Red FN-R azo dye removal. J Hazard Mater 154:484–490
3. Pinheiro HM, Touraud E, Thomas O (2004) Aromatic amines from azo dye reduction: status review with emphasis on direct UV spectrophotometric detection in textile industry wastewaters. Dyes Pigm 61:121–139
4. Sessa DJ, Palmquist DE (2008) Effect of heat on the adsorption capacity of an activated carbon for decolorizing/deodorizing yellow zein. Biores Technol 99:6360–6364
5. Ong SA, Toorisaka E, Hitara M, Hano T (2005) Treatment of azo dye Orange II in aerobic and anaerobic-SBR systems. Process Biochem 40:2907–2914
6. Junghanns C, Neumann JF, Schlosser D (2012) Application of the aquatic fungus Phoma sp. (DSM22425) in bioreactors for the treatment of textile dye model effluents. J Chem Technol Biotechnol 87:1276–1283. doi:10.1002/jctb.3797
7. Bonakdarpour B, Vyrides I, Stuckey DC (2011) Comparison of the performance of one stage and two stage sequential anaerobic–aerobic biological processes for the treatment of reactive-azo-dye-containing synthetic wastewaters. Int Biodeterior Biodegrad 65:591–599
8. Gopinath KP, Kathiravan MN, Srinivasan R, Sankaranarayanan S (2011) Evaluation and elimination of inhibitory effects of salts and heavy metal ions on biodegradation of Congo red by *Pseudomonas* sp. mutant. Bioresource Technol 102:3687–3693
9. Waghmode TR, Kurade MB, Khandare RV, Govindwar SP (2011) A sequential aerobic/microaerophilic decolorization of sulfonated mono azo dye Golden Yellow HER by microbial consortium GG-BL. Int Biodeter Biodegrad 65:1024–1034
10. Jadhav SB, Phugare SS, Patil PS, Jadhav JP (2011) Biochemical degradation pathway of textile dye Remazol red and subsequent toxicological evaluation by cytotoxicity, genotoxicity and oxidative stress studies. Int biodeterior Biodegrad 65:733–743
11. Chen G, Huang MH, Chen L, Chen DH (2011) A batch decolorization and kinetic study of Reactive Black 5 by a bacterial strain *Enterobacter* sp. GY-1. Int Biodeterior Biodegrad 65:790–796
12. Srinivasan R, Kathiravan MN, Gopinath KP (2011) Degradation of Tectilon Yellow 2G by hybrid technique: combination of Sonolysis and biodegradation using mutant *Pseudomonas putida*. Biores Technol 102:2242–2247
13. Phugare SS, Kalyani DC, Patil AV, Jadhav JP (2011) Textile dye degradation by bacterial consortium and subsequent toxicological analysis of dye and dye metabolites using cytotoxicity, genotoxicity and oxidative stress studies. J Hazard Mater 186:713–723
14. Niebisch CH, Malinowski AK, Schadeck R, Mitchell DA, Cordeiro VK, Paba J (2010) Decolorization and biodegradation of reactive blue 220 textile dye by *Lentinus crinitus* extracellular extract. J Hazard Mater 180:316–322
15. Ip AWM, Barford JP, McKa G (2010) Biodegradation of Reactive Black 5 and bioregeneration in upflow fixed bed bioreactors packed with different adsorbents. J Chem Tech Biotechnol 85:658–667
16. Gopinath KP, Shreela M, Joanna A, Muthukumar K (2009) *Bacillus* sp. mutant for improved biodegradation of Congo red: random mutagenesis approach. Bioresource Technol 100:6295–6300
17. Karagoz B, Bayramoglu G, Altintas B, Bicak N, Arica MY (2011) Amine functional monodisperse microbeads via precipitation polymerization of *N*-vinyl formamide: immobilized laccase for benzidine based dyes degradation. Bioresource Technol 102:6783–6790
18. Yang Y, Hu H, Wang G, Li Z, Wang B, Jia X, Zhao Y (2011) Removal of malachite green from aqueous solution by immobilized *Pseudomonas* sp. DY1 with *Aspergillus oryzae*. Int Biodeterior Biodegrad 65:429–434
19. Saratale GD, Saratale RG, Chang JS, Govindwar SP (2011) Fixed-bed decolorization of Reactive Blue 172 by *Proteus vulgaris* NCIM-2027 immobilized on *Luffa cylindrica* sponge. Int Biodeterior Biodegrad 65:494–503
20. You SJ, Damodar RA, Hou SC (2010) Degradation of Reactive Black 5 dye using anaerobic/aerobic membrane bioreactor (MBR) and photochemical membrane reactor. J Hazard Mater 177:1112–1118
21. Lu H, Zhou J, Wang J, Si W, Teng H, Liu G (2010) Enhanced biodecolorization of azo dyes by anthraquinone-2-sulfonate immobilized covalently in polyurethane foam. Biores Technol 101:7185–7188
22. Asgher M, Bhatti HN (2010) Mechanistic and kinetic evaluation of biosorption of reactive azo dyes by free, immobilized and chemically treated *Citrus sinensis* waste biomass. Ecol Eng 36:1660–1665
23. Champagne PP, Ramsay JA (2010) Dye decolorization and detoxification by laccase immobilized on porous glass beads. Biores Technol 101:2230–2235
24. Osma JF, Toca-Herrera JL, Rodríguez-Couto S (2010) Transformation pathway of Remazol Brilliant Blue R by immobilised laccase. Biores Technol 101:8509–8514
25. Binupriya AR, Sathishkumar M, Ku CS, Yun SI (2010) Sequestration of Reactive Blue 4 by free and immobilized *Bacillus subtilis* cells and its extracellular polysaccharides. Coll Surf B 76:179–185
26. González EMP, Ramírez FLF, Villa GMRG (2009) Degradation of immobilized azo dyes by *Klebsiella* sp. UAP-b5 isolated from maize bioadsorbent. J Hazard Mater 161:769–774

Collection @ chosun

조선대학교
CHOSUN UNIVERSITY

Bioprocess Biosyst Eng (2014) 37:99–106
DOI 10.1007/s00449-013-0920-8

ORIGINAL PAPER

Comparison of biomass production and total lipid content of freshwater green microalgae cultivated under various culture conditions

Geun Ho Gim · Jung Kon Kim · Hyeon Seok Kim · Mathur Nadarajan Kathiravan · Hetong Yang · Sang-Hwa Jeong · Si Wouk Kim

Received: 25 December 2012 / Accepted: 26 January 2013 / Published online: 3 May 2013
© Springer-Verlag Berlin Heidelberg 2013

Abstract The growth and total lipid content of four green microalgae (*Chlorella* sp., *Chlorella vulgaris* CCAP211/11B, *Botryococcus braunii* FC124 and *Scenedesmus obliquus* R8) were investigated under different culture conditions. Among the various carbon sources tested, glucose produced the largest biomass or microalgae grown heterotrophically. It was found that 1 % (w/v) glucose was actively utilized by *Chlorella* sp., *C. vulgaris* CCAP211/11B and *B. braunii* FC124, whereas *S. obliquus* R8 preferred 2 % (w/v) glucose. No significant difference in biomass production was noted between heterotrophic and mixotrophic (heterotrophic with light illumination/exposure) growth conditions, however, less production was observed for autotrophic cultivation. Total lipid content in cells increased by approximately two-fold under mixotrophic cultivation with respect to heterotrophic and autotrophic cultivation. In addition, light intensity had an impact on microalgal growth and total lipid content. The highest total lipid content was observed at 100 μmol $m^{-2}s^{-1}$ for *Chlorella* sp. (22.5 %) and *S. obliquus* R8 (23.7 %) and 80 μmol $m^{-2}s^{-1}$ for *C. vulgaris* CCAP211/11B (20.1 %) and *B. braunii* FC124 (34.9 %).

Keywords Microalga · Autotrophic · Heterotrophic · Mixotrophic · Biomass · Total lipid content

G. H. Gim · H. S. Kim · M. N. Kathiravan · S. W. Kim (✉)
Department of Environmental Engineering and Pioneer Research Center for Controlling of HAB, Chosun University, Gwangju 501-759, South Korea
e-mail: swkim@chosun.ac.kr

G. H. Gim
e-mail: ma.geunho@gmail.com

J. K. Kim
Bioenergy Crop Research Center, National Institute of Crop Science, Rural Development Administration, 293-5, Cheongcheon, Cheonggye, Muan, Jeonnam 534-833, South Korea

J. K. Kim
Animal Environmental Division, National Institute of Animal Science, Rural Development Administration, 77 Chuksan gil (564 Omokchun-dong), Gwonsun-Gu, Suwon, South Korea

H. Yang
Biotechnology Center, Shandong Academy of Science, No.19 Keyuan Road, Jinan 250014, People's Republic of China

S.-H. Jeong
Department of Mechanical Engineering, Chosun University, Gwangju 501-759, South Korea
e-mail: shjeong@chosun.ac.kr

Introduction

In recent years, microalgae become one of the most potential candidates of renewable sources for alternative fuel production because of its higher lipid content, faster and abundant growth compared to other plant-based crops. The cost effective biodiesel production from microalgae primarily depends on high biomass productivity, high lipid yields, and efficient harvesting. Thus, there have been extensive researches and developments focused on photoautotrophic, heterotrophic and mixotrophic culture conditions to increase the biomass production and total lipid content [1–9]. Photoautotrophic growth represents that the microalgae can harvest energy source from the sunlight and assimilate atmospheric CO_2. However, the photoautotrophic growth makes slow cell growth, low biomass, and higher harvesting cost. The major limitations associated with photoautotrophic cultivations overcome by heterotrophic cultivation of microalgae using organic carbon sources. Heterotrophic growth

Collection @ chosun

조선대학교
CHOSUN UNIVERSITY

was supported by sugars and organic acids replacing the traditional light energy [10]. Glucose [2, 11–13], sodium acetate [11, 14] and sodium bicarbonate [15] are common carbon sources used for heterotrophic cultivation of microalgae. This mode of growth offers several advantages including elimination of light, good control of cultivation, high degree of biomass growth and high lipid content in cells [5, 16]. Conversely, the mixotrophic cultivation means that light is the main source of energy although both organic carbon sources and inorganic carbon (CO_2) are simultaneously assimilated. Thus, mixotrophic cultivation was a good strategy to obtain a large biomass and high lipid content [16], with the additional benefits that CO_2 released by microalgae via metabolic process will be trapped and reused under phototrophic cultivation [3]. Furthermore, a number of environmental factors such as salinity, nitrogen, iron, light intensity and culture conditions are known to strongly influence the microalgal growth and lipid content of microalgae. Most researches on microalgae have been dominated by the selection of cultivation conditions that lead to the highest yield of lipid in the shortest time [17, 18]. In the literature, much attention has not been given on comparison of biomass production and total lipid content in microalgae under various culture conditions. In the present study, we compared the microalgal growth and total lipid content of four green microalgal species such as *Chlorella* sp., *Chlorella vulgaris* CCAP211/11B, *Botryococcus braunii* FC124 and *Scenedesmus obliquus* R8 under autotrophic, heterotrophic and micotrophic conditions. The influence of six carbon sources, different glucose concentration and light irradiations on cell growth and total lipid content were also investigated.

Methods and materials

Microalgae and growth medium

Four green microalgal species including *Chlorella* sp. (obtained from Prof. EonSeon Jin of Hanyang University, Seoul, Korea), *Chlorella vulgaris* CCAP211/11B (obtained from Culture Collection of Algae and Protozoa, Argyll, UK), *Scenedesmus obliquus* R8 (obtained from Dr. Yang Hetong of the Biotechnology Center, Shandong Academy of Science, PR China), and *B. braunii* FC124 (obtained from Korea Marine Microalgae Culture Center, Busan, Korea) were studied. The media used in this study were TAP (Tris-Acetate-Phosphate) medium [19] for *Chlorella* sp., BG11 (Blue-Green) medium [20] for *C. vulgaris* CCAP 211/11B, Bold's Basal medium [21] for *S. obliquus* R8, and Chu 13 [22] medium for *B. braunii* FC124. TAP medium contained (per liter, pH 7.0): 0.8 g NH_4Cl, 0.1 g $CaCl_2{\cdot}2H_2O$, 0.2 g $MgSO_4{\cdot}7H_2O$, 0.3 g K_2HPO_4, 0.05 g EDTA·$2H_2O$, 0.005 g $FeSO_4{\cdot}7H_2O$, 0.022 g $ZnSO_4{\cdot}7H_2O$, 0.005228 g H_3BO_3, 0.0051 g $MnCl_2{\cdot}4H_2O$, 0.0011 g $CuCl_2{\cdot}2H_2O$, 0.0026 g $Na_2MoO{\cdot}2H_2O$, 0.0016 g $CoCl_2{\cdot}6H_2O$. BG11 medium contained (per liter, pH 7.1): 1.5 g $NaNO_3$, 0.04 g K_2HPO_4, 0.075 g $MgSO_4{\cdot}7H_2O$, 0.036 g $CaCl_2{\cdot}2H_2O$, 0.006 g citric acid, 0.006 g ammonium ferric citrate green, 0.001 g Na_2EDTA, 0.02 g Na_2CO_3, 0.00286 g H_3BO_3, 0.00181 g $MnCl_2{\cdot}4H_2O$, 0.00022 g $ZnSO_4{\cdot}7H_2O$, 0.00039 g $Na_2MoO{\cdot}2H_2O$, 0.00008 g $CuSO_4{\cdot}5H_2O$, 0.00005 g $Co(NO_3)_2{\cdot}2H_2O$. Bold's Basal medium included (per liter, pH 6.8): 0.175 g KH_2PO_4, 0.025 g $CaCl_2{\cdot}2H_2O$, 0.0075 g $MgSO_4{\cdot}7H_2O$, 0.255 g $NaNO_3$, 0.075 g K_2HPO_4, 0.025 g NaCl, 0.01 g Na_2EDTA, 0.0062 KOH, 0.00498 g $FeSO_4{\cdot}7H_2O$, 0.001 ml H_2SO_4, 0.01086 g H_3BO_3, 0.00181 g $MnCl_2{\cdot}4H_2O$, 0.00022 g $ZnSO_4{\cdot}7H_2O$, 0.00039 g $Na_2MoO{\cdot}2H_2O$, 0.000079 g $CuSO_4{\cdot}5H_2O$, 0.0000494 g $Co(NO_3)_2{\cdot}6H_2O$. Chu 13 medium contained (per liter, pH 7.5): 0.4 g KNO_3, 0.08 g K_2HPO_4, 0.107 g $CaCl_2{\cdot}2H_2O$, 0.2 g $MgSO_4{\cdot}7H_2O$, 0.02 g ferric citrate, 0.1 g citric acid, 0.00002 g $CoCl_2$, 0.00572 g H_3BO_3, 0.00362 g $MnCl_2{\cdot}4H_2O$, 0.00044 g $ZnSO_4{\cdot}7H_2O$, 0.00016 g $CuSO_4{\cdot}5H_2O$, 0.000084 g Na_2MoO, 1 drop of 0.072 N H_2SO_4.

Pre-cultivation conditions

Each microalga was pre-cultured in 500 ml Erlenmeyer flask of modified medium with pH adjusted to 6.8–7.5 and incubated at 25–27 °C. The light intensity and illumination period (light:dark) provided for each microalga were: 100 μmol m^{-2} s^{-1} and 12:12 h for *Chlorella* sp.; 80 μmol m^{-2} s^{-1} and 12:12 h for *C. vulgaris* CCAP211/11B and *S. obliquus* R8; and 100 μmol m^{-2} s^{-1} and 16:8 h for *B. braunii* FC124, respectively. The cultivation periods for each microalgal species were 12, 15, 20, and 30 days for *Chlorella* sp., *C. vulgaris* CCAP211/11B, *S. obliquus* R8, and *B. braunii* FC124, respectively.

Culture conditions

The photoautotrophic cultivations of the above four microalgae were performed under the same pre-cultivation conditions in the 2 l Erlenmeyer flasks. The effects of various organic carbon sources such as glucose, xylose, rhamnose, fructose, sucrose, and galactose on heterotrophic cultivation (without light irradiation) of the four microalgae were studied. The initial concentrations of the carbon sources were 0.01 M. In addition, the influence of glucose concentration (0.2–2.0 %) on microalgal growth under heterotrophic condition was also determined. In the mixotrophic culture conditions, the start-up cultivation was the same as the phototrophic culture condition with an initial glucose concentration 1 % (w/v) for *Chlorella* sp., *C. vulgaris* CCAP211/11B and *B. braunii* FC124 and 2 % (w/v) for *S. obliquus* R8. To study the effect of light

Collection @ chosun

조선대학교
CHOSUN UNIVERSITY

intensity on microalgal growth and total lipid content, 0, 15, 35, 80, 100, and 150 μmol m^{-2} s^{-1} of light intensities were provided by fluorescence lamp. Under mixotrophic conditions, *Chlorella* sp., *C. vulgaris* CCAP211/11B, *S. obliquus* R8, and *B. braunii* FC124 were cultivated for 11, 15, 12, and 20 days, respectively.

Estimation of biomass production

To estimate dry weight of the microalgae, 100 ml of stationary microalgal cultures were centrifuged at 5,000×*g* for 30 min. The resulting pellets were washed three times with 0.9 % NaCl. After washing, the pellet fraction was filtered through a 0.8 μm glass membrane (Pall, USA) and dried at 105 °C for 8 h in an electric oven (Advantec FUW243PA, Japan) and then weighed using electronic balance.

Estimation of total lipid content

The cultured microalgal cells were harvested by centrifugation at 5,000×*g* for 30 min, and the precipitate was frozen overnight at −30 °C and freeze-dried at −50 °C under vacuum. One gram of the dry cell biomass was blended with 200 ml of distilled water and the biomass mixture was disrupted by autoclaving at 121 °C with 0.2 MPa for 60 min. Analysis of the total lipids from microalgal biomass was performed according to the modified procedure described by Folch et al. [23]. Total lipid was extracted with a mixture of chloroform–methanol (2:1, v/v) for 1 h and then separated into chloroform and aqueous methanol layers overnight. The chloroform layer was washed with distilled water and evaporated by rotary vacuum evaporator (Rotavapor R-205; Buchi, switzerland). All the experiments were performed in triplicate and the average values and standard deviations were described.

Results and discussion

Effect of organic carbon sources on biomass production

In heterotrophic culture condition, effect of different carbon sources supplemented to the mineral medium on biomass production of the four microalgae was shown in Fig. 1. Six carbon sources used were glucose, xylose, rhamnose, fructose, sucrose and galactose. When the initial concentration of carbon source was 0.01 M, significant biomass growth variations were observed in all four microalgal species. Among the various carbon sources, glucose was the most effective carbon source for four microalgal growths, especially for *B. braunii* FC124 and *S. obliquus* R8, whereas the other carbon sources did not stimulate significantly the biomass production. This is mainly due to that the glucose is a simple hexose monosaccharide, which is first catabolised into glucose-6-phosphate (important intermediate product for various metabolic precursors) and subsequently to pyruvate through anaerobic glycolysis process, and then entered into TCA cycle followed by mitochondrial oxidative phosphorylation for ATPs production [24, 25]. However, the other carbon sources need more complicated inter-conversion metabolic process to provide energy for algal growth as well as lipid production. Although glucose and fructose had the same number of carbon atoms, fructose cannot directly be converted into glucose-6-phosphate in the microalgae. The lowest biomass production was observed with the sucrose supplementation, because sucrose is a non-reducing disaccharide molecule consisting of equimolar amount of glucose and fructose and requiring to be hydrolyzed before entering glycolysis pathway. From the overall results, it was revealed that different biomass productions of the four microalgal species were due to their different metabolic pathways of carbon and energy sources supplemented.

Effect of glucose concentration on biomass growth

Influence of glucose concentration (0.2–2.0 %, w/v) on biomass growth under heterotrophic cultivation of four microalgal species was monitored (Fig. 2). Generally, biomass concentrations of the four green microalgal species increased in proportional to the increase of glucose concentration. Among the cultures supplemented with glucose, the highest biomass production was achieved with the concentration of 1.0 % (w/v) glucose; however, higher concentration severely inhibited the growth. When 2.0 % glucose supplementation resulted in 30–40 % decrease of biomass productions, this is because of substrate inhibition of growth. Meanwhile, the biomass of *S. obliquus* R8 exhibited strong tolerance to higher glucose concentration (2.0 %). The results obtained in these studies are in good agreement with the results previously reported in the literature. The concentration of glucose had a marked effect on the biomass yield. For example, *C. protothecoides* and *C. saccharophila* have been reported to grow heterotrophically using organic compounds as a carbon source and produce higher yield of biomass [26, 27]. Conversely, Tan and Johns [28] and Hongjin and Guangce [11] reported that the microalgal growth was strongly inhibited at higher concentrations.

Comparison of biomass and total lipid content in different culture conditions

Microalgal growth and total lipid content of all four microalgae under photoautotrophic, heterotrophic and

Collection @ chosun

조선대학교
CHOSUN UNIVERSITY

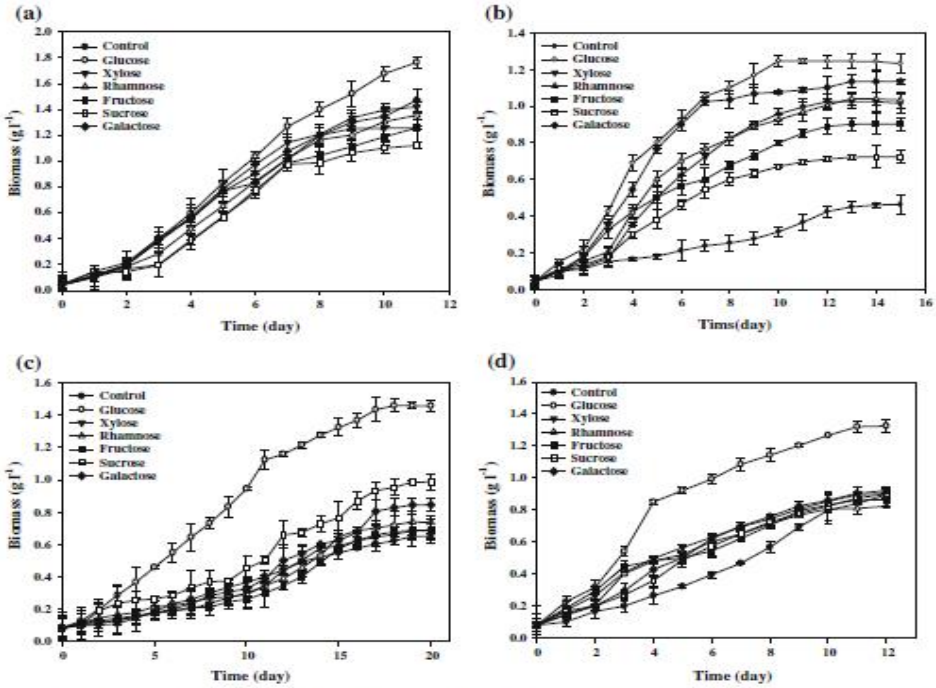

Fig. 1 Effect of various carbon sources (0.01 M) on biomass production of four microalgae under heterotrophic cultivation. **a** *Chlorella* sp.; **b** *C. vulgaris* CCAP211/11B; **c** *B. braunii* FC124; and **d** *S. obliquus* R8

mixotrophic cultivation were compared (Fig. 3). In this study, 1.0 % (w/v) glucose was used in both heterotrophic and mixotrophic (with light) conditions. The maximum biomass production under photoautotrophic, heterotrophic and mixotrophic culture conditions were as follows: 1.3, 2.5, and 2.7 g l^{-1} for *Chlorella* sp.; 0.5, 1.7, and 1.8 g l^{-1} for *C. vulgaris* CCAP211/11B; 1.1, 2.2, and 2.3 g l^{-1} for *S. obliquus* R8; and 0.6, 2.1, and 2.4 g l^{-1} for *B. braunii* FC124, respectively (Fig. 3a). Biomass production under autotrophic culture condition was significantly lower than heterotrophic and mixotrophic culture systems. These variations occur due to two major reasons; first, the microalgal cells transferred lower amount of light energy into ATPs production [29]. Second, some of the ATP produced during photochemical reactions is not utilized for anabolic process [30]. In heterotrophic culture conditions, due to the absence of light source, the supplied organic carbon source (glucose) was directly used for cell metabolism. Moreover, the growths of the four microalgal species were better when they were cultivated in mixotrophic conditions as given below: 100 µmol m^{-2} s^{-1}, 1 % glucose and 11 days incubation for *Chlorella* sp.; 100 µmol m^{-2} s^{-1}, 2 % glucose and 12 days incubation for *S. obliquus* R8; 80 µmol m^{-2} s^{-1}, 1 % glucose and 15 days incubation for *C. vulgaris* CCAP211/11B; and 80 µmol m^{-2} s^{-1}, 1 % glucose and 20 days incubation for *B. braunii* FC124, respectively. These results are in accordance with Liang et al. [2] and Arroyo et al. [31] who stated that mixotrophic cultivation produced higher biomass than heterotrophic and autotrophic cultivation. This phenomenon is mainly because glucose and light energy can be utilized for energy metabolism for ATP and NAD(P)H production, and therefore cell growth can be accelerated [29].

Total lipid contents of the four microalgal species under different growth modes were compared and presented in Fig. 3b. Total lipid content increased in the order of mixotrophic–autotrophic–heterotrophic culture conditions. Lipid production under heterotrophic condition decreased

Collection @ chosun

조선대학교
CHOSUN UNIVERSITY

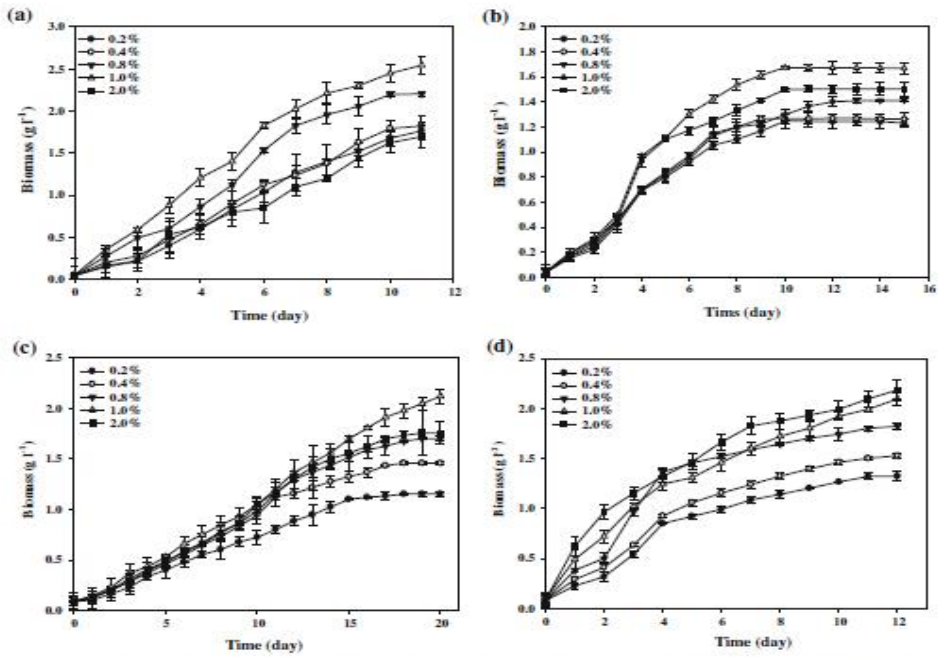

Fig. 2 Influence of glucose concentration on biomass production under heterotrophic cultivation of four microalgal species. **a** *Chlorella* sp.; **b** *C. vulgaris* CCAP211/11B; **c** *B. braunii* FC124; **d** *S. obliquus* R8

when compared with autotrophic and mixotrophic culture conditions: 21 and 49 % in *Chlorella* sp.; 23 and 40 % in *C. vulgaris* CCAP211/11B; 38 and 51 % for *S. obliquus* R8; and 41 and 55 % for *B. braunii* FC124, respectively. Based on the above experimental results, it was revealed that the mixotrophic cultivation of the four microalgal species stimulates both biomass production and total lipid content when compared with heterotrophic cultivation. As shown in Fig. 3a, lower lipid content was obtained in heterotrophic system because most of organic carbon sources supplied were completely utilized for algal growth. In mixotrophic culture condition, however, simultaneous assimilation of the glucose (carbon source) and CO_2 was took place in the algal cells. In the presence of light energy and glucose, most of the metabolizing enzymes present in the algal cells got more activity. Especially, the activities of fatty acid synthesizing enzymes such as acetyl-CoA carboxylase, desaturase, acyl-carrier protein synthase, and ATP:citrate lyase increased and the accumulation of lipids in the algal cells also subsequently increased [31].

Effect of light intensity on biomass and lipid production

Microalgal acclimatization can be occurred based on the variations in environmental factor such as light intensity. When microalga is cultured with carbon dioxide as a sole carbon source, the cell growth, biochemical composition (structural and storage molecules) and lipid accumulation are depending on the availability of light intensity [32]. Figure 4 shows the effect of light intensity on biomass growth and total lipid content of the four microalgal species, which were cultured in mixotropic culture conditions. In our study, when the microalgal cells were grown with increasing light intensity range from 0 to 150 μmol m^{-2} s^{-1}, no significant difference in biomass growth was found in *Chlorella* sp. and *C. vulgaris* CCAP211/11B. However, *B. braunii* FC124 showed higher biomass content (2.6 g l^{-1}) at 80 μmol m^{-2} s^{-1} of light irradiation, but a higher light intensity inhibited cell growth. Conversely, the *S. obliquus* R8 growth increased with increasing light intensity.

Collection @ chosun

조선대학교
CHOSUN UNIVERSITY

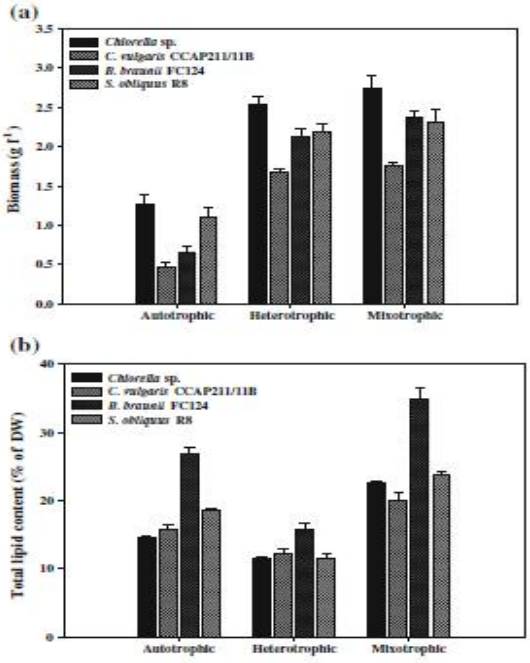

Fig. 3 Comparison of **a** biomass production and **b** total lipid content of four *green* microalgae under autotrophic, heterotrophic and mixotrophic culture conditions

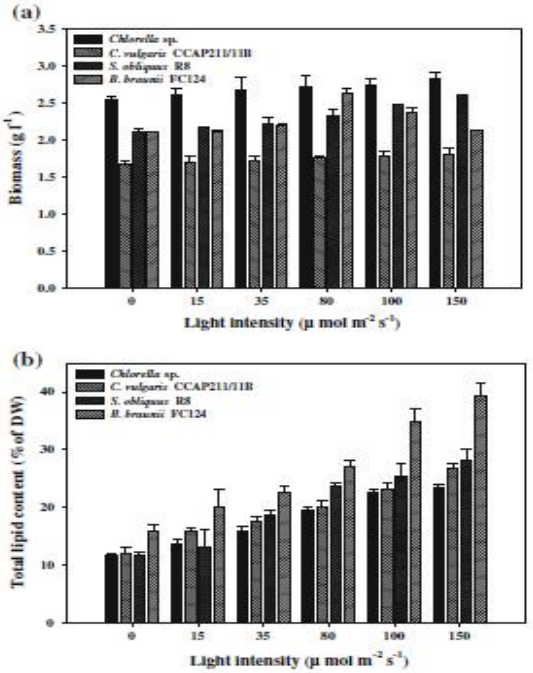

Fig. 4 Effect of light intensity on **a** biomass growth and **b** total lipid content of four microalgae grown under mixotrophic condition

Total lipid content in these four species increased in proportional to light intensity. *B. braunii* FC124 was found to be the highest lipid producing microalga (39.4 %) compared with the other species. These results are in good agreement with Tansakul et al. [33]. According to the literature, because light intensity has a profound impact on lipid accumulation, higher light irradiance was favored for the lipid production rather than biomass growth. When microalgae are exposed to a large quantity of light energy, more metabolic fluxes generated from photosynthesis are directed to lipid accumulation [33] and enhance free fatty acid synthesis in chloroplasts [34]. Furthermore, a low light intensity may cause a higher Chl *a* content in cell [35]. This trend is because, under the low light irradiation, the microalgal cells increase their photosynthetic pigments such as Chl *a* and antenna pigments to maximize their ability to harvest light for their normal growth of microalgae [36]. In addition, the algal cells had a relatively large volume of chloroplast, a high surface density of thylakoid membrane and a small volume of lipid storage body [37]. In contrast, at higher light intensity, the dimensions of microalgal light harvesting antenna pigments and Chl *a* contents decreased and thylakoid membranes worked more efficiently for lipid accumulation [38].

Table 1 shows the outline of the biomass production and total lipid content of various microalgal species cultivated under different culture conditions. From the comparative analysis, it was proposed that all the four green microalgal species used in this study show relatively high total lipid content in cell. Among them, *B. braunii* FC124 was found to be the best lipid producing microalgae under mixotrophic culture conditions (80 μmol m^{-2} s^{-1}, 1 % glucose and 20 days). Our study firmly proves that higher lipid production was obtained at a relatively lower light intensity (80 or 100 μmol m^{-2} s^{-1}). And it was known that the light intensity also influences the fatty acid composition such as triglyceric acid, glycolipids, phospholipids, and PUFA. In the near future, the effect of light intensity on microalgal fatty acid composition profile during mixotrophic cultivation should be investigated.

Collection @ chosun

조선대학교
CHOSUN UNIVERSITY

Table 1 Comparison of biomass production and total lipid content of four green microalgae with other related microalgae

Microalgae	Culture condition	Carbon source	Light intensity ($\mu mol\ m^{-2}\ s^{-1}$)	Biomass production ($g\ l^{-1}$)	Total lipid content (%)	References
S. obliquus AS-6-1	Photobioreactor	CO_2	140	1.6	11.7	[39]
S. obliquus CNW-1	Photobioreactor	CO_2	140	1.4	9.2	[39]
S. obliquus ESP-5	Photobioreactor	CO_2	140	1.9	8.3	[39]
S. obliquus	Photobioreactor	12 % CO_2	43.2	2.1	ND	[40]
Nannochloropsis sp.	Batch reactor	N-depleted medium and 2 % CO_2	700	0.6	21.0	[41]
Dunaliella viridis	Batch reactor	N-Limited and 1 % CO_2	1500	~0.6	31.8	[42]
D. salina DCCBC2	Photobioreactor	3 % CO_2		3.2	ND	[43]
C. protothecoides	Heterotrophic/batch reactor	Glucose	–	15.3	7.7	[44]
C. protothecoides	Heterotrophic/batch reactor	Pure glycerol	–	19.2	9.8	[44]
C. protothecoides	Heterotrophic/batch reactor	Crude glycerol	–	23.5	14.6	[44]
C. vulgaris LEB-104	Batch reactor	5 % CO_2	47.3	1.9	10.0	[45]
B. braunii SAG-30.81	Batch reactor	5 % CO_2	47.3	3.1	33.0	[45]
Chlorella sp.	Mixotrophic/batch reactor	1 % Glucose	100	2.7	22.5	This study
C. vulgaris CCAP211/11B	Mixotrophic/batch reactor	1 % Glucose	80	1.8	20.1	This study
B. braunii FC124	Mixotrophic/batch reactor	1 % Glucose	80	2.4	34.9	This study
S. obliquus R8	Mixotrophic/batch reactor	2 % Glucose	100	2.3	23.7	This study

Conclusion

In the present study, four green microalgal growth and total lipid contents were compared in three different modes of cultivations. Comparing to autotrophic cultivation, higher biomass production was observed in heterotrophic cultivation. Among the various carbon sources tested, glucose was the best carbon source for four microalgal growths, and 1 % glucose was optimum for higher biomass production in three microalgal species except *S. obliquus* R8 (2 % glucose). The *B. braunii* FC124 was found to be a best lipid producing microalga under 80 $\mu mol\ m^{-2}\ s^{-1}$ of light intensity, 1 % of glucose and 20 days incubation. Lipid accumulation increased with increasing light intensity in the mixotrophic cultivation. Total lipid content was lesser in the heterotrophic mode when compared with other two modes. Nevertheless, no significant variations in the biomass production was noted between heterotrophic and mixotrophic cultivations. These algal species can be used for the industrial scale-up of lipid production.

Acknowledgments This work was supported by the grant of New & Renewable Energy Program of the Korea Institute of Energy Technology Evaluation and Planning (KETEP) funded by the Ministry of Knowledge Economy, Korea (20103020090020).

References

1. Cho S, Ji SC, Hur S, Bae J, Park IS, Song YC (2007) Optimum temperature and salinity conditions for growth of green algae *Chlorella ellipsoidea* and *Nannochloris oculata*. Fish Sci 73:1050–1056
2. Liang YN, Sarkany N, Cui Y (2009) Biomass and lipid productivities of *Chlorella vulgaris* under autotrophic, heterotrophic and mixotrophic growth conditions. Biotechnol Lett 31:1043–1049
3. Mata TM, Martins AA, Caetano NS (2010) Microalgae for biodiesel production and other application: review. Renew Sustain Energy Rev 14:217–232
4. Yoo C, Jun SY, Lee JY, Ahn CY, Oh HM (2010) Selection of microalgae for lipid production under high levels carbon dioxide. Bioresour Technol 101:S71–S74
5. Miao X, Wu Q (2006) Biodiesel production from heterotrophic microalgal oil. Bioresour Technol 97:841–846
6. Xu H, Miao XL, Wu QY (2006) High quality biodiesel production from a microalga *Chlorella protothecoides* by heterotrophic growth in fermenters. J Biotechnol 126:499–507
7. Li XF, Xu H, Wu QY (2007) Large-scale biodiesel production from microalga *Chlorella protothecoides* through heterotrophic cultivation in bioreactors. Biotechnol Bioeng 98:764–771
8. Cheng Y, Zhou WG, Gao CF, Lan K, Gao Y, Wu QY (2009) Biodiesel production from Jerusalem artichoke (Helianthus Tuberosus L.) tuber by heterotrophic microalgae *Chlorella protothecoides*. J Chem Technol Biotechnol 84:777–781
9. Mandal S, Mallick N (2009) Microalga *Scenedesmus obliquus* as a potential source for biodiesel production. Appl Microbiol Biotechnol 84:281–291
10. Huang GH, Chen F, Wei D, Zhang XW, Chen G (2010) Biodiesel production by microalgal biotechnology. Appl Energy 87:38–46
11. Hongjin Q, Guangce W (2009) Effect of carbon source on growth and lipid accumulation in *Chlorella sorokiniana* GXNN01. Chinese J Oceanol Limnol 27:762–768
12. Leesing R, Nontaso N (2010) Microalgal oil production by green microalgae under heterotrophic cultivation. KKU Res J 15:787–793
13. Wan M, Liu P, Xia J, Rosenberg JN, Oyler GA, Betenbaugh MJ, Nie Z, Qiu G (2011) The effect of mixotrophy on microalgal

Collection @ chosun

조선대학교
CHOSUN UNIVERSITY

growth, lipid content, and expression levels of three pathway genes in *Chlorella sorokiniana*. Appl Microbiol Biotechnol 91:835–844
14. Ratledge C, Kanagachandran K, Anderson AJ, Grantham DJ, Stephenson JC (2001) Production of docosahexaenoic acid by *Crypthecodinium cohnii* grown in a pH-auxostat culture with acetic acid as principal carbon source. Lipids 36:12410–12416
15. Yeh KL, Chang JS, Chen YM (2010) Effect of light supply and carbon source on cell growth and cellular composition of a newly isolated microalga *Chlorella vulgaris* ESP-31. Eng Life Sci 10:201–208
16. Lee K, Lee C (2002) Nitrogen removal from wastewaters by microalgae without consuming organic carbon sources. J Microbiol Biotechnol 12:979–985
17. Doan TTY, Sivaloganathan B, Obbard JP (2011) Screening of marine microalgae for biodiesel feedstock. Biomass Bioenergy 35:2534–2544
18. Yeesang C, Cheirsilp (2011) Effect of nitrogen, salt, and iron content in the growth medium and light intensity on lipid production by microalgae isolated from freshwater sources in Thailand. Bioresour Technol 102:3034–3040
19. Harris EH (1989) The *Chlamydomonas* source book: a comprehensive guide to biology and laboratory use. Academic Press, San diego, p 780
20. Stanier RY, Kunisawa R, Mandel M, Cohen-Bazire G (1971) Purification and properties of unicellular blue-green algae (order *Chroococcales*). Bacteriol Rev 35:171–205
21. Bold HC (1949) The morphology of *Chlamydomonas chlamydogama* sp. nov. Bull Torrey Bot Club 76:101–108
22. Chu SP (1942) The influence of the mineral composition of the medium on the growth of planktonic algae. J Ecol 30(2):284–325
23. Folch J, Lees M, Stanley GHS (1956) A simple method for isolation and purification of total lipides from animal tissues. J Biol Chem 226:497–509
24. Droop MR (1974) Heterotrophy of carbon. In: Stewart WDP (ed) Algal physiology biochemistry. Blackwell Scientific Oxford, UK, pp 530–559
25. Neilson AH, Lewin RA (1974) The uptake and utilization of organic carbon by algae: an essay in comparative biochemistry. Phycologia 13:227–264
26. Shi XM, Liu HJ, Zhang XW, Chen F (1999) Production of biomass and lutein by *Chlorella protothecoides* at various glucose concentrations in heterotrophic cultures. Process Biochem 34:341–347
27. Hosoglu MI, Gultepe I, Elibol M (2012) Optimization of carbon and nitrogen sources for biomass and lipid production by *Chlorella saccharophila* under heterotrophic conditions and development of Nile red fluorescence based method for quantification of its neutral lipid content. Biochem Eng J 61:11–19
28. Tan CK, Johns MR (1991) Fatty acid production by heterotrophic *Chlorella saccharophila*. Hydrobiologia 215:13–19
29. Yang C, Hua Q, Shimizu K (2000) Energetics and carbon metabolism during growth of microalgal cells under photoautotrophic, mixotrophic and cyclic light-autotrophic/dark-heterotrophic conditions. Biochem Eng J 6:87–102
30. Yokota A, Harada A, Kitaoka S (1989) Characterization of ribulose 1,5-bisphosphate carboxylase/oxygenase from *Euglena gracilis* Z. J Biochem 105:400–405
31. Arroyo TH, Wei W, Ruan R, Hu B (2011) Mixotrophic cultivation of *Chlorella vulgaris* and its potential application for oil accumulation from non-sugar materials. Biomass Bioenergy 35:2245–2253
32. Khotimchenko SV, Yakovleva IM (2005) Lipid composition of the red alga *Tichocarpus crinitus* exposed to different levels of photon irradiance. Phytochemistry 66:73–79
33. Tansakul P, Savaddirakasa Y, Prasertsan P, Tongurai C (2005) Cultivation of the hydrocarbon-rich alga, *Botryococcus braunii* in secondary treated effluent from a sea food processing plant. Thai J Agric Sci 38:71–76
34. Sauer A, Heise KP (1984) Regulation of acetyl-coenzyme A carboxylase and acetyl-coenzyme A synthetase in spinach chloroplasts. Z Naturforschung 39:268–275
35. Guihéneuf F, Mimouni V, Ulmann L, Tremblin G (2009) Combined effects of irradiance level and carbon source on fatty acid and lipid class composition in the microalgae pavlova lutheri commonly used in mariculture. J Exp Marine Biol Ecol 369:136–143
36. Mock T, Kroon BMA (2002) Photosynthetic energy conversion under extreme conditions-II: the significance of lipids under light limited growth in antractic sea ice diatoms. Phytochemistry 61:53–60
37. Sukenik A, Carmell Y, Berner T (1989) Regulation of fatty acid composition by irradiance level in the eustigmatophyte *Nannochloropsis* sp. J Phycol 25:686–692
38. Rammus J (1990) A form-function analysis of photon captures for seaweeds. Hydrobiologia 204–205:65–71
39. Ho SH, Lu WB, Chang JS (2012) Photobioreactor strategies for improving the CO_2 fixation effiency of indigenous *Scenedesmus obliquus* CNW-N: statistical optimization of CO_2 feeding. Bioresour Technol 105:106–113
40. Morais MG, Costa JAV (2007) Carbon dioxide fixation by *Chlorella kessleri*, *C. vulgaris*, *Scenedesmus obliquus* and *Spirulina* sp. cultivated in flasks and vertical tubular photobioreactors. Biotechnol Lett 29:1349–1352
41. Pal D, Goldberg IK, Cohen Z, Boussiba S (2011) The effect of light, salinity, and nitrogen availability on lipid production by *Nannochloropsis* sp. Appl Microbiol Biotechnol 90:1429–1441
42. Gordillo FJL, Goutx M, Figueroa FL, Niell FX (1998) Effects of light intensity, CO_2 and nitrogen supply on lipid class composition of *Dunaliella viridis*. J Appl Phycol 10:135–144
43. Kim W, Park JM, Gim GH, Jeong S, Kang CM, Kim D, Kim SW (2012) Optimization of culture conditions and comparison of biomass productivity of three green algae. Bioprocess Biosyst Eng 35:19–27
44. Chen YH, Walker TH (2011) Biomass and lipid production of heterotrophic microalgae *Chlorella protothecoides* by using biodiesel-derived crude glycerol. Biotechnol Lett 33:1973–1983
45. Sydney EB, Sturm W, Carvalho JC, Soccol VT, Larroche C, Pandey A, Soccol CR (2010) Potential carbon dioxide fixation by industrially important microalgae. Bioresour Technol 10:5892–5896

Collection @ chosun

조선대학교
CHOSUN UNIVERSITY

Journal of Microbiology (2015) Vol. 53, No. 11, pp. 767–775
DOI 10.1007/s12275-015-5454-0
Copyright © 2015, The Microbiological Society of Korea

Enhanced method for microbial community DNA extraction and purification from agricultural yellow loess soil

Mathur Nadarajan Kathiravan[1], Geun Ho Gim[1], Jaewon Ryu[2], Pyung Il Kim[3], Chul Won Lee[4], and Si Wouk Kim[1]*

[1]*Department of Environmental Engineering and Ptoneer Research Center for Controlling of Harmful Algal Bloom, Chosun University, Gwangju 61452, Republic of Korea*
[2]*Department of Energy Convergence, Chosun University, Gwangju 61452, Republic of Korea*
[3]*Bio Control Research Institute, IBF, Jeonnam 516-944, Republic of Korea*
[4]*Department of Chemistry, Chonnam National University, Gwangju 61186, Republic of Korea*

(Received Sep 8, 2015 / Revised Oct 2, 2015 / Accepted Oct 2, 2015)

In this study, novel DNA extraction and purification methods were developed to obtain high-quantity and reliable quality DNA from the microbial community of agricultural yellow loess soil samples. The efficiencies of five different soil DNA-extraction protocols were evaluated on the basis of DNA yield, quality and DNA shearing. Our suggested extraction method, which used CTAB, EDTA and cell membrane lytic enzymes in the extraction followed by DNA precipitation using isopropanol, yielded a maximum DNA content of 42.28 ± 5.59 μg/g soil. In addition, among the five different purification protocols, the acid-treated polyvinyl polypyrrolidone (PVPP) spin column purification method yielded high-quality DNA and recovered 91% of DNA from the crude DNA. Spectrophotometry revealed that the ultraviolet A_{260}/A_{230} and A_{260}/A_{280} absorbance ratios of the purified DNA were 1.82 ± 0.03 and 1.94 ± 0.05, respectively. PCR-based 16S rRNA amplification showed clear bands at ~1.5 kb with acid-treated PVPP–purified DNA templates. In conclusion, our suggested extraction and purification protocols can be used to recover high concentration, high purity, and high-molecular-weight DNA from clay and silica-rich agricultural soil samples.

Keywords: microbial community DNA, metagenomics, soil texture, DNA extraction purification

Introduction

The microbial diversity of environmental samples is enormous; however, only 1–10% of the microbial population can be cultured through the traditional isolation techniques. Numerous works in the literature have indicated that most bacteria in environmental samples cannot be isolated via the recognized methods. In recent years, researchers have paid great attention to the culture-independent metagenomic approach, using either a sequence- or a functional-based application. Metagenomics is a reliable alternative approach for providing insights into microbial diversity. This approach has also been considered as a promising molecular method for the isolation and identification of novel and unusual proteins, enzymes, and secondary metabolites from soil samples (Forsberg *et al.*, 2012; McGarvey *et al.*, 2012; Selvin *et al.*, 2012; Yeh *et al.*, 2013). In addition, this approach has become one of the powerful research tools to overcome the limitation of the traditional culture-based methods. Construction of a metagenomic library requires a sufficiently great quantity of high-quality DNA, which makes the extraction and purification of DNA from the environmental samples a critical step (Wilkinson *et al.*, 2002). The molecular techniques used in metagenomic studies, including DNA extraction from the environmental samples, followed by purification, restriction digestion, cloning, and sequencing, are affected mainly by humic acid contaminants. Humic substances are known to inhibit the activities of imperative enzymes that are used in molecular studies, such as *Taq* DNA polymerase and restriction enzymes. Even at extremely low concentrations, humic acid substances significantly influence the binding efficiency and annealing of double-stranded DNA in polymerase chain reaction (PCR) amplification. Hence, to obtain high-quality microbial community DNA, researchers have developed different types of protocols and applied modified methods in each step. The efficiency of soil microbial community DNA extraction depends on the soil quality and chemical composition of the soil, including sand, clay, and silt. Several previous studies have indicated that the extraction process is also influenced by the tight interaction of microorganisms on soil colloids, the formation of clay-organic matter aggregates, and the interaction of DNA with the soil matrix (Harry *et al.*, 1999). The soil samples contain microbial populations including bacteria, actinomycetes, fungi, protozoa, mycelia, spores, and different types of unicellular and multicellular organisms (Krsek and Wellington, 1999). However, the data on high quality DNA extractions from soil communities are significantly limited. This may be due to different trace elements, pH, and clay contents of the soil and sediments. A variety of extraction protocols have been applied to obtain high-quality microbial community DNA from diverse environmental samples.

Over the past two decades, different protocols of physical, chemical, and enzymatic lysis have been developed for direct DNA extraction. Generally, common physical disruption methods have been employed, such as sonication (Yeates *et al.*, 1997), bead beating (Kozdroj and Van Elsas, 2000), freezing-

*For correspondence. E-mail: swkim@chosun.ac.kr; Tel.: +82-62-230-6649

Collection @ chosun

조선대학교
CHOSUN UNIVERSITY

thawing (Tsai and Olson, 1990), liquid nitrogen freezing-thawing (Erb and Wagner-Dobler, 1993), and microwaving (Orsini and Romano-Spica, 2001). Although these techniques yield high DNA concentrations, a major drawback of direct lysis is the coextraction of extra humic acid, cellulose-derived compounds, and other phenolic compounds. The lysis buffer commonly contains detergents such as sodium dodecyl sulfate (SDS) (Miller *et al.*, 1999) and sarkosyl (Smith and Tiedje, 1992), however in recent years a variety of chemical lysis approaches have been used to obtain higher purity DNA, including high-temperature boiling with polyvinyl polypyrrolidone (PVPP), phenol, chloroform, ethylenediamine tetraacetic acid (EDTA), cetyl trimethylammonium bromide (CTAB), and Triton X-100, respectively. Arbeli and Fuentes (2007) used polyethylene glycol (PEG) as a precipitate instead of isopropanol, which resulted in a higher reduction of PCR inhibitors without loss of DNA concentration. The final method of DNA extraction is an enzymatic digestion step that frequently employs lysozyme and proteinase K to quicken the process and increase the DNA yield.

The extracted DNA product is light brown to dark brown in color owing to the presence of phenolic compounds. As mentioned above, because these contaminants inhibit the activities of DNA polymerase and restriction-digestion enzymes, further purification is required to obtain greater purity. So far, several purification methods-including Sephadex spin columns, ion exchange chromatography, gel filtration chromatography, agarose gel electrophoresis, PVPP, bovine serum albumin (BSA), gelatin, and skim milk-have been developed to remove PCR inhibitors (Romanowski *et al.*, 1993; More *et al.*, 1994; Harry *et al.*, 1999; Kauffmann *et al.*, 2004). Amsaleg *et al.* (2001) reported that each step of the purification procedure suffers from shortcomings of inappropriate removal of humic acids and high cost, and every additional step inevitably results in DNA loss. The choice of extraction and purification protocol should consider the desired concentration and quality of the recovered DNA.

Because yellow loess is an aeolian sediment formed by the accumulation of wind-blown silt, typically in the 20–50 μm size range, twenty percent or less clay and balance equal parts sand and silt that are loosely cemented by calcium carbonate, its moisture content is relatively low as 10–15%. And main chemical composition is as follows: 50–60% silica (SiO_2), 8–12% alumina (Al_2O_3), 2–4% ferric ion (Fe_2O_3), 0.8–1.1% ferrous ion (FeO), 0.5% titanium oxide (TiO_2), and Manganese oxide (MnO), 4–16% calcium oxide (CaO), and 2–6% Magnesium oxide (MgO). These indicate that yellow loess is a unique environmental habitat for growth of microorganisms, from which DNA is difficult to extract and purify.

The purpose of this study was to develop novel methods for efficient extraction and purification of microbial community DNA from agricultural yellow loess soil (AYLS) samples. To obtain high quantity of DNA from six soil samples, five different extraction methods were investigated. In addition, five different purification methods were developed to gain high-quality DNA from crude extracted DNA. The purity of DNA was assessed both by analysis of the A_{260}/A_{230} and A_{260}/A_{280} spectrophotometry absorbance ratios and by analysis of 16S rRNA gene amplification.

Materials and Methods

Soil sample collection and characterization

AYLS samples were collected in sterile plastic bags from three different sites around Jeollanamdo, the southwestern province in South Korea: Muan-Hyeongyeong (34°59′25.63″N, 126°28′54.07″E), Yeongam-Sinbuk (34°53′25.04″N, 126°41′33.35″E), and Yeongam-Miam (34°41′57.20″N, 126°34′18.94″E). The collected soil samples were labeled AYLS01, AYLS02, AYLS03, AYLS04, AYLS05, and AYLS06. All soil samples were immediately transferred to the laboratory and stored at -20°C until further use. To identify the soil characteristics, its textures were analyzed by the method described by Kathiravan *et al.* (2011) with a slight modification. The required amount of sterilized soil sample was placed in a glass jar and mixed with an equal volume of distilled water. The resulting soil-water mixture was vigorously stirred for 1 h and then left without further agitation for 1 day. Next, the volume of each particle size was visually measured and the percentage of sand, silt, and clay was calculated with reference to a soil texture analysis chart. The AYLS trace element composition was analyzed as follows. Briefly, 1 g of homogenized soil was placed into a Teflon vessel containing a solution of 20 ml concentrated HNO_3:HCl (3:2), after which the total volume was increased by a further 50% by the addition of ultrapure water. The sample vessels were sealed and stored at 120°C overnight. After incubation, the vessels were allowed to cool, and 10 ml of ultrapure water was added when the acid-extracted digestate reached room temperature. This digestate was further diluted into a 100- to 1000-fold series, and injected into inductive-coupled mass spectroscopy (ICP-MS) (Elan DRC II, PerkinElmer). The pH values of all soil samples were determined by using a glass electrode in a soil:water ratio of 1:1.25. The moisture content of the samples was determined by drying 10 g of soil samples at 100°C for 2 days. The concentration of humic acid was determined using a UV-visible spectrophotometer at a wavelength of 230 nm.

Soil DNA extraction methods

Five different methods were used for DNA extraction, as described below:

Method 1: The PowerSoil® DNA Extraction Kit (MO BIO Laboratories, Inc.): AYLS microbial community DNA extraction was performed according to the manufacturer's protocol using 250 mg of the soil sample. For further purification, the resultant DNA was washed three times with 70% ethanol.

Method 2: Modified Porteous method (Porteous *et al.*, 1994): Briefly, 100 mg of soil sample and 350 μl of homogenization solution A [250 mM NaCl, 100 mM Na_2-EDTA, and 0.2% CTAB (w/v), pH 8.0] were mixed by vortexing for 30 sec. The samples were then sonicated (Branson 5200 sonicator-bath) at room temperature for 3 min. The resultant products were treated with 10 μl proteinase K (10 mg/ml), 10 μl lysozyme (10 mg/ml), and 2 μl glusulase (1,000 U/ml). The tubes were vortexed for 10 sec and incubated at 37°C for 1 h. Each sample was treated with 350 μl of lysis solution B [250 mM NaCl, 100 mM Na_2-EDTA, and 4% SDS (w/v), pH 8.0] and 50 μl of 5 M guanidine isothiocyanate. The samples

Collection @ chosun

조선대학교
CHOSUN UNIVERSITY

were incubated at 68°C for 1 h and then centrifuged for 15 min at 12,000 × *g* at 4°C. The resultant supernatant was mixed with 0.6× volume of isopropanol and incubated at -20°C for 30 min, followed by centrifugation for 15 min at 12,000 × *g*. The pellet was washed three times with 70% ethanol, centrifuged, air dried, and then resuspended in 100 µl of TE buffer (10 mM Tris-HCl, 1 mM EDTA; pH 8.0).

Method 3: Modified Yeates method (Yeates *et al.*, 1997): Yeates's protocol with a minor modification was applied for DNA extraction. Briefly, 1 g of soil was mixed with 2 ml of extraction buffer (100 mM Tris-HCl, 100 mM Na_2-EDTA, 1.5 M NaCl, pH 8.0) and 1 g of sterilized glass beads, before being blended in a mini-bead beater (Biospec instruments) for 2 min at 50 shaking speed/min. The sample was incubated at 65°C for 10 min then centrifuged for 15 min at 12,000 × *g*. The supernatant was transferred to centrifuge tubes containing a half volume of PEG (30%, w/v)/NaCl (1.5 M) and incubated at room temperature for 2 h. Then, 0.5 M potassium acetate (7.5 M) was added to the samples, which were transferred to ice for 5 min and then centrifuged at 12,000 × *g* for 30 min at 4°C to precipitate proteins and polysaccharides. The aqueous phase was extracted with the addition of equal volumes of phenol/chloroform and chloroform/isoamyl alcohol (Sambrook *et al.*, 1987), and DNA was precipitated by adding 0.6× volume of isopropanol. After 2 h at room temperature, the samples were centrifuged at 12,000 × *g* for 30 min and the DNA was resuspended in 250 µl of TE buffer.

Method 4: Modified Bürgmann method (Bürgmann *et al.*, 2001): The Bürgmann protocol was used with a slight modification. Briefly, 0.5 g soil sample and 0.5 g glass beads were suspended in 1 ml of extraction buffer (0.2 M Na_3PO_4, 0.1 M NaCl, 50 mM EDTA, pH 8.0) containing 2 µl glusulase (1,000 U/ml) and incubated with agitation at 200 rpm for 30 min at 37°C. DNA extraction was performed by using a mini-bead beater for 1 min of 10 cycles at 50–60 Hz, and thereafter DNA was purified by adding 2 ml chloroform/isoamyl alcohol (24/1, v/v). DNA precipitation was performed by the addition of 3 ml of a precipitation solution (20% PEG 6000, 2.5 M NaCl), followed by incubation at 37°C for 1 h and then centrifugation at 12,000 × *g* for 5 min. The resultant pellet was washed three times with 70% ice cold ethanol, air dried, and resuspended in 1 ml of TE buffer.

Method 5: Our suggested method: An alternative and efficient method was developed to obtain high-quantity, -quality, and -molecular-weight microbial community DNA. In this protocol, 250 mg of soil sample in 1.5 ml Eppendorf tubes was mixed with 270 µl of DNA extraction buffer [100 mM Tris-HCl, 100 mM Na_2-EDTA, 100 mM NaH_2PO_4, 1.5 M NaCl, and 1% (w/v) CTAB pH 8.0], 2 µl proteinase K (10 mg/ml), and 2 µl glusulase (1,000 U/ml), followed by agitation at 200 rpm for 30 min at 37°C. After shaking, 30 µl of 20% (w/v) SDS was added and incubated in a 65°C water bath for 2 h with gentle mixing every 20 min. The supernatant was collected after centrifugation at 6,000 × *g* for 10 min at room temperature and transferred into 1.5 ml Eppendorf tubes. About 10 µl of RNase A (10 mg/ml) was added to 1.5 ml tubes, which were incubated at room temperature for

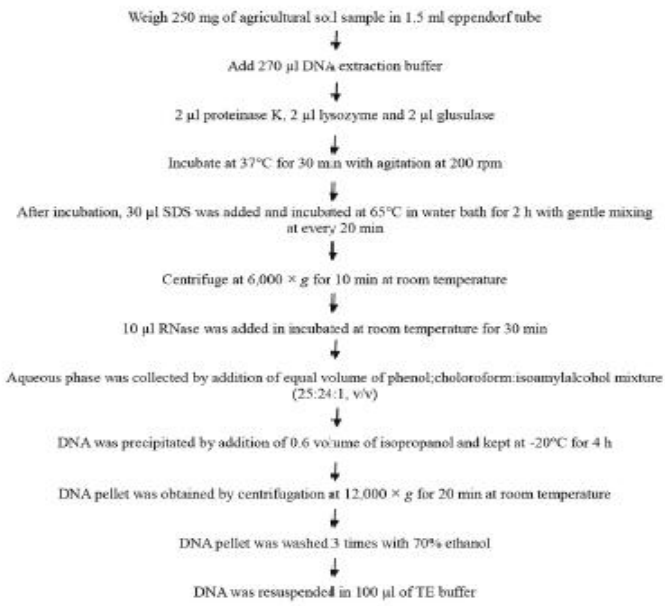

Fig. 1. **Schematic diagram of microbial community DNA extraction from AYLS samples as suggested by this study.**

Collection @ chosun

조선대학교
CHOSUN UNIVERSITY

30 min, and then mixed with an equal volume of phenol: chloroform:isoamyl alcohol (25:24:1, v/v). Next, the aqueous phase was obtained by centrifugation at 6,000 × *g* for 10 min at room temperature and precipitated with 0.6× volume of isopropanol at -20°C for 4 h. The samples were centrifuged at 12,000 × *g* (20 min, room temperature) and the resulting pellet was washed three times with ice cold 70% ethanol and resuspended in 100 µl of TE buffer (Fig. 1).

DNA purification methods

Removal of humic acids and phenolic compounds from a soil sample is very difficult and therefore DNA purification is a critical step. The presence of humic acid is revealed by the development of a brownish color in the recovered DNA extract. This crude DNA is not suitable for PCR amplification or restriction digestion. Generally, during purification, humic acid and contaminated proteins can be removed; however, a significant amount of DNA will inevitably be lost. In this study, five different DNA purification methods were applied and compared as follows:

Method 1: Genomic DNA purification kit: The extracted soil DNA was further purified using a genomic DNA purification kit (Nucleogen Biotechnology) according to the manufacturer's instructions, using 100 µl of sample with slight modifications. Briefly, 20 mg polyvinyl pyrrolidone (PVP) was added to the spin columns, which were then washed three times with ice cold 70% ethanol to remove the excess contaminants present in the extracted sample.

Method 2: Sephadex G-100 spin column: The Sephadex G-100 spin column was constructed by adding 25 mg Sephadex G-100 into the commercial spin column, followed by washing with sterilized DNase-free water. The excess water was removed by centrifugation. Approximately 100 µl of the extracted DNA was added into the spin column. The contaminants were washed with ice cold 70% ethanol, and then 100 µl of TE buffer was added to the spin column and left for 2 min. The purified DNA was collected in a collection tube by centrifuging the spin column at maximum speed for 2 min.

Method 3: PVP-low melting point (LMP) agarose gel: The PVP-LMP agarose gel was prepared by the addition of 1.5% (w/v) PVP and 1% (w/v) LMP agarose in 100 µl of 1× TAE buffer (40 mM Tris-acetate, 1 mM EDTA; pH 7.0). This mixture was dissolved by heating in a microwave oven for 3 min and then cooled to 50°C. After cooling, 10 µl Top Red nucleic acid gel stain (Genomicbase) was added and the mixture was poured into a gel casting tray. After setting the gel, about 40 µl of crude DNA sample was added into each well. Electrophoresis was performed for 30 min at 100 V. The separated DNA was visualized using UV light. After electrophoresis, the separated bands were extracted using a commercial kit.

Method 4: Formamide–agarose gel purification (our suggested method): A 2% agarose solution in 1× TAE was prepared in a sterile glass beaker, heated in a microwave oven, and left to cool to 45°C. It was mixed briefly to ensure that the agarose solution was homogeneous. Then, 100 µl of 2% agarose was mixed with 100 µl of DNA extract. A solution of 1 ml 80% formamide prepared in a 1.3 M NaCl solution was added into the agarose-DNA mixture before being inverted slowly then incubated at 4°C for 1 h. After incubation, the formamide was removed by centrifugation at 6,000 × *g* for 10 min. Purified DNA was obtained using a commercial gel extraction kit.

Method 5: Acid-treated PVPP (AT-PVPP) spin column (our suggested method): Acid treatment of PVPP was performed by the addition of 10 g of insoluble PVPP to 1 L of 1 M HCl. This reaction mixture was incubated at room temperature for 24 h. After incubation, the solution was filtered through Whatman filter paper No. 1. The filtered PVPP was added to 1 L of 20 mM phosphate buffer (pH 8.0) and mixed by stirring for 2 h. This washing process was repeated with the same buffer until the pH of filtered PVPP suspension reached 7.0. After washing, the AT-PVPP residue was air dried over-

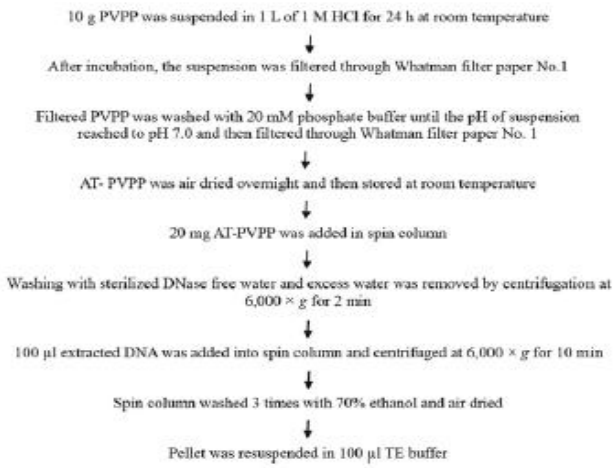

Fig. 2. **Schematic purification steps of crude DNA by AT-PVPP.**

Collection @ chosun

조선대학교
CHOSUN UNIVERSITY

Table 1. Soil properties of agricultural yellow loess

Property		Sample Nos.					
		AYLS01	AYLS02	AYLS03	AYLS04	AYLS05	AYLS06
pH		6.5 ± 0.04	7.2 ± 0.03	6.8 ± 0.07	6.2 ± 0.05	6.8 ± 0.04	7.1 ± 0.06
Soil type		Loam	Loam	Sandy loam	Sandy clay loam	Sandy loam	Clay loam
Soil texture[a]	Sand (%) (2-0.05 mm)	41.4 ± 1.2	50.7 ± 2.4	59.6 ± 1.9	52.6 ± 2.1	43.6 ± 1.6	38.7 ± 2.3
	Silt (%) (0.05-0.002 mm)	43.0 ± 3.2	39.8 ± 1.8	30.0 ± 1.3	26.9 ± 1.8	39.0 ± 1.7	41.7 ± 1.9
	Clay (%) (<0.002 mm)	15.6 ± 1.7	9.5 ± 0.5	10.4 ± 0.6	20.4 ± 1.1	17.4 ± 0.9	19.6 ± 1.4

[a] The soil type was determined with soil texture analysis chart.

night at room temperature. About 20 mg AT-PVPP was added to the DNA purifying spin column and washed with sterilized DNase-free water. The excess water was removed by centrifugation. Approximately 100 µl of the extracted DNA was added into the spin column and washed three times with 70% ethanol to remove the excess contaminants present in the extracted sample. In this purification method, the eluant was collected, and DNA was washed with 70% ethanol, air dried, and then resuspended in 100 µl of TE buffer (Fig. 2).

PCR amplification

16S rRNA genes were amplified by PCR from the soil-extracted community DNA templates using universal bacterial primers 27F (5′-AGAGTTTGATCCTGGCTCAG-3′) and 1494R (5′-TGACTGACTGAGGYTACCTTGTTAC-3′). PCR amplification of 16S rRNA genes was performed using two templates; crude DNA obtained using our suggested protocol, and DNA that had been purified using the AT-PVPP approach. A total volume of 20 µl PCR mixture was used, containing 1 µl undiluted DNA template, 2.5 µl 10× PCR buffer (TaKaRa Bio Inc.), 2 µl 20 mM $MgCl_2$, 1 µl 1% (w/v) BSA, 1 µl 1.5% (w/v) PVP, 0.5 µl dNTPs, 1 µl each of forward and reverse primers, 0.2 U of *Taq* DNA polymerase (TaKaRa Bio Inc.), and 9.5 µl DNase-free water. The PCR conditions were as follows: 1 cycle of 5 min at 94°C, then 30 cycles of denaturation at 94°C for 1 min; annealing at 60°C for 1.3 min; and extension at 72°C for 1.3 min, followed by a final extension at 72°C for 20 min. About 2 µl of PCR-amplified products were analyzed by 0.8% agarose gel electrophoresis in 1× Tris/borate/EDTA buffer.

Results and Discussion

Soil properties

The texture of AYLS samples was analyzed to define the percentage of clay, silt, and sand present in soil. Generally, the sand particles were settled at the bottom, the silt was layered above the sand, and the clay lay on top in the measuring jar. The general properties of the AYLS samples are listed in Table 1. In this experiment, all six samples were found to be loam, sandy loam, and sandy clay loam with pHs of 6.2–7.2. The soil type plays an important role in DNA extraction; for example, higher clay content is an especially problematic factor (Lakay *et al.*, 2007). Furthermore, the size of soil pores among sand, silt, and clay determine the interaction of soil particles with microorganisms. As mentioned earlier, the efficiency of DNA extraction depends on clay content and organic matter content. Moreover, microorganisms strongly bind with clay through a variety of binding forces (Bakken and Lindahl, 1995). The high clay content leads to an explanation of lowered DNA yields because of the adsorption of free DNA onto the clay particles. Young *et al.* (2014) reported that soil samples containing high levels of clay and organic compounds also influence DNA extraction. Furthermore, the AYLS04 DNA was found to be more dark brown in color than other samples, due to coextraction of high humic acid contaminants.

In addition, metal contaminants are often coextracted with DNA from soil because of their similar physicochemical properties. The analysis of the mineral contents in the AYLS samples facilitates the selection of the DNA extraction method (Table 2). The concentrations of trace elements were determined using ICP-MS after soil extraction with acid extraction (conc. HNO_3/conc. HCl). It is known that Fe and Si concentrations in soil samples have a major effect on soil DNA extraction. The Fe content in AYLS03 was found to be higher than that in other soil samples tested (Table 2). Fe may be present in the form of iron oxides and iron hydroxides in agricultural soils (Kozdroj and Van Elsas, 2000). DNA extraction increases with an increase in Fe concentration in the soil sample and *vice versa*. On the other hand, the presence of high Si in the soil may retard the release of DNA from clay particles, which subsequently affects the efficiency of DNA extraction from soil. The concentrations of soluble ele-

Table 2. Trace elements composition of AYLS samples analyzed by ICP-MS

Samples	Concentration of trace elements (mg/g of soil)[a]					
	Fe	K	Ca	Mg	Mn	Si
AYLS01	20660 ± 32	2657 ± 13	1312 ± 5	2252 ± 10	222 ± 5	38.4 ± 2.1
AYLS02	18770 ± 25	1980 ± 10	1600 ± 5	2040 ± 15	319 ± 6	41.1 ± 3.0
AYLS03	23100 ± 39	1693 ± 11	514 ± 6	1417 ± 7	270 ± 5	34.7 ± 1.4
AYLS04	22330 ± 23	2786 ± 12	2804 ± 7	2567 ± 14	185 ± 4	40.2 ± 2.0
AYLS05	15030 ± 18	1215 ± 10	795 ± 5	1147 ± 6	162 ± 7	41.0 ± 1.9
AYLS06	14060 ± 12	496 ± 5	274 ± 6	1604 ± 7	321 ± 8	34.7 ± 2.0

[a] Soil samples were prepared by acid treatment method.

Collection @ chosun

조선대학교
CHOSUN UNIVERSITY

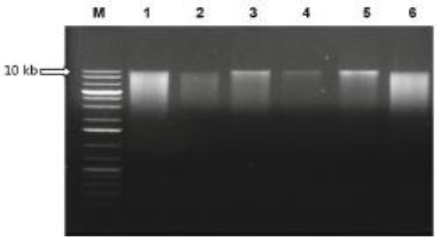

Fig. 3. **Agarose gel electrophoresis of soil microbial community DNA extracted as per the Powersoil® DNA extraction protocol.** Lanes: M, molecular marker; 1, AYLS01; 2, AYLS02; 3, AYLS03; 4, AYLS04; 5, AYLS05; and 6, AYLS06.

ments varied significantly, but can be ordered by abundance with the following: K>Mg>Ca>Mn>Si (Table 2). High metal concentrations in the soil can negatively affect microbial activities, provoking a low mineralization of organic materials during plant growth.

Soil DNA extraction

For functional- and sequence-based DNA analysis, it is essential to develop novel protocols that yield high quantity and quality DNA. However, DNA extraction from soil is extremely complicated due to coextraction of humic acid and other contaminants. The successful extraction depends on the type of soil, because the soil's composition requires optimization of the extraction protocol used. It is important to obtain DNA samples that are free of or contain an extremely low concentration of humic contaminants. In order to evaluate the best protocol for DNA extraction from agricultural soil samples, we used a commercial kit and four different methods with slight modifications. DNA yields from six AYLS samples varied considerably from sample to sample depending on the extraction method used.

The microbial community DNA extractions from six samples using the commercial PowerSoil® DNA extraction kit showed different sizes of fragments on agarose gel (Fig. 3), and yielded very low DNA concentrations (2.47–6.96 ± 1.56 μg/g soil) (Fig. 4). It is known that highly fragmented DNA may allow generation of chimeric amplicons during PCR amplification (Liesack *et al.*, 1991). The purity of extracted DNA was determined based on the spectrophotometry absorption ratios at A_{230}, A_{260}, and A_{280}, where the absorption peaks of coextracted humic acids and phenolic compounds with DNA are visible at 230 nm, whereas those of DNA and protein are observed at 260 and 280 nm, respectively (Yeates *et al.*, 1997). An A_{260}/A_{230} ratio greater than 2 and an A_{260}/A_{280} ratio greater than 1.7 indicate high-purity DNA, whereas the lower absorbance ratios indicate the contamination of DNA with humic acid and protein, respectively. The A_{260}/A_{230} and A_{260}/A_{280} ratios of DNA extracted from six AYLS samples by the PowerSoil® DNA extraction method were 1.28–1.58 and 1.13–1.64, respectively. Our results show that the commercial DNA extraction kit was not suitable for problematic soil samples that contain high levels of organic compounds, clay or heavy metals. Moreover, because commercial kits are typically optimized for a small volume of soil sample, their uses for obtaining high-quantity and -quality DNA are often limited. Therefore, we tested four alternative DNA extraction methods.

A modified Porteous DNA extraction protocol yielded a high DNA concentration of 15.89 ± 1.34 μg/g soil from AYLS01 and a low concentration of 9.31 ± 0.77 μg/g soil from AYLS05 (Fig. 4). This method adopts sonication to disturb the microbial cell wall and release DNA. Although a long period of sonication was required to obtain high DNA concentration, excessive sonication makes DNA highly fragmented (data not shown). The absorption ratios of DNA extracted by this method were assessed as 0.80 ± 0.01 for A_{260}/A_{230} and 1.04 ± 0.02 for A_{260}/A_{280}. These ratios indicate that the extracted DNA samples were highly contaminated with humic acid and proteins. As shown in Fig. 4, a modified Yeates DNA extraction method yielded a DNA concentration of 23.62 ± 4.65 μg/g soil from AYLS03, however, the amounts of DNA extracted from other soil samples were relatively low and the absorption ratios of A_{260}/A_{230} and A_{260}/A_{280} ratios were found

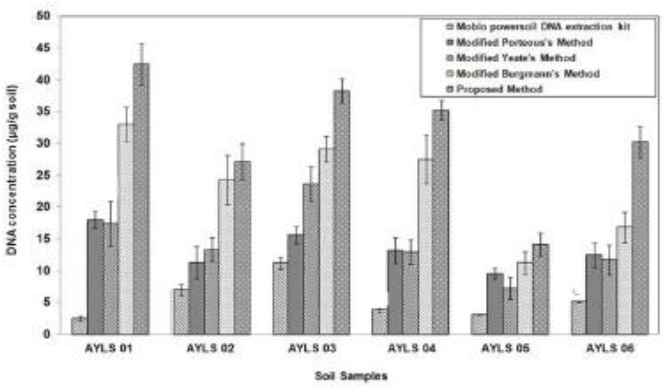

Fig. 4. **Microbial community DNA concentrations (μg/g soil [dry wt]) obtained from various extraction protocols.** The results are presented as mean ± SD of triplicate experiments.

Collection @ chosun

조선대학교
CHOSUN UNIVERSITY

Table 3. **Comparison of the quantity of crude DNA obtained by different extraction methods from diverse types of soil samples**

No	Soil type	Extraction buffer	Detergent (% SDS)	Precipitating agent	Maximum DNA concentration (μg/g soil)	Reference
1	Paddy soil	NaCl, EDTA, and lysozyme	10	Isopropanol	20.17	Islam *et al.* (2012)
2	Paddy soil	NaCl	1	Isopropanol	11.36	Islam *et al.* (2012)
3	Paddy soil	NaCl, CTAB and proteinase K	20	Isopropanol	18.65	Islam *et al.* (2012)
4	Pristine polluted soil	NaCl, EDTA and glass beads	20	PEG/NaCl	23.50	Yeates *et al.* (1997)
5	Bakery industry soil	EDTA and NaCl	4	PEG	3.8	Sagar *et al.* (2014)
6	Compost and organic rich soil	NaCl and EDTA	1	PEG	20.0	LaMontagne *et al.* (2002)
7	Arable soil	NaCl, EDTA, glass beads and skim milk	2	Potassium acetate	3.76	Ikeda *et al.* (2004)
8	AYLS	PowerSoil® DNA extraction kit	-	-	6.96	This study
9	AYLS	NaCl, EDTA, glusulase and glass beads	-	PEG/NaCl	33.71	This study
10	AYLS	NaCl, EDTA and glusulase	4	Isopropanol	16.86	This study
11	AYLS	Tris, NaCl, EDTA, glusulase and glass beads	20	PEG/NaCl	18.35	This study
12	AYLS	Tris, EDTA, NaCl, CTAB, proteinase K, lysozyme and glusulase	20	Isopropanol	42.48	This study (proposed method)

to be 0.92 ± 0.04 and 1.23 ± 0.06, respectively. The extracted DNA was also highly contaminated with proteins and humic acids. When we used a modified Bürgmann DNA extraction protocol, 33.8 ± 2.71 μg/g soil of DNA was extracted from AYLS01 (Fig. 4). It seems that a relatively higher DNA yield was due to glass bead-beating cell disruption, and the PEG precipitated DNA extraction. A combination of PEG and NaCl could provide an alternative to isopropanol precipitation, although the purity was low, as assessed by the absorbance ratios of 0.86 ± 0.02 at A_{260}/A_{230} and 1.27 ± 0.03 at A_{260}/A_{280}. The extracted DNA was still contaminated with high contents of humic acid and proteins. Based on these results, it is concluded that the above-mentioned DNA extraction protocols are not suitable for obtaining high quantity and quality of DNA.

Therefore, we suggested an alternative soil DNA extraction protocol, which yielded the highest DNA concentration among the methods used in this study. The maximum DNA yield was 42.48 ± 5.59 μg/g soil from AYLS01, which had loam soil and a pH of 6.5. We exploited the combined action of chelating agents (EDTA and CTAB), which were added into the DNA extraction buffer. These long-tailed surfactants turn random coil DNA structures into the compact globular structure and subsequently increase the efficiency of DNA precipitations. Also, these chemical agents help to detach microbes from soil matrix. Additionally, the collective actions of hydrolytic enzymes such as lysozyme, proteinase K, and glusulase break microbial cells and release more DNA. Agarose gel electrophoresis of soil microbial community DNA extracted by our suggested protocol showed that the size of extracted crude DNA was found to be > 10 kb, and no fragmented DNA was noted (data not shown). The range of absorption ratios of A_{260}/A_{230} of six soil samples was from 0.52 to 0.96. Similarly, that of A_{260}/A_{280} of extracted crude DNA was 1.24–1.43. The quantity of DNA was high enough to study metagenomics, and was much higher than the maximum DNA concentrations obtained from other methods (Table 3). Soil type, DNA extraction buffer composition, SDS concentration, and precipitating agents influence successful DNA extraction.

DNA purification

Metagenomic studies requires highly purified and plentiful high-molecular-weight DNA, because humic acid and protein contaminants have severe negative effects on DNA polymerase, restriction enzymes, DNA ligase, and DNA-DNA hybridization. To remove the contaminants from crude DNA, several purification methods have been adopted. The conventional purification methods have many limitations, including low quality products, significant DNA loss, and comigration of phenolic compounds. Therefore, in this study, we applied five different purification methods that enhance purity and high-molecular-weight DNA and incur low DNA loss.

A commercial DNA purification kit consists of a silica-coated spin column and a DNA collection tube. The binding buffer in the column neutralizes the silica's surface negative charge due to its high ionic strength, so that it helps binding of DNA to the silica surface. The unbound humic acid contaminants were eluted during centrifugation. By increasing the elution buffer temperature, the purified DNA can be obtained. The resultant DNA showed the absorbance ratios of A_{260}/A_{230} and A_{260}/A_{280} as 1.62 and 1.75, respectively, and was therefore a good quality. However, the major drawback of this method is a notable loss (41.7%) of DNA caused by inappropriate binding of DNA with the silica surface in the column.

When the crude DNA was purified by PVP–agarose gel electrophoresis and subsequent gel extraction, the A_{260}/A_{230} and A_{260}/A_{280} ratios of purified DNA were 1.68 and 1.81, respectively. These ratios indicate that the purified DNA was also of good quality. The high purification is obtained by the strong hydrogen interaction of PVP with humic acid and phenolic compounds. This complex retards comigration during electrophoresis. However, because a remarkable loss of DNA (56.8%) was incurred by this method, PVP–agarose gel purification failed to yield the required quantity of purified DNA. This confirms the findings of Young *et al.* (1993), who mentioned that although PVP reduces electrophoretic mobility of DNA, it strongly binds to humic acid.

The Sephadex G-100 mini-column purification method

Collection @ chosun

조선대학교
CHOSUN UNIVERSITY

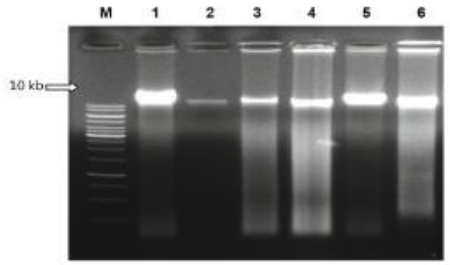

Fig. 5. **Agarose gel electrophoresis of DNA after formamide-LMP agarose gel plug purification.** Lanes: M, molecular marker; 1, AYLS01; 2, AYLS02; 3, AYLS03; 4, AYLS04; 5, AYLS05; and 6, AYLS06.

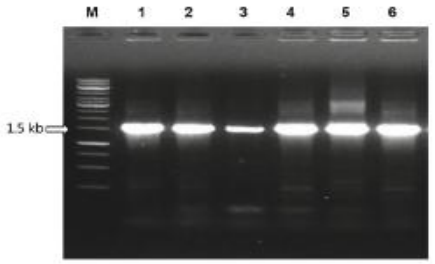

Fig. 7. **Agarose gel electrophoresis of PCR-amplified products of purified DNA after AT PVPP spin column purification.** Lanes: M, molecular marker; 1, AYLS01; 2, AYLS02; 3, AYLS03; 4, AYLS04; 5, AYLS05; and 6, AYLS06.

allowed effective removal of humic contaminants from crude DNA. The A_{260}/A_{230} and A_{260}/A_{280} ratios were found to be 1.66 and 1.78, respectively. The high-molecular-weight humic acid substances passed through the larger pore size of the Sephadex G-100 matrix. Although this method was better than DNA purification kit, a loss of about 19% of DNA was still observed. Sephadex G-50, Sephadex G-200, and Sephadex 4B were ineffective in purifying DNA from soil samples.

The formamide–LMP agarose gel plug purification method showed effective removal of humic acids. After the contaminated DNA was mixed with formamide, LMP-agarose, and NaCl, the humic acid and phenolic compounds tightly interacted with formamide, while the DNA strongly binds with the agarose gel. To prevent denaturation of DNA by formamide, NaCl was used as a stabilizer. The absorption ratios of A_{260}/A_{230} and A_{260}/A_{280} were 1.78 and 1.86, respectively, which indicates the high purity of the DNA. The purified DNA from each of the six soil samples was visualized by band analysis after electrophoresis (Fig. 5). All of the DNA fragment sizes were larger than 10 kb without shearing fragments, however this protocol also lost a meaningful amount (20%) of DNA.

Therefore, we suggested a novel AT-PVPP spin column purification protocol to minimize DNA loss with high purity.

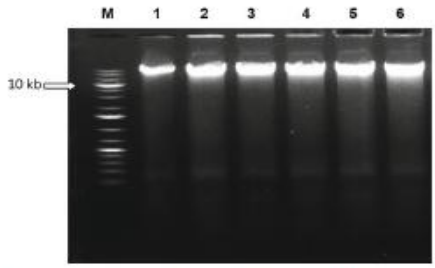

Fig. 6. **Agarose gel electrophoresis of DNA after AT-PVPP spin column purification.** Lanes: M, molecular marker; 1, AYLS01; 2, AYLS02; 3, AYLS03; 4, AYLS04; 5, AYLS05; and 6, AYLS06.

The absorbance ratios of A_{260}/A_{230} of six DNA samples ranged from 1.82 to 2.03 and those of A_{260}/A_{280} ranged from 1.89 to 2.05. It suggests that this method was found to yield the highest quality DNA and to be the most simple, most convenient, and least time-consuming protocol. DNA purity was further evaluated by agarose gel electrophoresis (Fig. 6). The band profile indicated that DNA sizes were larger than 10 kb in all six soil samples. Moreover, DNA loss in AT-PVPP spin column purification was significantly lower than the other methods (9%).

Furthermore, the quality of purified DNA by the AT-PVPP plug method was confirmed through 16S rRNA gene amplification by PCR. There were no appropriate sizes of 16S rRNA amplicon bands when the crude DNA was used as a template but clear primer dimer bands appeared in gel electrophoresis (data not shown). This is due to the fact that humic acid binds more strongly to *Taq* polymerase than to DNA strands. The purified DNA with AT-PVPP spin column showed high-quality clear bands with a PCR amplification product of ~1.5 kb in all soil samples (Fig. 7). Consequently, it was suggested that our proposed DNA extraction and purification methods were found to be the most reliable, simple, and cost-effective for obtaining microbial community DNA from all kinds of soil samples. In addition, it was found that each DNA color purified by each method showed "clear to white".

Conclusion

The main objective of a DNA extraction protocol is to obtain high DNA yields of high purity by a method that is convenient, less time-consuming, and cost-effective. Our assessment of DNA extraction methods depends mainly on the soil type, pH, and clay content of the soil samples. Our proposed DNA extraction method permits a wide range of DNA extraction from bacteria, fungi, and soil-associated organisms. The results demonstrated 3- to 7-fold increased DNA extraction from all six AYLS samples compared to previously described methods. Among the five purification methods assessed, the AT-PVPP spin column purification protocol was found to be the best choice to obtain high

Collection @ chosun

조선대학교
CHOSUN UNIVERSITY

concentrations of high-purity and high-molecular-weight DNA. The purity absorbance ratios of A_{260}/A_{230} and A_{260}/A_{280} were found to be 1.82 ± 0.03 and 1.94 ± 0.05, respectively. Both novel DNA extraction and purification methods were suitable for use in a large-scale study involving the comparative analysis of microbial diversity depending on soil types. However, further research is required to evaluate the efficiency of the purified DNA with restriction enzymes and DNA ligase for successful larger-sized DNA cloning.

Acknowledgements

This study was supported by Bio-industry Technology Development Program 2012, Ministry for Food, Agriculture, Forestry and Fisheries, Republic of Korea (Grant no. 112003-3) and was partially supported by the Research Fund of Chosun University (2014), Republic of Korea.

References

Amsaleg, C.L.R., Garnier-Sillam, E., and Harry, M. 2001. Extraction and purification of microbial DNA from soil and sediment samples. *Appl. Soil Ecol.* **18**, 47–60.

Arbeli, Z. and Fuentes, C.L. 2007. Improved purification and PCR amplification of DNA from environmental samples. *FEMS Microbiol. Lett.* **272**, 269–275.

Bakken, L.R. and Lindahl, V. 1995. Recovery of bacterial cells from soil. Nucleic Acids in the Environ, pp. 9–27. Springer-Verlag, Berlin, Germany.

Bürgmann, H., Pesaro, M., Widmer, F., and Zeyer, J. 2001. A strategy for optimizing quality and quantity of DNA extracted from soil. *J. Microbiol. Methods* **45**, 7–20.

Erb, R.W. and Wagner-Dobler, I. 1993. Detection of polychlorinated biphenyl genes in polluted sediments by direct DNA extraction and polymerase chain reaction. *Appl. Environ. Microbiol.* **59**, 4065–4073.

Forsberg, K.J., Reyes, A., Wang, B., Selleck, E.M., Sommer, M.O.A., and Dantas, G. 2012. The shared antibiotic resistome of soil bacteria and human pathogens. *Science* **337**, 1107–1111.

Harry, M., Gambier, B., Bourezgui, Y., and Garnier-Sillam, E. 1999. Evaluation of purification procedures for DNA extracted from organic rich samples: interference with humic substances. *Analysis* **27**, 439–442.

Ikeda, S., Watanabe, K.N., Minamisawa, K., and Ytow, N. 2004. Evaluation of soil DNA from arable land in Japan using a modified direct-extraction method. *Microbes Environ.* **19**, 301–309.

Islam, M.R., Sultana, T., Joe, M.M., Cho, J.C., and Sa, T. 2012. Comparisons of direct extraction methods of microbial DNA from different paddy soils. *Saudi J. Biol. Sci.* **19**, 337–342.

Kathiravan, M.N., Karthick, R., and Muthukumar, K. 2011. *Ex situ* bioremediation of Cr (VI) contaminated soil by *Bacillus* sp.: Batch and continuous studies. *Chem. Eng. J.* **169**, 107–115.

Kauffmann, I.M., Schmitt, J., and Schmid, R.D. 2004. DNA isolation from soil samples for cloning in different hosts. *Appl. Microbiol. Biotechnol.* **64**, 665–670.

Kozdroj, J. and Van Elsas, J.D. 2000. Bacterial community DNA extracted from soils polluted with heavy metals. *Polish J. Environ. Studies* **9**, 403–407.

Krsek, M. and Wellington, E.M.H. 1999. Comparison of different methods for the isolation and purification of total community DNA from soil. *J. Microbiol. Methods* **39**, 1–16.

Lakay, F.M., Botha, A., and Prior, B.A. 2007. Comparative analysis of environmental DNA extraction and purification methods from different humic acid-rich soils. *Appl. Microbiol.* **102**, 265–273.

LaMontagne, M.G., Michel, F.C.Jr., Holden, P.A., and Reddy, C.A. 2002. Evaluation of extraction and purification methods for obtaining PCR-amplifiable DNA from compost for microbial community analysis. *J. Microbiol. Methods* **49**, 255–264.

Liesack, W., Weyland, H., and Stackebrandt, E. 1991. Potential risks of gene amplification by PCR as determined by 16S rDNA analysis of a mixed-culture of strict barophilic bacteria. *Microb. Ecol.* **21**, 191–198.

McGarvey, K.M., Queitsch, K., and Fields, S. 2012. Wide variation in antibiotic resistance proteins identified by functional metagenomic screening of a soil DNA library. *Appl. Environ. Microbiol.* **78**, 1708–1714.

Miller, D.N., Bryant, J.E., Madsen, E.L., and Ghiorse, W.C. 1999. Evaluation and optimization of DNA extraction and purification procedures for soil and sediment samples. *Appl. Environ. Microbiol.* **65**, 4715–4724.

More, M.I., Herrick, J.B., Silva, M.C., Ghiorse, W.C., and Madsen, E.L. 1994. Quantitative cell lysis of indigenous microorganisms and rapid extraction of microbial DNA from sediment. *Appl. Environ. Microbiol.* **60**, 1572–1580.

Orsini, M. and Romano-Spica, V. 2001. A microwave-based method for nucleic acid isolation from environmental samples. *Lett. Appl. Microbiol.* **33**, 17–20.

Porteous, L.A., Armstrong, J.L., Seidler, R.J., and Watrud, L.S. 1994. An effective method to extract DNA from environmental samples for polymerase chain reaction amplification and DNA finger print analysis. *Curr. Microbiol.* **29**, 301–307.

Romanowski, G., Lorenz, M.G., and Wackernagel, W. 1993. Use of polymerase chain reaction and electroporation of *Escherichia coli* to monitor the persistence of extracellular plasmid DNA introduced into natural soils. *Appl. Environ. Microbiol.* **59**, 3438–3446.

Sagar, K., Singh, S.P., Goutam, K.K., and Konwar, B.K. 2014. Assessment of five soil DNA extraction methods and a rapid laboratory-developed method for quality soil DNA extraction for 16S rDNA-based amplification and library construction. *J. Microbiol. Methods* **97**, 68–73.

Sambrook, J., Fritsch, E.F., and Maniatis, T. 1987. Molecular cloning-a laboratory manual. Cold Spring Harbor, USA, Cold Spring Harbor Laboratory Press, London.

Selvin, J., Kennedy, J., Lejon, D.P.H., Kiran, G.S., and Dobson, D.W. 2012. Isolation identification and biochemical characterization of a novel halo-tolerant lipase from the metagenome of the marine sponge *Haliclona simulans*. *Microb. Cell Fact.* **11**, 72.

Smith, G.B. and Tiedje, J.M. 1992. Isolation and characterization of a nitrite reductase gene and its use as a probe for denitrifying bacteria. *Appl. Environ. Microbiol.* **58**, 376–384.

Tsai, Y.L. and Olson, B.H. 1990. Effects of Hg^{2+}, CH_3-Hg^+, and temperature on the expression of mercury resistance genes in environmental bacteria. *Appl. Environ. Microbiol.* **56**, 3266–3272.

Wilkinson, D.E., Jeanicke, T., and Cowan, D.A. 2002. Efficient molecular cloning of environmental DNA from geothermal sediments. *Biotechnol. Lett.* **24**, 155–161.

Yeates, C., Gillings, M.R., Davison, A.D., Altavilla, N., and Veal, D.A. 1997. PCR amplification of crude microbial DNA extracted from soil. *Lett. Appl. Microbiol.* **25**, 303–307.

Yeh, Y.F., Chang, S.C., Kuo, H.W., Tong, C.G., Yu, S.M., and Ho, T.H. 2013. A metagenomic approach for the identification and cloning of an endoglucanase from rice straw compost. *Gene* **519**, 360–366.

Young, C.C., Burghoff, R.L., Keim, L.G., Minak-Bernero, V., Lute, J.R., and Hinton, S.M. 1993. Polyvinylpyrrolidone-agarose gel electrophoresis purification of polymerase chain reaction-amplifiable DNA from soils. *Appl. Environ. Microbiol.* **59**, 1972–1974.

Collection @ chosun

조선대학교
CHOSUN UNIVERSITY

Biotechnology and Bioprocess Engineering 20: 267-275 (2015)
DOI 10.1007/s12257-014-0689-x

RESEARCH PAPER

Evaluation of Steady State and Unsteady State Mass Transfer Rate of Cr(VI) in Immobilized *Bacillus* sp.

Mathur Nadarajan Kathiravan, Geun Ho Gim, Jaewon Ryu, Gui Hawn Han, and Si Wouk Kim

Received: 8 October 2014 / Revised: 4 December 2014 / Accepted: 13 December 2014
© The Korean Society for Biotechnology and Bioengineering and Springer 2015

Abstract A novel hexavalent chromium (CrVI)-removing *Bacillus* sp. was isolated from leather industry wastewater-contaminated soil. This potential isolate was subjected to Cr(VI) removal under free and immobilized states in a stirred batch reactor (SBR). Two biokinetic parameters, V_{max} and K_m, and the effective diffusivity (D_e) for various bead sizes were calculated from Lineweaver-Burk and Eadie-Hoftsee plots, respectively. With respect to bead size, D_e decreased significantly from a maximum of 3.024×10^{-6} cm^2/sec in the 0.20 cm bead to 2.948×10^{-6}, 1.775×10^{-7}, and 1.144×10^{-7} cm^2/sec in the 0.40-, 0.60- and 0.80 cm beads, respectively. Additionally, steady and unsteady state modeling of diffusional mass transfer into the immobilized beads was conducted to determine the mass transfer rate as a function of time and the beads' radial profile. Furthermore, the space-time yield (STY) was modeled according to the residence time of the reactor. The reactor's STY was reasonable and could be further boosted by increasing the fractional biocatalyst.

Keywords: effective diffusivity, unsteady state mass transfer, STY, SBR, Cr(VI) removal

1. Introduction

Hexavalent chromium is toxic to the environment, and aquatic and human life. It poses a hazard to flora and fauna in various morphs by acting as a carcinogen and mutagen. Compared to Cr(VI), however, Cr(III) is non-toxic, has low environmental mobility, and therefore has a negligible environmental impact. Industrial effluents from a wide range of industries such as leather tanning, electroplating and chemical processing are usually rich in Cr(VI). Many conventional methods are available to remove toxic chromium from wastewaters, including chemical reduction, precipitation, reverse osmosis, ion exchange, biosorption and adsorption [1-3]. However, these methods suffer serious disadvantages such as high cost, low efficiency, and generation of toxic sludge or other wastes that require disposal problems and necessitate operational complexity [4,5]. The biological conversion of Cr(VI) to Cr(III) remains the novel method for the treatment of chromium-containing waste due to its ecofriendly nature. Compared to Cr(VI) removal by free cells, biological removal of Cr(VI) with enzymes secreted by immobilized bacteria offers many advantages such as ease of operation under very mild conditions without any damage to living bacterial cells. The operational stability is assured by the immobilized whole cell, due to its high mechanical strength [6], high efficiency, long-term operation [7] and reusability. Several studies have examined hexavalent chromium removal by biocatalysis using various immobilized bacterial species such as *Desulfovibrio desulfuricans* [8,9], *Amphibacillus* KSUCr3 [10] and *Pseudomonas* sp. [11]. However, the alginate immobilization technique often leads to a decrease of biocatalytic activity, with the decrease in immobilized whole cell catalyst activity having been attributed to internal diffusion limitations and steric hindrance [12-14]. The substrate diffusional limitations reduced the catalytic efficiency of immobilized biocatalysts. Therefore, developing efficient bioreactors with immobilized catalysts will require knowledge of diffusional limitations in such biocatalysts.

Mathur Nadarajan Kathiravan, Geun Ho Gim, Jaewon Ryu, Gui Hawn Han, Si Wouk Kim*
Department of Environmental Engineering, Pioneer Research Center for Controlling of Harmful Algal Bloom, Chosun University, Gwangju 501-759, Korea
Tel: +82-62-230-6649, Fax: +82-62-225-6040
E-mail: swkim@chosun.ac.kr

Collection @ chosun

조선대학교
CHOSUN UNIVERSITY

Various investigators studied different catalysts to investigate the intrinsic mass transport limitations. Diffusion of substrates within the porous beads in batch reactors was studied and reported by Backer and Baron [15]. The effective diffusivity (D_e) of glucose in porous glass beads was reported by Arnaud and Lacroix [16]. Dursun and Tepe [17] investigated and reported the effective diffusion coefficient of phenol in Ca-alginate-immobilized *Ralstonia eutropha* in batch system. Recently, the influence of mass transfer resistance on formaldehyde degradation in kissiris-immobilized *R. eutropha* has been reported [18]. Ha and his group [19] studied the diffusion characteristics of chlorferon and diethylthiophosphate in Ca-alginate gel beads. The internal mass transfer limitations of phenol biodegradation using Ca-alginate-immobilized *P. putida* beads in a batch system have been reported, and a literature review presented of the effective diffusion coefficient and effectiveness factor along with Thiele's modulus [20]. The steady state internal mass transfer limitation involved in substrate diffusion to the reaction system is still the major drawback in the application of immobilization by entrapment method. An unsteady state model was developed to measure the effective substance diffusivity within an entrapment matrix used for whole cell immobilization [21,22]. Further studies investigated the effects of internal diffusion on the biodegradation rate of ferrous (II) cyanide complex (ferrocyanide) ions by Ca-alginate gel-immobilized *P. fluorescens* beads and reported that the diffusion characteristics for each combination of diffusing substrate and immobilized matrix are necessary to determine the diffusion coefficients for the analysis and design of reactors using immobilized cells [23,24]. Hence, to design, optimize and construct an efficient bioreactor for microorganism-immobilized catalyst systems, it is necessary to understand the internal mass transfer limitations.

The present study investigates the Cr(VI) removal efficiency and estimates the internal diffusion limitations in *Bacillus* sp.-immobilized beads. In addition, the characteristics of the alginate beads such as viable cell counts and mechanical strength were studied. The internal mass transfer rate within these biocatalysts was predicted using steady state, unsteady state and space-time yield (STY) models. These parameters were used to predict the reactor performance.

2. Materials and Methods

2.1. Characterization and identification of bacterial isolates

The microorganisms used in this study were isolated from the soil samples of tannery effluent-contaminated sites in Pallavaram, Chennai, India. These soil samples (10% w/v) were inoculated in nutrient broth containing 100 mg/L of Cr(VI) and then incubated at 37°C under controlled conditions. After 2 days of incubation, 10 mL of the culture was serially diluted and samples (0.1 mL) were withdrawn from 10^{-5} dilution. The samples were then inoculated on nutrient agar plates containing the desired concentration of Cr(VI). After 2 days incubation at 37°C, the colonies were screened for their ability to survive in the chromium-amended agar plates. The potential isolates were inoculated with fresh nutrient broth and purified by streak plate techniques. The isolated colonies were subjected to biochemical tests to identify the species.

2.2. Chromium removal by free cells

The isolated *Bacillus* sp. was used for chromium removal in minimal salt medium containing (g/L) glucose- 1.0; $Na_2HPO_4{\cdot}2H_2O$- 6.0; KH_2PO_4- 3.0; NaCl- 0.5; $CaCl_2$- 0.01; $MgSO_4$- 0.246 with various initial concentrations of chromium ranging from 10 to 500 mg/L. For the removal, the medium was inoculated with mid-logarithmic phase bacterial culture and was incubated at 37°C and pH 7.0 at 150 rpm.

2.3. Immobilization of *Bacillus* sp. in calcium alginate

The alginate entrapment of cells was performed according to the method previously described in the literature [25]. Alginate was dissolved in boiling water and autoclaved at 121°C for 15 min. The acclimatized *Bacillus* sp. was inoculated in NB broth and incubated at 37°C for 48 h. After incubation, the culture was harvested during the mid-logarithmic growth phase by centrifugation (6,000 rpm, 10 min) and resuspended in 15 mL of saline solution. Then the biomass was added into sterilized 3% sodium alginate under aseptic condition (cell loading: 1.35 g/100 mL of sodium alginate). This alginate-cell mixture was extruded drop by drop into sterile 3% $CaCl_2$ solution through various nozzle sizes to prepare gel beads of different diameters. The beads were hardened by resuspending into a fresh 0.01 M $CaCl_2$ solution for 24 h at 4°C with gentle agitation. Finally, these beads were washed with distilled water to remove excess calcium ions and free cells. The alginate beads without *Bacillus* sp. cells were prepared to act as control. Beads with diameters ranging from 0.2 to 0.8 cm were obtained and stored in moist condition until further use.

2.4. Viability cell counts

To determine the number of cells encapsulated within a specific bead, the bead was submerged in 1 mL of a saturated phosphate buffer solution, which was maintained at room temperature until the alginate completely dissolved.

Collection @ chosun

조선대학교
CHOSUN UNIVERSITY

The liquefied alginate-cell suspension was shaken for several minutes with a vortex mixer, and 0.1 mL samples were taken for each bead size. The viable cell counts were carried out within the agar plate cultivation.

2.5. Determination of bead density and bead size

The immobilized bead density was measured by water displacement method. The total mass of ~30 wet beads was measured and the beads were placed in a measured volume of water in a graduated cylinder. The increase in volume after bead addition was measured, and the density was calculated from the mass and volume. The alginate beads were blot dried with filter paper before measuring the mass. The bead diameters were measured directly using a glass ruler and the average for 40 beads was calculated. This result obtained was compared with the size calculated from the average volume determined using the water displacement method.

2.6. Chromium removal experiment using immobilized beads

The Cr(VI) removal experiments were carried out in batch mode at 37°C, pH 7.0 and glucose 1.0 g/L. Predetermined quantities of alginate-immobilized *Bacillus* sp. beads were added in the beaker and stirring was achieved by thermally controlled shaker (Scigenics-ORBITEK) at 150 rpm. The batch experiments were conducted by varying the initial Cr(VI) concentration from 10 to 500 mg/L of 100 mL working volume in 250 mL Erlenmeyer flask. The cell-free beads were used for control experiments. In all experiments, initial pH was adjusted to 7.0 by adding 0.1 N H_2SO_4 and 0.1 N NaOH. At 6 h intervals, 3 mL of the samples was withdrawn and centrifuged at 6,000 rpm for 5 min.

2.7. Analytical methods

The Cr(VI) removal was estimated as the decrease in Cr(VI) concentration in the supernatant with time using hexavalent chromium specific colorimetric reagent S-diphenylcarbazide (DPC) prepared in 0.25% (w/v) acetone (AR) reported by Pattanapipitpaisal [9]. Samples of 200 or 400 µL were made up to 1mL with distilled water. After the addition of 330 µL of 6 M H_2SO_4 and 400 µL of DPC, this solution was made up to 10 mL with distilled water. UV-Visible spectrophotometry was used to measure the Cr(VI) content at 540 nm.

2.8. Kinetics studies

Measurements of the enzymatic reaction rate are used to characterize enzymes with regard to their substrate affinities and maximal reactions rate. Several numerical models are available for simulating the fate and transport of contaminants in the subsurface. Kinetic data on Cr(VI) removal by microorganisms is important in assessing their potential application to remediation of contaminated wastewaters. In this investigation, the chromium reductase catalyzes the removal of Cr(VI) substrate. Michaelis-Menten kinetics is the best available mathematical model for predicting the kinetics of enzyme-catalyzed reactions, according to the following equation,

$$V = \frac{V_m[S]}{K_m + [S]} \tag{1}$$

Where V_m is the maximum reaction rate, K_m the rate constant and $[S]$ the substrate concentration.

2.9. Internal mass transfer studies

The immobilized cells cause extra diffusional limitations as compared to free cells. The significant effect of diffusional limitations (internal and external mass transfer) determines the relative bioconversion. The transfer of substrate from the bulk liquid phase to the immobilized biocatalyst surface is called internal mass transfer. Internal mass transfer studies within the immobilized bead were carried out under the following six assumptions: the *Bacillus* sp.-immobilized particles are spherical in shape, a single substrate limits the growth, the Cr(VI) removal is dependent on the initial bulk concentration of the substrate, the effective diffusivity of the substrate is constant throughout the catalytic surface, the effects of outward diffusion of metabolic products are negligible, and the substrate is transported into the catalyst through diffusion according to Fick's first law of diffusion.

2.10. Steady state modeling of internal diffusion in immobilized beads

Consider an immobilized bead consisting of *Bacillus* sp. Let 'R' be the radius of the bead. Consider an elemental shell of thickness Δr. The chromium reductase is secreted within the bead and let W be the molar flux of the substrate inside the bead. Applying mole balance at steady state, over the shell of thickness r, we have,

$$(moles)_{in} - (moles)_{out} + (rate\ of\ generation\ inside\ \Delta r) = 0 \tag{2}$$

$$W\cdot(4\pi r^2)_2 - W\cdot(4\pi r^2)_{r+\Delta r} - r_c\cdot 4\pi r_m^2 \Delta r = 0 \tag{3}$$

Where r_m is the mean radius.

$$W\frac{((r^2)_{r+\Delta r} - W(r^2)_r}{\Delta r} = -r_c\cdot r_m^2 \tag{4}$$

On limiting Δr to zero,

$$Lt_{\Delta r\to 0}\left[W\frac{(r^2)_{r+\Delta r} - (r^2)_r}{\Delta r}\right] = -r_c\cdot r_m^2 \tag{5}$$

Collection @ chosun

조선대학교
CHOSUN UNIVERSITY

Thus, $\frac{d(W \cdot r^2)}{dr} = -r_c \cdot r_m^2$ (6)

By Fick's law of diffusion, we have, $W = -D_e \cdot \frac{d[S]}{dr}$

Substituting Fick's first law of diffusion in Eqn. (6) gives,

$$\frac{d\left(-D_e \cdot \frac{d[S]}{dr} \cdot r^2\right)}{dr} = -r_c \cdot r^2 \quad (7)$$

On simplifying,

$$\frac{d^2[S]}{dr^2} + \frac{2}{r}\frac{d[S]}{dr} - \frac{r_c}{D_e} = 0 \quad (8)$$

Assuming that the enzymatic reaction follows Michaelis-Menten kinetics,

$$r_c = \frac{V_m[s]}{[s]+K_m} \quad (9)$$

Including the effect of effectiveness factor η (average dimensionless rate), the rate becomes,

$$r_c = \eta \frac{V_m[S]}{[S]+K_m} \quad (10)$$

Hence, $\frac{d^2[S]}{dr^2} + \frac{2}{r}\frac{d[S]}{dr} = \frac{\eta}{D_e}\frac{V_m[S]}{[S]+K_m}$ (11)

Converting the above equation into dimensionless form by introducing the following variables, $\hat{S} = \frac{[S]}{[S_s]}$, $\hat{r} = \frac{r}{R}$ and $\alpha = \frac{K_m}{[S_s]}$, where $[S_s]$ is the substrate concentration at the catalytic bead surface,

$$\frac{d^2\hat{S}}{d\hat{r}^2} + \frac{2}{\hat{r}}\frac{d\hat{S}}{d\hat{r}} = \Phi^2 \eta \frac{\alpha \cdot \hat{S}}{\hat{S}+\alpha} \quad (12)$$

Such that $\Phi = R\sqrt{\frac{V_m}{K_m \cdot D_e}}$ (13)

The boundary conditions for the above equation are,

i. At surface of the immobilized bead, $\hat{r} = 1$ and $\hat{S} = 1$

ii. At center of the immobilized bead, $\hat{r} = 0$ and $\frac{d\hat{S}}{dr} = 0$

Equation (13) shows that the substrate diffusion is also a function of Thiele's modulus. Hence, the effectiveness factor for a first order system is:

$$\eta = \frac{3}{\phi}\left(\frac{1}{\tanh\phi} - \frac{1}{\phi}\right) \quad (14)$$

For small values of φ, $\eta \to \varphi$ and intraparticle mass transport has no effect on the rate. The rate at the center is the same as that at the outer surface, so that all the volume is fully effective. The biodegradation step controls the rate. For large φ, $\eta << 1$, so that intraparticle diffusion has a large effect on the rate. Practically, these conditions mean that diffusion into the particle is relatively slow and hence biodegradation occurs before the substrate has diffused far into the particle and only the surface of the particle is effective. For $\varphi > 5$ a good approximation for above Eqn. (12) is (21 and 26):

$$\eta = \frac{1}{\varphi} \quad (15)$$

2.11. Unsteady state mass transfer modeling

In reactors, non-uniformity arises over time due to non-ideal stirring concentration, which increases interest in studying the rate of unsteady mass transfer in this system. Hence, the batch stirred reactor is modeled for unsteady state with a first-order reaction assumption that is valid for large substrate concentrations for any elemental shell Δx inside the spherical biocatalyst as,

$$\frac{\partial C}{\partial t} = D_e \cdot \frac{\partial^2 C}{\partial x^2} - k \cdot C \quad (16)$$

This can be solved by implementing Danckwert's [27] method of transformation by which the rate of mass transfer by diffusion within the spherical catalyst is given by,

$$D_e \cdot \frac{\partial C}{\partial N} = \chi \cdot (C_0 - C_s) \quad (17)$$

Where C_s is the actual concentration on the surface at that time, C_0 the equilibrium surface concentration attained after infinite time, and dC/dN the concentration gradient measured in the outward direction along the radius of the bead. Here χ is a constant for a given radius of the spherical bead.

For convenience in writing we put $h = \chi/D$ in what follows. Hence, this problem is transformed as,

C = 0 when t = 0, within the spherical catalyst
C = C_0 when t > 0, at all points on the surface of the bead

And

$D \cdot \frac{\partial C}{\partial N} = \chi \cdot (C_0 - C_s)$ when t > 0, at any distance within the bead.

The solution for such problem is,

$$C = k\int_0^t C_1 e^{-ky} dy + C_1 e^{-kt} \quad (18)$$

Collection @ chosun

조선대학교
CHOSUN UNIVERSITY

where C_i is the solution of the unsteady diffusion equation to the same environment without reaction. Thus, on solving by adopting the aforesaid strategy, the rate of diffusional mass transfer (F) within the spherical catalyst at any radii 'a' and time 't' is,

$$F = 8\pi \cdot a \cdot D_e \cdot C_0 \sum_{n=0}^{\infty} \frac{ka^2 + D_e n^2 \pi^2 \cdot \exp\left(-t\left[k + \frac{D_e n^2 \pi^2}{a^2}\right]\right)}{ka^2 + D_e n^2 \pi^2} \quad (19)$$

2.12. Space Time Yield (STY) of the Stirred Batch Reactor (SBR)

STY refers to the quantity of product obtained per quantity of catalyst per unit time in immobilized beads. The space time, t, is equal to the average residence time (τ).

For a stirred batch reactor (SBR) of elemental volume dV, the following relationship applies:

$$([S_0]-[S])\frac{dV}{dt} = \frac{\eta \cdot \sigma \cdot V_{max} \cdot [S] \cdot dV}{K_m + [S]} \quad (20)$$

Where σ is the immobilized biocatalyst volume as a fraction of the reactor volume. Defining the relative substrate concentration as $\gamma = \frac{[S]}{Km}$, the above expression is transformed as,

$$-\frac{d\gamma}{dt} = \frac{\eta\sigma \cdot V_{max} \cdot \gamma}{K_m(1+\gamma)} \quad (21)$$

Which, on rearrangement yields,

$$dt = -\frac{K_m(1+\gamma) \cdot d\gamma}{\eta \cdot \sigma \cdot V_{max} \cdot \gamma} \quad (22)$$

Integrating the reactor holding time (τ) for the required relative substrate concentration conversion, we have,

$$\tau = \int_0^t dt = \frac{K_m}{\eta \cdot \sigma \cdot V_{max}} \int_{\gamma}^{\gamma_0} \frac{(1+\gamma) \cdot d\gamma}{\gamma} \quad (23)$$

Thus,

$$\tau = \frac{K_m}{\eta \cdot \sigma \cdot V_{max}} \cdot \left[\ln\left(\frac{\gamma_0}{\gamma}\right) + (\gamma_0 - \gamma)\right] \quad (24)$$

Where $\gamma_0 = \frac{[S]_0}{Km}$ is the initial relative substrate concentration and by an analogous derivation we obtain the STY for the reactor as,

$$\tau_{STY} = \eta \cdot V_{max} \cdot \sigma \frac{(\gamma_0 - \gamma)}{\ln\left(\frac{\gamma_0}{\gamma}\right) + (\gamma_0 - \gamma)} \quad (25)$$

3. Results and Discussion

A potential chromium-reducing bacteria was isolated from chromium-contaminated leather industrial effluent. From the colony morphology, cell morphology and biochemical test results of the isolated species presented in Table 1, the isolated species was identified as *Bacillus* sp. We have previously determined the minimum inhibitory concentration (MIC) of Cr(VI) of *Bacillus* sp. to be 600 mg/L [28]. This isolate was used for calcium alginate immobilization and other mass transfer studies. The number of viable cells within the beads ranged from 2.0×10^9 to 2.8×10^9 cfu/mL.

3.1. Chromium removal by free cells

The effect of initial concentration on Cr(VI) removal by free cells *Bacillus* sp. was studied over an initial concentration range of 10 ~ 500 mg/L and the results are shown in Fig. 1. The percentage Cr(VI) removal increased with increasing

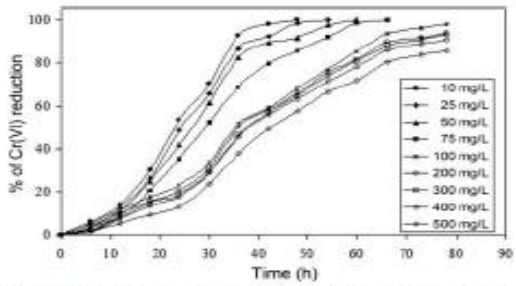

Fig. 1. Effect of initial concentration on Cr(VI) removal by *Bacillus* sp. (conditions: pH: 7.0, temperature: 37°C, and carbon source: glucose).

Table 1. Biochemical characteristics of the isolate

Analysis	Results
Gram staining	+
Endospore staining	+
Motility	+
Morphology	rod
Anaerobic growth	−
Catalase test	+
Indole test	−
Urease	+
Lactose	−
Amylase test	+
Nitrate reduction test	+
Voges-Proskquer	+
Growth in 10% NaOH	+
MR/VP test	+/−

+: positive; −: negative

Collection @ chosun

조선대학교
CHOSUN UNIVERSITY

incubation time and decreased with increasing concentration. After 66 h of incubation, 100% Cr(VI) removal was obtained for 10, 25, 50, and 75 mg/L initial concentrations, whereas after 78 h of incubation the chromium removal was 95.2, 94.1, 93.2 92.8, and 87.8% for initial concentrations of 100, 200, 300, 400, and 500 mg/L, respectively. Similar results were reported in using *Streptomyces griseus*, in which the chromium removal percentage decreased with increasing an increase in Cr(VI) concentration [29]. The *P. fluorescence LB 300* showed 99.7% removal for 112.5 mg/L of Cr(VI) but only 61% removal for 314 mg/L [30]. Thacker and Madamvar [31] reported that *Bacillus* sp. isolated from soil reduced Cr(VI) in the concentration range of 80 ~ 400 mg/L in 42 h. In the current study, the isolate tolerated Cr(VI) toxicity over the concentration range of 10 ~ 500 mg/L and exhibited a promising chromium removal potential.

3.2. Enzyme kinetics

The bio-kinetic parameters of the Michaelis-Menten kinetics were calculated by plotting the inverse substrate – removal rate in the Lineweaver-Burk model. The maximum reaction rate decreased with increasing biocatalyst particle diameter, whereas the trend was contrary with the Michaelis-Menten constants. For the smallest particle diameter of 0.20 cm, the Lineweaver-Burk plot is linear, indicating that the immobilized system is reaction limited ($\eta \approx 1$) (Fig. 2). As the particle size increases, the plot's nonlinearity correspondingly increases, indicating the enhanced effect of intra-particle diffusional mass transfer on the overall reaction rate.

3.3. Effect of Thiele's modulus over the rate of reaction

The influence of intra-particle diffusion in immobilized porous catalysts on the kinetic behaviors of immobilized cells has been theoretically considered as an effectiveness factor. Therefore, we can assess the overall performance of the SBR by classical effectiveness factor (η) and Thiele's modules (Φ) approach. The intrinsic kinetic parameters of immobilized cells cannot be directly measured by any analytical parameters, but the observable Thiele modulus is one of the significant parameters that can be used to determine the internal diffusion limitations. Thiele's modulus is a dimensionless factor that depicts the highest degree of catalysis that could be attained with the given catalyst. It depends on the effective diffusivity, radius of the bead and Michaelis-Menten constants of the biocatalyst. The values of Thiele's modulus were calculated from the intercept on the ordinate of the Eadie-Hoftsee plot ($K_m/V_{max}\Phi$) for each bead particle diameter, as shown in Fig. 3, and its variation according to the initial Cr(VI) concentration is presented in Fig. 4. The same trend was observed in the hydrolysis of rice bran oil using immobilized lipase [32]. The diffusional limitation increases with increasing biocatalyst particle diameter, as evident from the increase in nonlinearity of the plots for respective diameters.

The results reveal that Thiele's modulus increases with decreasing Cr(VI) concentration to a maximum value at

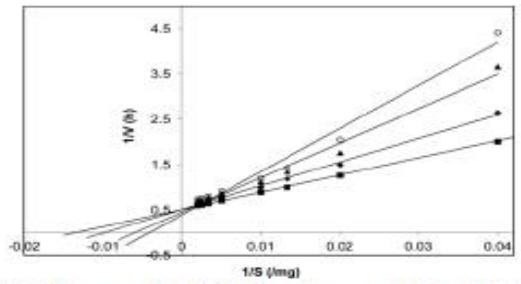

Fig. 2. Lineweaver Burk plot for chromium removal by immobilized *Bacillus* sp. for various bead sizes. (■; 0.2-, ◆; 0.4-, ▲; 0.6-, and ○; 0.8-cm beads).

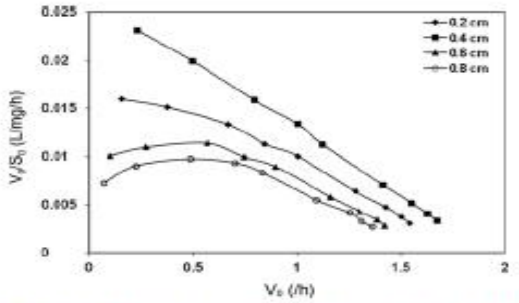

Fig. 3. Eadie-Hoftsee plot for various bead sizes (◆; 0.2-, ■; 0.4-, ▲; 0.6-, and ○; 0.8 cm beads).

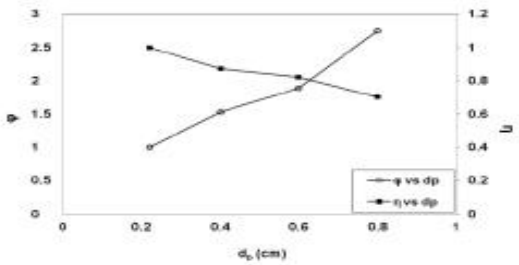

Fig. 4. Effect of biocatalyst bead size on Thiele's modulus (Φ) and effectiveness factor (η).

Collection @ chosun

조선대학교
CHOSUN UNIVERSITY

very low Cr(VI) concentrations. This suggests that the size of the catalytic beads significantly affects Thiele's modulus and Thiele's modulus increased with increasing bead diameter. The reaction is diffusion controlled for larger values of Thiele's modulus ($d_p = 0.8$ cm), but surface reaction controlled for lower values ($d_p = 0.2$ cm).

3.4. Significance of effectiveness factor

The effectiveness factor is the main parameter that indicates the maximum extent to which the reaction could be driven with the given catalyst. The effectiveness factor is calculated using Eqn. (14) and is an inverse function of Thiele's modulus. Hence, the values were expected to offer contradictory effects among the various parameters against Φ. The effect of the catalytic bead size on the effectiveness factor of the catalyst could be well inferred from Fig. 4. The plot suggests that the effectiveness factor increases with increasing initial Cr(VI) concentration, which again was attributed to the increasing concentration gradient facilitating mass transfer. Furthermore, the effectiveness factor decreases with increasing particle diameter, which was attributed to the fact that the diffusional resistance to mass transport and the tortuous effects of the catalysts are more pronounced in larger particles. These explanations support the study finding that the 0.20 cm bead exhibited the highest effectiveness factor.

3.5. Space-time Yield (STY)

The residence time (τ_R) and STY (τ_{STY}) expressions for various bead diameters inside the SBR are given by Eqns. (24) & (25) and are presented in Figs. 5 and 6. STY increases with decreasing biocatalyst particle diameter, which was attributed to the diffusional limitation trend existing with the biocatalyst particle diameter. STY was maximized at approximately 0.4 mg/L/min for the 0.20 cm bead with a substrate load of 500 mg/L. STY increased with increasing substrate concentration, which was attributed

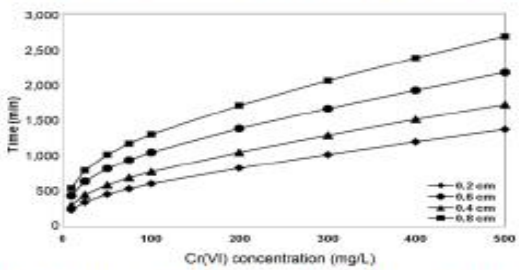

Fig. 5. Effect of initial Cr(VI) concentration on holding time for Cr(VI) removal in the stirred batch reactor (SBR). (◆; 0.2-, ●; 0.4-, ▲; 0.6-, and ■; 0.8 cm beads).

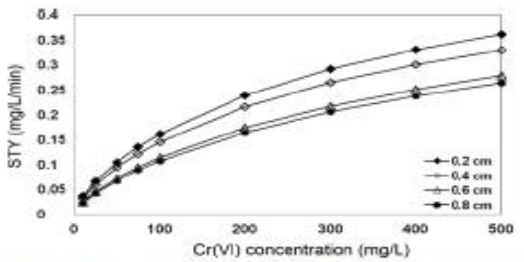

Fig. 6. Effect of biocatalyst particle diameter on the space-time yield (STY) of the stirred batch reactor (SBR). (◆; 0.2-, ◇; 0.4-, △; 0.6-, and ●; 0.8 cm beads).

to the increased driving force for mass transfer. The fractional biocatalyst volume (α) was maintained below 0.5 for all bead diameters. STY can be considerably increased by increasing the fractional biocatalyst volume in the reactor to within the range of 0.60 ~ 0.75, but this in turn will introduce undesirable side effects such as elevated abrasion in the catalysts and increased shear force during stirring.

3.6. Influence of effective diffusivity (D_e) over the reaction rate

The reaction dependence on mass transfer necessitates further elucidation of the diffusion of the reactant into the immobilized catalytic bead. The diffusivity of the catalytic bead reveals the extent to which the substrate could diffuse. More accurate information is given by the effective diffusivity, which assumes that not all of the area normal to the concentration flux is available for the molecules to diffuse, that the diffusion path is tortuous and that the pores are of varying cross sections. From Thiele's modulus, the effective diffusivity for various biocatalyst diameters was determined from Eqn. (13) and the results are presented in Table 2. The effective diffusivity is inversely correlated with bead diameter, which reveals the vibrant diffusional substrate transfer existing in the smaller particles. Again, as D_e is an inverse function of Φ and bead diameter. This effect can clearly be explained by the large effectiveness

Table 2. Mean effective diffusivity for various bead sizes during Cr(VI) reduction using immobilized *Bacillus* sp

No.	Catalytic bead diameter (cm)	Mean effective diffusivity (D_e) (cm^2/sec)
1	0.20	3.024×10^{-6}
2	0.40	2.947×10^{-6}
3	0.60	1.775×10^{-7}
4	0.80	1.144×10^{-7}

Collection @ chosun

조선대학교
CHOSUN UNIVERSITY

factor for small particles, which indicates the ease of diffusional transfer into them.

3.7. Dynamics in mass transfer rate within the biocatalyst

The rate of mass transfer for each bead size as a function of both bead radius and time was calculated using Eqn. (19) and simulated in MATLAB 7.0. For the bead diameters, the simulation results revealed that the mass transfer ceased beyond 77% radius for the 0.20 cm bead after 62 h, 69% radius for the 0.4 cm bead after 54 h, 54% radius for the 0.6-cm bead after 47 h and 43% radius for 0.8-cm bead after 12 h. Hence, the dynamics of the mass transfer rate within the entire biocatalyst diameters at an optimum location of 60% biocatalyst radii (0.6 r) until an optimum time period of 20 hours were monitored so that the mass transfer rate completely prevailed in the study range and the results are depicted in Figs. 7 and 8. The rate of mass transfer exponentially decayed over time to a minimum of almost zero after a mean time period of 17 h for all the catalysts. In addition, the mass transfer rate was high during the process start up. In comparison with the residence time data for all biocatalyst diameters in the steady state reactor, these mass transfer exhaust time data are promising. To conclude, the unsteady infinite series model for internal mass transfer satisfactorily predicts the actual biocatalyst conditions.

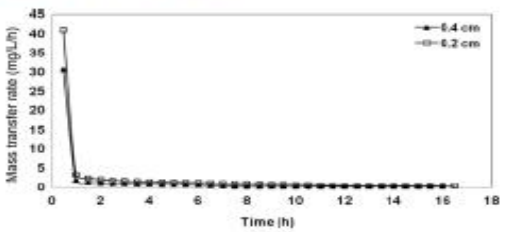

Fig. 7. Effect of time course on the Cr(VI) mass transfer rate within the bio-catalyst. (□; 0.2- and ▲; 0.4 cm beads).

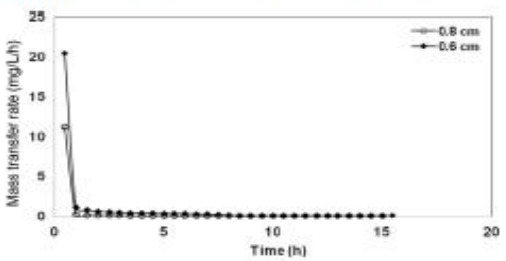

Fig. 8. Effect of time on the Cr(VI) mass transfer rate within the bio-catalyst. (◆; 0.6- and ○; 0.8 cm beads).

4. Conclusion

The use of immobilized *Bacillus* sp. for the biological removal of Cr(VI) in an SBR was shown to be technically feasible. Reaction engineering studies were conducted to assess the biocatalyst effectiveness, which was shown to be satisfactory. The STY of the SBR showed a moderate yield of around 0.4 mg/l min for a given fractional biocatalyst volume. Furthermore, to gain more insight into the dynamics of the mass transfer rate into a specific biocatalyst, the catalytic system was modeled with an unsteady state, infinite series, mass transfer model, which well modeled the time dependence of the mass transfer rate. This model has a promising potential for the scale-up and control of bioreactors.

Acknowledgement

This study was supported by a Research Fund of Chosun University (2013), Gwangju, Republic of Korea.

References

1. Park, D., Y. Yun, H. Y. Cho, and J. M. Park (2004) Chromium biosorption by thermally treated biomass of the brown seaweed, *Eckloniа* sp. *Ind. Eng. Chem. Res.* 43: 8226-8232.
2. Lee, S. H. (2014) Two metal biosorption of chromium and copper by Ca-loaded *Laminaria japonica* biomass. *Biotechnol. Bioproc. Eng.* 19: 696-702.
3. Sumathi, K. M. S., S. Mahimairaja, and R. Naidu (2005) Use of low-cost biological wastes and vermiculite for removal of chromium from tannery effluent. *Bioresour. Technol.* 96: 309-316.
4. Arica, M. Y. and G. Bayramoglu (2005) Cr(VI) biosorption from aqueous solutions using free and immobilized biomass of *Lentinus sajor-aju*: Preparation and kinetic characterization. *Colloids and Surfaces A: Physicochem. Eng. Asp.* 253: 203-211.
5. Sahin, Y. and A. Ozturk (2005) Biosorption of chromium (VI) ions from aqueous solution by the bacterium *Bacillus thuringiensis*. *Proc. Biochem.* 40: 1895-1901.
6. Kukubu, T., I. Karube, and S. Suzuki (1981) Protease production by immobilized mycelia of *Streptomyces fradiae*. *Biotechnol. Bioeng.* 23: 29-37.
7. Ramakrishna, S. V., R. Jamuna, and A. N. Emery (1992) Production of ethanol by immobilized yeast cells. *Appl. Biochem. Biotechnol.* 37: 275-282.
8. Tucker, M. D., L. L. Barton, and B. M. Thomson (1998) Reduction of Cr, Mo, Se and U by *Desulfovibrio desulfuricans* immobilized in polyacrylamide gels. *J. Ind. Microbiol. Biotech.* 20: 13-19.
9. Pattanapipitpaisal, P., N. L. Brown, and L. E. Macaskie (2001) Chromate reduction by *Microbacterium liquefaciens* immobilised in polyvinyl alcohol. *Biotechnol. Lett.* 23: 61-65.
10. Ibrahim, A. S. S., A. A. Al-Salamah, A. M. El-Toni, M. A. El-Tayeb, Y. B. Elbadawi, and G. Antranikian (2013) Detoxification of hexavalent chromate by *Amphibacillus* sp. KSUCr3 cells immobilised in silica-coated magnetic alginate beads. *Biotechnol. Bioproc. Eng.* 18: 1238-1249.

Collection @ chosun

조선대학교
CHOSUN UNIVERSITY

11. Konovalova, V. V., G. M. Dmytrenko, R. R. Nigmatullin, M. T. Bryk, and P. I. Gvozdyak, Chromium(VI) reduction in a membrane bioreactor with immobilized *Pseudomonas* cells. *Enz. Microb. Technol.* 33: 899-907.
12. Klibanov, A. M. (1983) Immobilized enzymes and cells as practical catalysts. *Science* 219: 722-727.
13. Gunther, K. and S. Helmut (1993) Immobilization of *Proteus vulgaris* for the reduction of 2-oxo acids with hydrogen gas or formate to D-2-hydroxy acids. *Appl. Microbiol. Biotechnol.* 38: 441-446.
14. Guobin, S., X. Jianmin, G. Chen, L. Huizhou, and C. Jiayong (2005) Biodesulfurization using *Pseudomonas delafieldii* in magnetic polyvinyl alcohol beads. *Lett. Appl. Microbiol.* 40: 30-36.
15. De Backer, L. and G. Baron (1993) Effective diffusivity and tortuosity in a porous glass immobilization matrix. *Appl. Microbiol. Biotechnol.* 39: 281-284.
16. Arnaud, J. P. and C. Lacroix (2004) Diffusion of lactose in *k*-carrageenan/locust bean gum gel beads with or without entrapped growing lactic acid bacteria. *Biotechnol. Bioeng.* 38: 1041-1049.
17. Dursun, A. Y. and O. Tepe (2005) Internal mass transfer effect on biodegradation of phenol by Ca-alginate immobilized *Ralstonia eutropha*. *J. Hazard. Mat.* 126: 105-111.
18. Habibi, A. and F. Vahabzadeh (2013) Degradation of formaldehyde in packed-bed bioreactor by kissiris-immobilized *Ralstonia eutropha*. *Biotechnol. Bioproc. Eng.* 18: 455-464.
19. Ha, J., C. R. Engler, and S. J. Lee (2007) Determination of diffusion coefficients and diffusion characteristics for chlorferon and diethylthiophosphate in Ca-Alginate gel beads. *Biotechnol. Bioeng.* 100: 698-706.
20. Aksu, Z. and G. Bulbul (1991) Determination of the effective diffusion coefficient of phenol in Ca-alginate-immobilized *P. putida* beads. *Enz. Microb. Technol.* 25: 344-348.
21. Pilkington, P. H., A. Margaritis, N. A. Mensour, and I. Russell (1998) Fundamentals of immobilised Yeast cells for continuous beer fermentation: A review. *J. Insti. Brew.* 104: 19-31.
22. Merchant, F. J., A. A. Margaritis, J. B. Wallace, and A. Vardanis (1987) A novel technique for measuring solute diffusivities in entrapment matrices used in immobilization. *Biotech. Bioeng.* 30: 936-945.
23. Dursun, A. Y. and Z. Aksu (2002) Effect of internal diffusivity of ferrous (II) cyanide complex ions in Ca-alginate immobilized *Pseudomonas fluorescens* gel beads on the biodegradation rate. *Proc. Biochem.* 37: 747-752.
24. Brito, E., J. D. Juan, F. Dominguez, and L. T. Casas (1990) Diffusion coefficients of carbohydrates in modified *k*-carrageenan gels with and without *Escherichia coli* immobilized. *J. Ferment. Bioeng.* 69: 135-137.
25. Johnsen, A. and J. M. Flink (1986) Influence of alginate properties and gel reinforcement on fermentation characteristics of immobilized yeast cells. *Enz. Microb. Technol.* 8: 737-748.
26. Chung, T. P., H. Y. Tseng, and R. S. Juang (2003) Mass Transfer effect and intermediate detection for phenol degradation in immobilized *Pseudomonas putida* systems. *Proc. Biochem.* 38: 1497-1507.
27. Danckwerts, P. V. (1950) Absorption by simultaneous diffusion and chemical reaction. *Trans. Faraday Soc.* 46: 300-304.
28. Kathiravan, M. N. R. Karthick, and K. Muthukumar (2011) *Ex situ* bioremediation of Cr(VI) contaminated soil by *Bacillus* sp.: Batch and continuous studies. *Chem. Eng. J.* 169: 107-115.
29. Lakshman, R. S. and S. More (2002) Reduction of hexavalent chromium by *Streptomyces griseus*. *Minerals Eng.* 15: 831-837.
30. Deleo, P. C. and H. L. Ehrlich (1994) Reduction of hexavalent chromium by *Pseudomonas fluorescens LB 300*, in batch and continuous culture. *Appl. Microbiol. Biotechnol.* 40: 756-759.
31. Thacker, U. and D. Madamvar (2005) Reduction of toxic chromium and partial localization of chromium reductase activity in bacterial isolate DM1. *World J. Microb. Biotechnol.* 21: 891-899.
32. Murty, V. R. C., J. Bhat, and P. K. A. Muniswamn (2005) External mass transfer effects during the hydrolysis of rice bran oil in immobilized lipase packed bed reactor. *Chem. Biochem. Eng. Q.* 19: 57-61.

Collection @ chosun

조선대학교
CHOSUN UNIVERSITY

J Ind Microbiol Biotechnol (2016) 43:605–616
DOI 10.1007/s10295-016-1741-y

BIOENERGY/BIOFUELS/BIOCHEMICALS

Effects of carbon source and light intensity on the growth and total lipid production of three microalgae under different culture conditions

Geun Ho Gim[1] · Jaewon Ryu[2] · Moon Jong Kim[2] · Pyung Il Kim[3] · Si Wouk Kim[1]

Received: 5 August 2015 / Accepted: 28 December 2015 / Published online: 8 February 2016
© Society for Industrial Microbiology and Biotechnology 2016

Abstract We attempted to enhance the growth and total lipid production of three microalgal species, *Isochrysis galbana* LB987, *Nannochloropsis oculata* CCAP849/1, and *Dunaliella salina*, which are capable of accumulating high content of lipid in cells. Low nitrogen concentration under photoautotrophic conditions stimulated total lipid production, but a decreasing total lipid content and an increasing biomass were observed with increasing nitrogen concentration. Among the different carbon sources tested for heterotrophic cultivation, glucose improved the growth of all three strains. The optimal glucose concentration for growth of *I. galbana* LB987 and *N. oculata* CCAP849/1 was 0.02 M, and that of *D. salina* was 0.05 M. Enhanced growth occurred when they were cultivated under heterotrophic or mixotrophic conditions compared with photoautotrophic conditions. Meanwhile, high total lipid accumulation in cells occurred when they were cultivated under photoautotrophic or mixotrophic conditions. During mixotrophic cultivation, biomass production was not affected significantly by light intensity; however, both chlorophyll concentration and total lipid content increased dramatically with increasing light intensity up to 150 μmol/m^2/s. The amount and composition ratio of saturated and unsaturated fatty acids in cells were different from each other depending on both species and light intensity. The highest accumulation of total fatty acid (C16–C18) among the three strains was found from cells of *N. oculata* CCAP849/1, which indicates that this species can be used as a source for production of biodiesel.

Keywords Microalgae · Biomass · Lipid content · Light intensity · Chlorophyll · Fatty acid

✉ Si Wouk Kim
swkim@chosun.ac.kr

[1] Department of Environmental Engineering, Chosun University, Gwangju 61452, Republic of Korea

[2] Department of Energy Convergence, Chosun University, Gwangju 61452, Republic of Korea

[3] Bio Control Research Institute, Goksung-gun, Jeollanam-do 516-944, Republic of Korea

Introduction

In recent years, many researchers have increased efforts to find a better alternative renewable fuel because of depletion of fossil fuels. Microalgae promise to be a suitable energy resource through the photoautotrophic mechanism that can convert atmospheric carbon dioxide into biomass, fatty acid, and lipids. The total lipid content of microalgae varies from 1 to 70 % of the dry cell weight [19, 33, 43]. The lipids present in microalgae are mainly in the form of esters of glycerol and fatty acids, which are suitable for producing biodiesel. Microalgae such as *Scenedesmus pectinatus* var XJ-1 [42], *Chlorella* sp. [6], and *Chlorella vulgaris* [20] generally are cultured photoautotrophically. Unfortunately, the photoautotrophic cultivation of microalgae has many limitations, such as low biomass and lipid productivity, and this is mainly because of photolimitation (high cell density inhibits light penetration). Heterotrophic growth of microalgae can be performed in a culture medium supplemented with external organic/inorganic carbon sources. For heterotrophic microalgal cultivation, several carbon sources, such as glucose [5, 11, 29], fructose [11, 29], sucrose [11, 29], glycerol [5], and acetate [39], have been used. Heterotrophic cultivation offers many advantages, including good control of cultivation, higher biomass and lipid, and elimination of the requirement for light. However, mixotrophic

Collection @ chosun

조선대학교
CHOSUN UNIVERSITY

growth that combines phototrophic and heterotrophic cultivation (i.e., with light and organic sources) is particularly useful for overcoming the problems imposed by phototrophic or heterotrophic growth [11]. One of the most notable advantages is that the CO_2 released from microalgae during carbon metabolism is trapped and reused. Recently, many studies have focused on the enhanced biomass and lipid productivity achieved by mixotrophic cultures of microalgae such as *C. vulgaris* [17], *Scenedesmus* sp. ZTY3, and *Chlorella* sp. ZTY4 [37]. Furthermore, it is known that many environmental factors influence the growth, lipid content and fatty acid composition of microalgae. Microalgal cultivation requires rigorous control of various factors, such as carbon sources, salinity, nitrogen, iron, pH, temperature, CO_2 concentration, and light intensity. It is most noteworthy that carbon source, light-intensity and -wavelength have been reported to change the lipid metabolism in microalgae by enhancing the biomass production and lipid content, as shown for *Nannochloropsis* sp. [8], *Haematococcus pluvialis* [16], *Scenedesmus* sp. [23], and *C. vulgaris* ESP-31 [46]. In addition, a number of nutritional factors, including phosphate [12], sulfur [34], iron [22], and nitrogen [12, 45], have been reported to influence the growth and lipid content of algae. Nitrogen starvation especially affects the lipid accumulation in microalgal cells [25]. However, to date, the studies on various modified and enhanced microalgal cultivation, lipid production, lipid extraction, and transesterification techniques are still in progress.

In this study, three microalgal species *Isochrysis galbana* LB987, *Nannochloropsis oculata* CCAP849/1, and *Dunaliella salina*, which have relatively higher biomass and lipid productivity, were cultivated under photoautotrophic, heterotrophic, and mixotrophic conditions to obtain higher biomass and total lipid content. Effects of various carbon sources and light intensity on growth, chlorophyll concentration, total lipid content, and fatty acid composition under the different culture conditions were investigated.

Materials and methods

Microalgae and media

Three marine microalgae, which accommodate high content of lipid in cells, were used in this study. *I. galbana* LB987 (obtained from UTEX Culture Collection of Algae at The University of Texas at Austin, Austin, TX, USA) and *N. oculata* CCAP849/1 (obtained from Culture Collection of Algae and Protozoa, UK) were cultured in f/2 medium [14], with the following composition (per liter of sea water): 75 mg $NaNO_3$, 5.65 mg $NaH_2PO_4{\cdot}2H_2O$, 4.16 mg Na_2-EDTA, 3.15 mg $FeCl_3{\cdot}6H_2O$, 0.01 mg $CuSO_4{\cdot}5H_2O$, 0.02 mg $ZnSO_4{\cdot}7H_2O$, 0.01 mg $CoCl_2{\cdot}6H_2O$, 0.18 mg $MnCl_2{\cdot}4H_2O$, 0.006 mg $Na_2MoO_4{\cdot}2H_2O$, 0.0005 mg cyanocobalamin (vitamin B_{12}), 0.1 mg thiamine-HCl (vitamin B_1), and 0.0005 mg biotin. *D. salina* (a gift from Hanyang University, Seoul, Korea) was cultured in modified D medium [4], with the following composition (per liter of distilled water): 58.44 g NaCl, 4.844 g Tris, 0.5055 g KNO_3, 0.92 g $MgCl_2{\cdot}6H_2O$, 0.12 g $MgSO_4{\cdot}7H_2O$, 0.044 g $CaCl_2$, 0.023 g K_2HPO_4, 0.55 mg $FeCl_3$, 2.45 mg EDTA, 0.31 mg H_3BO_3, 0.20 mg $MnCl_2{\cdot}4H_2O$, 0.023 mg $ZnSO_4{\cdot}5H_2O$, 0.01 mg $CuSO_4{\cdot}5H_2O$, 0.048 mg $NaMoO_4{\cdot}2H_2O$, 0.005 mg $CoCl_2{\cdot}6H_2O$, 0.027 mg $NaVO_3$, and 2.1 g $NaHCO_3$.

Microalgal culture conditions

Photoautotrophic batch cultivation of the three marine microalgae was performed in 1-L Erlenmeyer flask containing a working volume of 0.3 L medium at pH 8.0 with cotton plugs that allow exchange with the atmosphere. Cells were cultivated at 25 °C. Cultures were illuminated with cool-white fluorescent lamps, which were fixed on the wall, and light intensity was attenuated by adjusting distance from lamps and was measured with an illuminance meter (LT Lutron LM-81LX; Lutron Electronic Enterprise, Co., Taipei, Taiwan). From our previous results of optimal growth conditions, light intensity was maintained at 80 μmol/m^2/s for *I. galbana* LB987 and *N. oculata* CCAP849/1 and at 100 μmol/m^2/s for *D. salina*, and the photoperiods were 12/12-h light/dark in all three microalgae. Their photoautotrophic cultivation period was 10 days. To determine the optimal nitrogen concentration for maximal biomass and lipid productivity, each of *I. galbana* LB987 and *N. oculata* CCAP849/1 was cultivated in a modified f/2 medium containing different $NaNO_3$ concentrations ranging from 0.75 to 1.0 mM; *D. salina* was cultivated in a modified D medium containing various KNO_3 concentrations ranging from 1 to 10 mM. For heterotrophic cultivation, the above two different culture media were supplemented with six different carbon sources: glucose, xylose, rhamnose, fructose, sucrose, and galactose (0.01 M). The influence of initial glucose concentration on microalgal growth was performed within a range of 0.01–0.05 M. Mixotrophic cultivation was evaluated with an initial glucose concentration of 0.02 M for *I. galbana* LB987 and *N. oculata* CCAP849/1 and 0.05 M for *D. salina*. The effect of light intensity on algal cell growth and total lipid content under mixotrophic cultivation was tested with different light intensities ranging from 0 to 200 μmol/m^2/s.

Determination of biomass production

Dry biomass was determined with 100 mL of microalgal culture, which was collected and filtered through a 0.8 μm

Collection @ chosun

조선대학교
CHOSUN UNIVERSITY

glass membrane (Pall Corporation, Port Washington, NY, USA). The filtrate was dried at 105 °C for 8 h in an electric oven (Advantec FUW243PA; Advantec, Ehime, Japan) and then weighed by using an electronic balance (Ohaus Explorer EX623; Ohaus Corporation, Newark, NJ). All of the experiments were conducted in triplicate.

Measurement of reducing sugar concentration

Reducing sugar was quantitatively analyzed by DNS (3,5-dinitrosalicylic acid) assay method suggested by Miller [27]. DNS reagent was prepared as follows: 0.25 g of DNS and 75 g of sodium potassium tartrate were dissolved in 250 mL of 0.4 M sodium hydroxide solution. Glucose with different concentrations, from 1.0 to 10.0 mg/mL, was used to create the calibration curve. To analyze the residual glucose concentration in the microalgal medium according to the cell growth, 500 µL of each medium sample was mixed with 5.0 mL of DNS reagent and heated at 100 °C for 10 min to develop the red-brown color. 8 mL of distilled water was added into the samples when temperature dropped to the room temperature. Then the samples were detected by UV–visible spectrophotometer (DU800; Beckman Coulter, Brea, CA, USA) at 540 nm. All of the tests were conducted in triplicate.

Determination of chlorophyll content

Chlorophylls in fresh microalgal cells were extracted with acetone. The concentration of chlorophylls in the extracted solution was determined by measuring the absorbance at 645 and 663 nm with a UV–visible spectrophotometer (DU800; Beckman Coulter, Brea, CA, USA) and then calculating with the following equation [2]: Chlorophylls (mg/L) $= 8.02 \times A_{663} + 20.21 \times A_{645}$.

The chlorophyll contents in the microalgal cells (milligram per gram) were calculated by dividing the concentration of the chlorophylls (milligram per liter) by the dry weight (gram per liter) of microalgae.

Estimation of total lipid content

Microalgal cells were harvested by centrifugation at 5000×*g* for 30 min. The cell pellets were frozen overnight at −30 °C and freeze-dried at −50 °C under vacuum (FD 8508 Bench-Top freeze-dryer; Ilshin BioBase, Co. Ltd., Gyeonggi-do, South Korea). One gram of dried cell biomass was blended with 200 mL of distilled water, and the cell mixture was disrupted by a sonicator (Sonifier 250; Branson Ultrasonics, Danbury, CT, USA) at a resonance of 10 kHz for 5 min. Lipid extraction was performed according to the modified method described by Folch et al. [10]. Total lipid was extracted with a mixture of chloroform–methanol (2:1, v/v) for 1 h. The chloroform layer was removed by evaporation with rotary vacuum (Rotavapor R-205; Buchi Labortechnik, Flawill, Switzerland) and weighed.

Analysis of fatty acid composition

The extracted lipid was used to analyze fatty acid composition by a modified saponification and methylation procedure described by Metcalfe et al. [26]. The composition of each microalgal strain was determined by gas chromatography (GC-2010 Plus; Shimadzu Corporation, Kyoto, Japan), with an art-2560 capillary column (length 100 m, 0.25 mm inner diameter, 0.25 µm film thickness) and a flame ionization detector. Operation conditions were as follows: inlet temperature 260 °C, initial oven temperature 140 °C held for 5 min and then ramped by 4 °C per min and held for 15 min, and the detector temperature 260 °C. Fatty acids were identified by a comparison of their retention times with known standards.

Results

Effect of nitrogen concentration on photoautotrophic growth and total lipid content

To examine the effect of nitrogen on the biomass and total lipid production of the three microalgae under photoautotrophic cultivation (light intensity was maintained at 80 µmol/m^2/s for *I. galbana* LB987 and *N. oculata* CCAP849/1, and at 100 µmol/m^2/s for *D. salina*), different concentrations of nitrogen were supplemented to the modified culture media. As shown in Fig. 1, a low nitrogen concentration did not support cell growth but stimulated total lipid accumulation in cells. As nitrogen concentration increased, biomass production increased. High amounts of biomass from *I. galbana* LB987 (0.58 g biomass per liter) and *N. oculata* CCAP849/1 (0.56 g/L) were obtained at a concentration of 0.95 mM $NaNO_3$, whereas a biomass of 0.62 g/L was obtained from *D. salina* at 7.5 mM KNO_3. In contrast to biomass production, total lipid content decreased significantly in all three strains by increasing nitrogen concentration. In particular, total lipid content decreased >35 % in *D. salina* as nitrogen concentration increased from 1.0 to 10.0 mM.

Effect of carbon source on heterotrophic growth

Figure 2 shows the growth of the three microalgae under heterotrophic culture conditions with various carbon sources (0.01 M), such as glucose, galactose, fructose, xylose, rhamnose, and sucrose. The three microalgal

Collection @ chosun

조선대학교
CHOSUN UNIVERSITY

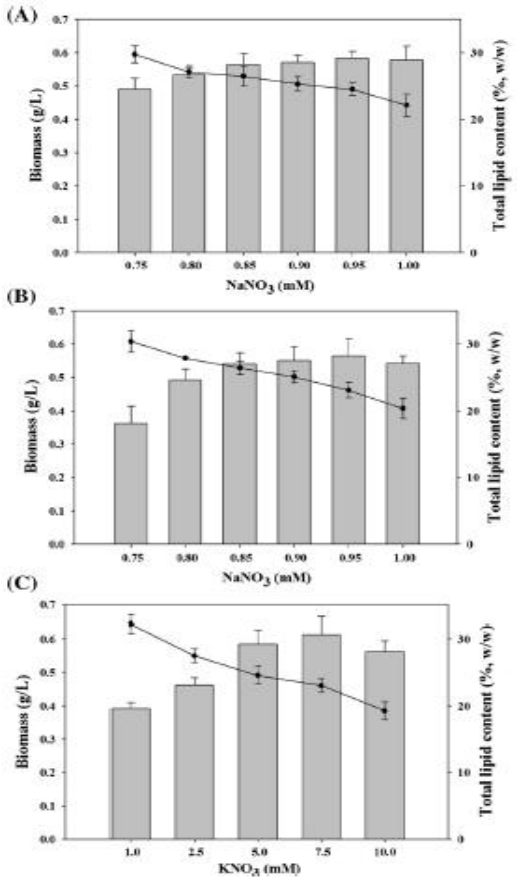

Fig. 1 Effect of nitrogen concentration on biomass and total lipid content under photoautotrophic condition. **a** *Isochrysis galbana* LB987; **b** *Nannochloropsis oculata* CCAP849/1; **c** *Dunaliella salina*. *Filled rectangle* biomass, *filled circle* total lipid content

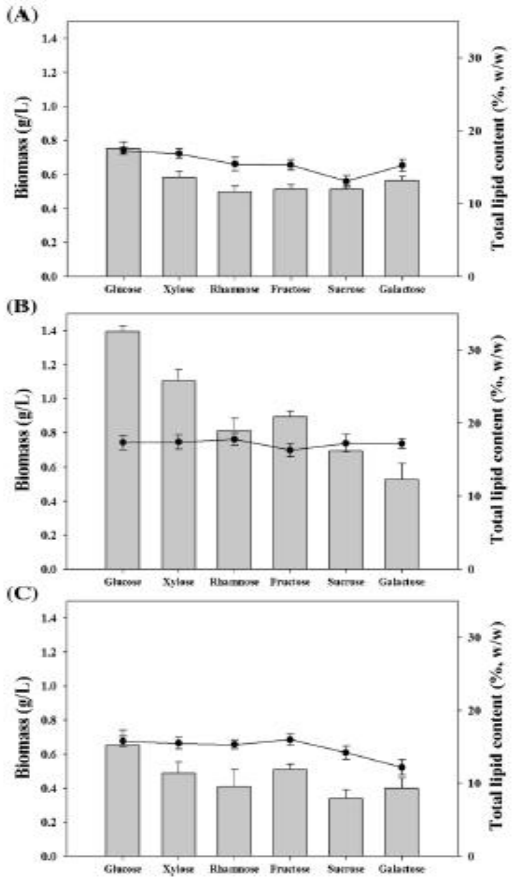

Fig. 2 Effect of six different carbon sources (0.01 M) on heterotrophic microalgal growth. **a** *I. galbana* LB987; **b** *N. oculata* CCAP849/1; and **c** *D. salina*

species can use all of the carbon sources tested. However, among the carbon sources tested, glucose was the best, with maximal biomass of 0.75 g/L for *I. galbana* LB987, 1.40 g/L for *N. oculata* CCAP849/1, and 0.65 g/L for *D. salina*, respectively, during 10 days cultivation. Compared with photoautotrophic cultivation, heterotrophically cultured biomass increased remarkably; especially, that of *N. oculata* CCAP849/1 increased approximately threefold. On the other hand, poor biomass production was observed from *I. galbana* LB987 and *D. salina* when supplemented with sucrose and from *N. oculata* CCAP849/1 with galactose as the sole carbon source. It is obvious from the data shown in Fig. 2 that the total lipid contents in cells cultured in heterotrophic conditions were relatively low.

To learn about the effect of initial glucose concentration on cell growth, all three microalgae were cultured in different modified media supplemented with various glucose concentrations (0.01–0.05 M) for 10 days. The results are illustrated in Fig. 3. When 0.02 M glucose

Collection @ chosun

조선대학교
CHOSUN UNIVERSITY

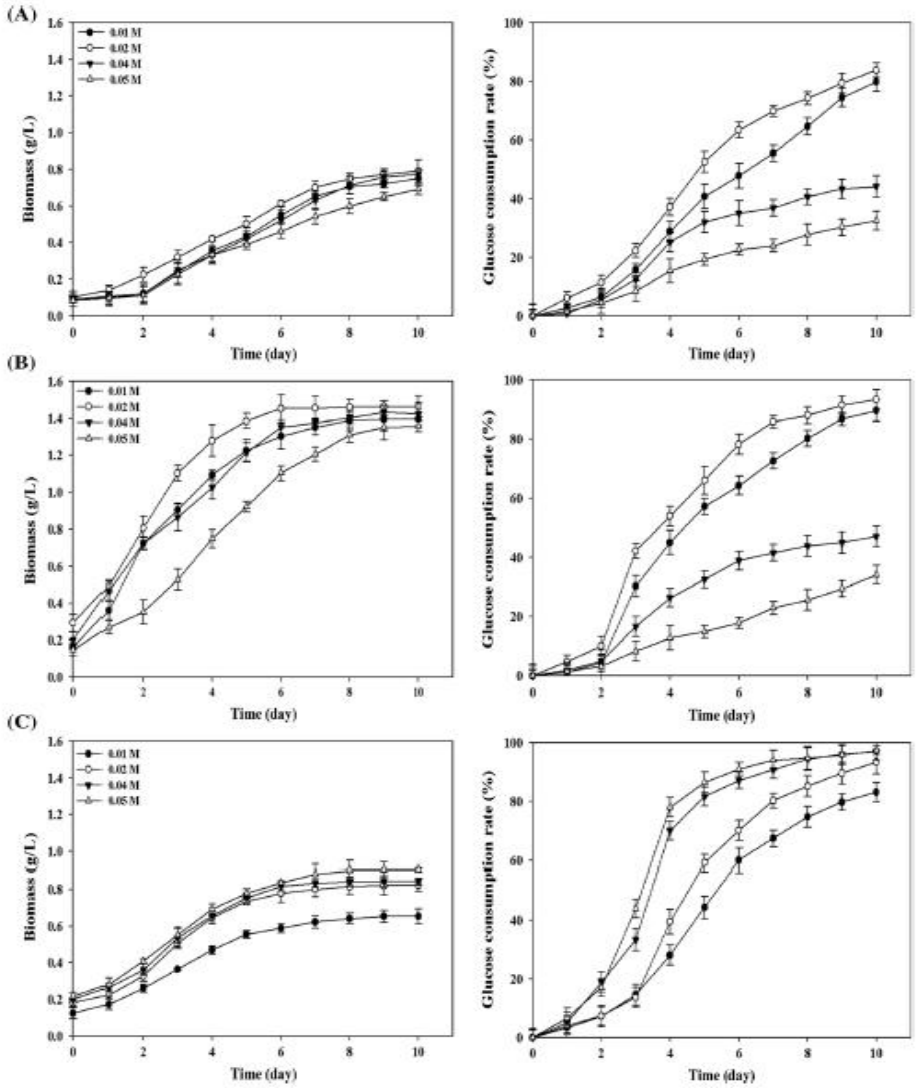

Fig. 3 Influence of glucose concentration (0.01–0.05 M) on microalgal growth under heterotrophic cultivation and glucose consumption rate according to cell growth. **a** *I. galbana* LB987; **b** *N. oculata* CCAP849/1; and **c** *D. salina*

Collection @ chosun

조선대학교
CHOSUN UNIVERSITY

was supplemented, the highest amount of biomass was observed in *I. galbana* LB987 (0.79 g/L) and *N. oculata* CCAP849/1 (1.46 g/L). On the other hand, 0.90 g/L biomass was observed in *D. salina* with 0.05 M glucose. In addition, glucose consumption rates of three microalgae in different initial concentration were also determined as cells grew (Fig. 3). After 10 days incubation with 0.02 M glucose, the consumption rates of *I. galbana* LB987 and *N. oculata* CCAP849/1 were found to be 83.8 and 93.3 %, respectively. In contrast, no more than 50 % of glucose was utilized in higher concentrations (>0.04 M). Similarly, *D. salina* showed the highest consumption rate (97.3 %) when grown on initial 0.05 M glucose concentration, but substrate inhibition was also happened at higher concentrations (data not shown). Moreover, the pH changes in the medium during cells growth were also monitored. Medium pH deceased from initial 8.0 to final 6.8–7.2 for 10 days incubation in all three microalgae, but it did not inhibit cell growth significantly.

Biomass, total lipid, and chlorophyll content under different culture conditions

The effect of culture mode on biomass, chlorophyll, and total lipid content was investigated. For heterotrophic and mixotrophic cultivation, 0.02 M glucose for *I. galbana* LB987 and *N. oculata* CCAP849/1 and 0.05 M glucose for *D. salina* were supplemented to the media, and light intensity for mixotrophic conditions was the same as that for photoautotrophic conditions. As shown in Fig. 4, biomass production of all strains improved dramatically when they were grown under mixotrophic conditions. Biomass obtained under phototrophic, heterotrophic, and mixotrophic culture conditions were as follows: 0.56, 0.83, and 0.89 g/L for *I. galbana* LB987; 0.54, 1.46, and 1.69 g/L for *N. oculata* CCAP849/1; and 0.59, 0.90, and 1.16 g/L for *D. salina*, respectively.

As described above, microalgal cells grown under heterotrophic condition, which means dark conditions, maintained low-level chlorophyll and total lipid content. However, under mixotrophic conditions, light stimulated the production of chlorophyll and total lipid to the maximal level. Chlorophyll concentration in cells grown under photoautotrophic, heterotrophic, and mixotrophic cultivation were as follows: 32.3, 4.1, and 29.1 mg/g for *I. galbana* LB987; 41.9, 3.7, and 39.2 mg/g for *N. oculata* CCAP849/1; and 38.5, 2.6, and 35.2 mg/g for *D. salina*, respectively (Fig. 4). In addition, total lipid contents (%, w/w) in cells obtained from photoautotrophic, heterotrophic, and mixotrophic cultivation were as follows: 26.5, 17.4, and 30.1 % for *I. galbana* LB987; 26.5, 18.4, and 37.3 % for *N. oculata* CCAP849/1; and 24.6, 15.8, and 31.3 % for *D. salina*, respectively. The increase or decrease patterns for chlorophyll and total lipid production under different culture conditions were very similar.

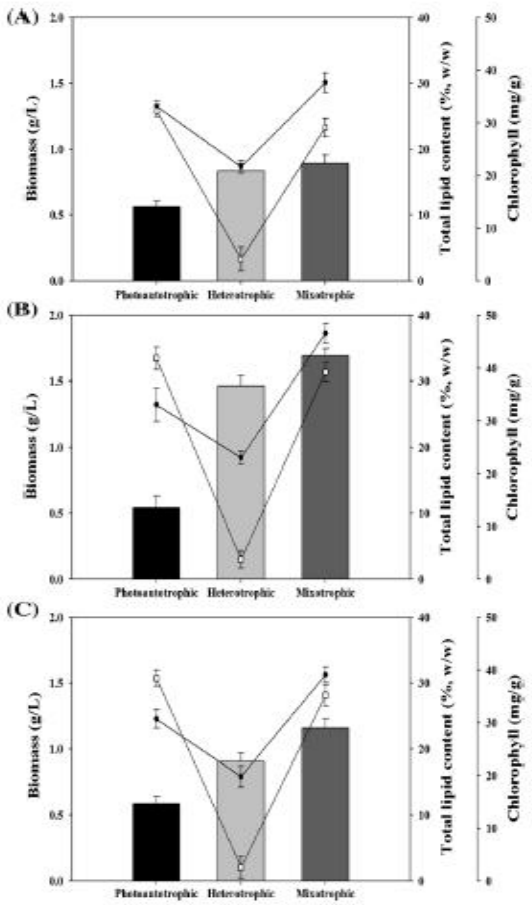

Fig. 4 Biomass, total lipid and chlorophyll content of three green microalgae grown under photoautotrophic, heterotrophic and mixotrophic culture conditions. **a** *I. galbana* LB987; **b** *N. oculata* CCAP849/1; and **c** *D. salina*. *Filled rectangle* biomass, *filled circle* total lipid content, and *unfilled circle* chlorophyll content

It is known that light intensity directly influences microalgal cell growth and photosynthesis. Therefore, the effect of light intensity on biomass, total lipid, and chlorophyll concentrations was assessed under mixotrophic cultivation, with

Collection @ chosun

조선대학교
CHOSUN UNIVERSITY

varying light intensity ranging from 0 to 200 μmol/m^2/s and a constant photoperiod (12/12-h light/dark). It is noteworthy that light intensity did not have a significant impact on cell growth but stimulated chlorophyll synthesis and lipid production in cells remarkably (Fig. 5). Optimal range of light intensity for maximum total lipid production of all three strains was found to be from 80 to 150 μmol/m^2/s.

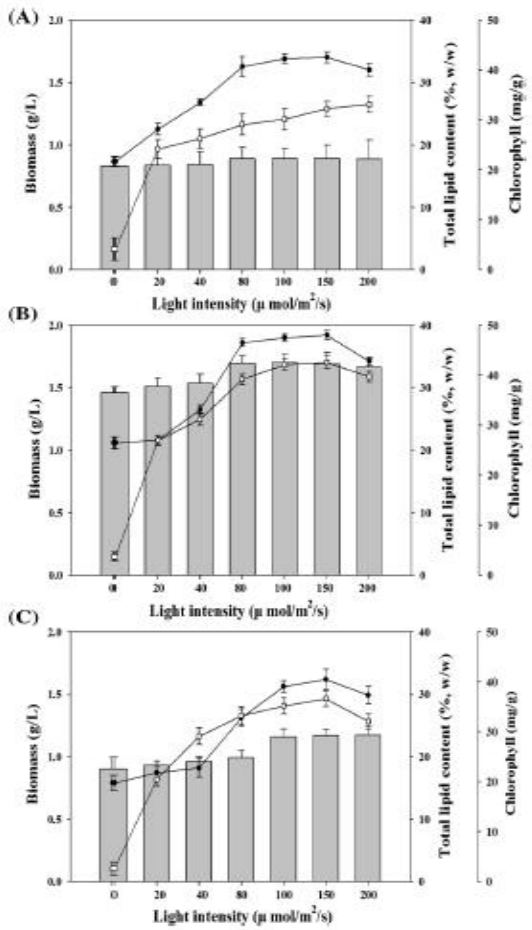

Fig. 5 Effect of light intensity on cell growth, total lipid and chlorophyll content under mixotrophic cultivation. **a** *I. galbana* LB987; **b** *N. oculata* CCAP849/1; and **c** *D. salina*. *Filled rectangle* biomass, *filled circle* total lipid content, and *unfilled circle* chlorophyll content

Effect of light intensity on fatty acid composition

Effect of light intensity on total fatty acid concentration and composition of total lipid in all three strains was analyzed with different light intensities ranging from 0 to 200 μmol/m^2/s. Fatty acid composition was determined as palmitic acid (C16:0), palmitoleic acid (C16:1), stearic acid (C18:0), oleic acid (C18:1), linoleic acid (C18:2), and linolenic acid (C18:3) from extracted lipid to focus on the quality improvement of biodiesel. As light intensity increased up to 150 μmol/m^2/s, fatty acid concentrations in the three microalgae increased slightly (Table 1). *N. oculata* CCAP849/1 produced the highest amount of C16–C18 fatty acids among the three strains, 67.0 mg/mL with a light intensity of 150 μmol/m^2/s. Unlike *I. galbana* LB987 and *N. oculata* CCAP849/1, the concentration of C16–C18 fatty acids of *D. salina* increased remarkably according to the increase of light intensity up to 150 μmol/m^2/s, although its relative concentration level (approximately 20 mg/mL) was low. More than 40 mg/mL fatty acids were involved as forms of lignoceric acid (C24:0), docosahexaenoic acid (C22:6), and eicosapentaenoic acid (C20:5), in decreasing order.

Meanwhile, light intensity variations did not change C16–C18 fatty acids composition significantly in all three strains (Table 1). Regardless of light intensity, the major constituents of *I. galbana* LB987 were long-chain fatty acid of palmitic (C16:0) and oleic acid (C18:1), whereas those of *N. oculata* CCAP849/1 were palmitic (C16:0) and palmitoleic acid (C16:1). In the case of *D. salina*, linolenic (C18:3) and linoleic acids (C18:2) were found to be dominant in cells. It is noteworthy that all three strains contained a relatively low concentration of stearic acid (C18:0), a common fatty acid in microalgae.

Discussion

Nitrogen concentration in the culture medium is one of the vital factors that affect lipid synthesis of microalgae. It has been reported that lipid content in *Chlorella* could be doubled or even tripled under N-depletion conditions [7, 31], and a reciprocal relationship between nitrogen concentration and lipid content was also observed [41]. Under nitrogen starvation, the capacity for de novo lipid synthesis seems a characteristic of some algal species by converting excess of carbon and energy into triacylglycerols (TAG) [36]. TAG consisted mainly of saturated and monounsaturated fatty acids can be efficiently stored in the cell and generate more energy than carbohydrates upon oxidation, thus forming the efficient carbon sink for rebuilding the cell after the stress. Although nitrogen starvation is well known to trigger a high amount of lipid accumulation, it can cause poor cell growth as well. Therefore, it is important

Collection @ chosun

조선대학교
CHOSUN UNIVERSITY

Table 1 Relative fatty acid (C16–C18) composition (%) of lipids in cells grown under mixotrophic condition with different light intensities

Microalgae	Light intensity (umol/m^2/s)	Fatty acid concentrations						
		C16:0	C16:1	C18:0	C18:1	C18:2	C18:3	Total fatty acid
		mg/mL (%)	mg/mL (%)	mg/mL (%)	mg/mL (%)	mg/mL (%)	mg/mL (%)	mg/mL (%)
I. galbana LB987	0	17.4 (41.2)	0.9 (2.0)	3.1 (7.3)	10.9 (25.8)	6.9 (16.3)	3.1 (7.3)	42.3 (100)
	20	17.6 (38.7)	0.9 (2.0)	5.9 (13.0)	11.2 (24.7)	6.5 (14.3)	3.3 (7.3)	45.4 (100)
	40	17.9 (38.8)	0.9 (2.0)	6.0 (13.0)	11.6 (25.1)	7.0 (15.1)	2.8 (6.1)	46.2 (100)
	80	18.3 (36.2)	1.0 (1.9)	6.3 (12.5)	12.0 (23.7)	7.1 (14.0)	5.9 (11.7)	50.6 (100)
	100	19.4 (38.3)	0.9 (1.8)	6.4 (12.6)	12.4 (24.4)	7.5 (14.8)	4.1 (8.0)	50.7 (100)
	150	19.7 (38.5)	1.0 (1.9)	6.4 (12.5)	12.6 (24.6)	7.2 (14.1)	4.3 (8.4)	51.1 (100)
	200	17.3 (36.6)	0.9 (1.9)	6.1 (12.9)	12.7 (26.8)	6.7 (14.2)	3.6 (7.6)	47.3 (100)
N. oculata CCAP849/1	0	21.3 (41.9)	20.8 (41.1)	0.8 (1.7)	4.1 (8.0)	3.0 (5.8)	0.8 (1.5)	50.7 (100)
	20	23.8 (43.3)	21.5 (39.0)	1.4 (2.5)	4.1 (7.5)	3.5 (6.3)	0.8 (1.4)	55.0 (100)
	40	25.8 (44.1)	22.5 (38.5)	1.4 (2.4)	4.3 (7.3)	3.7 (6.3)	0.8 (1.4)	58.5 (100)
	80	27.3 (42.3)	26.0 (40.2)	1.7 (2.6)	6.3 (9.7)	2.7 (4.1)	0.8 (1.2)	64.7 (100)
	100	26.2 (40.0)	26.4 (40.2)	1.5 (2.3)	6.9 (10.5)	3.7 (5.6)	0.9 (1.4)	65.6 (100)
	150	26.4 (39.4)	27.2 (40.6)	1.5 (2.2)	6.3 (9.4)	4.8 (7.1)	0.9 (1.3)	67.0 (100)
	200	25.7 (41.6)	23.2 (37.6)	1.4 (2.3)	6.6 (10.6)	4.1 (6.6)	0.8 (1.2)	61.6 (100)
D. salina	0	0.2 (8.8)	0.2 (7.1)	0.2 (8.0)	0.1 (4.6)	0.6 (25.6)	1.1 (45.8)	2.4 (100)
	20	0.4 (11.7)	0.2 (6.7)	0.2 (7.0)	0.2 (5.0)	0.7 (24.8)	1.3 (44.6)	3.0 (100)
	40	0.9 (13.2)	0.4 (6.3)	0.6 (8.4)	0.3 (4.1)	1.2 (16.7)	3.6 (51.2)	7.0 (100)
	80	1.5 (10.8)	0.5 (3.7)	0.9 (6.9)	0.7 (4.8)	2.7 (19.6)	7.4 (54.3)	13.7 (100)
	100	1.6 (8.5)	0.5 (2.8)	1.1 (5.9)	1.2 (6.2)	4.0 (21.6)	10.3 (55.0)	18.6 (100)
	150	1.6 (7.8)	0.6 (2.7)	1.3 (6.5)	1.2 (6.0)	4.3 (20.8)	11.7 (56.3)	20.8 (100)
	200	1.6 (8.0)	0.6 (3.0)	1.4 (6.8)	1.2 (5.9)	4.4 (21.7)	11.0 (54.6)	20.1 (100)

The values in parenthesis indicate the relative compositions of fatty acid of total lipid accumulated in microalgal cells

to establish an appropriate concentration of nitrogen in culture medium to obtain maximal lipid productivity. This study shows that the total lipid content in cells decreased but cell growth improved with increasing nitrogen concentration (Fig. 1).

Some photoautotrophic microalgal cells can grow under mixotrophic conditions, with the addition of external organic carbon sources. This phenomenon exists in a number of microalgal genera and species distributed in major taxonomic divisions [9, 38]. Most of the previous works have focused on the use of organic carbon as precursor for cell growth and for the accumulation of macromolecules, such as lipids, saccharides, proteins, and other active biochemicals under heterotrophic cultivation [24]. Heterotrophic cultivation has many advantages such as pure and high cell density culture without photolimitation effect and ease of harvesting. The use of carbon source is species-specific. In the present study, among the carbon sources tested, the supplementation of glucose led to a significant improvement of growth in all three microalgal cells (Fig. 2). In general, glucose is the most commonly used carbon source in the heterotrophic cultivation of many microalgae. Based on the finding from Griffiths et al. [13], we found that high biomass concentrations were obtained when glucose was added as the sole carbon source. Liang et al. [20] showed that the highest biomass and a 14-fold higher lipid productivity of *C. vulgaris* were obtained under heterotrophic conditions in the presence of glucose. In addition, Liu et al. [21] stated that glucose is the best carbon source for microalgal growth and lipid accumulation. This is mainly because the supplementation of glucose in the culture medium induces the membrane-bound H^+-glucose symport system [15] and enhances the driving force of glucose uptake [35]. The major metabolic pathways of glucose in algal cells are the glycolytic and pentose phosphate pathways. The reducing equivalents ($FADH_2$ and NADPH) are produced from glucose metabolism involved in ATP synthesis during oxidative phosphorylation. As a consequence, all of the produced ATPs are used for cell growth and lipid accumulation.

In our study, increasing growth trend was observed with increasing glucose concentrations; however, higher glucose concentrations provoked a decrease in biomass amount, which might be attributed to substrate inhibition (Fig. 3). In this case, excess glucose molecules would compete with the glucose molecules on the membrane-bound glucose permease.

Collection @ chosun

조선대학교
CHOSUN UNIVERSITY

The influence of three different culture modes on growth, chlorophyll, and total lipid content in three microalgae is presented in Fig. 4. Low biomass production occurred under photoautotrophic cultivation compared with heterotrophic or mixotrophic cultivation. The major reason for this outcome was that, in phototrophic conditions, only one factor acts as an energy source (light). Meanwhile, both light energy and organic carbon source were used for ATP production under mixotrophic conditions. In mixotrophic conditions, light energy is the major source for ATP production in the early stage of cell growth. Furthermore, in the presence of an organic carbon source, the concentration of photosynthetic pigments was low, and the formation of thylakoids was disturbed within the cell. Yang et al. [44] stated that total ATPs produced under photoautotrophic, heterotrophic, and mixotrophic conditions were 34.4, 19.4, and 27.4 mmol/g/h, respectively. However, the percentages of ATP consumption/production were 56.8, 18.2, and 36.3 % during photoautotrophic, heterotrophic, and mixotrophic cultivation, respectively. A low ATP consumption during heterotrophic cultivation was attributed to the absence of the Calvin cycle (no light energy), and most of ATP was consumed only for glucose uptake and biomass synthesis. Among the three different culture mode operations, the highest total lipid content was observed under mixotrophic cultivation. This is because mixotrophic cultivation uses both light energy and carbon sources for cell growth and lipid accumulation.

The effect of light intensity on microalgal growth and total lipid content is depicted in Fig. 5. Our previous studies indicated that cell growth and total lipid production of freshwater green microalgal cells under mixotrophic conditions are notably affected by light intensity [11]. Cheirsilp et al. [6] reported that the number of photosynthetic pigments (chlorophyll *a* and light-harvesting pigments such as chlorophyll *c*, phycobilins, and carotenoids) increases with increasing light intensity. In the present study, the total lipid content increases with increasing light intensity; this is because excessive light energy was converted into fatty acids. Under optimal growth conditions, light energy absorbed by antenna pigments is converted to ATP or NADPH, and this chemical energy is stored ultimately as starch and/or lipids by fixing CO_2 through the Calvin cycle and lipogenesis. Furthermore, when high light energy was supplied into the microalgal culture, the enzymes involved in fatty acid biosynthesis were very active, particularly acetyl-CoA carboxylase, desaturase, acyl-carrier protein synthase, ATP/citrate lyase, and membrane-bound glucose permease [1, 11]. In contrast, photo-oxidative cell damage occurred when microalgal cells were grown under higher light intensity. Under these conditions, the light-harvesting chlorophyll molecules were converted to unstable forms, which in turn react with dissolved oxygen species. These reactive oxygen species then react with free fatty acids to make lipid peroxidase in inactive form, which reduces the fatty acid concentration. Furthermore, microalgal cells can accumulate excessive light energy in the form of other macromolecules such as polysaccharides and proteins. Instead, low light intensity may increase the light reaction center pigments and light-harvesting (antenna) pigments to absorb maximal photons for normal cell growth. Moreover, a large volume of chloroplasts and a high density of thylakoid membranes lead to reduced lipid storage [11].

It has been shown that light intensity influences fatty acid composition of microalgal cells such as triglyceric acids, glycolipids, phospholipids, and polyunsaturated fatty acids (PUFA) [44]. Fatty acid composition plays an important role in the evaluation of biodiesel quality. The changes in fatty acid composition attributed to light intensity are highly species-specific. Furthermore, when the cells were grown at a higher light intensity, this led to an increased concentration of saturated fatty acids but a decrease in PUFA [3]. In contrast, low light intensity induces the formation of membrane polar lipids associated with chloroplasts. In this situation, more electron receptors were synthesized in thylakoids. Under low light intensity, the photosynthetic pigments and PUFA increased [47]. It is noteworthy that Solovchenko et al. [32] reported that the fatty acid composition of lipids in *Desmodesmus* sp. were most likely changed in chloroplasts accompanied by the dismantling of thylakoid membranes under very high light intensity.

In this study, the effect of light intensity on total amount and composition of fatty acid (C16–C18) of total lipid in three microalgal cells was investigated. As shown in Table 1, fatty acid concentration increased slightly with increasing light intensity up to 150 μmol/m^2/s, and the order of microalgal species containing high fatty acids (C16–C18) concentration was *N. oculata* CCAP849/1 > *I. galbana* LB987 > *D. salina*. However, relative fatty acid compositions of total lipid were not changed by the variation of light intensity. Regardless of light intensity, *I. galbana* LB987 contained approximately 40 % palmitic (C16:0) and 25 % oleic acids (C18:1) as major fatty acids but stearic (C18:0) and linoleic acids (C18:2) as minor fatty acids, whereas *N. oculata* CCAP849/1 contained >40 % palmitic (C16:0) and >40 % palmitoleic acids (C16:1) as major fatty acids but oleic acid (C18:1) as minor fatty acid. In the case of *D. salina*, total fatty acid concentration was 62.1 mg/mL, however, C16–C18 concentration was found to be only 20 mg/mL. More than 40 mg/mL fatty acid was involved as forms of lignoceric (C24:0), docosahexaenoic (C22:6), and eicosapentaenoic acids (C20:5) in *D. salina*. From these results, we can expect that the species of *N. oculata* CCAP849/1 and *I. galbana* LB987 can be used as sources for biodiesel production, whereas *D. salina* species can be used as a source for omega-3 production, which is

Collection @ chosun

조선대학교
CHOSUN UNIVERSITY

Table 2 Comparison of biomass and total lipid productivities of three microalgae with other related marine microalgae

Microalgae	Reactor type (L)	Culture conditions			Biomass		Lipid			References
		Culture mode	Light intensity (umol/m^2/s)	Carbon sources	Production (g/L)	Productivity (mg/L/d)	Contents (%, dry weight)	Production (g/L)	Productivity (mg/L/d)	
I. galbana	Circular cylindrical (20 L)	Photoautotrophic	36	–	0.57	24.9	23.2	–	–	Lee et al. [18]
I. galbana	Circular cylindrical (5 L)	Photoautotrophic	110	–	0.80	66.6	24.0	–	–	Ra et al. [28]
I. galbana LB987	Erlenmeyer flask (1 L)	Mixotrophic	150	0.02 M glucose	0.89	89.1	30.1	0.27	26.8	In this study
N. oculata	Circular cylindrical (20 L)	Photoautotrophic	36	–	0.57	20.4	8.2	–	–	Lee et al. [18]
N. oculata	Circular cylindrical (5 L)	Photoautotrophic	110	–	0.51	47.5	17.0	–	–	Ra et al. [28]
N. oculata CCMP525	–	Mixotrophic	270	0.06 M glucose	0.61	–	–	0.16	14.0	Wan et al. [40]
N. oculata CCAP849/1	Erlenmeyer flask (1 L)	Mixotrophic	150	0.02 M glucose	1.69	169.4	38.5	0.63	63.1	In this study
D. tertiolecta	Circular cylindrical (5 L)	Photoautotrophic	110	–	0.28	44.2	23.0	–	–	Ra et al. [28]
D. salina	Circular cylindrical (5 L)	Photoautotrophic	110	–	0.25	37.5	22.0	–	–	Ra et al. [28]
D. salina FACHB435	–	Mixotrophic	270	0.08 M glucose	0.52	–	–	0.15	12.0	Wan et al. [40]
D. salina	Erlenmeyer flask (1 L)	Mixotrophic	150	0.05 M glucose	1.17	115.9	32.4	0.36	36.3	In this study

effective for human health benefits of cancer, cardiac disease, stroke, high blood pressure, and arrhythmia [30, 39].

Table 2 shows the comparative analysis of the biomass and lipid production in the three marine microalgae species with other related species under the different culture conditions. From this analysis, it was confirmed that mixotrophic cultivation is more efficient for lipid production than photoautotrophic culture in the same microalgal species and glucose can be used for growth as a better organic source. Among the microalgal species described in this Table 2, *N. oculata* CCAP849/1 was the best biomass- and lipid-producing microalga under mixotrophic culture conditions with 0.02 M glucose and light intensity of 150 µmol/m^2/s. Maximal biomass and lipid productivities of this species were 169.4 and 63.1 mg/L/d, respectively.

Conclusion

In this study, the improvement of biomass and total lipid production of three microalgal species under different culture modes was investigated. Nitrogen starvation under photoautotrophic conditions could increase lipid synthesis of microalgae. Cells cultivated under mixotrophic condition with 0.02 M glucose and light intensity of 150 µmol/m^2/s showed the maximal biomass and lipid productivities. Light intensity stimulated chlorophyll synthesis and lipid production in cells significantly, but did not increase cell growth. Meanwhile, light intensity variations did not change C16–C18 fatty acids composition significantly in all three strains. *N. oculata* CCAP849/1 used in this study can be applicable for industrial level lipid production.

Collection @ chosun

조선대학교
CHOSUN UNIVERSITY

Acknowledgments This work was supported by the Ministry of Science, ICT, and Future Planning Research Grant (NRF-2015R1D1A3A01020290) and in part by the Human Resources Development program (20114010100090) of the KETEP grant funded by the Ministry of Trade, Industry and Energy, Republic of Korea.

References

1. Arroyo J, Hutzler J, Bermejo C, Ragni E, GarcÃ-a-Cantalejo J, BotÃ-as P, Piberger H, Schott A, Sanz BS, Strahl S (2011) Functional and genomic analyzes of blocked protein O-mannosylation in baker's yeast. Mol Microbiol 79:1529–1546
2. Becker EW (1994) Microalgae: biotechnology and microbiology. Cambridge University, New York
3. Brown MR, Dunstan GA, Norwood SJ, Miller KA (1996) Effects of harvest stage and light on the biochemical composition of the diatom *Thalassiosira pseudinana*. J Phycol 32:64–73
4. Castenholz RW (1969) Thermophilic blue-green algae and the thermal environment. Bact Rev 33:476–504
5. Cerón-García MC, Fernández-Sevilla JM, Sánchez-Mirón A, García-Camacho F, Contreras-Gómez A, Molina-Grima E (2013) Mixotrophic growth of *Phaeodactylum tricornutum* on fructose and glycerol in fed-batch and semi-continuous modes. Bioresour Technol 147:569–576
6. Cheirsilp B, Torpee S (2012) Enhanced growth and lipid production of microalgae under mixotrophic culture condition: effect of light intensity, glucose concentration and fed-batch cultivation. Bioresour Technol 110:510–516
7. Converti A, Casazza AA, Ortiz EY, Perego P, Del Borghi M (2009) Effect of temperature and nitrogen concentration on the growth and lipid content of *Nannochloropsis oculata* and *Chlorella vulgaris* for biodiesel production. Chem Eng Process 48:1146–1151
8. Das P, Lei W, Aziz SS, Obbard JP (2011) Enhanced algal growth in both phototrophic and mixotrophic culture under blue light. Bioresour Technol 102:3883–3887
9. Feuillade M, Feuillade J (1989) Heterotrophic capabilities of blue–green alga *Oscillatoria rubescens*. Arch Hydrobiol 117:61–76
10. Folch J, Lees M, Sloane Stanley GH (1957) A simple method for the isolation and purification of total lipids from animal tissues. J Biol Chem 226:497–509
11. Gim GH, Kim JK, Kim HS, Kathiravan MN, Yang H, Jeong SH, Kim SW (2014) Comparison of biomass production and total lipid content of freshwater green microalgae cultivated under various culture conditions. Bioprocess Biosyst Eng 37:99–106
12. Gouveia L, Oliveira AC (2009) Microalgae as raw material for biofuels production. J Ind Microbiol Biotechnol 36:269–274
13. Griffiths DJ, Thresher CL, Street HE (1960) The heterotrophic nutrition of *Chlorella vulgaris*. Ann Bot 24:1–11
14. Guillard RRL, Ryther JH (1962) Studies of marine planktonic diatoms I. *Cyclotella nana* hustedt and *Detonula confervaceae* (Cleve) gran. Can J Microbiol 8:229–239
15. Haass D, Tanner W (1973) Regulation of hexose transport in *Chlorella vulgaris*. Plant Physiol 53:14–20
16. Imamoglu E, Sukan FV, Dalay MC (2007) Effect of different culture media and light intensities on growth of *Haematococcus pluvialis*. Int J Natural Eng Sci 1:5–9
17. Kong WB, Yang H, Cao YT, Song H, Hua SF, Xia CG (2013) Effect of glycerol and glucose on the enhancement of biomass, lipid and soluble carbohydrate production by *Chlorella vulgaris* in mixotrophic culture. Food Technol Biotechnol 51:62–69
18. Sj Lee, Go S, Jeong GT, Kim SK (2011) Oil production from five marine microalgae for the production of biodiesel. Biotechnol Bioprocess Eng 16:561–566
19. Li Y, Wang B, Wu N, Lan CQ (2008) Effects of nitrogen sources on cell growth and lipid production of *Neochloris oleoabundans*. Appl Microbiol Biotechnol 81:629–636
20. Liang Y, Sarkany N, Cui Y (2009) Biomass and lipid productivities of *Chlorella vulgaris* under autotrophic, heterotrophic and mixotrophic growth conditions. Biotechnol Lett 31:1043–1049
21. Liu J, Hung J, Fan KW, Jiang Y, Zhong Y, Sun Z, Chen F (2010) Production potential of *Chlorella zofingiensis* as a feedstock for biodiesel. Bioresour Technol 101:8658–8663
22. Liu ZY, Wang GC, Zhou BC (2008) Effect of iron on growth and lipid accumulation in *Chlorella vulgaris*. Bioresour Technol 99:4717–4722
23. Liu J, Yuan C, Hu G, Li F (2012) Effects of light intensity on the growth and lipid accumulation of microalga *Scenedesmus* sp. 11-1 under nitrogen limitation. Appl Biochem Biotechnol 166:2127–2137
24. Mata TM, Martins AA, Caetano NS (2010) Microalgae for biodiesel production and other applications: a review. Renew Sustain Energy Rev 14:217–232
25. Merzlyak MN, Chivkunova OB, Gorelova OA, Reshetnikova IV, Solovchenko AE, Khozin-Goldberg I, Cohen Z (2007) Effect of nitrogen starvation on optical properties, pigments, and arachidonic acid content of the unicellular green alga *Parieto-chloris* incise rebouxiophyceae, Chlorophyta). J Phycol 43:833–843
26. Metcalfe LD, Schmitz AA, Pelka JR (1966) Rapid preparation of fatty acid esters from lipids for gas chromatographic analysis. Anal Chem 38:514–515
27. Miller GL (1959) Use of dinitrosalicylic acid reagent for determination of reducing sugar. Anal Chem 31:426–428
28. Ra CH, Kang CH, Kim NK, Lee CG, Kim SK (2015) Cultivation of four microalgae for biomass and oil production using a two-stage culture strategy with salt stress. Renew Energy 80:117–122
29. Ren HY, Liu BF, Ma C, Zhao L, Ren NQ (2013) A new lipid-rich microalga *Scenedesmus* sp. strain R-16 isolated using Nile red staining: effects of carbon and nitrogen sources and initial pH on the biomass and lipid production. Biotechnol Biofuels 6:143
30. Romieu I, Tellez-Rojo MM, Lazo M, Manzano-Patino A, Cortez-Lugo M, Julien P, Belanger MC, Hernandez-Avila M, Holguin F (2005) Omega-3 fatty acid prevents heart rate variability reductions associated with particulate matter. Am J Respir Crit Care Med 12:1534–1540
31. Scott SA, Davey MP, Dennis JS, Horst I, Howe CJ, Lea-Smith DJ, Smith AG (2010) Biodiesel from algae: challenges and prospects. Curr Opinion Biotechnol 21:277–286
32. Solovchenko AE, Chivkunova OB, Semenova LR, Selyakh IO, Shcherbakov PN, Karpova EA, Lobakova ES (2013) Stress-induced changes in pigment and fatty acid content in the microalga *Desmodesmus* sp. isolated from a white sea hydroid. Russ J Plant Physiol 60:313–321
33. Spolaore P, Joannis-Cassan C, Duran E, Isambert A (2006) Commercial applications of microalgae. J Biosci Bioeng 101:87–96
34. Sugimoto K, Midorikawa T, Tsuzuki M, Sato N (2008) Upregulation of PG synthesis on sulfur-starvation for PS I in *Chlamydomonas*. Biochem Biophys Res Commun 369:660–665
35. Tanner W (1969) Light-driven active uptake of 3-*O*-methylglucose via an inducible hexose uptake system of *Chlorella*. Biochem Biophys Res Commun 36:278–283
36. Thompson GA Jr (1996) Lipids and membrane function in green algae. Biochim Biophys Acta 1302:17–45
37. Tian-Yuan Z, Yin-Hu Wu, Shu-feng Z, Feng-Min L, Hong-Ying H (2013) Isolation and heterotrophic cultivation of mixotrophic microalgae strains for domestic wastewater treatment and lipid production under dark condition. Biresour Technol 149:586–589
38. Ukeles R, Rose WE (1976) Observations on organic carbon utilisation by photosynthetic marine microalgae. Marine Biol 7:11–28

Collection @ chosun

조선대학교
CHOSUN UNIVERSITY

39. Vazhappilly R, Chen F (1998) Eicosapentaenoic acid and docosahexaenoic acid production potential of microalgae and their heterotrophic growth. J Am Oil Chem Soc 75:393–397
40. Wan M, Liu P, Xia J, Rosenberg JN, Oyler GA, Betenbaugh MJ, Nie Z, Qui G (2011) The effect of mixotrophy on microalgal growth, lipid content, and expression levels of three pathway genes in *Chlorella sorokiniana*. Appl Microbiol Bitechnol 91:825–844
41. Widjaja A, Chien CC, Ju YH (2009) Study of increasing lipid production from fresh water Microalgae *Chlorella vulgaris*. J Taiwan Institute of Chem Eng 40:13–20
42. Xia L, Ge H, Zhou X, Zhang D, Hu C (2013) Photoautotrophic outdoor two-stage cultivation for oleaginous microalgae *Scenedesmus obtusus* XJ-15. Bioresour Technol 144:261–267
43. Xin L, Hong-ying H, Ke G, Ying-xue S (2010) Effects of different nitrogen and phosphorus concentrations on the growth, nutrient uptake, and lipid accumulation of a freshwater microalga *Scenedesmus* sp. Bioresour Technol 101:5494–5500
44. Yang C, Hua Q, Shimizu K (2000) Energetics and carbon metabolism during growth of microalgal cells under photoautotrophic, mixotrophic and cyclic light-autotrophic/dark-heterotrophic conditions. Biochem Eng J 6:87–102
45. Yeesang C, Cheirsilp B (2011) Effect of nitrogen, salt, and iron content in the growth medium and light intensity on lipid production by microalgae isolated from freshwater sources in Thailand. Bioresour Technol 102(3):3034–3040
46. Yeh KL, Chang JS, Chen WM (2010) Effect of light supply and carbon source on cell growth and cellular composition of a newly isolated microalga *Chlorella vulgaris* ESP-31. Eng Life Sci 10:201–208
47. Zhukova NV, Titlyanov EA (2006) Effect of light intensity on the fatty acid composition of dinoflagellates symbiotic with hermatypic corals. Bot Mar 49:339–346

Collection @ chosun